Targeting of methotrexate to melanoma by way of melanocyte stimulating hormone

Richards, Andrew Colin

Award date:
1993

Awarding institution:
University of Bath

TARGETING OF METHOTREXATE TO MELANOMA BY WAY OF MELANOCYTE STIMULATING HORMONE

Submitted by Andrew Colin Richards

for the degree of

Doctor of Philosophy

of the University of Bath

1992

ProQuest LLC
789 East Eisenhower Parkway
P.O. Box 1346
Ann Arbor, MI 48106-1346

Abstract

The work in this thesis relates to the efficiency of cell-specific uptake of drugs mediated by peptide hormones. A model system was used to study hormonal targeting to B16 melanoma cells using melanocyte stimulating hormone. The rate of fluid-phase endocytosis was measured at 37^0C, in B16 murine melanoma cells, by determining the fluid-associated accumulation of ^{125}I-PVP. Fluid uptake was bi-phasic. A rapid phase of uptake in the first 10 minutes was thought to represent the filling of the cell endosomal compartment (the volume of which was estimated as 109 ± 40nl/10^6cells). After the establishment of steady-state fluid turnover by the endosomes, a slower linear accumulation of fluid (thought to be by the lysosomes) was observed for up to 100 minutes. The rate of this second phase was $0.038 \pm 0.001\mu$l/hr/10^6cells. Different uptake profiles were observed for two other cell lines.

The interaction of methotrexate (MTX) with B16 cells was assessed using the tritiated drug. Binding at 4^0C had a relatively low affinity, K_d 0.21μM, with approximately 270,00 binding sites/cell. At 37^0C the labelled drug was internalised presumably through the reduced folate carrier in the cell membrane, as uptake was inhibited by PCMPS and thiamine pyrophosphate. It was not possible to establish the growth of B16 cells in low folate medium.

The analogue of α-MSH, [Nle^4,D-Phe^7]-αMSH (NLDP-MSH), was successfully labelled with ^{125}I, and the mono-iodinated product separated. Binding to B16 cells at 4^0C had high affinity, K_d c.0.6nM, but a low number of binding sites, c.4500 per cell. After 30 minutes at 37^0C, 40% of the cell associated ^{125}I activity was acid-wash resistant, and thus considered internalised. Cell surface binding reached a maximum after 30 minutes before declining. Uptake occurred through the binding site observed at 4^0C, and displayed no signs of cooperativity.

MTX was successfully conjugated to NLDP-MSH, forming four equal products. This was due to racemization around the linkage to the α-carbon of the gluta-

mate moiety of MTX. The conjugate displayed no specific inhibition of ^{3}H-MTX binding to B16 cells. However in a competition assay against ^{125}I-NLDP-MSH, the affinity of the conjugate compared to the labelled peptide was ten fold lower (K_d c.6.5nM).

NLDP-MSH-MTX was iodinated and the mono-labelled product purified. ^{125}I-NLDP-MSH-MTX was internalised by B16 cells at 37^{0}C and demonstrated similar profiles of surface binding to the free peptide.

Using a spectrophotometric assay, the inhibition of dihydrofolatereductase (DHFR), the target enzyme for MTX, was examined. Free MTX and NLDP-MSH-MTX displayed IC_{50} values of 0.01 and 0.25μM respectively, i.e. the conjugate had a forty fold lower affinity than MTX for DHFR. In vitro lysosomal degradation of the conjugate after a 16 hour incubation at 37^{0}C, released products of an equipotent nature to free MTX.

Acknowledgements

I would like to thank my supervisor Dr Colin Pouton for his constant support and enthusiasm throughout the time spent on this thesis. I would also like to thank Dr George Olivier at Bath University for synthesising the peptide and the peptide conjugate employed in this work. I would like to thank Gail Adams, Elena De Angelis and in particular Roger Mepstead for their friendship and support. Also my family for proof reading, encouragement and for being there when I needed them most. Finally I would like to thank SERC and Cyanamid (U.K.) Ltd. for financial support, the collaboration of members of the SERC/DTI funded LINK programme in 'Selective Drug Delivery and Targeting' and the University of Bath for providing research facilities.

Abbreviations

ATP	Adenosine Triphosphate
BSA	Bovine Serum Albumin
DHFR	Dihydrofolate Reductase
DMSO	Dimethyl Sulphoxide
DNA	Deoxyribonucleic Acid
ECDI	1-Ethyl-3-[3-(dimethylamino)propyl] carbodiimide
EDT	Ethane Diol
EDTA	Ethylenediaminetetraacetic Acid
EGF	Epidermal Growth Factor
FAB-MS	Fast Atom Bombardment- Mass Spectrometry
FCS	Foetal Calf Serum
FH_2	7,8-Dihydrofolate
FH_4	5,6,7,8-Tetrahydrofolate
HMPA	N-(2-Hydroxypropyl) methacrylamide
HPLC	High Performance Liquid Chromatography
HRP	Horseradish Peroxidase
HSA	Human Serum Albumin

i.p. Intraperitoneal

i.v. Intravenous

LDL Low Density Lipoprotein

5-MFH_4 5-Methyltetrahydrofolate

MSH Melanocyte Stimulating Hormone

MTX Methotrexate

NADPH β-Nicotinamide Adenine Dinucleotide Phosphate

NEAA Non-Essential Amino Acids

NLDP-MSH [Nle^4,D-Phe^7]-αMSH

NLDP-MSH-MTX [Nle^4,D-Phe^7]-αMSH-MTX Conjugate

PB Phosphate Buffer

PBS Phosphate Buffer Saline

PCMPS p-Chloromercuribenzylsulphonic Acid

PVP Polyvinyl Pyrrolidone

RNA Ribonucleic Acid

TFA Trifluoroacetic Acid

Amino Acids:

Ala Alanine
Arg Arginine
Asn Asparagine

Asp	Aspartic Acid
Cys	Cysteine
Gln	Glutamine
Glu	Glutamic Acid
Gly	Glycine
His	Histidine
Ile	Isoleucine
Leu	Leucine
Lys	Lysine
Met	Methionine
Phe	Phenylalanine
Pro	Proline
Ser	Serine
Trp	Tryptophan
Tyr	Tyrosine
Val	Valine

Contents

Chapter 1

Introduction

Most medications are associated to some degree with toxic side-effects, the clinical use of these therapeutic agents can only be justified if their therapeutic effects outweigh these undesirable actions. This is best illustrated in cancer chemotherapy where inhibition of tumour growth by various agents is invariably accompanied by toxicity to rapidly proliferating normal cells. The therapeutic effectiveness of these agents could be improved, and the toxic responses limited, by increasing their amount and duration at the site of action (tumour cells); whilst reducing the exposure of non-target cells. This principle is the very basis of site-specific drug delivery, or drug targeting. Although the reference of drug-complexes will mainly be related to cancer chemotherapy, site-specific drug delivery is pertinent to many other illnesses including diseases of the central nervous system, immune system, some cardiovascular related diseases and arthritis.

The lack of target specificity of conventional drugs is mainly attributable to the formidable barriers presented by the body, e.g. cell membranes, enzymes, passage through certain organs etc. A major approach to solving this problem has been the advent of prodrugs [1, 2] which appears the most promising means of improving drug delivery. Here the active chemical is transformed into an inactive derivative which reverts to the parent compound due to enzyme and/or chemical

lability before or after reaching its site of action within the body. To this end the association or linkage of a drug to a carrier has been employed in an attempt to alter the tissue localisation [3]. The absorption and biodistribution of the drug is now largely dictated by the physico-chemical properties of the macromolecular carrier and so the choice of carrier. By definition these site-specific drug carrier delivery systems are of prodrug nature, unless the drug exerts its pharmacological action while attached to the carrier.

1.1 Design of Macromolecular-Drug Conjugates

In order to achieve the successful site-specific delivery of drugs via a carrier, the resulting conjugate must conform to a multitude of guidelines which as yet have not been satisfied by any reported complex.

1. The carrier must protect the drug from inactivation and premature release during transit.
2. The carrier must localise the drug at the site of action via the vasculature possibly involving endothelial passage. This may require the interaction with specific membrane or intracellular sites with the target cells.
3. The release of active drug should be regulated by biological processes at controlled and predictable rates. This release should be restricted to the target site.
4. The drug and host must be protected from one another during drug transit.
5. The carrier should be biodegradable (or not display any serious accumulation in the body), biochemically inert and non-immunogenic.
6. The carrier itself must not modulate the disease in question.
7. The complete entity should be convenient and cost-effective to prepare in a reproducible manner with homogenous yields.

8. The complete entity should be chemically and physically stable in its dosage form.

1.1.1 Choice of Macromolecular Carrier

The choice of carrier will be dependent on many factors including any known pharmacokinetic distribution of the macromolecule. Other important properties a carrier should posess are:

1. Lack of intrinsic toxicity and antigenicity by the carrier and its metabolic degradation products.
2. The carrier must have adequate functional groups for chemical fixation.
3. The carrier-drug conjugate must retain the desirable specificity of the original carrier compound.

There are two distinct classes of drug carriers, 1), particulate carriers such as liposomes [4], proteinaceous capsular particles [5] and cell carriers [6], and 2), soluble macromolecular carriers. Although particulate carriers offer many advantages such as the well protected delivery of a relatively large amount of drug to a site of action, their use is limited due to their poor extravasation [2] and will not be considered in any further detail here.

Soluble macromolecular conjugates can be further subdivided into biological carriers e.g. proteinaceous, and synthetic polymers e.g. poly-l-lysine. Examples of some carriers so far investigated include antibodies [7, 8], albumin [9], glycoproteins [10], lipoproteins [11], lectins [12], hormones [13], dextran [14], deoxyribonucleic acid [15] and N-(-2-hydroxypropyl)-methacrylamide (HMPA) [16], some of which will be mentioned in further detail.

1.1.2 Choice of Drug

There are three main properties the cytotoxic component must posess:

1. It must have adequate groups in its molecular structure for chemical fixation.
2. It must be chemically stable in the conjugated form until released.
3. It must display sufficient toxicity at relatively low doses in order to decrease the load of the carrier molecule.

Although most cytotoxic agents used in cancer chemotherapy may prove good candidates especially in the experimental stage of development, the potential of site-specific drug delivery is more likely to be reached in the long term with new chemical entities [17]. Theoretically this mode of drug delivery permits the use of highly toxic components not used in standard therapy e.g. animal or plant toxins [18].

Linkage to the macromolecule is usually covalent employing functional groups such as amino, carboxyl and hydroxyl groups. The conditions for attachment must be mild enough to ensure no adverse effects on the biological activity of the drug, yet the nature of the linkage can alter the pharmacokinetics of the formed conjugate. For example when ricin-A chain was conjugated to a monoclonal antibody via a disulphide bridge, a protected -S-S- link or a sulphide link, the latter was found to be cleared more slowly from the circulation [19].

1.1.3 Passive/Active Targeting

In general soluble and particulate macromolecular drug-conjugates are rapidly cleared from the blood by the cells of the reticuloendothelial system, mainly in

the liver and spleen. Indeed when Hashida et al. [20] injected rats with ^{14}C-labelled mitomycin C-dextran conjugates of diverse molecular weights, radioactivity rapidly disappeared from the blood. The extent of accumulation in the liver and spleen increased with the molecular weight of the carrier from 10,000 to 500,000. The net charge also determined the distribution of the conjugate which was polycationic at physiological pH. Conjugates with a carrier weight of 10,000 were rapidly distributed to the kidney where they were subsequently lost in the urine, whereas higher molecular weights were unaffected. It appears that the net charge and molecular weight of a macromolecular carrier can predetermine the biodistribution of the drug-conjugate, in particular to the liver and spleen. This localisation of drug away from the target site of action (in most situations) is the basis of 'passive' targeting which utilises the passive or natural distribution pattern of the carrier to deliver the drug to a specific site. However this does not generally lead to selective uptake at the appropiate target site. The normal distribution has to be selectively altered by specific means, i.e. active targeting. This is mainly achieved through specific membrane receptor recognising moieties such as sugar residues [12], hormones [13] and in particular antibodies [7, 8]. Note a limited degree of targeting can be achieved physically e.g. by intracompartment or intratumoural injection.

The addition of a targeting moiety to a conjugate will most probably alter the interaction with individual cells, especially those which represent the target. These macromolecular complexes are unable to enter cells by diffusion across the plasma membrane; their general mechanism of entry is by endocytosis. Knowledge of this complex and intricate process has led to the improved design of drug-conjugates to increase cell-targeting, uptake and release of active drug at the target site.

1.2 Endocytosis

Due to their large size and hydrophilic nature, macromolecules are incapable of permeating cellular membranes without the assistance of specific cell-membrane transporters or carriers. Undoubtedly the most important transport process with respect to cell-function and macromolecular drug-delivery is endocytosis. Here plasma membrane invaginates and pinches off, internalising membrane proteins, lipids and extracellular solutes. These newly-formed vesicles and their contents are then processed through various intracellular organelles before ligands or receptors generally reach the lysosomes, or are recycled back to the plasma membrane, figure 1.1. In polarised cells, e.g. epithelial cells, internalised macromolecules can be transported to the opposite side of the cell, a process known as transcytosis. Both endocytosis and transcytosis although well reviewed [21, 22, 23, 24] are very complex processes not yet fully understood. However a knowledge of their function is essential for the rational design of site-specific drug delivery systems as it is a process pertinent to almost all animal cells. Endocytosis is an essential part of many physiologic pathways including the transport of nutrients, regulation of hormone actions, the control of metabolic reactions and the processing of antigens [21].

Interaction of macromolecules with cell membranes can result in basically one of two types of endocytic uptake, receptor-mediated or non-receptor mediated endocytosis.

1. Receptor-mediated endocytosis involves the precise binding of the macromolecular conjugate to a specific plasma membrane-associated protein, for example the ligand for such a high affinity protein may include an antibody, hormone or polysaccharide. Following binding, receptor-ligand complexes may concentrate in coated pits (clathrin-coated regions) which subsequently invaginate to form clathrin-coated vesicles. Many physiological ligands are internalised via this pathway e.g. LDL, insulin, EGF [25] but binding of the

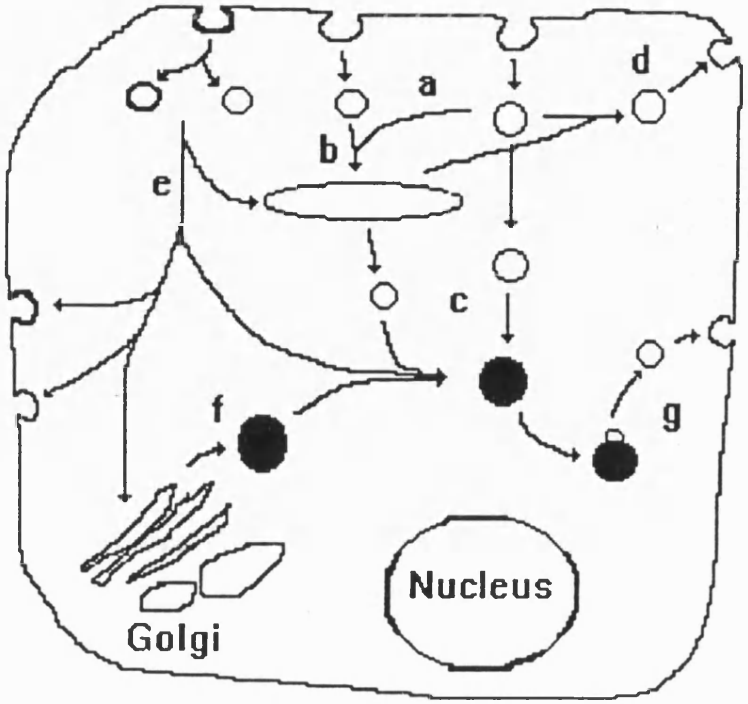

Figure 1.1: A schematic representation of the vesicular pathways of endocytosis. (a) Formation of uncoated vesicles from uncoated pits which may fuse with each other before reaching the early endosomes (b). Vesicles from the endosomes, or directly from invagination of cell membrane, fuse with primary lysosomes to form secondary lysosomes (c). Some vesicles recycle back to the cell membrane (d). Coated regions of the membrane can give rise to vesicles with or without a clathrin coat (e). These either fuse with early endosomes, primary lysosomes, the Golgi complex, or the opposing cell membrane (transcytosis). (f) Vesicles from Golgi complex fuse with primary lysosomes. (g) Vesicles arising from lysosomes may fuse with the plasma membrane.

ligand is not always a prerequisite for triggering this process. Transferrin receptors can concentrate in coated pits in the absence of ligand and become internalised unoccupied [26]. Other receptors (e.g. for EGF and insulin) can be randomly distributed on the plasma membrane in the absence of ligand and will only concentrate in coated-pits and be endocytosed upon binding [27]. Different ligands can be internalised within the same coated pit but divergence of the ligands and/or receptors may occur through intracellular sorting.

In some cases endocytosis may not be required for the physiologic function of ligands e.g. EGF or insulin [28], however internalisation of the ligand-receptor complex may serve to regulate and control the membrane associated signal. Conversely endocytosis of receptor-bound ligands such as transferrin [29] or LDL [30] is essential for their physiologic function.

2. Non-receptor mediated endocytosis can occur without the specific involvement of a membrane receptor. Instead this type of endocytosis is derived from the constant internalisation of plasma membrane to form vesicles containing the trapped extracellular fluid and a portion of cell membrane. Thus extracellular molecules are internalised either in the fluid phase or through non-specific adsorption to the membrane.

1.2.1 Fluid-Phase Endocytosis (Pinocytosis)

This is a constitutive cellular process involving internalisation of plasma membrane and a portion of extracellular fluid. Since it does not require a membrane receptor the amount of uptake is only dependent upon the extracellular concentration of macromolecules and the rate of internalisation. Unlike receptor-mediated endocytosis, it is a non-saturable, non-concentrative and non-specific uptake process.

1.2.2 Adsorptive Endocytosis

This involves the same cellular process as pinocytosis, except macromolecules gain entry by non-specific adsorption to the plasma membrane. The cell surface contains both cationic and anionic sites [31] so macromolecules which express a net electrostatic charge will adsorb readily onto the surface of the membrane. Positively charged macromolecules have a greater affinity towards the cell membrane as the latter contains glycosylated proteins distributed on its outer surface which posess a net negative charge due to an abundance of carbohydrate residues. Also the hydrophobicity of the cell membrane lipid bilayer may accommodate strongly hydrophobic molecules. Unlike pinocytosis, this mode of internalisation is a saturable process due to the limited number of available membrane binding sites.

In order to appreciate the design and cellular processing of drug-conjugates a more detailed understanding of the intracellular organelles involved and their interplay with each other is required.

1.2.3 The Endocytic Vesicular Pathway

Coated and Uncoated Vesicles

Coated regions of the plasma membrane are composed of clathrin and it has been recently demonstrated that the cytoplasmic tail of the LDL and the mannose-6-phosphate receptors will bind to this protein [29]. The position of a tyrosine residue in the tail may be essential for this process [32]. This binding is probably linked to the clustering of receptors into coated pits before the formation of coated vesicles. Once internalised, these vesicles rapidly lose their coat (c.15-60 seconds). The newly formed uncoated vesicles have a half-life of 1-2 minutes and transport the receptor-ligand complexes and solutes to the early endosomes. It should be noted that a controversial issue is still unresolved as to whether fluid-phase uptake

occurs through coated pits or a clathrin independent pathway.

Early Endosomes

Early endosomes are a heterogenous population of vesicles, tubules and vacuoles (0.4-0.7μm in diameter) that receive ligands 2-5 minutes after uptake. They have an internal pH of 6.0-6.2 which is lower than that of the extracellular medium (pH 7.2) but higher than that of lysosomes (pH 5.3) [33]. This acidic milieu is created by vacuolar H^+-ATPase, however the internal pH of early endosomes is not uniform and may be regulated by the presence of Na^+/K^+ ATPase in some endosomes and not others [33]. This pump is electrogenic and increases the vesicular membrane potential that then limits the activity of the H^+-ATPase, although how endosomes acquire the latter is unknown.

Early endosomes have been referred to as CURL (compartment for uncoupling receptor and ligand [34]) as it is the site where membrane and dissociated ligands are sorted to various destinations. Certain receptors, for example those for LDL, asialoglycoprotein and mannose receptors are transported back to the plasma membrane [35]. Fluid that is trapped in these vesicles is also returned to the cell surface (diacytosis). Indeed the majority of the fluid internalised through pinocytosis does undergo diacytosis (see chapter 3). Recycling is thought to occur mainly from the endosomes due to the rapid recycling times (< 5 minutes) inferred for several receptors [36]. Other receptors (e.g. EGF), ligands and solutes are directed to the prelysosomes whilst in polarised epithelial cells some molecules (e.g. polymeric immunoglobulin) are transported to the opposing membrane [23]. Some ligands do not dissociate from their receptors and so may also recycle, e.g. transferrin [37], or be transported to the lysosomes e.g. polyvalent immune complexes [38]. Small amounts of some receptors that escape recycling e.g. the transferrin receptor, are transported to the trans Golgi reticulum.

The mechanism of early endosome sorting is still unresolved but the low pH

appears to account for a basic step in the process, allowing ligands and receptors to dissociate and follow separate pathways [23]. It is generally believed that solutes, ligands and membrane components then follow a non-selective pathway to the lysosomes with only selected membrane receptors being diverted away and recycled to the cell surface. However it was demonstrated recently that three different receptors were recycled to the plasma membrane at identical rates [39], the interpretation of selective sorting may now shift from recycling receptors to those that escape this process, as the former would predict different rates of recycling.

The biogenesis of endosomes is still under debate due to their heterogenous composition and transient nature. Two models for the process have been proposed [40]:

1. The Maturation Model assumes no permanent endosomal membrane components and that uncoated vesicles fuse with one another to form early endosomes. Plasma membrane components are then removed for recycling and lysosomal membrane supplied.

2. The Vesicle Shuttle model simply assumes the delivery of the contents from uncoated vesicles to pre-existing endosomes by fusion.

Although doubt remains over each model, the latter seems the most plausible as if the maturation model was appropiate then uncoated vesicles and endosomes would be expected to display similar properties, but this is not the case.

Prelysosomes

Following sorting in the early endosomes ligands are next observed in prelysosomes which probably mature from the former, but the transport of endocytosed molecules via vacuoles to prelysosomes in a microtuble dependent manner has

been observed. Prelysosomes are thought to be the site where lysosomal enzymes are delivered from the trans Golgi reticulum to the endocytic pathway via the mannose-6-phosphate receptor. However the delivery of prelysosome contents to the lysosomes remains unclear. Another maturation model assumes the vesicle changes with time as the lysosomal enzymes are delivered, whilst a second model proposes the fusion of prelysosomes with lysosomes (which has recently been demonstrated in vitro [41]).

Lysosomes

Lysosomes are generally considered inactive organelles with respect to membrane traffic, being the end-point of the endocytic pathway. But a lysosomal membrane protein has recently been discovered to be slowly transported from the lysosomes to the plasma membrane [42].

Lysosomes are 0.2-0.4μm in size and are composed of a variety of acid-dependent hydrolases capable of degrading most biological macromolecules. Although they are considered the terminal degradative compartment of the endocytic pathway, earlier organelles, e.g. early endosomes, do contain some proteases [43]. However they are not termed lysosomes as they lack the full complement of enzymes. Once within lysosomes endocytosed ligands and tracers are either degraded or reside indefinitely within the organelle, they are not generally released intact into the cytosol.

From the brief description of the endocytic pathway it can be appreciated that many factors can determine the cellular uptake and fate of a macromolecular conjugate, which in turn can dictate subsequent alterations in its design.

1.2.4 Enhancement of Endocytic Uptake Of Macromolecular Conjugates

Interaction of conjugates with the plasma membrane can be altered to enhance uptake via non-specific pathways (i.e. adsorption to the membrane) or through specific interactions with distinct membrane sites.

Non-Specific Carriers

Poly-l-lysine is a good example of carrier-mediated uptake via adsorptive endocytosis due to its net cationic charge. Indeed it can increase the uptake of the fluid-phase marker HRP (horseradish peroxidase) by 1000-fold in cultured mammalian cells [44]. The same principle of non-specific adsorption onto cell membranes is applied to cationised proteins, which after conjugation of di- or polyamine molecules through carboxylic acid residues, have a resultant net positive charge. For example when β-endorphin, a non-transported peptide, was conjugated to cationised albumin, it experienced adsorptive endocytosis into the brain capillary endothelium [45].

The group of glycoproteins referred to as lectins have affinity towards certain carbohydrate and sugar residues on the cell surface. For example when the plant lectin wheat germ agglutin (WGA) binds to sialic acid and N-acetylglucosamine residues on the cell surface, it is internalised via adsorptive endocytosis [46]. Lectins can therefore be used as carriers to increase binding and uptake of other compounds, e.g. WGA linked to HRP increased the uptake of the latter [47].

Finally it should be noted that the uptake of proteins and peptides can be enhanced through increasing their lipophilicity by conjugation with lipophilic molecules. For example fatty acid binding to albumin has been shown to increase transcytosis of the latter across lung capillary endothelium by 2-3 fold over unconjugated protein [48].

Specific Carriers

Targeting to particular cells and tissues can be achieved by using ligand containing carriers which interact with specific receptors on the cell surface, e.g. EGF [49], transferrin [50] and in particular antibodies which have been studied extensively in drug delivery. However from the general overview of the endocytic pathway, many factors of targeting via a membrane bound receptor have to be considered:

1. The number of binding sites per cell.
2. The distribution of binding sites on other (non-target) cells.
3. Does ligand binding induce receptor-mediated internalisation?
4. If the receptor is recycled does the ligand dissociate wthin the cell and if so, is it transported further along the endocytic pathway or is it returned to the cell surface intact with the receptor?
5. How long before re-expression of the receptor on the plasma membrane after internalisation?

In particular the number of receptors per cell will determine the amount of drug required to be associated with each macromolecule. If there are a small number of available receptors then the conjugation ratio of drug to macromolecule will need to be high (unless the cytotoxic agent was very potent, e.g. ricin-A-chain).

1.2.5 Optimisation of Drug Release and/or Carrier Degradation

The major site for enzymatic metabolism of an endocytosed conjugate will be in the lysosomes, although some proteases are present in earlier organelles e.g. early

endosomes [43]. Lysosomal sensitive peptide spacer linkages have been employed between drug and carrier in order to enhance the release of active drug from the conjugate (see chapter 7). Also drug complexes employing carbohydrate linkages, using either the side-chain of a glycoprotein [51] or dextran as a spacer [52], are most likely to be processed by glycosidases present in lysosomes.

Most drug conjugates which release their cytotoxic component once selectively delivered to the lysosomes can be termed as 'lysosomotropic' agents, as defined by De Duve et al. [53]. Some agents which are not lysosomotropic can be converted through the conjugation to a macromolecule, as in many cases for selective-drug delivery.

Organelles of the endocytic pathway are acidified soon after their formation near the cell surface (pH 6.2 for early endosomes) and the pH decreases to about 4.5-5.0 in the lysosomes [33]. This change in enviroment has led to the development of several acid-sensitive linkages [54] for the release of drugs from macromolecular carriers.

Reductive cleavage of disulphide bonds is known to be important in the processing of endocytosed proteins [55], however the molecular mechanisms and the site of action in the internalisation pathway is relatively unknown. Disulphide reduction is required for the activation of several protein toxins, e.g. ricin [56]. Knowledge of this has been utilised in the formation of immunotoxins (toxin-antibody conjugates) where a disulphide linkage between the two components is essential for an active conjugate [57].

It can be clearly observed that knowledge of the endocytic pathway has influenced the development of macromolecular-drug conjugates, in order to improve their efficiency and therapeutic effectiveness.

1.3 Types of Macromolecular Carriers and/or Targeting Agents

1.3.1 Antibodies

The advent of high yield and purity of monoclonal antibodies by the application of hybridoma technology has offered new approaches in the targeting of cytotoxic drugs. Many of these antibodies react with cell surface associated glycoproteins and glycolipids of malignant cells, specificity relying on the sole, or increased expression of these antigens when compared to normal tissue.

Although still in the experimental stage, many antibody conjugates have been studied containing various cytotoxic elements [7, 8], e.g. antibiotics (daunomycin, adriamycin), alkylating agents (trenimon, p-phenylenediamine mustard), plant (saporin, gelonin, ricin, abrin) and bacterial (diphtheria) toxins. Here antibody conjugates containing methotrexate (MTX) will primarily be described in detail as a model example of the design and development of a macromolecular drug-conjugate.

Design and Mode of Action of Antibody Drug Conjugates

The mode of synthesis is very important in order to incorporate as many drug molecules per antibody, whilst maintaining its immunological reactivity. Kulkarni et al. [58] produced MTX conjugates by three different methods, the first via direct ECDI reaction produced unwanted cross-linking between antibodies and resulted in reduced binding activity of the final product. Activation by the initial production of a MTX mixed anhydride before linkage failed to incorporate 2-3 molecules of MTX before a significant decrease in antibody activity. However when an active-ester method was employed 10 molecules of MTX were linked whilst the antibody retained 90% of its immunological activity.

It is generally considered that incorporation of more than 10 drug residues often results in unacceptable loss of antibody reactivity, although in some cases this can be lower [59]. Estimations have suggested that conjugation ratios of this value have limited potential and will prove insufficient in achieving the desired level of toxicity [60]. This has resulted in the use of carriers such as HSA [61] and dextran [62], which can be loaded with drug molecules and then linked to the antibody. Using HSA, incorporation values of 32-96 molecules of MTX per antibody have been achieved [60].

In order to reduce non-specific toxicity in any form of macromolecular drug targeting, linkage of drug to carrier must be stable. This is particulary important when employing carriers like serum albumin which in the case of MTX, will physically bind the drug to some extent [63]. Conjugation of MTX to this protein [64] or directly to antibodies [65] has resulted in unstable complexes which slowly release the drug in solution and so give false toxicity values. When MTX was directly linked to an antibody [65] the cytotoxicity of the conjugate was found to decrease in the presence of thiamine pyrophosphate (a MTX uptake inhibitor [66]), thus implying some of the toxic action was due to free MTX. Hydroxalamine treatment of the conjugate was found to remove the less stable bound MTX and so decrease the non-specific toxicity.

Although some of the MTX-antibody conjugates formed can inhibit the drug's target enzyme, DHFR [58, 65, 67, 68], the proposed route of cellular entry will be via the lysosomal pathway. Evidence to support this includes a decrease in cytotoxicity when in the presence of ammonium chloride [69, 70]. This compound is thought to inhibit lysosomal enzymes by raising their pH optimum [71, 72]. Also the lysosomal protease inhibitor leupeptin has demonstrated partial protection against conjugates [69, 73] indicating that some lysosomal enzymes are involved in the degradation of the conjugates. In view of this Umemoto et al. [69] synthesised a MTX-antibody conjugate containig an oilgopeptide (-Leu-Ala-Leu-Ala-) spacer linkage, which was more cytotoxic than the parent conjugate. To confirm the linkage was being degraded by lysosomes, identical conjugates were synthesised

with poly-d-lysine replacing the antibody. This polymer is totally resisitant to lysosomal attack [74] and non-toxic, however when linked to MTX via the peptide spacer linkage toxicity was observed. Although the cytotoxic action appears to be linked to the endocytic pathway, it has been suggested that internalisation does not occur for all antibody conjugates [75].

The in-vitro growth inhibition and cytotoxic assays for MTX-antibody conjugates display equal or greater potency than free MTX [67, 68, 73], but they tend to be weaker inhibitors of DHFR [67]. This implies an efficient delivery of MTX to the cell cytoplasm via endocytosis or defective membrane transport of MTX. In vivo testing is difficult to interpret due to limitations in experimental design, although some conjugates have revealed promising results with increased effectiveness over free MTX [7, 58].

Antibody-conjugates display good selectivity to antigen expressing cells in vitro [60, 67], with toxicity being related to the degree of antibody binding [60]. Shen et al. [73] effectively blocked the antigen sites on mouse F-9 bearing teratocarcinoma cells with free antibody thereby preventing any internalsation (and toxicity) until after 4 hours. At this point the free antibody had either dissociated or the antigen had recycled.

Limitations of Use

The i.v. injection of radio-labelled antibody results in only a small proportion accumulating in solid tumour deposits [7]. This resides primarily in the periphery of the main tumour and its metastases. Once the antibody is part of a conjugate its biodistribution is likely to be highly altered due to its new size, charge etc. Pimm et al. [76] demonstrated a direct antibody-drug linked conjugate to deliver drug to subcutaneous human xenografts in mice, however the achievable tumour drug concentration was unlikely to be therapeutic. When Garnett et al. [60] employed a MTX-antibody conjugate with HSA as a carrier, it was rapidly cleared

from the circulation of mice by the liver and spleen. It appeared that the overall net negative charge encouraged removal from the vasculature by phagocytes.

A major limitation for antibody and indeed most macromolecular conjugates, is their poor extravasation partly due to their large molecular size (e.g. up to 340,000 Da). This results in insufficient levels being attained in tumour tissue. Extravasation is a highly desirable characteristic for a site-specific drug conjugate in cancer chemotherapy as it would permit exposure of the metastatic tumours mostly responsible for the high fatality associated with this disease. The widespread location and number of these secondary tumours renders conventional therapy with surgery and irradiation virtually useless, thereby leaving chemical therapy practically the only option.

Immunotoxins (antibody conjugates to animal or plant toxins) posess a great advantage due to their high potency (only one toxin molecule generally rquired to cause cell death). In vivo they are rapidly cleared from the blood by the liver (probably due to mannose and fucose residues present in the toxin) which causes further problems due to the release of free antibody [7, 77]. This may then saturate the antigen binding sites preventing any intact immunotoxin from binding. The highly toxic component of these conjugates may prove undesirable if there are low levels of cross-reactivity, i.e. antigen expression, albeit at a low level, on normal tissues.

Various methods have been employed to improve tumour localisation and toxicity, including intracavity administration, enhancement of target antigen expression by interferons and the use of vasoactive agents to increase tumour blood flow [7]. An interesting development has been the production of bi-specific antibodies with dual specificity i.e. one Fab site reacting with tumour antigen, the other with the drug and/or carrier [78]. This would allow the separate administration of both components which would not only allow better tissue penetration, but the antibody retains fully immunoreactive in the process. Using this in vivo conjugation approach Pimm et al. [78] discovered they could deliver up to 40

molecules of MTX per antibody via a carrier.

Another approach for increased drug incorporation has been the use of IgM as opposed to the usual IgG antibodies, the former posessing ten antigen binding sites instead of two. Persiani et al. [79] incorporated 65 molecules of MTX directly to an IgM antibody without a significant decrease in its immunoreactivity. The resulting conjugate was more effective than free MTX during in vivo experiments, but this could be due to it functioning as a slow release form for MTX. The high molecular mass of such a conjugate would however restrict it to the vasculature.

The use of Fab-fragments has resulted in a more rapid passage through the vasculature, but absolute levels achieved in tumours make them less effective targeting agents than whole antibodies [7]. Also lower incorporation values result from fewer lysine residues present and a more rapid decline in immunoreactivity per bound drug molecule [80].

Another potential problem is the heterogeneity in antigen expression among malignant cells, even within a single tumour and its metastases, which will limit the antibody directed localisation e.g. in lung cancers [81], breast carcinoma [82]. This could theoretically be overcome with a mixture or cocktail of antibodies to different antigens, however in order to saturate each individual antigen the amount of antibody would have to be increased resulting in further non-specific binding and immunogenicity problems.

A major drawback to the use of antibody conjugates, besides poor tumour localisation, is the problem of immnuogenicity. Antibodies of mouse or rat origin used for tumour imaging in clinical practice have evoked the production of antibodies to these foreign proteins [83]. If this area of targeting is to succeed the use of human antibodies is advantageous but their production to a wide range of antigens and their immunogenicity will need to be evaluated.

A Macromolecular Conjugate Model

Form this brief overview of antibody conjugate design the basic model for a macromolecular drug complex can be envisaged (figure 1.2). The drug carrier, in this case a polymer, can have three different functional groups attached. The therapeutic agent is usually joined via a covalent linkage either directly or by a spacer moiety (to enhance drug release if related to a steric function i.e. enzyme cleavage). A control device may also be present to maintain the desired overall physiochemical properties of the conjugate, e.g. molecular weight, solubility, hydrophilic/lipophilic balances and electric charge. Finally site specific moieties can be incorporated for guiding or 'homing' the conjugate to the target site.

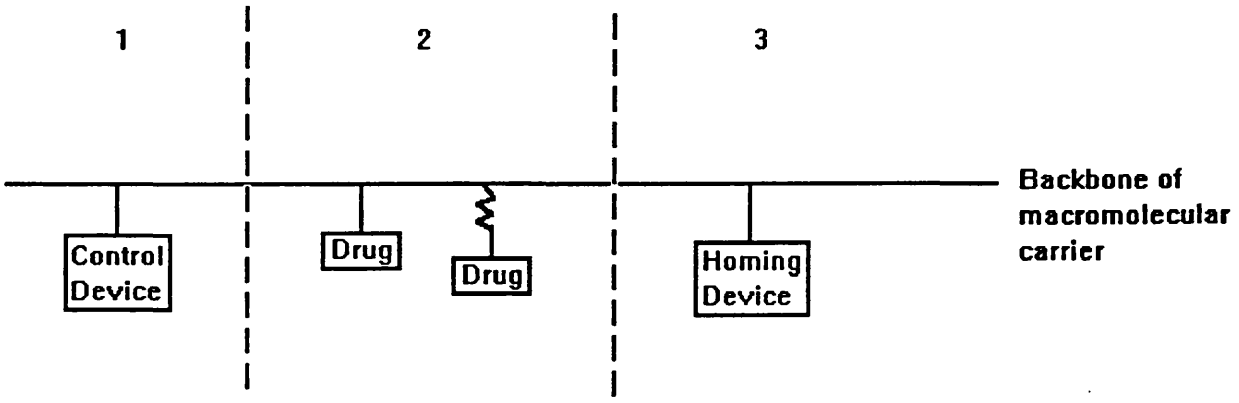

Figure 1.2: A basic model for a macromolecular-drug conjugate. This is composed of three components; a control device for maintaining the overall physicochemical properties of the conjugate (1), a cytotoxic agent covalently linked either directly or via a spacer (2), and a targeting moiety (3).

1.3.2 Albumin and Glycoproteins

Albumin has proved a popular choice of carrier in experimental studies, it offers many advantages including its ready availability in a pure form, good biological

stability, large numbers of free carboxyl and amino-groups for chemical substitution, low toxicity and antigenicity and lastly established properties for cellular interaction and pharmacokinetics. The protein itself lacks intrinsic site-selectivity but specificity has been provided when used as a carrier with antibodies (see previous section).

Conjugation to albumin is generally via covalent bonds, the drug being released by enzymatic cleavage inside the cell. When the two inhibitors of DNA synthesis, 5-fluorodeoxyuridine and cytosine arabioside were linked to albumin [84], both were effective in inhibiting cellular growth. Cleavage of drug from the carrier was inferred to occur inside the cell since the covalent bond present involved the primary hydroxy groups of both drugs which must be phosphorylated before either can exert their pharmacological action.

However the stability of other conjugates has been in doubt, especialy when MTX is used (see previous section). The conjugate of MTX to bovine serum albumin (BSA) was found to be more effective than equivalent doses of free drug when delivered i.p. in reducing the growth of tumours, and the number of subsequent metastases, in female mice implanted subcutaneously with Lewis lung carcinoma [85]. However the same conjugate was found to be relatively ineffective against a MTX transport resistant strain of Reuber hepatoma 1135 cells in vitro [86]. This implied a proportion of the pharmacological action of MTX-BSA was due to the extra-cellular liberation of free MTX with its subsequent uptake across the cell membrane. This underlines the importance of chemical stability when the drug is linked to a carrier.

The use of glycoproteins as drug carriers has been investigated [87], although they display no site selectivity. However when the sialic acid moieties are removed from the terminal sugar branches, the resulting asialoglycoproteins are rapidly recognised and cleared by certain cells of the liver (depending on the sugar group(s) exposed). Therefore glycoproteins can be modified to deliver drugs in a site specific manner e.g. hepatocytes posess receptors for galactosyl-terminated gly-

coconjugates [88] which has resulted in asialofetuin (galactosyl-terminated fetuin) being developed as a hepatocyte-specific drug carrier [89].

Other plasma proteins in addition to albumin have been suggested as carriers of anticancer agents including fibrinogen and globulin [90].

1.3.3 Dextran

The polysaccharide dextran has been used for many years as a plasma expander but has generated much interest as a drug carrier due to the following properties:

1. A well characterised polymeric structure.
2. High water solubility.
3. High stability.
4. Availability of different molecular weight fractions.
5. Presence of numerous reactive hydroxy groups for chemical fixation.
6. Low pharmacological activity and toxicity.
7. Protection of conjugated drugs from biodegradation.

Drugs can be coupled to the hydroxyl groups of dextran by a variety of techniques including periodate oxidation, cyanogen bromide activation and diazotization [14]. This demonstrates the versatility of dextran as a drug carrier.

The antitumour antibiotic mitomycin C was conjugated to dextran of varying molecular weights (10,000, 70,000 and 500,000) [91]. The resulting polycationic conjugates were almost as effective as free drug in growth inhibition of L1210 mouse leukemia cells after continuous exposure (short term acute exposure showed little cytotoxic activity). It was concluded that the conjugates acted as a

prodrug of mitomycin C, exhibiting their activity after release of the drug probably by chemical liberation and not by the lysosomal enzymes. In vivo experiments employed murine models inoculated i.p. with various tumour cell types followed by i.p. drug treatment [92]. Although the conjugate was effective against some tumours in prolonging survival time the relevance of such an in vivo model has to be questioned when the tumour inoculation and subsequent treatment are via the same anatomical compartment. When the conjugate was administered by intravenous injection it displayed only modest activity.

Dextran has also been used as drug-carrier for linkage to antibodies [93] allowing a greater drug to antibody ratio.

1.3.4 Polypeptides

Synthetic polypeptides such as poly-l-lysine, polyaspartic acid and polyglutamic acid have been proposed as drug carriers, in particular the polycationic polypeptide poly-l-lysine. This compound itself has some affinity for specific tumour cells and is capable of arresting their growth [94], furthermore its cellular uptake by endocytosis and susceptibility to degradation by trypsin, enhances its potential use as a drug carrier.

Ryser and Shen [95] conjugated MTX to poly-l-lysine and tested it against a MTX-uptake resistant Chinese Hamster ovary cell line. They discovered enhanced uptake and increased cytotoxicity compared to the free drug or the carrier and drug administered separately. Cell death was caused by the intracellular hydrolysis and subsequent release of free drug. When poly-d-lysine was used as the carrier, the conjugate was internalised but inactive [74]. It was suggested that intracellular enzymes could degrade and release free MTX only from the natural l-isomeric derivative. Thus by conjugating MTX to the polypeptide enabled the drug to enter the cell via an alternative route, thereby overcoming one form of resistance that is characteristic of its treatment.

An identical conjugate was found to express differential toxicities against various tumours in vitro [96], being predominantly more inhibitory to solid tumours. However these effects were not totally reflected in vivo,demonstrating in vitro situations can be misleading. The original antineoplastic activity of poly-l-lysine can complicate the evaluation of results and in fact the limiting factor in the use of MTX-poly-l-lysine conjugates was suggested to be the toxicity of the carrier [97]. In all reports of poly-l-lysine conjugates cytotoxicity only occurred when active free drug was liberated upon lysosomal degradation i.e. the conjugates can be considered lysosomotropic agents.

Polyanionic polypeptides have also been employed as drug-carriers, for example when daunomycin was coupled to poly-l-aspartic acid the conjugate was less effective than free drug in vitro. The situation was reversed in vivo and was attributed to a significant reduction in drug toxicity. The anion charge of these carriers (and the cationic charge of poly-l-lysine) may alter the bio-distribution of conjugated drugs due to the affinity of these charged polymers for any cationic or anionic charges in the body respectively.

1.3.5 Deoxyribonucleic Acid

Site specificity of deoxyribonucleic acid (DNA) is based on the concept of lysosomotropic chemotherapy [53], the drug-carrier complex enters the cell by endocytosis and is transported to the lysosomal compartment. The basis for the site-specificity of DNA is that certain tumour cells exhibit higher endocytic activity than normal cells, plus DNA is a potent inducer of pinocytosis and easily degraded by lysosomal hydrolases [98].

Relatively stable drug-carrier conjugates have been formed between DNA and daunorubicin or adriamycin [99]. Both conjugates displayed equal or increased effectiveness over free drug in animal models. The conjugates were also associated with decreased toxicity as the bio-distribution of the drugs had been altered. In

clinical trials the amount of cardiac toxicity was greatly reduced, this was credited to the fact that the myocardium has little endocytic activity and would therefore not be expected to accumulate the drug-conjugate [100].

The use of DNA drug complexes alone is fairly limited as generally they have to be administered by the same route as the tumour cells in order to be effective [53], otherwise the conjugates become located in non-specific areas, mainly the cells of the reticuloendothelial system.

1.3.6 Synthetic Polymers

Although most macromolecular drug-conjugates employ biological molecules, some synthetic polymers have been studied, in particular poly [N-(2-hydroxypropyl)-methacrylamide] (HMPA). The biological and chemical properties of this hydrophilic polymer have been extensively studied and reviewed [16]. Uptake of HMPA in various tissues occurred slowly via pinocytosis. Modification of the polymer e.g. with targeting residues thus had the potential for delivery to specific cells. When tyrosinamide residues were incorporated an increase in endocytic uptake followed. The increased hydrophobicity of the modified polymer led to increased membrane binding and so adsorptive endocytosis. Cellular delivery was still occurring in a passive, non-specific manner, therefore high levels of drug loading had to be avoided as they were likely to precipitate unwanted carrier-membrane interactions.

Site-specific drug delivery was then attempted through the inclusion of carbohydrate moieties such as glucose, mannose and galactose which are known to be involved in receptor-mediated endocytosis in macrophages and hepatocytes [101, 102]. Polymers containing galactose residues had altered bio-distribution and were cleared from the blood more rapidly than unmodified HMPA. Further studies demonstrated that the galactose-containing polymer was delivered predominantly to the hepatocytes of the liver, whereas with the inclusion of mannose

it was mainly found in the Kupffer cells of the liver. Thus the use of carbohydrate moieties in low molecular weight (c.25,000) HMPA polymers can selectively alter body distribution. Other targeting residues studied included monoclonal antibodies which posed problems in direct conjugation.

Uptake of HMPA polymers by endocytosis resulted in the carrier being exposed to the lysosomes of the cell. Extensive studies with various oligopeptidyl side chains terminating with a drug analogue were performed to optimise the amount and rate of drug release by lysosomal proteases (see chapter 7). Therefore through the inclusion of targeting residues and peptide spacer linkages, HMPA offers the advantage of being tailor-made or modified to suit the tumour line in question.

Other potential soluble synthetic drug carriers include Pyran (divinyl ether-maleic anhydride), polyphosphazenes, poly(ethylene-oxide) and derivatives of poly(methacrylic acid) [103]. A major drawback to their use is their interaction with the body, e.g. heamolytic activity, pyrogenicity, osmotic properties, but in particular immunogenicity. When HMPA was used in five genetically different strains of mice it was not recognised as a foreign molecule, however when oilgopeptide side chains were present immunogenic activity occurred [104, 105]. Whether immunogenicity of synthetic polymers will pose a severe drawback remains to be resolved.

1.3.7 Lectins

Lectins are proteins that agglutinate cells by binding to specific carbohydrate residues which has resulted in their study as drug carriers [12]. They contain the usual functional groups of proteins which has permitted the coupling of various drugs, e.g. daunomycin [106], MTX [107], chlorambucil [107] and toxins such as ricin A-chain [108]. Although the conjugates have proved effective against various tumour types their use is limited to local chemotherapy [109]. Due to the widespread distribution of sugar residues in the body, an injected lectin con-

taining solution remains at the site of injection as there is immediate binding to carbohydrate residues. Also the adverse interactions of lectins [12] with tissues severely limits their use to local chemotherapy e.g. the lectin Concanavalin A has been shown to be cytotoxic to most tissues.

1.3.8 Hormones

As hormones generally exert their effects after binding to specific receptors on their target cells, they have potential for selective drug-delivery. Hormones that have been investigated as drug or toxin carriers include human placental lactogen [110], human chronionic gonadotrophin (hCG) [111] and EGF [112]. They were studied primarily to investigate if the hormones were internalised after binding.

When diphtheria toxin fragment A was conjugated to human placental lactogen the conjugate bound but was non-toxic to cells expressing the hormone receptor. This demonstrates that if a hormone exerts its biological action merely by binding to the cell surface without any subsequent internalistion it is unlikely to be an efficient cell-specific carrier.

Ricin A-chain when conjugated to hCG was toxic to rat Leydig cells expressing the receptors for the β-subunit of hCG but did not affect mouse L-cells which are devoid of these receptors. This demonstrated the in vitro specificity of the hormone binding and subsequent internalisation. The same toxin linked to EGF displayed a toxic effect at a similar concentration range (10^{-9}-10^{-10}M) at which the hormone exerts its biological action. The very high affinity demonstrated by some hormone receptors may permit the advantageous use of hormone conjugates at low concentrations. One such hormone that has received particular attention is MSH (α-melanocyte stimulating hormone), which will be briefly described as it has formed the basis of this study.

α-Melanocyte Stimulating Hormone

This basic tridecapeptide [113] is synthesised by the pars intermedia of the pituitary gland of most vertebrates. In man this region of the gland is only present during foetal growth when large amounts of MSH are found in the pituitary. The hormone shares the same pre-cursor, pro-opiomelanocortin (POMC) as other related peptides or melanotropins. The peptides only become biologically active when they are cleaved from POMC by glycosylation, amidation or acetylation. The predominant form of MSH in man is α-MSH which shares an identical central sequence with β-MSH and ACTH (adrenocorticotrophic hormone), (figure 1.3). It is hardly suprising that these peptides also display some MSH-like activity.

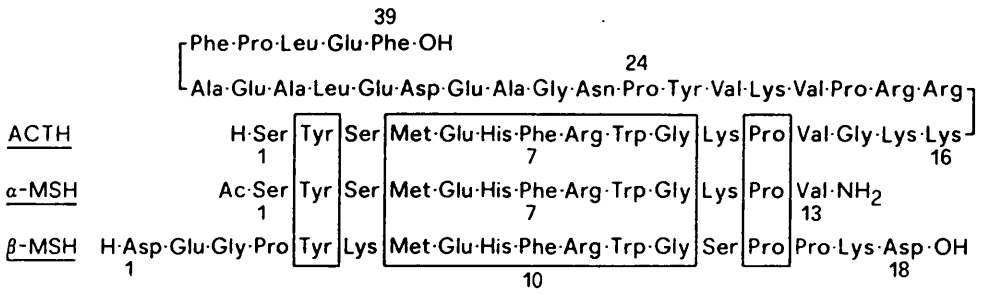

Figure 1.3: The amino acid sequences of αMSH, βMSH and ACTH.

Secretion of the hormone by the pituitary is under the control of the hypothalamus and is subject to circadian rhythm. Various peripheral tissues are MSH sensitive, primarily the skin where melanocytes are situated. Circulating hormone is mainly inactivated by the skin and skeletal muscles as well as the kidneys, liver, lung and intestines. This inactivation is due to enzymatic cleavage primarily by an endopeptidase at Phe^7-Arg^8 in the sequence, followed by exopeptidases causing degradation to free amino acids. The peptide is also synthesised and secreted within the brain, it is considered a neuropeptide with various CNS related ef-

fects on development, adaptive behaviour, learning, neurotransmission and nerve regeneration.

Distribution of the native peptide is not well understood. However when a radiolabelled MSH analogue was injected into B16 melanoma bearing mice, initial uptake occurred in the kidney, liver, spleen, tumour and adrenals. No preferance was displayed for the tumour and transport across the blood-brain barrier was minimal.

The primary effect of MSH in the periphery is related to skin darkening, it stimulates melanogenesis, proliferation and differentation of melanocytes. The complex process of skin pigmentation although well defined in other species, e.g. amphibia, is less well defined in man. Skin darkening is basically caused by cell melanisation by melanin involving the enzymatic (tyrosinase) oxidation of tyrosine to melanin.

The hormone elicits its biological effect by binding to an extracellular receptor since intracellular administration of MSH displayed no response [113]. MSH binding and subsequent signal transduction appears to require extracellular calcium. Binding stimulates adenylate cyclase causing intracellular levels of cAMP to rise, this in turn activates protein kinase(s) and causes protein phosphorylation. It is unknown how the signal caused by MSH binding is terminated, but one or more of three possibilities is thought to occur:

1. Dissociation of MSH from the receptor.
2. Internalisation of the receptor/ligand complex.
3. Inactivation of MSH.

Although at least part of the receptor/ligand complex is known to be internalised [114] its intracellular pathway and localisation is unknown.

MSH binding and subsequent signal transduction appears to require extracellular calcium. Binding stimulates adenylate cyclase causing intracellular levels of

cAMP to rise, this in turn activates protein kinase(s) and causes protein phosphorylation.

The use of MSH as a drug carrier has several advantages in addition to its 'targeting' potential. It is relatively easy to obtain in a pure form, its small size avoids the problems associated with larger conjugates and permits the study of chemical manipulations in the peptide sequence (which has shown identical homology in all mammals so far investigated). Low immunogenicity would be expected due to its natural structural similarity but this may pose the potential problem of cross-recognition of the hormone by different receptors. The sequence homology with other hormones is very close, ACTH has an identical central sequence to α-MSH.

To envisage the use of MSH for selective drug delivery the pertinent characteristics for receptor-mediated endocytosis have to be elucidated (see section 1.2.4). This therefore involves the determination of receptor binding characteristics, kinetics and the subsequent fates of ligand and receptor.

1.4 Therapeutic Agents

Although the use of different cytotoxic agents has been mentioned already ranging from conventional drugs to toxins, it seems logical to employ a well characterised drug in the experimental stage of any conjugate system. If the pharmacological effects of this component are already established (in vitro and in vivo), it permits a more defined interpretation of experimental results with the conjugate form. For these reasons MTX has proved a popular choice for experimental studies.

1.4.1 Methotrexate

Methotrexate (MTX) is a widely used antimetabolite in cancer chemotherapy and its structure consists of three components. A multi-ring pteridine group linked to para-aminobenzoic acid, which in turn is connected to a terminal glutamic acid residue (this displays chirality in its l-form). MTX (4-amino-4-deoxy-N^{10}-methylpteroyl-L-glutamic acid) is a strutural analogue of the natural substrate folic acid (figure 1.4), with a 4-amino group instead of a hydroxyl group on the pteridine ring, and a methyl group at the N^{10} position. Since its synthesis in 1949 [115] MTX has proved an effective antitumour agent and has been well reviewed [116, 117, 118, 119], particulary with respect to its cellular entry, antimetabolic activity, formation of active metabolites and cellular resisitance.

Membrane Transport

MTX is a weak bicarboxylic acid and is essentially ionised and lipid insoluble at physiological pH. The intracellular accumulation of MTX is via a carrier mediated system which has the plasma folate, 5-methyl tetrahydrofolate, as its preferred substrate (reviewed by Sirotnak [120]). Transport of MTX results from the dynamic interplay between two distinct membrane carrier systems, influx displays high affinity for reduced folates and MTX, but low affinity for folic acid. Although the carrier has a high saturability (K_m 3-26μM for MTX), entry of these compounds is mediated by a low capacity process. Uptake is saturable, demonstrates competitive inhibition by structural analogues, is pH and temperature dependent and requires the interaction with specific membrane receptor sites containing sulphydryl groups [121]. Although an energy linked process, the carrier can continue to operate in a 'facilitated' diffusion mode if uncoupled from its energy source [122].

Unlike the entry mechanism, efflux occurs as a first order process with low saturability for folate analogues. The pump appears to be obligately coupled to

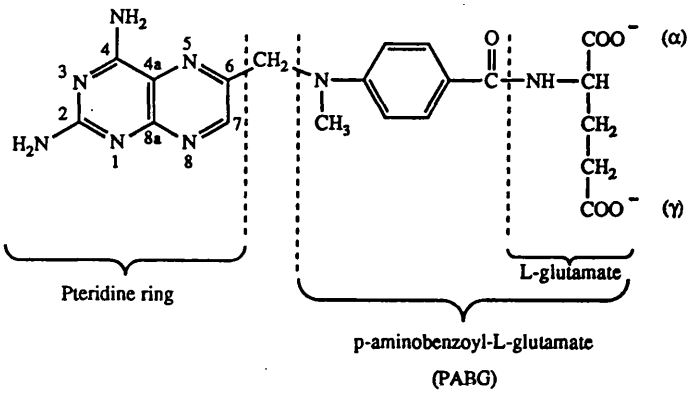

Methotrexate

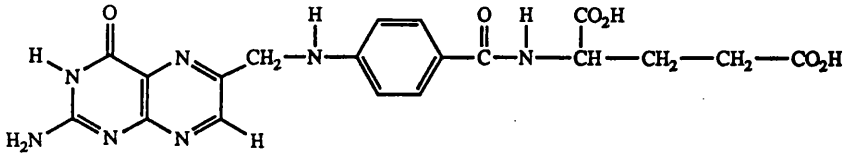

Folic acid

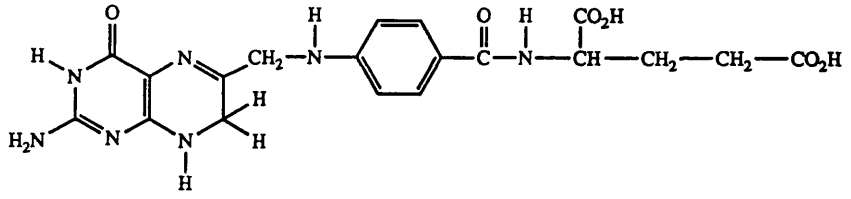

7,8-Dihydrofolate

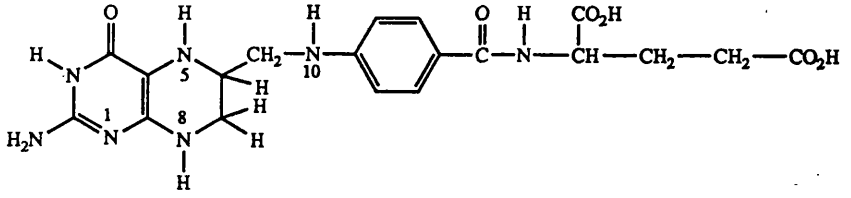

5,6,7,8-Tetrahydrofolate

Figure 1.4: The chemically related structures of MTX, folic acid, 7,8-dihydrofolate and 5,6,7,8-tetrahydrofolate.

metabolic energy [123] and if blocked results in net augmentation of MTX into the cell.

Recently the existence of a second folate membrane binding protein has been observed in cells grown in low folate medium ([124, 125, 126, 66, 127, 128]). It has a very high affinity (K_m < nM) for folic acid over reduced folates, followed by MTX [124, 125, 126], and is capable of accumulating folate such that intracellular concentrations exceed those in the media [129]. The exact transport process is unclear, however it is regulated by the folate content of the cell [129, 130] possibly explaining its late discovery as cells in culture are usually folate replete (due to the high extracellular folate concentrations in the media). Some authors have suggested uptake by this membrane protein via receptor-mediated endocytosis with recycling of the receptor [126, 66, 129, 130, 131, 132, 133].

Mechanism of Action

MTX exerts its cytotoxic action through the competitive inhibition [74, 134] of dihydrofolate reductase (DHFR) due to its structural similarity with the natural substrates (figure 1.5). This enzyme catalyses the NADPH-dependent reduction of folic acid and its 7,8-dihydro- derivative, dihydrofolate (FH_2) to 5,6,7,8-tetrahydrofolate (TH_4).

TH_4 is responsible for at least 17 single carbon transfer reactions which form the building blocks for purine and pyrimidine bases of the nucleic acids, and hence DNA synthesis. One of the most important of these reactions is the conversion of deoxyuridylate (dUMP) to thymidylate (dTMP) by thymidylate synthetase. Here the methylene group of 5,10-methylene-TH_4 (formed enzymatically in the presence of TH_4 and serine) is transferred to the 5-position of the pyrimidine ring of deoxyuridylate. In this process TH_4 is oxidised to FH_2 and DHFR is required to complete the cycle by forming TH_4 again. However TH_4 is not solely used as a 1-carbon fragment source but also as a reductant, thereby being used in

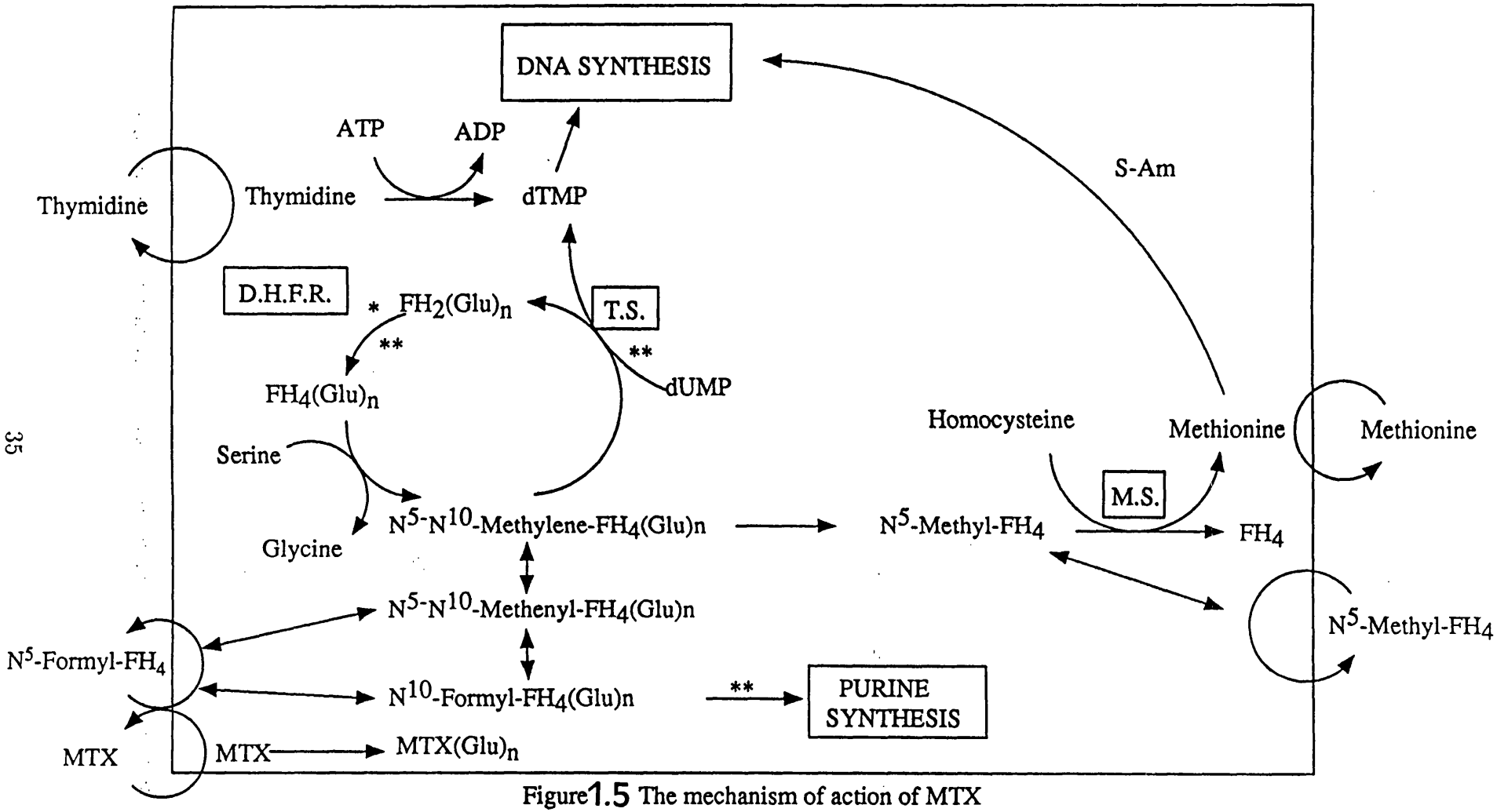

Figure 1.5 The mechanism of action of MTX

* -MTX Block; ** -$MTX(Glu)_n$ Block

D.H.F.R.: Dihydrofolate Reductase, T.S.: Thymidylate Synthetase, FH_4: Tetrahydrofolate

FH_2: Dihydrofolate, S-Am: S-Adenosyl Methionine, Glu: Glutamyl, M.S.: Methionine Synthetase

substrate rather than coenzyme amounts [135]. This exceeds the delivery from exogenous 5-methyl-TH_4 sources and relies upon DHFR to replenish the TH_4 pool. Inhibition of DHFR leads to decrease in the cellular pool of TH_4 derivatives and so a deficiency in thymidylate (thus disrupting nucleic acid production). This method of DNA synthesis disruption is the biochemical mechanism by which antifolates such as MTX exert their cytotoxic action.

The binding of MTX to DHFR, although not irreversible [136] results in a build-up of FH_2 behind the block [137]. The FH_2 then interacts with unoccupied enzyme to an extent proportional to its increased concentration. For this reason, 95% of the intracellular DHFR activity has to be inhibited to achieve an appreciable reduction in cell growth [138]. Inhibition of DHFR is thereby determined by the levels of free intracellular MTX which are dependant on the extracellular drug concentration and the membrane transport system.

In humans MTX appears to inhibit DNA synthesis to a greater extent than RNA synthesis, suggesting that inhibition of thymidylate synthesis is the most important mechanism of MTX cytotoxicity [139]. The drug is thus highly cell-cycle dependant, so those tissues undergoing rapid cellular turnover with a high fraction of cells in cycle are the most susceptible to the cytocidal effects.

Metabolism of MTX

Folates exist primarily in the cell with 5-7 extra glutamyl residues added via the γ-carboxyl of the terminal glutamate residue [140]. These derivatives, formed by folate polyglutamate synthetase in the cell cytosol, are actually the preferred substrates of DHFR [141]. MTX is also a substrate for this enzyme [142, 143, 144], the polyglutamates being formed having equal or even greater affinity for DHFR than the unaltered drug [145, 146]. They also dissociate at a much reduced rate making themselves less reversible inhibitors than MTX, they are also direct inhibitors of thymidylate synthetase [137] and aminomidazolecarboxamide

ribonucleotide transformylase [147], the latter involved in de novo purine synthesis.

Once formed intracellulary, polyglutamates exit the cell much more slowly than the parent compound, the extent of their retention being dependent on the cell type and the glutamyl chain length [148, 149]. This indicates that the MTX polyglutamates play an important role in the overall pharmacological effects of the native drug. MTX is also oxidised in the liver by aldehyde-oxidase to 7-hydroxy-MTX, although reviewed [147], it will not be considered in this report.

Resistance to MTX

From the studies of experimental resistance to MTX, cells may display one or more of the following changes:

1. **Decreased Membrane Transport**

   This represents a frequent basis for resisitance both in cultured human and murine cell lines [150, 151, 152]. This may arise for a number of reasons, e.g. a reduced affinity of the binding protein for MTX, a diminished number of the former, or even a decrease in the rate of its translocation.

2. **Decreased Affinity of DHFR for MTX**

   This has been demonstrated in murine and human models [153, 154, 155, 156] and the altered DHFR may have a 2.5-270 fold decreased affinity for MTX [155, 157].

3. **Increased Levels of DHFR**

   This can occur through the process of gene amplification leading to the over production of the target enzyme (reviewed [158]). In the experimental situation, large increases in DHFR can be induced by long-term incubation with increasing amounts of MTX [159].

4. **Decreased Polyglutamation**

   There is only preliminary evidence of this type of resistance to date, a mechanism has been described in human breast cancer cell line [160], and a similar situation with leukemic cells where resistance was thought to occur by an alteration in folypolyglutamate synthetase [161].

5. **Thymidylate Synthetase Activity**

   Low rates of thymidylate synthesis make cells less susceptible to MTX [162] as their demand for reduced folates is decreased.

Clinical Use and Toxicity of MTX

The antineoplastic activity of this drug is used (often in combination therapy) against a variety of tumours including acute (non) lymphocyte leukemia, breast carcinoma, ovarian cancer, osteocarcinoma, head and neck carcinomas and small cell-lung carcinoma [117]. MTX is also used as an immunosuppressive in the complication of 'graft versus host disease' in allogeneic bone marrow transplant [163], and in the treatment of inflammatory diseases e.g. rheumatoid arthritis.

MTX exerts its toxicity primarily on growing, self-renewing tissues, mainly the bone marrow and the gastrointestinal system [119].

MTX Use in Site-Specific Drug Delivery

Throughout this brief review of site-specific drug delivery conjugates utilising MTX as the cytotoxic component has often been quoted to emphasise its widespread use in this field. Its well characterised pharmacological action and physiochemical properties makes it an ideal choice in the experimental stage of conjugate development, although it does posess some disadvantages e.g. some weak, non-covalent bonds when conjugated to proteins and peptides (see section 1.3.1). However in the clinical situation it is envisaged that MTX will be superseeded

by a more potent drug moiety. It has been estimated that at least one million molecules of MTX are required to achieve cell death which would demand high drug incorporation ratios into a conjugate or a very efficient mode of cell uptake and drug release. A more potent compound would ease these demanding limitations.

1.5 Summary

The development of macromolecular drug conjugates can be established depending upon the disease state in question. Most work has involved cancer chemotherapy with limited success in vivo. The design of these conjugates has to be based on the characteristics of the tumour cells (e.g. cell type, localisation), the physiochemical properties of the drug employed and their interaction depending upon the (un)modified carrier. The success of these 'tailor-made' complexes will be linked to their pharmacological and physiochemical properties plus their degree of specificity. Therefore the field of site-specific drug delivery involves a multidisciplinary approach.

1.6 Overview

In order to assess the cellular interactions of a macromolecular conjugate the binding characteristics and fate of the individual components must be evaluated before using the entire complex. As already emphasised, the fate of a targeting moiety alone will partly predetermine its potential use, i.e. it should ideally be readily internalised and display minimal cross-reactive binding. Non-specific uptake processes also need to be assessed in order to estimate the degree of toxicity to non-targeted cells. This entails investigating any cellular binding due to the carrier and drug molecules of the conjugate, plus an evaluation of non-selective pinocytic uptake by cells.

The conjugate system under investigation in this study employed an analogue of the hormone αMSH as a potential targeting group and MTX as the cytotoxic component, the two were then linked in a ratio of 1:1. The binding and uptake characteristics of the individual components on B16 murine melanoma cells was studied with the use of radio-isotopes before being compared to their conjugate forms. The non-specific process of pinocytosis was also assessed for this tumour cell line and two others in order to ascertain the importance of this non-selective entry route into the cell.

Finally toxicity was studied by investigating the release of active fragments from the lysosomal degradation of the conjugate in vitro through the inhibition of DHFR, the target enzyme for MTX. The assumption was that if the conjugate gained cell entry through the endocytic pathway it would eventually reside in the lysosomal compartment.

Chapter 2

Materials and Methods

2.1 Cell Culture

Cell Lines

Three different transformed cell lines were employed, studies with B16 murine melanomas formed the majority of the cell-culture based work. The two other cell lines were of human origin, HMB-2 melanoma cells and SVK-14 keratinocytes. The B16 and SVK-14 cells were propagated in RPMI 1640 medium, whilst HMB-2 cells utilised DMEM.

2.1.1 Solutions

Water

All water employed in the preparation of cell culture media and solutions was freshly double glass distilled by a bi-distillation Fistreem still (Fisons Ltd) fitted with a Fistreem predionizer (Fisons Ltd).

Balanced Salt Solution

Phosphate buffered saline (PBS) (without calcium and magnesium) was obtained from Oxoid Ltd in a tablet form. Ten tablets were dissolved in 1L of freshly double distilled water and divided into 125ml Flow bottles before being sterilized and stored at 4^0C.

Base Solutions

Both sodium bicarbonate (7.5% $^w/_v$) and sodium hydroxide (2M), from BDH Chemicals, were prepared with double distilled water, sterilized and stored at room temperature.

Ethylenediaminetetraacetic Acid (EDTA)

A 0.02% $^w/_v$ EDTA solution prepared with sterile PBS was passed through a 0.2μm diameter filter and 20ml fractions aliquoted into sterile universals (Sterilin Ltd). These were stored at -20^0C until required.

Trypan Blue

The stain, obtained from Sigma Ltd, was stored at room temperature as a 0.4% solution in PBS.

Growth Media and Components

RPMI 1640 (Flow Laboratories) and DMEM (Gibco Ltd) were both obtained as 10x liquid concentrates containing phenol red indicator but deficient in l-glutamine and sodium bicarbonate. The following media supplements were all

obtained sterile from Flow Laboratories, l-glutamine (200mM), an antibiotic solution (pen/strep) of penicillin (5000 IU/ml) and streptomycin (5000μg/ml), and non-essential amino acids (NEAA). Growth media and NEAA were stored at 4^{0}C whilst l-glutamine and pen/strep were kept frozen at -20^{0}C.

Foetal calf serum (FCS) from Flow Laboratories was batch-tested for the support of cell growth supplemented at 10% $^v/_v$ to normal growth medium. Maximum growth occurred with batch number 9130102 which was used throughout the work. Serum arrived in 500 ml bottles and was stored at -20^{0}C.

Cell growth media was aseptically prepared from sterile components according to the following recipe, stored at 4^{0}C and used within two weeks:

	RPMI 1640	DMEM
10x Media	50 ml	50 ml
Water	421.5 ml	410 ml
l-Glutamine	5 ml	5 ml
Pen/Strep	5 ml	5 ml
NEAA	5 ml	5 ml
$NaHCO_3$	13.5 ml	25 ml
FCS	55.6 ml	55.6 ml

Both media required a small addition (c.1ml) of sterile 2M NaOH (BDH Chemicals) to attain a final pH of 7.2-7.4.

Autoclave labile solutions were sterilized in small volumes by membrane filtration using sterile 0.2μm filters from Gelman Sciences. All other solutions were sterilized in an autoclave (British Sterilizer Co. Ltd, Swingclave Type SFT-LAB) at 121^{0}C for 15 minutes.

2.1.2 Equipment

All manipulations involving the mammalian cell lines were performed in a vertical recirculating laminar flow cabinet (MDH Ltd). Experimental protocols not requiring sterile technique were performed at the bench.

A LEEC PF2 anhydric incubator (Laboratory and Engineering Company) with forced air circulation was used with thermostatic controls adjusted to give a temperature of 37^0C for culture incubation. It was regularly checked with a digital thermometer with a thermocouple probe (Jenway Ltd).

All cells were stored in 2ml ampoules shelved in the vapour phase of a Union Carbide LR-40 liquid nitrogen refrigerator at approximately -148^0C.

An inverted biological microscope WILD M40 (Wild Heerbrugg Ltd) was used for the examination of growing cell cultures and haemocytometer counting (a standard double grid haemocytometer (Fisons Ltd) was used throughout).

Sterile tissue culture flasks (25, 75 and 150cm^2 in size) were regularly obtained from Flow Laboratories or Sterilin Ltd. Tissue culture tubes, 100x16mm with screw caps and 30ml screw capped universal containers were also obtained sterile from Sterilin Ltd. Polypropylene 2ml ampoules with screw-caps used for the storage of cells in the vapour phase of liquid nitrogen were obtained sterile from J. Bibby Sciences.

2.1.3 Cell Culture Methods

Preparation of Glassware and Non-Glassware Items

All recycled items were rinsed in tap water immediately after use and then processed as follows. Glassware was soaked in a 2% solution of RBS 25 (Fisons Ltd) at approximately 40^0C for 30 minutes, then thoroughly cleaned using a nylon

brush. Articles were subsequently rinsed in three changes of tap water, leaving for 30 minutes in the last rinse. The process was then repeated using single distilled water. Finally all glassware was left to stand in a large volume of freshly collected double distilled water for no longer than 1 hour. After drying in a hot air oven (Gallenkamp) all items were capped with aluminium foil and sterilized by dry heat at 160^{0}C (Gallenkamp Sterilising Oven) for a minimum of 1 hour.

Non-glass items, mainly tips for replicating pipettes, bottle caps and syringes were rinsed immediately after use and then cleaned by boiling in three changes of fresh distilled water. Finally they were rinsed and left for 1 hour in a large volume of freshly double distilled water, dried, sealed in autoclave bags (DRG Hospital Supplies) and sterilized in an autoclave (Drayton Castle Laboratory Steriliser) at 121^{0}C for 15 minutes.

Cell Line Sub-Culture

Sub-culture was undertaken when the cells had reached confluency and the growth rate had almost ceased. In this state the cells completely covered the floor of the tissue culture flask and further growth was limited by contact-inhibition and the availability of nutrients in the media (the latter turned orange/yellow in appearance the longer cells remained confluent). At this point the culture was subject to a sub-culture routine which involved removing a fraction of the cells and seeding them into a new flask with fresh media.

Initially the existing culture was optically examined to ensure the cells were healthy in appearance with no free-floating cellular debris or any signs of contamination. At the laminar flow cabinet the old media was then decanted off before the culture received two 5ml washes of pre-warmed PBS (37^{0}C) and was gently agitated to ensure the cell monolayer was entirely rinsed during each wash. The flask was then incubated at 37^{0}C containing 2ml of pre-warmed 0.025% EDTA for 10 minutes.

Upon removal from incubation the flask was gently agitated to dislodge the cells from the surface of the plastic before the addition of 5ml of fresh media. Using a sterile plugged pasteur pippette, the cell suspension was gently aspirated and transferred to a sterile test-tube in order for the cell density to be determined. A new 150cm^2 tissue culture flask containing 45ml of pre-warmed media was then innoculated with a known number of cells and purged with 5% CO_2 in air (BOC Special Gases) for 20 seconds before the cap was tightly sealed. The culture was then gently dispersed by agitation and placed in a dark, 37^{0}C enviroment until confluent.

B16 cells were sub-cultured three times a week in order to maintain the culture in an active state of growth i.e. confluency was never fully achieved. This was attained by seeding new cultures on a Monday and Wednesday with 4.5x10^{6}cells, and on a Friday with 3.0x10^{6}cells. Other cell lines employed were maintained in a similar state of growth.

Determination of Cell Density and Cell Viability

Cells prepared in a suspension form were thoroughly mixed and a small volume removed from just below the fluid surface with a pasteur pipette before being loaded into a haemocytometer chamber under a coverslip. Each chamber was divided into nine large squares by triple white lines, the four corner squares being further sub-divided into 16 squares per corner. A total count was made on eight large squares of the haemocytometer grid (using a double chambered haemocytometer) with an inverted microscope.

If cell clumping was observed the count was abandoned and the cell suspension further aspirated before a new sample was taken. If the cell density was greater than 150 per large square then counting became impeded by over-crowding and the original cell susupension was diluted accordingly before a new count. Conversely if a low count was observed ($<$ 25 cells per large square) the cell suspension

was concentrated by centrifugation (1000g for 5 minutes).

Each large square had an area of $1mm^2$, when the coverslip was pressed down such that interferance patterns appeared, the depth of the chamber was 0.1mm. The total volume of each square was therefore:

$$1 \times 1 \times 0.1 = 0.1mm^3 = 0.0001cm^3 = 10^{-4}ml$$

The total count per ml, i.e. cell density, was given by 10^4n, where n is the average number of cells per large square.

Cell viability could also be determined during a haemocytometer count with the use of trypan blue. Viable cells exclude the dye whilst non-viable cells are stained a dark blue, a cell density count would include the former only.

This procedure involved mixing 0.2ml of cell suspension with 0.3ml PBS and 0.5ml of 0.4% trypan blue (Sigma Ltd) and allowed to stand for 10-15 minutes (any longer involved the loss of viable cells). A dilution factor of 1 in 5 had to be considered due to the mixture.

Cell Storage

All cells were routinely stored frozen in the vapour phase of liquid nitrogen, in the presence of a cryoprotectant (10% dimethyl sulphoxide, DMSO). Cells were required to be in an active state of growth for storage, hence cells ready for routine sub-culture were suitable. Cell suspensions were prepared from the monolayer state and centrifuged at 1000g for 5 minutes (Jouan B3-11 bench centrifuge). The supernatant was removed and the cell pellet resuspended in a volume of filter-sterilised growth media containing 10% DMSO to attain a final cell density of $2x10^6$cells/ml. Replicate volumes of 1ml were placed in 2ml polypropylene ampoules (J.Bibby Sciences) and a maximum of eight were placed in a Union

Carbide BF6 biological freezer unit plug in the top of a Union Carbide LR 33-10 liquid nitrogen refrigerator. Here the cells cooled to below -70^{0}C in the vapour of the liquid nitrogen at a rate of about 1^{0}C/minute before being rapidly transferred to a liquid nitrogen freezer (Union Carbide LR-40) for long term storage.

Recovery of Cells from Storage

Immediately upon removing an ampoule from storage it was placed in a 37^{0}C waterbath until completely thawed and then swabbed in 70% ethanol (care was taken to ensure the ampoule was not completely immersed above the screw-cap lid). The contents were aseptically removed and diluted in 9ml of normal growth media before being centrifuged at 1000g for 5 minutes. The supernatant was removed and the cells resuspended in 3ml of growth medium before being transferred to a culture flask containing 40ml of pre-warmed medium. After 2-3 days the cells had formed a monolayer suitable for routine sub-culture.

Preparation of B16 Cells in Multi-Well Plates

Many experiments employed B16 cells grown in multi-well plates that had just attained confluency. The cell density was determined for a cell suspension from routine sub-culture before 12-well plates (2.4x1.7cm, Flow Laboratories) were innoculated with 0.6x10^5 viable cells per well plus growth medium to reach a final volume of 1ml in each well. A maximum of eight plates were then placed in a rigid clear polystyrene 3.25 litre box (Gallenkamp) containing a small beaker of sterile water, the box sealed with gas tight vinyl tape (Intech Tapes Ltd) and incubated at 37^{0}C in the dark. After seven days the cells were ready for experimental use.

2.2 Cellular Uptake of Iodinated Polyvinyl-Pyrrolidone (PVP)

It was decided from the outset to employ a cell-suspension technique rather than to use cell monolayers. The latter method can give rise to apparent non-cellular uptake due to entrapment in extracellular spaces. The first attempt was a shake-flask method. $5x10^6$cells were suspended in 5ml of serum free medium contained in a cotton-wool stoppered flat-bottom flask. The suspensions were agitated in a shaking water bath at 37^0C. Cell clumps began to form after 15 minutes so the method was abandoned in favour of the current method described below.

The uptake of ^{125}I-PVP (ICN Radiochemicals Ltd.) was measured in three cell lines, B16 mouse melanomas, HMB-2 human melanomas and SVK-14 human keratinocytes. A cell suspension from one of the lines was prepared using three pre-confluent 150cm^2 culture flasks (four flasks with SVK-14 cells) and centrifuged at 100g for 5 minutes. The supernatant was discarded and the cell pellet re-suspended in 4.5ml of growth media before the cell density and viability were determined. A volume of 4.1ml of cell suspension was subsequently transferred to a glass test-tube and incubated in a 37^0C waterbath. Cells were held in suspension by a glass paddle being rotated at approximately 70-90 rpm by a Gallenkamp motor.

After one hour 0.9ml of pre-warmed media containing c.1.8 million cpm/ml of ^{125}I-PVP was supplemented to the suspension, this point being time zero. At desired time points 0.5ml of the suspension was removed and diluted with 4.5ml of ice-cold media devoid of FCS but containing 1mg/ml of unlabelled PVP (in order to minimise non-specific binding of the radio-label to the plastic [164]). The sample was then centrifuged at 100g for 1 minute at 0^0C before the supernatant was removed and retained for assessment of radioactivity. The cells were resuspended in 5ml of identical fresh ice-cold media and recentrifuged. Each of the nine samples received five centrifugation washes, the cell pellet from the

final wash being resuspended in 1ml of media and the activity assayed (along with the supernatants of each wash) using a gamma-counter (LKB Wallac 1277 Gammamaster).

A control experiment in the absence of radio-labelled PVP revealed no appreciable decrease in cell viability during the 37^{0}C incubation or the centrifugation washes.

2.3 Interaction of Tritiated Methotrexate with B16 Cells

Tritiated Methotrexate (^{3}H-MTX) was obtained from Sigma Chemical Co. and stored in a diluted form with 160mM Hepes buffer (pH 7.4) at -20^{0}C. Cyanamid UK Ltd supplied the unlabelled drug which was prepared fresh in solution with an identical buffer immediately before use. All binding and uptake experiments hereafter employing radioligands used a 160mM Hepes buffer (Calbiochem) adjusted to pH 7.4 with 1M HCl.

2.3.1 Binding of ^{3}H-MTX at 4^{0}C

Media from 12-well plates containing cell monolayers (see section 2.1.3) was removed by vacuum and each well received one 3ml PBS (4^{0}C) wash. Ice-cold incubation buffer (1ml/well) was supplemented to each plate and incubated at 4^{0}C for 30 minutes unless otherwise stated. Incubation buffer consisted of 160mM Hepes containing either ^{3}H-MTX and/or an excess of unlabelled MTX (100μM). At high concentrations of MTX insufficient labelled compound was available, instead ^{3}H-MTX was mixed with a known amount of 'cold' MTX and a dilution factor taken into consideration (this assumed equal binding affinities of the two compounds).

When the 4^0C incubation was terminated, binding buffer was removed by pipette and each well received 3x3ml ice-cold PBS washes. At this point if an acid-wash was employed desired wells received 0.5ml of citrate buffer (pH 2.5) for 5 minutes at 4^0C after which the citrate buffer was removed and the well exposed to a 1ml PBS wash. Cells were then digested with 1ml of 1M NaOH per well and transferred to scintillation vials containing 1ml of 1M HCl. Vials were supplemented with 8ml Optiphase (from LKB Scintillation Products) scintillation fluid. Vials were then thoroughly mixed and left overnight before being counted on a beta-counter (LKB Wallac 1215 Rackbeta liquid scintillation counter).

The PBS and acid-wash routine, plus the cell monolayer digestion with NaOH was standard for all experiments employing radiolabelled compounds. The acid-wash buffer consisited of 21.01g of citric acid.$1H_2O$, 5.43g of NaCl and 23.44ml of 1M NaOH made up to 1L with distilled water.

The cell density per well for this type of experiment was determined from a single plate exposed to the experimental procedure but in the absence of radioligand. Cells were detached with a 0.025% EDTA solution.

2.3.2 Binding and Uptake of ^{3}H-MTX at 37^0C

The experimental protocol was essentially identical to that at 4^0C, except the cells were initially washed with 3ml of pre-warmed (37^0C) PBS before incubation with the radio-ligand (incubation buffer was also pre-warmed before use). Plates were incubated at 37^0C until removed and subjected to the standard PBS and acid-wash protocol.

2.3.3 Inhibition of ^{3}H-MTX Binding (4^{0}C) by NLDP-MSH-MTX

These experiments was performed in order to investigate the binding inhibition by the conjugate against a fixed concentration of ^{3}H-MTX (25nM). Cells grown for 7 days were washed with ice-cold PBS and incubated with 1 ml of Hepes binding buffer containing 200nM NLDP-MSH (to minimise binding of the conjugate due to the NLDP-MSH moiety) and 0.2% BSA for 1 hour at 4^{0}C. A further volume of 0.11ml was then supplemented to each well containing labelled and/or unlabelled MTX plus increasing concentrations of the conjugate. This was incubated for a further 1 hour at 4^{0}C before plates were washed and the activity assayed by the standard procedure. Two 12-well plates contained labelled and/or unlabelled MTX only (total and non-specific binding respectively).

Two 'forms' of NLDP-MSH-MTX were used corresponding to two peaks from the HPLC purification of the conjugation reaction, probably corresponding to linkage via the α or γ carboxyl groups of the MTX glutamyl moiety (see chapter 6).

2.4 Interaction of ^{125}I-Nleu^{4}-DPhe^{7}-αMSH with B16 Murine Melanoma

2.4.1 Synthesis of Nleu^{4}-DPhe^{7}-αMSH (NLDP-MSH)

The synthesis of the peptide and its conjugate with MTX was performed by Dr G. W. Olivier, therefore the protocol for their manufacture will not be described in full. Peptides were prepared by solid-phase synthesis using the Fmoc strategy as developed by Atherton and Sheppard [165]. The peptides were prepared as their carboxyamide forms using the AM-linker on Pepsyn K resin. All the amino-acid reagents were used as their pentafluorophenyl esters with the

exception of serine in which the 3,4-dihydro-4-oxobenzotriazin-3-yl ester was employed, and Fmoc-DPhe-OH which was treated with DIC and HOBT to form its HOBT active ester in situ. Side chains were protected as follows: Arginine, methoxytrimethylbenzene-sulphonyl (Mtr); Glutamic acid, t-butoxy (OBut); Histidine, t-butoxy-carbonyl (Boc); Lysine, (Boc); Serine, t-butyl (But); Tyrosine (But). A four-fold molar excess of reagents was used in all instances.

Deprotection and cleavage was performed using 2% EDT, 2% anisole and 1% water in TFA for 8 hours at room temperature. Peptide was purified using semi-preparative HPLC employing a gradient elution of 0.1% TFA in water and 0.1% TFA in acetonitrile:water (70:30) at a flow rate of 3ml/minute. The eluent was continuously monitored by UV spectrophotometry at 217nm. Fractions were collected in 1.5ml aliquots and each fraction was tested by analytical scale HPLC. Fractions were bulked according to their chromatographic profile and freeze-dried. Identity was confirmed by co-chromatography with authentic [Nleu^4, DPhe^7]αMSH (Sigma Chemical Co.) and by FAB-MS. Prior to experiments the peptide was prepared at a stock concentration of 1mg/ml in sterile 0.1mM HCl and stored at 4^0C.

2.4.2 Synthesis of Nα-MTX-[Nleu^4,DPhe^7]-αMSH (NLDP-MSH-MTX)

The peptide conjugate was prepared by addition of NHS-MTX in DMF to 300mg of the resin after deprotection of the N-terminus. The target peptide was obtained after deprotection and cleavage of the petidyl resin and HPLC purification using the same conditions as for the NLDP-MSH analogue. Identity was confirmed by FAB-MS.

2.4.3 Iodination of NLDP-MSH

The peptide was iodinated at the tyrosine residue (position 2) using a procedure based on the protocol described by Eberle [113]. The following stock solutions were routinely prepared and stored at 4^0C:

1. 0.25M Na_2HPO_4 in H_2O.
2. 0.25M NaH_2PO_4 in H_2O.
3. 1% TFA (trifluoroacetic acid) in H_2O.
4. 50, 60 and 80% methanol with 1% TFA.

The following solutions were prepared daily prior to each iodination:

1. 0.25M phosphate buffer (PB), pH 7.4 (from Na_2HPO_4 and NaH_2PO_4 stock solutions).
2. 0.25% BSA in 0.25M PB.
3. 1% Polypep in 0.25M PB.
4. 0.1% Chloramine T (BDH Chemicals Ltd) in H_2O (dissolved immediately prior to use).

Initial iodinated peptide was purified with a C18 reverse-phase column with Spherisorb ODS 'Bond Elut' (Analytical International, MFG Code OH53). The column was prepared and conditioned by receiving the following wash routine (each wash being 1ml):

1. 3x1% TFA.
2. 3x80% methanol/1% TFA.

3. 1x1% Polypep.

4. 3x80% methanol/1% TFA.

5. 3x1% TFA.

A 1.5ml eppindorf containing 20μl of 0.25M PB and 1.5μl of peptide (from a 1mg/ml stock) was transferred to a radioactive fume hood for the addition of 1.5mCi of ^{125}INa. This was followed by 10μl of freshly prepared 0.1% Chloramine T which marked the start of the reaction. After 30 seconds 0.6ml of 0.25% BSA was added to the eppindorf to halt the reaction. The entire contents were then loaded onto the pre-conditioned C18 column which received the following 1ml washes:

1. 2x0.25M PB.

2. 4x50% methanol/1% TFA.

3. 2x60% methanol/1% TFA.

The last two sets of washes were saved (6ml in total) and the peptide was further purified by HPLC using a C18 reverse-phase wide pore (300Å) column, 25cm in length and 4.6mm in diameter. The methanolic wash was loaded onto the column which was run with an exponential gradient starting at 95% A, 5% B and after 55 minutes reaching 40% A, 60% B before returning to the original values. The solvents were 0.1% TFA in water (A) and 70% acetonitrile/0.1% TFA (B). A UV detector was employed at 217nm. Ten 1 ml fractions were collected after 28 minutes (flow rate 1ml/minute) and their activity assayed on a gamma counter.

2.4.4 Iodination of NLDP-MSH-MTX

The iodination procedure was identical to that for the unconjugated peptide except 5μl of NLDP-MSH-MTX stock (1mg/ml) was used, the reaction time with Chloramine T was extended to 5 minutes and the washings of the C18 pre-conditioned reverse-phase column once loaded with the reaction products were altered to:

1. 2x1ml 0.25M PB.
2. 2x1ml 40% methanol/1% TFA.
3. 2x1ml 50% methanol/1% TFA.
4. 2x1ml 60% methanol/1% TFA.

The remaining 2ml from the 60% methanol/1% TFA wash was retained and further purified by analytical HPLC. The chromophore of MTX permitted increased UV detection of the peptide conjugate with a change in the wavelength from 217nm to 300nm, whereas NLDP-MSH has a poor UV absorbance.

2.4.5 Binding Isotherm of ^{125}I-NLDP-MSH on B16 Cells

The 4^{0}C binding experiments, and all subsequent work with ^{125}I-NLDP-MSH and B16 cells involved the 7 day growth of the latter in 12-well tissue culture plates as previously described. The structure of the protocols were similar to those employed for tritiated MTX.

Media was removed from confluent plates and each well received a 3ml ice-cold PBS wash. Plates were then incubated at 4^{0}C with 0.5ml/well of binding buffer (160mM Hepes, 0.2% BSA and 0.3mM 1,10-phenanthroline) supplemented with ^{125}I-NLDP-MSH with or without an excess (1μM) of unlabelled NLDP-MSH.

A standard incubation period of 8 hours was employed (unless otherwise stated) for each binding isotherm which was terminated by the standard PBS wash procedure. Cell-monolayers were digested as previously mentioned with 1M NaOH and the 1ml solution transferred to counting tubes and the activity assayed with a gamma counter.

2.4.6 Uptake of ^{125}I-NLDP-MSH at 37^{0}C

Medium was removed from the plates and each well washed with 3ml of PBS (37^{0}C) before being supplemented with 0.5ml of pre-warmed binding buffer and incubated at 37^{0}C. Uptake was terminated by the standard PBS wash routine after which some wells (exposed to ^{125}I-NLDP-MSH only, i.e. no unlabelled peptide present) received an acid-wash. Monolayers were then digested and the activity assayed.

2.4.7 Binding and Uptake of ^{125}I-NLDP-MSH at 37^{0}C

Plates were washed with 3ml of ice-cold PBS and incubated at 4^{0}C with 0.5ml/well binding buffer containing 0.5nM iodinated NLDP-MSH (with or without excess unlabelled peptide). After one hour plates were removed from the 4^{0}C enviroment and received the standard PBS wash before being reincubated with binding buffer with or without 1μM cold peptide at 37^{0}C for various lengths of time. The cells were finally washed again before being digested and the activity assayed. Some wells received an acid-wash after the final PBS rinse.

2.4.8 Binding Inhibition of ^{125}I-NLDP-MSH by the NLDP-MSH-MTX Conjugate

These experiments studied the binding inhibition of 0.25nM labelled NLDP-MSH by increasing concentrations of the NLDP-MSH-MTX conjugate at 4^{0}C. Wells were first washed with ice-cold PBS and then incubated for 30 minutes at 4^{0}C with 0.45ml/well of Hepes binding buffer containing 0.3mM MTX (in order to minimise any binding of the conjugate due to the MTX moiety). A further volume of 0.05ml was supplemented containing ^{125}I-NLDP-MSH and the conjugate. After an 8 hour incubation cells were washed, digested and the activity assayed.

2.4.9 Interaction of ^{125}I-NLDP-MSH-MTX with B16 Murine Melanoma

Two types of experiments were employed, incubation at 37^{0}C only, and exposure to ^{125}I-NLDP-MSH-MTX first at 4^{0}C, the cells washed and then reincubated at 37^{0}C in binding buffer only. The protocols used were identical to those for ^{125}I-NLDP-MSH, substituting the labelled conjugate for iodinated NLDP-MSH.

2.5 Dihydrofolate Reductase Enzyme Assay

2.5.1 Materials

The main buffer employed in the assay was 0.5M sodium acetate with 0.6M potassium chloride (BDH Chemicals), adjusted to pH 6.0 with glacial acetic acid. A second buffer was also prepared consisting of 0.15M mercaptoethanol (Sigma Chemical Co.) in the former sodium acetate buffer.

The enzyme, bovine dihydrofolate reductase, was obtained from Sigma Chemical

Co. and arrived in a stable form precipitated with ammonium sulphate to prevent hydrolysis of any hydrophobic groups on the protein surface. Five units of the enzyme were supplied and dissolved in 50ml of sodium acetate and KCl buffer pH 6. This was transferred to a cellulose acetate dialysis tube (pore diameter 1-20nM) and suspended overnight in 3L of the aforementioned buffer in order to remove the ammonium salt. The buffer was continuously agitated with a magnetic stirrer. The contents of the tubing were then aliquoted in 1ml volumes into glass vials and stored at -20^{0}C. Note:- 1 unit of enzyme will convert 1.0μmole of dihydrofolate and NADPH to tetrahydrofolate and NADP per minute at 25^{0}C, pH 6.

The compounds 7,8-dihydrofolic acid (dihydrofolate, FH_2) and 5,6,7,8-tetrahydrofolic acid (tetrahydrofolate, FH_4) were obtained in solid form (Sigma Chemical Co.). The entire contents of each vial were weighed and then dissolved in sodium acetate and KCl buffer (containing mercaptoethanol as an antioxidant) to give a final concentration of 2.41mM. Aliquots of 1ml were then stored in liquid nitrogen until used.

NADPH was obtained as a freeze-dried solid (Sigma Chemical Co.) in 1mg vials and dissolved with 1ml of sodium acetate and KCl buffer immediately prior to use.

Methotrexate (Cyanamid) and NLDP-MSH-MTX were dissolved in sodium acetate and KCl buffer and stored at 4^{0}C.

2.5.2 Assay Procedure

The spectrophotometric assay was based on a method described by Peterson et al. [166]. A quartz cuvette, with an optical path length of 1cm, contained 2.6ml of sodium acetate and KCl buffer (pH 6), 0.15ml of NADPH (from a 1mg/ml solution) and 0.1ml of DHFR enzyme stock. This was allowed to equilibrate

for 5 minutes at 37°C in a Pye Unicam cell temperature recorder connected to a Pye Unicam PU8610 UV/V15 kinetic spectrophotometer with a PU8605 cell programmer.

The reaction was initiated upon the addition of 0.15ml of FH_2 stock (120μM final concentration), each cuvette was thoroughly mixed by being inverted three times. The spectrophotometer was zeroed using a cuvette before the addition of FH_2. Absorbance readings were recorded for a maximum of six cuvettes every 30 seconds at 343nm for 10 minutes.

The aforementioned cuvette mixture constituted a standard test reaction, negative controls were performed twice daily and consisted of 2.75ml of sodium acetate and KCl buffer with 0.1ml of DHFR. After 5 minutes equilibration at 37°C, 0.15ml of NADPH (1mg/ml) was added and the absorbance recorded for 10 minutes.

Assays in the presence of inhibitors substituted 0.3ml of the buffer for 0.3ml of inhibitor solution, cuvettes in all experiments had a total volume of 3ml. The inhibitor was allowed to equilibrate with the enzyme before the addition of FH_2.

2.5.3 Isolation of Lysosomal Enzymes

Rat liver lysosomal enzymes were obtained by extraction based on the established method of Trouet [167]. Five large male Wistar rats were injected intraperitoneally with 20% $^{w}/_{v}$ Tyloxopol (formerly known as Triton WR1339) in water at a dose of 1ml per 100g body weight. Four days later the rats were sacrificed, their livers quickly removed and placed on ice in a 0.25M sucrose solution. The liver tissue was minced with scissors and homogenised in 0.25M sucrose solution using an Atomix homogeniser (MSE). The homogenate was then centrifuged at 15,000 rpm for 10 minutes using a High Speed 18 centrifuge (MSE). The supernatant was removed, the pellet resuspended in 0.25M sucrose and the process repeated. The combined supernatants were subsequently centrifuged for

60 minutes at 12,000 rpm. The supernatant was removed and the pellet resuspended in 45, 35.5 and 14.3% $^{w}/_{v}$ gradient sucrose solutions and centrifuged at 25,000 rpm for two hours at 4^{0}C in a Beckman L8-M centrifuge. A distinct band of lysosomes collected at the interface of the 34.5 and 14.3% sucrose layers and was removed using a Pasteur pipette before being placed in 5ml vials and stored at -20^{0}C.

This method permitted the separation of lysosomes from other cellular components of similar density as the surfactant specifically collects in the liver lysosomes producing a reduction in their equilibriation density. The Tyloxopol is unable to leave the vasculature except in the liver where the loose junctions of the sinusoidal capillaries allows the surfactant to penetrate the tissue.

2.5.4 Lysosomal Degradation of NLDP-MSH-MTX

This was adapted from the method described by R. J. Marriott [168]. A degradation mixture was prepared as follows and incubated at 37^{0}C with samples removed after 0, 2, 4 and 16 hours and then serially diluted in sodium acetate and KCl buffer (pH 6). The degradation mixture contained reduced glutathione for activation of the thiol proteases and the EDTA was used to chelate any metal ions present which may interfere with the enzyme activity. The sodium acetate and KCl buffer was adjusted to pH 5 to optimise the lysosomal activity.

Compound	Volume (ml)
1. NLDP-MSH-MTX (0.5mM)	0.50
2. Reduced glutathione (73.5mM)	0.08
3. EDTA (14.8mM)	0.08
4. 1% Superonic OP11 solution	0.03
5. Water	0.01
6. Tritisome solution	0.30
8. Sodium acetate and KCl buffer (pH 5.0)	0.50

Chapter 3

Accumulation of Extracellular Fluid by Pinocytosis

3.1 Introduction

Iodinated polyvinyl pyrrolidone (^{125}I-PVP) was used as a marker for fluid phase endocytosis as it has been shown not to adsorb to cell membranes, is not degraded and is easy to quantify [164, 169, 170]. The rate of fluid-associated uptake of this marker was measured at 37^{0}C in B16, SVK-14 and HMB2 cells prepared from monolayer cultures.

3.2 Methods

The suspension method employed for the three cell lines is described in section 2.2.

3.3 Results

These experiments were exquisitely sensitive and were required to be performed very carefully to avoid large error, as the amount of uptake being measured was so small. All extracellular ^{125}I-PVP had to be thoroughly removed and this was achieved using five centrifugation washes. This protocol was established by measuring the supernatants of each wash, an example of which is displayed in table 3.1.

Centrifugation	cpm of 1ml of supernatant	
Wash number	10 mins.	150 mins.
1	173985.4	174532.6
2	4418.0	6155.2
3	143.2	279.6
4	0.0	51.9
5	1.5	7.1

Table 3.1: The measured ^{125}I activity in 1ml of the centrifugation washes at 0^0C of samples of B16 cells exposed to ^{125}I-PVP for 10 and 150 minutes respectively at 37^0C.

The volume of fluid uptake expressed per 10^6 cells was calculated from three determined values;

1. The known concentration of ^{125}I-PVP in the medium (cpm per ml of medium) was determined from the supernatant washes. The activity of each supernatant from the five centrifugation washes was assayed for the first and last 0.5ml time samples. A mean value for the concentration of ^{125}I-PVP per 0.5ml sample expressed as cpm was obtained and converted to 'cpm per ml of medium.'

2. The cell density per 0.5ml sample (x) was determined from the known cell density in the experimental medium. The latter was innoculated with the

required number of cells from a cell suspension where the cell density and viability had been assayed by a haemocytometer count.

3. The ^{125}I-activity associated with the cell pellet from each experimental sample (cpm per 0.5ml sample).

Using these values the cpm associated with 10^6 cells was initially calculated (equation 3.1) and then expressed as the volume of fluid uptake per 10^6 cells (equation 3.2). It was noted that any small error in the activity of a sample e.g. poor washing of the pellet, is magnified due to this method of calculation.

$$\text{cpm per } 10^6 \text{ cells} = \frac{\text{cpm per 0.5ml sample}}{x}.\left(\frac{10^6}{x}\right) \tag{3.1}$$

$$\text{Volume of Fluid Uptake per } 10^6 \text{ cells} = \frac{\text{cpm per } 10^6 \text{ cells}}{\text{cpm per ml of medium}} \tag{3.2}$$

The results for each of the cell-lines are displayed graphically (figures 3.1, 3.2 and 3.3), demonstrating the uptake of fluid associated with the marker over a 150 minute period (105 minutes for B16 cells). Accumulation of extracellular fluid by the B16 cells was composed of two phases; an initial rapid uptake which was completed within the first 10 minutes of c.0.07-0.15μl per 10^6 cells followed by a reduced rate of continuous accumulation which was approximately linear for the remainder the experiment (figure 3.1). The four individual experiments showed variation in the volume taken up during the initial phase but accumulated ^{125}I-PVP at a similar rate during the linear phase. This could have been due to the use of different passages of B16 cells. Linear regression analyses of the data revealed the mean slope to be 6.28 ± 0.23 x$10^{-4}\mu$l/min/10^6 cells (mean and standard deviation) and the mean y-intercepts as $0.109\pm0.04\mu$l/10^6 cells.

The fluid uptake profile of the remaining two cell lines (figures 3.2 and 3.3) was different to that seen in B16 cells. Both the SVK-14 and HMB-2 cells demonstrated the rapid initial fluid uptake in the first 10 minutes (0.05-0.2μl) but there

was considerable variation thereafter. There was little apparent increase in fluid uptake with the SVK-14 cells over the remaining period, whereas the rate of uptake during the second phase diminished in HMB-2 cells after 20-30 minutes, reaching a plateau at approximately 100 minutes after a net increase of c.0.03-0.05μl.

A greater insight into the fate of the internalised marker, and the possibility of exocytosis (the release of ^{125}I-PVP back into the medium) occurring, would be gained by employing subcellular fractionation. This was attempted with the B16 cells using a technique described by England et al.[164]. A linear sucrose gradient (20-58% weight by weight sucrose) was prepared and the cells disrupted using a dounce homogeniser after being exposed to c.0.36x10^{6}cpm/ml ^{125}I-PVP for 100 minutes and then washed. After 4 hours centrifugation at 85,000g, 1ml fractions were collected from the centrifuge tubes and their activity and density were measured (the latter by refractive index).

The vast proportion of the radioactivity occurred in the earliest fractions suggesting endocytotic vesicles containing the marker were damaged (see figure 3.4). The vesicular bodies expected to contain the marker and hence display radioactivity are endosomes and lysosomes, of which the latter are reported to occur in the heavier fractions of a sucrose gradient(c.1.18gm/cm^3 [171]). Due to a shortage of ^{125}I-PVP it was not possible to refine this technique to remedy the probable breakage of the vesicles.

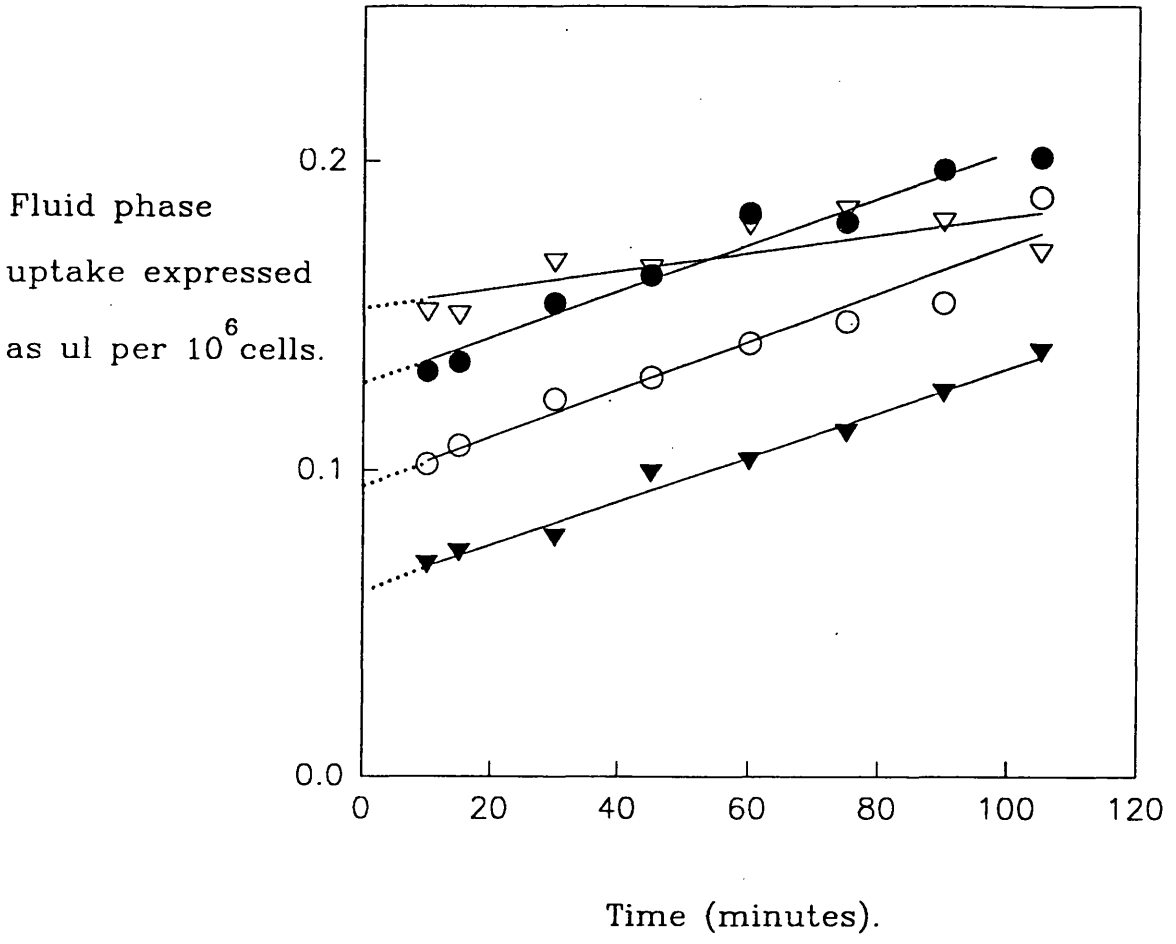

Figure 3.1: Fluid associated ^{125}I-PVP uptake with time by B16 cells in suspension at 37^{0}C. Data with linear regression represent individual experiments.

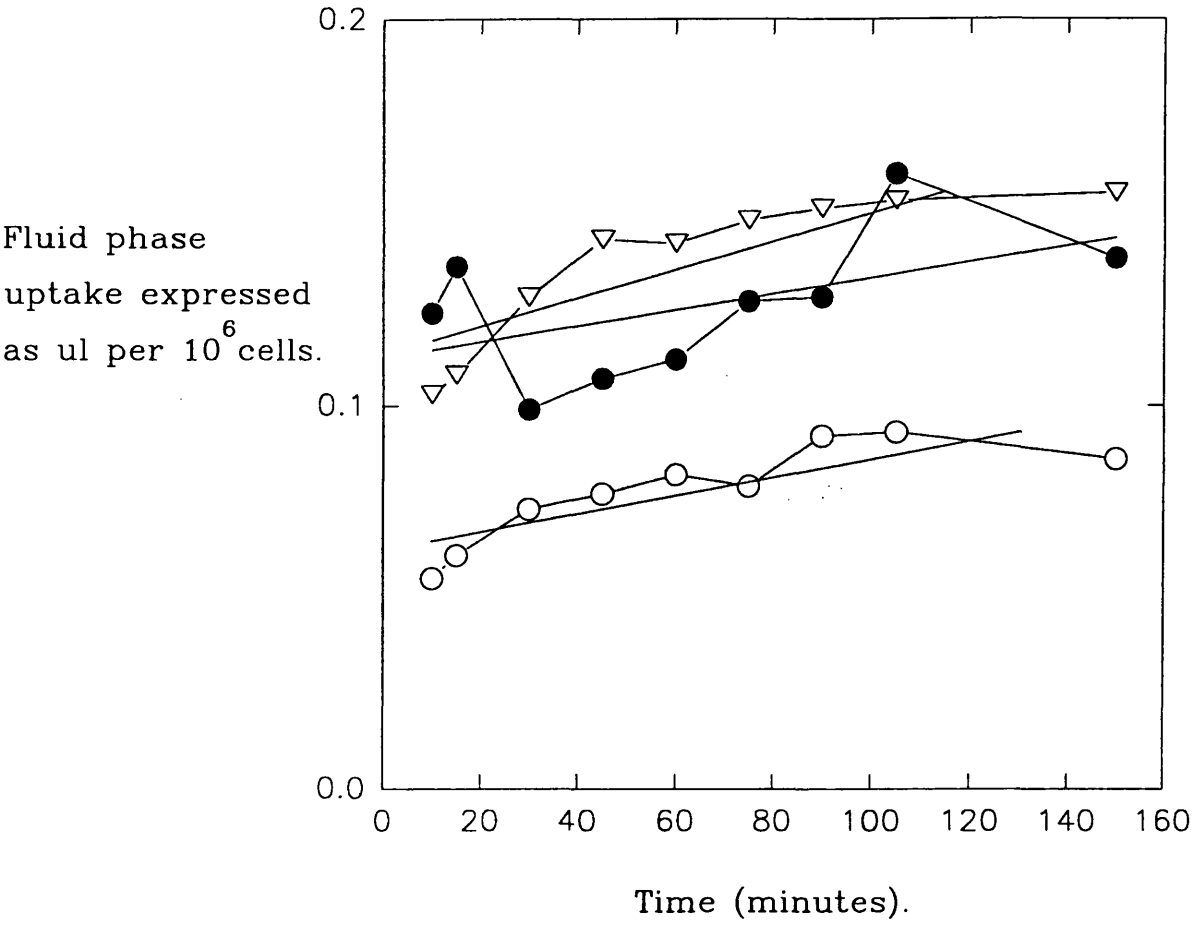

Figure 3.2: Fluid associated ^{125}I-PVP uptake with time by HMB-2 cells in suspension at 37^{0}C. Data with linear regression represent individual experiments.

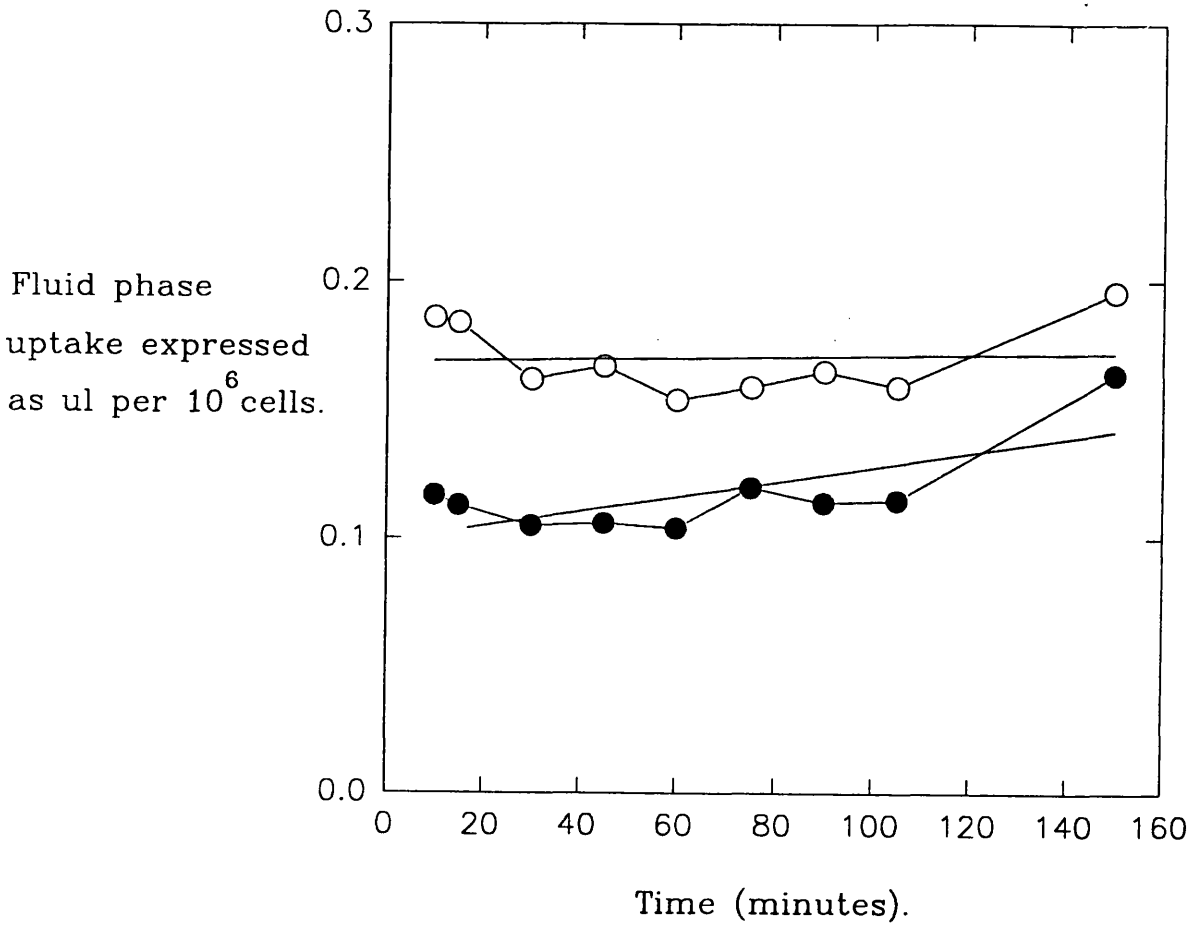

Figure 3.3: Fluid associated ^{125}I-PVP uptake with time by SVK-14 cells in suspension at 37^{0}C. Data with linear regression represent individual experiments.

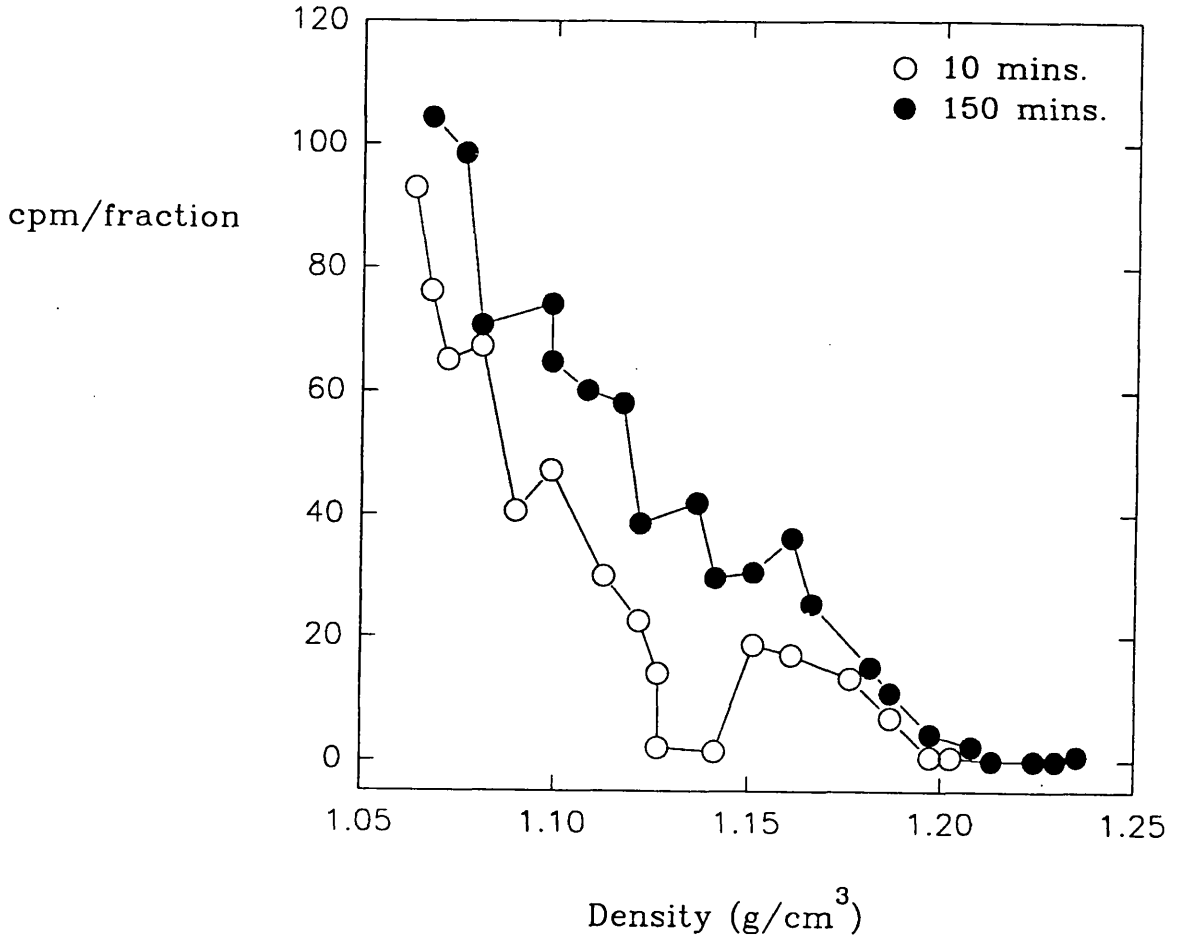

Figure 3.4: The activity per density fraction of a B16 cell homogenate after incubation for 10 and 150 minutes with ^{125}I-PVP (c.0.36x10^{6}cpm/ml) at 37^{0}C. Cells were then disrupted and separated on a linear sucrose gradient (20-58%).

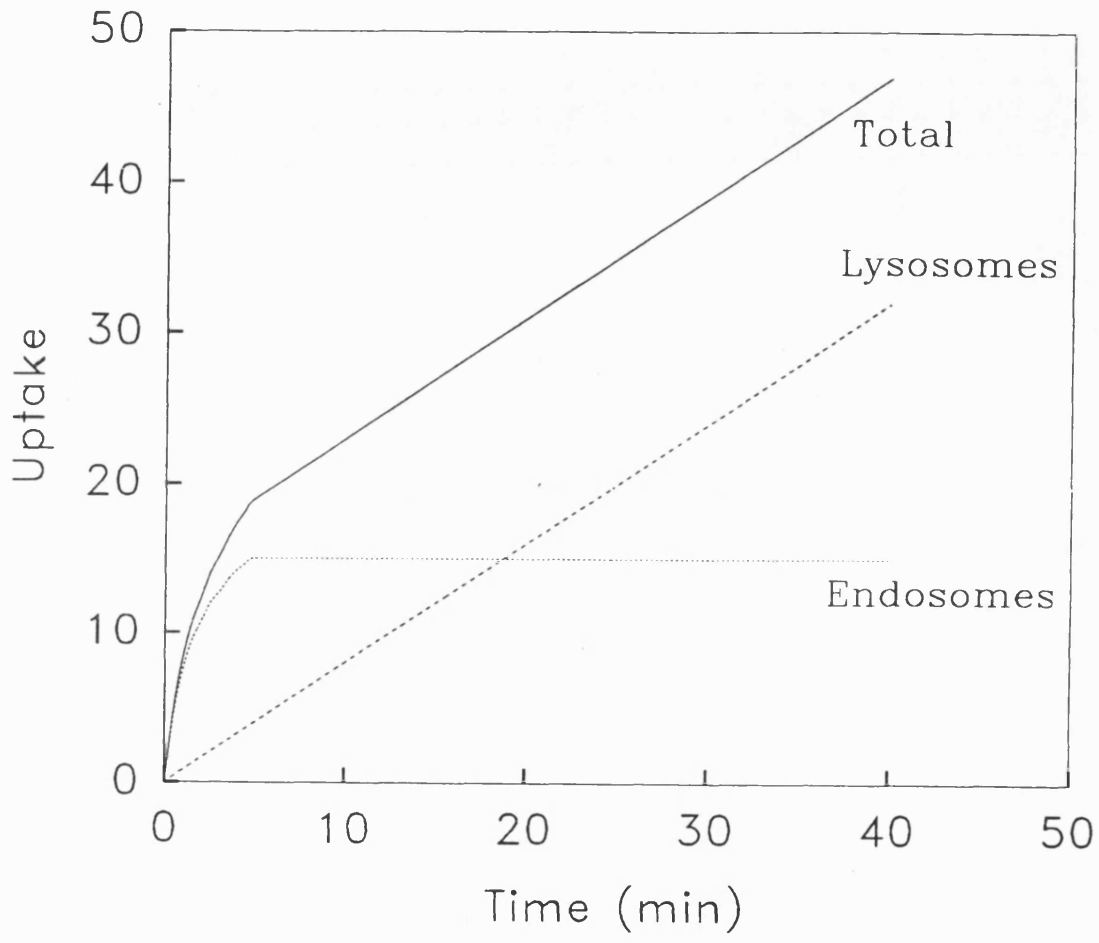

Figure 3.5: A graphical representation of the uptake (in arbitary units) of a fluid-phase marker into a mammamlian cell, and its vesicular compartments with time at 37^{0}C.

3.4 Discussion

The use of ^{125}I-PVP as a marker for fluid phase endocytosis is well documented with many examples in the literature of its use in varying cell types e.g. rat liver parenchymal cells [164, 170], macrophages [172], visceral yolk sacs [173, 174, 175], and human fibroblasts [176]. ^{125}I-PVP has been demonstrated to conform to the characteristics required for such a marker, i.e. does not adsorb or interact with cell membranes; it is internalised immediately upon addition to a cell-containing media at 37^{0}C; its rate of uptake is proportional to its extracellular concentration; it is not degraded and resides in a vesicular body after uptake.

Fluid uptake in the B16 cells appears bi-phasic with an initial rapid phase followed by a reduced but linear uptake for the remainder of the experiment. Similar profiles of this nature have been reported in the literature [164, 173, 174, 175, 177] using various markers but there are also examples of uptake proceeding with linearity from time zero [170, 172, 176, 178, 179].

The cellular uptake rate of a fluid-phase marker would be expected to be proportional to its extracellular concentration and so appear linear as the cell internalises a constant volume of fluid and solutes per unit time (providing the extracellular concentration of the marker and the rate of pinocytosis by the cell both remain constant). This would not explain the apparent bi-phasic uptake which occurred with the B16 cells which could be due to:

1. The rate of pinocytosis decreasing during the experiment.
2. Exocytosis of the ^{125}I-PVP after a time lag.
3. A proportion of cells exhibiting a 'leaky' membrane due to recent harvesting from a monolayer state.

The last point can be immediately discounted as all of the cell lines were checked for viability (>99%) before and after the experiment by trypan blue exclusion.

Commencing the experiment after varying lengths of cell suspension at 37^0C in the presence or absence of unlabelled PVP would examine any changes in the rate of endocytosis with time under these conditions, but there are no reports of this occuring in the current literature.

To examine the process of exocytosis, cells could be loaded with ^{125}I-PVP for various lengths of time, washed, and reincubated at 37^0C in the absence of marker. If ^{125}I-PVP was released into the medium relatively quickly it could explain the apparent decrease in the rate of pinocytosis observed. Various authors have indeed demonstrated this phenomenom with a variety of markers and cell types [164, 169, 172, 174, 176, 177, 178, 180, 181].

Fluid-phase uptake is thought to involve two intracellular compartments, early endosomes or pinosomes, and lysosomes; this has been established by using morphological and subcellular fractionation studies. England et al. [164] demonstrated that the appearance of ^{125}I-PVP in the cell was related to two distinct density fractions (1.13 and 1.20g/ml) in rat liver parenchymal cells, the latter associated with the lysosomal marker B-acetylglucosaminidase. Other authors have made similar observations [170, 178]. Upon incubation with a fluid-phase marker the less dense fraction appears to contain the marker during the early stages [178]. Steinman et al. [182] noted that in mouse fibroblasts exposed for 5-10 minutes to the marker HRP (horse-radish peroxidase), the enzyme first appeared to be localised in small vesicles near the cell surface. After 60 minutes the enzyme was found throughout the vacuolar apparatus. Further studies by Steinman et al. [179] demonstrated that this less dense, early endosome fraction equilibrated in about 5 minutes with HRP associated fluid and thereafter its volume remained constant whereas enzyme in the lysosomal compartment did not appear until after 5 minutes and gradually increased until reaching a plateau at around 45 minutes. It appears that marker is first taken into the cell by early endosomes and then slowly transferred to the secondary lysosomes.

Pulse-chase experiments have also revealed the kinetic interplay between these

two compartments. Release or exocytosis of previously intracellulary located marker has also displayed bi-phasic kinetics [172, 174, 177, 178, 180, 181] involving an initial rapid phase with a half-time in the order of 5 minutes, followed by a more gradual release of marker with a half-time in the range of 180-800 minutes. When internalisation of fluid was studied intracellulary marker was found to disappear from the endosomes whilst showing an increase in the lysosomes [178, 182].

The bi-phasic uptake profiles are due initially to the filling of the early endosome compartment which is complete and at steady state after 5-10 minutes. After which, marker is either returned to the extracellular enviroment (exocytosis or diacytosis) or transferred to the lysosomes (as represented in figure 3.5). Thus the second phase of uptake is an actual measure of fluid transfer to the lysosomal compartment of the cell. The initial rapid phase of uptake and of release would therefore be expected to be similar as they represent the filling and emptying of the endosomes respectively, with a proportion being transferred to the lysosomes. The half-life for the initial release of marker is in the order of 5-10 minutes [172, 180, 181]. The results with the three cell lines used in this study correspond favourably as after the first sample at 10 minutes there is no increase in the rate of uptake, i.e. the endosome compartment is already at a steady state of turnover. The volume of the endosomal compartment would then be reflected by the intercept of the ordinate axis at time zero on a graph of fluid uptake versus time. The value obtained using the regression plot for the B16 cells was 109 ± 40 nl/10^6cells (mean$\pm$standard deviation), greater than the value reported for rat liver parenchymal cells [164] of c.30nl, or values using other methods; human fibroblasts [176] 2-4nl, guinea pig macrophages [180] 4nl and fibroblasts 42nl, and bovine brain endothelia [177] 34nl. The reasons for this apparent high value are unclear, if not related to the experimental technique it may reflect a characteristic of tumour or melanoma cells.

The slopes of the plots for the B16 cells, 0.038μl/10^6cells/hr, which reflects the rate of lysosomal accummulation were of a similar order of magnitude to those reported by other authors:

Human fibroblasts [164] 0.12-0.02μl/10^6cells/hr.

Rat liver hepatocytes [170] 0.08μl/10^6cells/hr.

Rat liver non-parenchymal cells [170] 0.07 μl/10^6cells/hr.

Rat peritoneal macrophages [172] 0.034μl/10^6cells/hr.

Mouse peritoneal macrophages [179] 0.1μl/10^6cells/hr.

The rate of fluid uptake by the human melanoma HMB-2 appeared to decrease with time after the initial uptake of 0.06-0.12μl in the first 10 minutes. As the incubation time approached 100 minutes uptake had almost ceased. Non-linear uptake has been cited elsewhere [180, 181] but accummulation of fluid still proceeded albeit at a decreased rate. Both authors ascribed this deviation to the exocytosis from a slow release compartment with a half-time of release in the order of 500 minutes. The decrease in uptake observed with the HMB-2 cells could also result from the commencement of exocytosis from a slower release compartment, or a decrease in the amount fluid transfer from endosomes to lysosomes with time.

The rate of pinocytosis could have been diminishing due to cell death or length of incubation at 37^{0}C, but this was unlikely. Pre-loading the cells for various lengths of time, removing medium and replacing with 'marker' deficient medium to study the kinetics of release may give an insight to how the rate/amount of exocytosis compares to exposure time.

Uptake in the SVK-14 human keratinocytes has almost ceased after 10 minutes. This is unlikely to be explained by rapid entry into cells with damaged membranes (i.e. with no apparent ^{125}I-PVP accumulation amongst the healthy population) as cell viability was always >99%. Interaction of ^{125}I-PVP with the plasma membrane via non-specific adsorption binding sites which then become saturated after 10 minutes at 37^{0}C is unlikely as ^{125}I-PVP has not been reported to adsorb to cell membranes. However a balance of uptake versus release or a complete halt

in uptake would be possible. Similar results have been obtained in other cell lines in the literature, reaching an apparent plateau in uptake after similar periods of time; 10 minutes in human lymphoblasts [183], 20-30 minutes in rat hepatocytes [184] and 15-20 minutes in bovine brain endothelia [177]. It seems likely that there is little or no transfer of fluid and marker from the early endosomes to the lysosomes, resulting in a steady-state of turnover in fluid between the early endosomes and the extracellular enviroment. Sasaki et al. [184] did demonstrate uptake into a 'non-releaseable' compartment of hepatocytes, but the rate was very slow with a non-linear relation to loading time. It may have represented a gradual transfer of fluid to the lysosomes.

Data points that appeared to represent a sharp increase or decrease in the rate of fluid uptake probably reflect the sensitive nature of the experimental system and are likely to be caused by technical problems, for example:

1. Poor sampling of cells, e.g. cells not kept constantly in suspension.
2. Loss of cell viability during an experiment due to shearing forces of the paddle if the motor was not properly adjusted.
3. Poor centrifugation washing i.e. loss of cells during washing or incomplete removal of marker.

It is clear from these experiments that the profiles and kinetics of fluid phase uptake vary with differing cell types and origin. It is possible that the described uptake is pertinent only to ^{125}I-PVP or the experimental technique employed. The use of a second marker would help resolve the matter alongside subcellular fractionation studies. There was though, a similarity in the initial amount of uptake by all three cell lines but the values were much greater than those reported elsewhere in the literature. Further experiments to have helped validate that endocytosis was occurring by demonstrating the characteristics established for this particular mode of uptake [185, 22] are:

1. Examining the rate of uptake with varying concentrations of marker and cell density, pinocytosis being independant of these two parameters.

2. Demonstrate uptake at low temperatures.

3. Uptake should be metabolically dependant.

4. The use of other fluid-phase markers for comparision e.g. ^{14}C-Sucrose, horse-radish peroxidase (HRP).

Although fluid phase endocytosis is well reviewed [185, 22, 23] the precise interplay between the various vesicular compartments is unclear. For example Casey et al. [186] have described uptake of HRP in Chinese hamster ovary cells to be initially associated with two distinct populations of endosomes, separate from the lysosomes. However the value reported for the linear uptake of fluid into B16 cells appears in accordance with others cited in the literature.

Chapter 4

Binding and Uptake of Methotrexate

4.1 Introduction

The binding and uptake of methotrexate by B16 melanoma cells has been studied to allow the rate of accumulation of the free drug to be compared with that of the free hormone, (see chapter 5) and the drug conjugate. Cytotoxicity experiments would have provided a more useful direct measure of cellular uptake. Clonogenic cytotoxicity tests were attempted, however this line of approach proved difficult with the B16 system. In the absence of a cytotoxicity assay the kinetics of cellular binding and uptake have been used to give an indication of the differences between the free drug and its hormone derivative.

4.2 Methods

The protocols described in detail in section 2.3, concern the bulk of work when B16 cell monolayers were employed. Various attempts at ^{3}H-MTX binding (4^{0}C)

were made using centrifugation techniques to remove unbound ligand in order to avoid problems of desorption during washing steps. However none of these methods proved satisfactory as the non-specific binding remained high (see in figure 4.1). Briefly the centrifugation method used involved seeding 10^7cells per tube (10ml Cell-Cult centrifuge tubes) and incubation at 4^0C with radioactive tracer in a final volume of 1ml. After incubation the tubes were spun at 1000g for 15 minutes at 0^0C and the supernatant removed by pipette. An attempt to remove the final amount of fluid associated with the cells was made using small strips of filter paper in contact with the cell pellet for 10 seconds as described in the literature [187]. Further efforts to improve the technique with varying incubation vessels and wash protocols led to very erractic results. This method was investigated in anticipation of the relatively low binding affinity of MTX, as extensive washing of cells could potentially remove bound ligand by desorption. However the methods proved impractical and attentions were turned to use of monolayers.

4.3 Results

4.3.1 Washing Regime

Determination of the ^{3}H activity in washes of monolayers in wells, after exposure to ^{3}H-MTX, indicated that three rinses with ice-cold PBS were sufficient to remove the majority of unbound ligand (see table 4.1), but a small amount of bound ^{3}H-MTX appeared to be dislodged even after four washes when wash counts were compared to controls. (Background counts of the order of 50-60 dpm were obtained using 2ml of PBS and 8ml of Optiphase). Although washings were rapid care had to be taken not to dislodge cells from the wells.

Wash No.	Apparent dpm of PBS after washing	
1	158493.6	17120.3
2	778.4	425.3
3	205.3	95.6
4	120.0	118.1
5	181.4	115.8

Table 4.1: ^{3}H activity in washes for two wells exposed to 1ml of 10nM ^{3}H-MTX, initial activity in the order of 300,000 dpm. Each wash consisted of 3ml of ice-cold PBS, the resulting activity of which is shown above.

4.3.2 Binding of ^{3}H-MTX at 4^0C.

The B16 cells were initially incubated with 25nM ^{3}H-MTX to establish the binding profile with respect to time (figure 4.2). Maximum specific binding of c.60fmoles/10^6cells occurred between 30 minutes and 2 hours, the value apparently declining thereafter (low values at 4 hours may be explained by some cell detachment). A final incubation period of 30 minutes was chosen, there being no significant difference between specific binding after 30 minutes and 2 hours. It was noted that non-specific binding was a relatively high proportion of the total bound ligand. In retrospect this was probably due to the large surface area of plastic in relation to cell monolayer in the well. A smaller size well may have improved the assay by resulting in a lower proportion of non-specific binding.

Three binding isotherms are represented in figures 4.3, 4.4 and 4.5, ranging from 1-150nM extracellular ^{3}H-MTX. All three display specific binding of the tracer to the cells with a small degree of variation but apparently did not reach a state of saturation. At 150nM (see figure 4.3) binding reached c.200fmoles/10^6cells and was still increasing. Two further experiments carried out at higher concentrations (150-1000nM) figures 4.6 and 4.7, suggested that binding reached saturation at around 375fmoles/10^6cells although non-specific binding had greatly increased and represented a greater proportion of the total binding. It should be noted

at this stage that at higher concentrations ^{3}H-MTX had to be diluted with non-labelled MTX for economical reasons, the assumption being made that there was no difference in the binding affinity of tritiated and unlabelled ligand. This was found to be the case when 30nM pure ^{3}H-MTX and a 50% dilution with non-labelled MTX resulted in identical estimates of specific binding at 4^0C of 54.92±2.99 and 54.58±1.29fmoles/10^6cells respectively.

The data was considered to fit a Langmuir isotherm model and the appropiate parameters were obtained by least squares non-linear regression using a computer programme called MINSQ. The following equation (4.1) was used:

$$\text{Bound} = \frac{N.K_a[^3H - MTX]}{1 + K_a[^3H - MTX]} \tag{4.1}$$

Bound represented the specific binding per 10^6cells, N the number of binding sites per 10^6 cells and K_a the binding affinity. A model for a single population of binding sites was used for reasons explained later. It is observed however that in figure 4.4, the isotherm displays an inflection at c.15nM ^{3}H-MTX, and also in figure 4.5 at c.8nM ^{3}H-MTX. The exact nature of this is not apparent, such an inflection could represent the binding to a high affinity/low capacity site. However it is more likely to be an experimental artifact especially since the inflection is absent in figure 4.3.

A suitable isotherm model for figure 4.5 could not be found because binding saturation was not being reached as the curve did not start to plateau. The same problem might be anticipated with the two remaining isotherms, though a fit was obtained. To circumvent this problem the data from figure 4.7 expressing binding at high ^{3}H-MTX concentrations was added to data for each of the isotherms (now denoted as isotherm 1A, 2A and 3A). The resulting values for K_a (affinity constant) and N (maximum binding of ^{3}H-MTX) from the models are expressed in table 4.2.

Isotherm	Ka(x10^{-7} M^{-1})	N(fmoles/10^6cells)	Binding sites/cell
1	0.55 ± 0.61	420 ± 367	252966
2	0.39 ± 0.05	554 ± 50	333674
3	-	-	-
1A	0.46 ± 0.05	455 ± 23	274046
2A	0.48 ± 0.04	451 ± 18	271637
3A	0.47 ± 0.07	452 ± 27	272240
Mean	0.47	453	272842

Table 4.2: Values for binding affinity (K_a) and binding sites per cell (N) for binding of ^{3}H-MTX at 4^0C to B16 cells, obtained from a Langmuir model using a least squares minimisation regression programme.

The mean binding affinity of 0.47 x $10^{-7}M^{-1}$ corresponds to a K_d, dissociation constant (K_d=1/K_a) of 0.21μM which correlates well with work by Henderson et al. [187] using L1210 cells who reported a value of 0.35μM. However the number of binding sites per cell was lower in the latter study (80,000) than the present study (270,000).

4.3.3 Binding and Uptake at 37^0C.

In preliminary experiments B16 cells were incubated at 37^0C with 50 and 100nM ^{3}H-MTX and the cell association of the tracer measured with time, figures 4.8 and 4.9. However in these experiments the use of a Hepes-based acid buffer (pH 2.0) was unsuccessful in the removal of extracellular bound tracer. The buffer resulted in visual damage of the cells (vacuole-like bodies became apparent on the cell surface upon inspection with an inverted microscope) and caused inadequate removal of cellular material from the wells with 1M NaOH (insufficient washing of the well to remove residual acid-buffer could have been to blame). Therefore only a measure of cell-associated ^{3}H-MTX is recorded. At 50nM ^{3}H-MTX the amount associated with the cells after 15-30 minutes was c.45 fmoles/10^6cells

which was lower than that bound at 4^0C after 30 minutes c.80fmoles/10^6cells. Thereafter the amount bound increased to a maximum of c.70fmoles/10^6cells at 45 minutes before gradually declining over 100 minutes to a value lower than the first measurement at 15 minutes. This decrease could have been due to:

1. Loss of cells by detachment as the incubation period increased. It was observed that after a period at 37^0C occasionally cells detached rather easily when being washed with ice-cold PBS. Care had to be taken to avoid this problem.

2. Efflux rate of ^{3}H-MTX increasing as the experiment progressed. This was considered to be unlikely and would not give a lower value at the end of the experiment unless binding decreased (see below).

3. Decrease in the binding affinity at 37^0C coupled to an inactivation process. If this was the case initial amounts of cell associated ^{3}H-MTX would indeed be lower than values at 4^0C. If the folate carrier was 'inactivated' after transporting ^{3}H-MTX or took a long recovery time before it was capable of binding and transporting another molecule then the values in the latter part of the experiment would reflect internalised tracer only. The use of a reliable acid wash technique would enable the simultaneous study of surface bound and internalised ligand with respect to time.

The cell-association profile at 100nM extracellular concentration was slightly different, an initial value at 15 minutes of c.70fmoles/10^6cells increasing to c.125 fmoles/10^6cells at 30 minutes (c.160fmoles/10^6cells at 4^0C), and then remaining relatively constant for the next 75 minutes. The peak of cell associated ^{3}H-MTX occurred earlier at an extracellular concentration of 100nM but the non-specific value at 45 minutes seemed abnormally high (probably due to poor/insufficient washing in one or two wells) possibly masking a peak of specific cell association. A decrease in cell associated activity was not observed after 30 minutes indicating that the most likely reason for that seen with 50nM ^{3}H-MTX was due to cell

detachment.

Using an improved acid-wash treatment with a citrate buffer (pH 2.5), cells were incubated with 100nM ^{3}H-MTX at 4^{0}C and 37^{0}C (figure 4.10). Binding at 4^{0}C remained relatively constant between 1 and 2 hours with the acid-wash treatment totally removing all the ^{3}H-MTX specifically associated with the cells, thus demonstrating no uptake at 4^{0}C and confirming the suitability of the acid buffer.

At 37^{0}C total cell associated activity was lower than previously observed. Upon acid-washing the majority of the tracer was discovered to be internalised, increasing from c.60 to 80% from 1 to 2 hours respectively. However the total amount associated with the cells decreased over the second hour suggesting instability of the cells for this length of time under these conditions.

Specificity of uptake was investigated using various known inhibitors of folate previously cited in the literature. Using 100nM ^{3}H-MTX, cells were incubated at 37^{0}C for 1 hour in the presence of folinic acid, tetrahydrofolate (FH_4), dihydrofolate (FH_2), 5-methyltetrahydrofolate (5-MFH_4), aminopterin (all at 100nM), thiamine pyrophosphate (TP) at 50μM and p-chloromercuribenzylsulphonic acid (PCMPS) at 100μM. The results, displayed in table 4.3, demonstrate very little uptake of ^{3}H-MTX into the cells as determined by the acid-wash treatment, although total cell-associated ^{3}H-MTX is comparable to earlier experiments. Due to limited resources it was not feasable to purchase further stocks of ^{3}H-MTX to repeat the experiment so the present results from a single test must be treated with a degree of caution and so will not be discussed in detail.

Uptake was totally blocked by the two non-folates PCMPS and thiamine pyrophosphate, the former functions as a sulphydryl inhibitor and has been reported to inhibit MTX uptake [188], whilst the latter acts by competitive anion inhibition of uptake but does not affect binding [66]. The folate and antifolate (aminopterin) analogues display a degree of binding inhibition except for 5-methyltetrahydrofolate. Binding at 37^{0}C is relatively unaffected, except for

Inhibitor	Specific fmoles/10^6cells	Acid-Specific fmoles/10^6cells
Control	75.72 ± 22.37	18.50 ± 11.61
Folinic acid	121.33 ± 21.82	10.37 ± 14.48
FH_4	43.27 ± 13.79	-9.93 ± 12.54
FH_2	47.67 ± 11.68	4.22 ± 1.27
5-MFH_4	268.04 ± 89.93	22.15 ± 14.50
Aminopterin	70.99 ± 26.73	0.39 ± 12.11
PCMPS	169.32 ± 42.65	-14.49 ± 18.50
TP	75.14 ± 35.65	-7.27 ± 22.16

Table 4.3: The specific and acid-washed specific values for B16 cells incubated at 37^0C for 30 minutes with 25nM ^{3}H-MTX in the presence of various inhibitors. Non-specific values were 51.25 ± 11.03fmoles/10^6cells.

apparent increases caused by PCMPS, 5-methyltetrahydrofolate and folinic acid. A repitition of the experiment would provide a clearer explanation of the results.

4.3.4 Cell Growth in Low Folate Medium

An attempt was made to grow B16 cells at normal physiological folate levels 5-50 nM [189] rather than those found in the RPMI medium (2.2μM folic acid). The purpose being to enable the detection of a high affinity folate binding membrane protein that has been identified in cell lines predominantly grown only in low folate medium [66, 124, 125, 126, 127, 128]. However this adaptation to growth in a decreased amount of folate can take time; seven months in one example [125].

Folate free medium was obtained specially prepared from Gibco Ltd and medium was prepared in the absence of any form of folate except for that present in the serum. The growth passages of B16 cells with normal and low folate media were measured in parallel in 150cm^2 and then 75cm^2 (at passage 3) tissue culture flasks.

Both cultures received identical seeding values limited from passage 5-9 due to the slow growth of the cells in low folate media. Growth in low folate medium was expressed as a percentage of the total number of cells grown in normal media (with identical seeding and incubation values); and also as a direct measure of their own growth rate, by comparing the final number of cells to the seeded value (summarised in table 4.4).

Cell growth dropped dramatically upon incubation in low folate medium to only 2% of normal cells by passage 5. This was presumably due to depletion of the intracellular folate concentration. Growth actually ceased between passages 4-7 as the final number of cells was less than the seeded value. Growth was not improved upon the addition of 10nM 5-MFH_4 plus daily re-feedings to the medium but growth did proceed to a small extent at 100nM 5-MFH_4. From passage 7-9 normal B16 cells failed to reach previous values at confluency for a given time period, this is probably due to a very low seeding value. This would provide a sparse covering of cells initially in the flask causing an increase in the lag period before exponential growth. Consequently this would have hindered cell growth in low folate media as well. To circumvent this problem cells could have been transferred to a smaller flask. Returning the cells to standard media resulted in normal growth characteristics after three passages without daily re-feedings. It can be assumed that the cells were in a quiescent state in the low folate medium and were unable to divide until folate levels were increased to $>0.1\mu$M.

The growth of B16 cells in low folate medium was abandoned due to the length of time it was likely to take to achieve a similar growth rate to cells in ordinary media.

Passage	Seeding No. 10^5cells	Control 10^5cells	Low Folate 10^5cells	% of Control	Low Folate Growth Rate
1	30	260.4	224.0	86.0	7.47
2	45	392.0	91.0	23.0	2.02
3	15	195.3	19.3	9.89	1.29
4	15	207.3	11.81	5.7	0.79
5	10	207.0	4.2	2.0	0.42
6(10nM)	4.2	192.5	1.53	0.8	0.36
7(20nM)	1.5	111.2	0.92	0.8	0.61
8(0.1μM)	0.92	112.5	1.41	1.25	1.53
9	1.0	130	21.7	16.0	21.7
10	10	220	180	81.8	18.0
11	10	224	220	98.0	22.0

Table 4.4: Growth of B16 cells in standard RPMI media (control) and folate free RPMI both with 10% FCS. Seeding number varied according to total cell count from previous passage, cells were transferred from 150 to 75cm^2 culture flasks at passage 3. Values in brackets are 5-MFH$_4$ concentrations in the media with daily re-feedings, from passage 9 all cells were grown in standard media without re-feedings. Low folate growth rate corresponds to the total cell number obtained divided by the initial seeding value at each passage.

4.3.5 Binding Inhibition by NLDP-MSH-MTX Conjugates

Two conjugates of NLDP-MSH-MTX were purified corresponding to two peaks obtained by HPLC, these were thought to be due to linkage via the α or γ carboxyl groups on the glutamic acid moiety on MTX. Both conjugates, denoted as G0133/1 and G0133/3, were incubated at increasing concentrations for 1 hour at 4^0C in the presence of 25nM ^{3}H-MTX. Cells were pre-exposed to 200nM NLDP-MSH to prevent binding of the conjugate to MSH receptors. The results of three separate experiments are displayed in figures 4.11, 4.12 and 4.13 showing the dpm/well versus conjugate concentration. The total and non-specific binding show good consistancy between the experiments resulting in a difference of about 400-500 dpm. There was little difference between the two conjugates which appeared to show a weak general trend towards more inhibition as the concentration increased (figure 4.14). Over a wide-range of concentration of the conjugates there was only a small change in the degree of inhibition, indeed in figure 4.11 only the highest concentration of G0133/1 appeared to have caused a significant amount of inhibition, whereas in figure 4.12 there was no significant difference in the final three concentrations. Likewise in figure 4.13 conjugate G0133/3 displayed only a small increase in inhibition and G0133/3 acted in a similar manner. However the specific binding in the presence of conjugates was erratic and did not compare well with the controls (figures 4.12 and 4.13). When the mean and standard deviation of individual wells were plotted as % of control binding (control equals specific binding of ^{3}H-MTX in the absence of conjugate) versus conjugate concentration, a shallow decrease in binding with increasing conjugate concentration was observed, figure 4.14. However the size of the error bars illustrate that there was little if any difference over the complete range of concentrations used. Higher concentrations could not be used due to limited amounts of the conjugates.

The difficulty of the experiment was hampered by the low affinity of the system studied but it appeared that NLDP-MSH-MTX had no specific inhibitory effect

on MTX binding at concentrations up to 250nM.

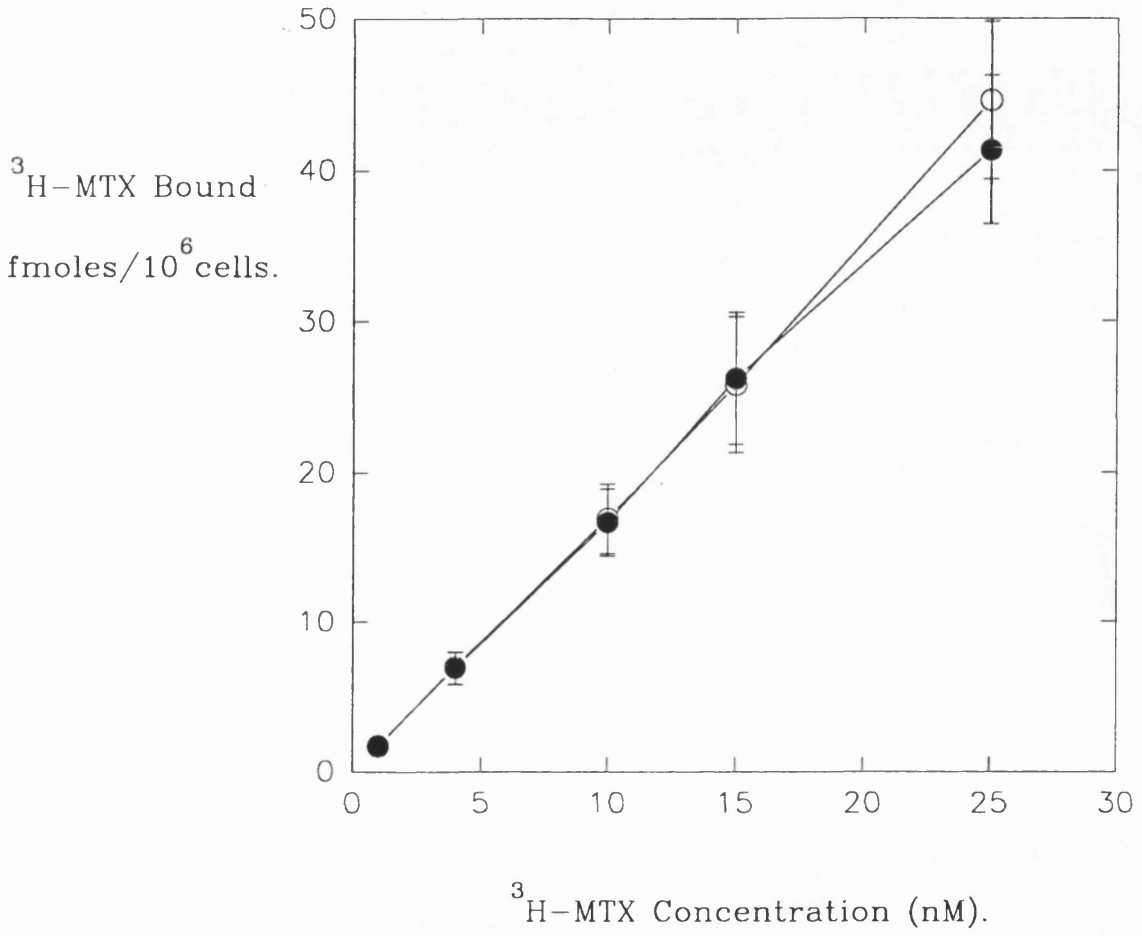

Figure 4.1: Incubation of B16 cells with ^{3}H-MTX at 4^0C in suspension for 30 minutes. Each point represents the mean±sd from three tubes each containing 10^6 cells. Total (●) and non-specific (○) binding.

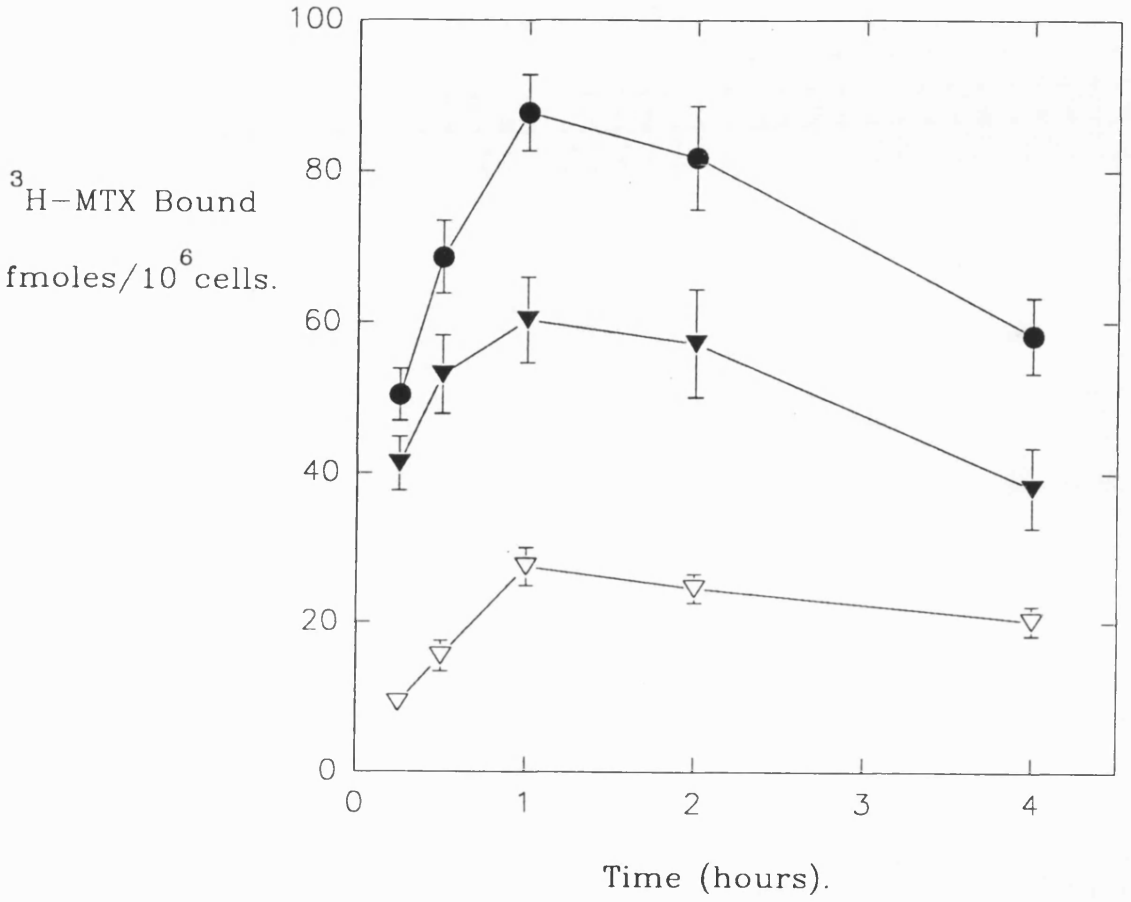

Figure 4.2: Binding of 25nM ^{3}H-MTX with B16 cells at 4^{0}C with time in a Hepes based buffer, pH7.4. Each point represents the mean±sd for 6 wells. Total (●), specific (▼) and non-specific (▽) binding respectively.

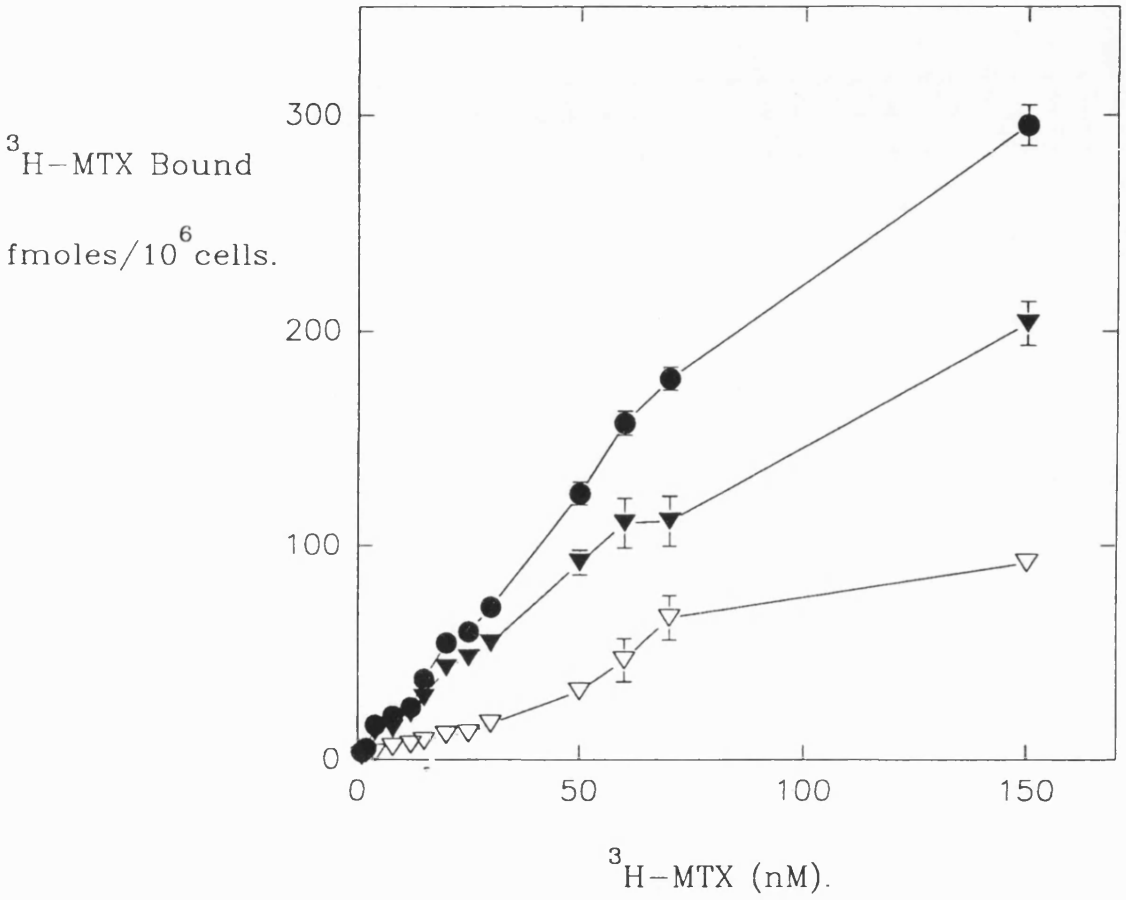

Figure 4.3: I. Adsorption isotherm of increasing concentrations of ^{3}H-MTX incubated with B16 cells at 4^0C for 30 minutes at pH 7.4. Each point represents the mean±sd for 6 wells. Total (●), specific (▼) and non-specific (▽) binding respectively.

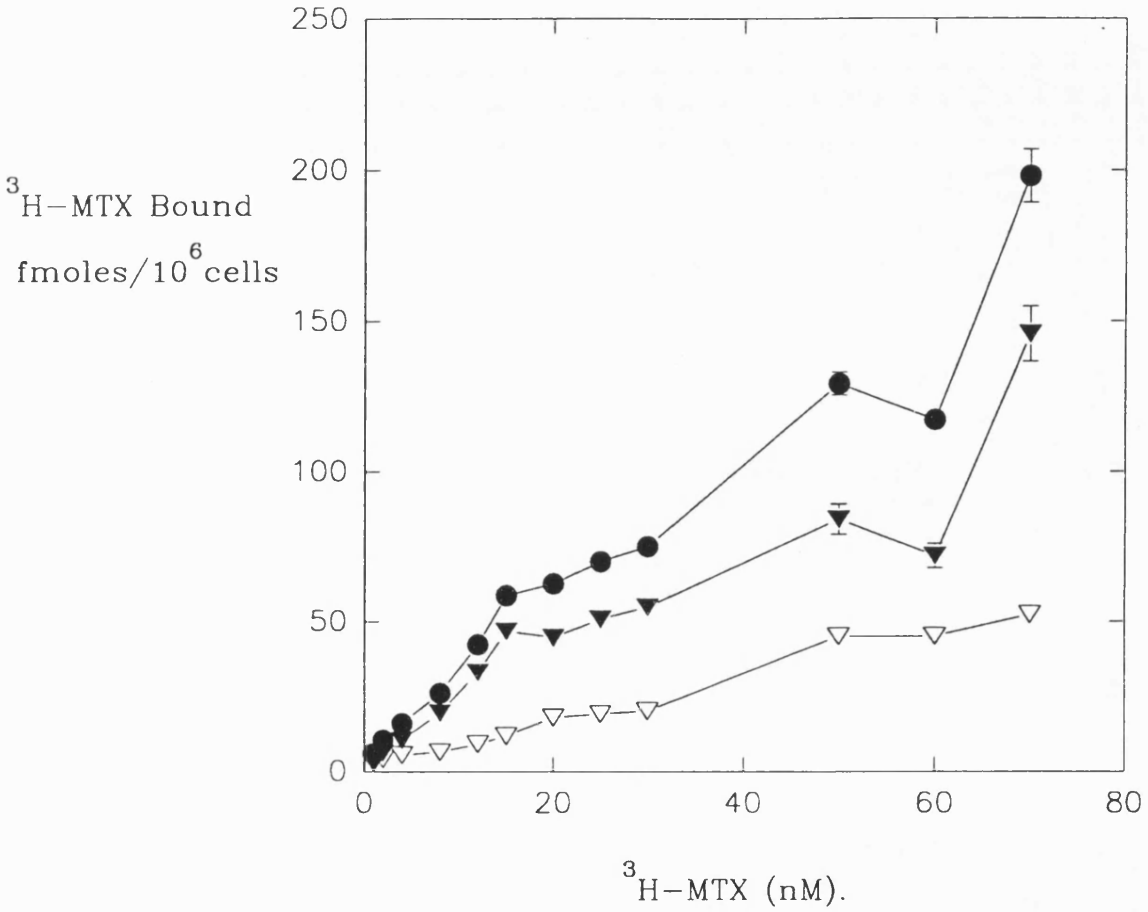

Figure 4.4: II. Adsorption isotherm of increasing concentrations of ^{3}H-MTX incubated with B16 cells at 4^0C for 30 minutes at pH 7.4. Each point represents the mean±sd for 6 wells. Total (●), specific (▼) and non-specific (▽) binding respectively.

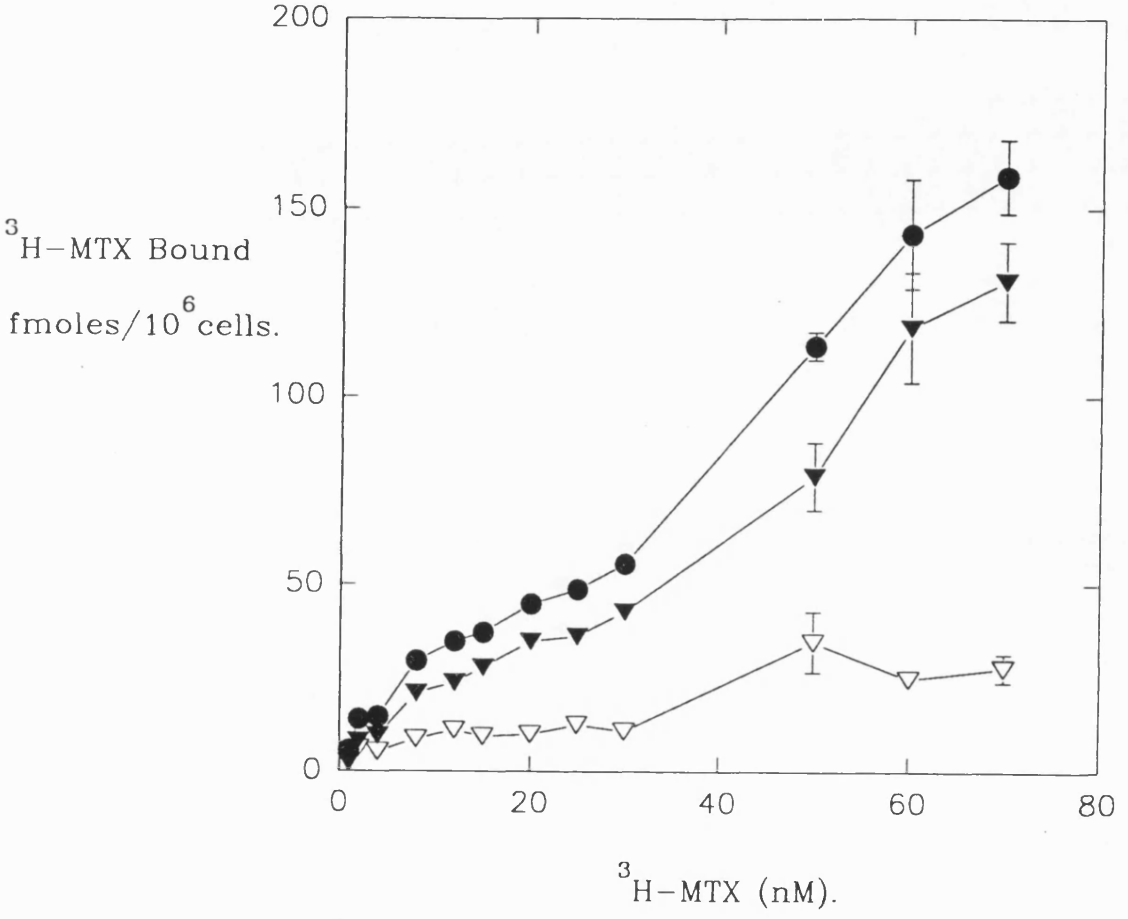

Figure 4.5: III. Adsorption isotherm of increasing concentrations of ^{3}H-MTX incubated with B16 cells at 4^{0}C for 30 minutes at pH 7.4. Each point represents the mean±sd for 6 wells. Total (●), specific (▼) and non-specific (▽) binding respectively.

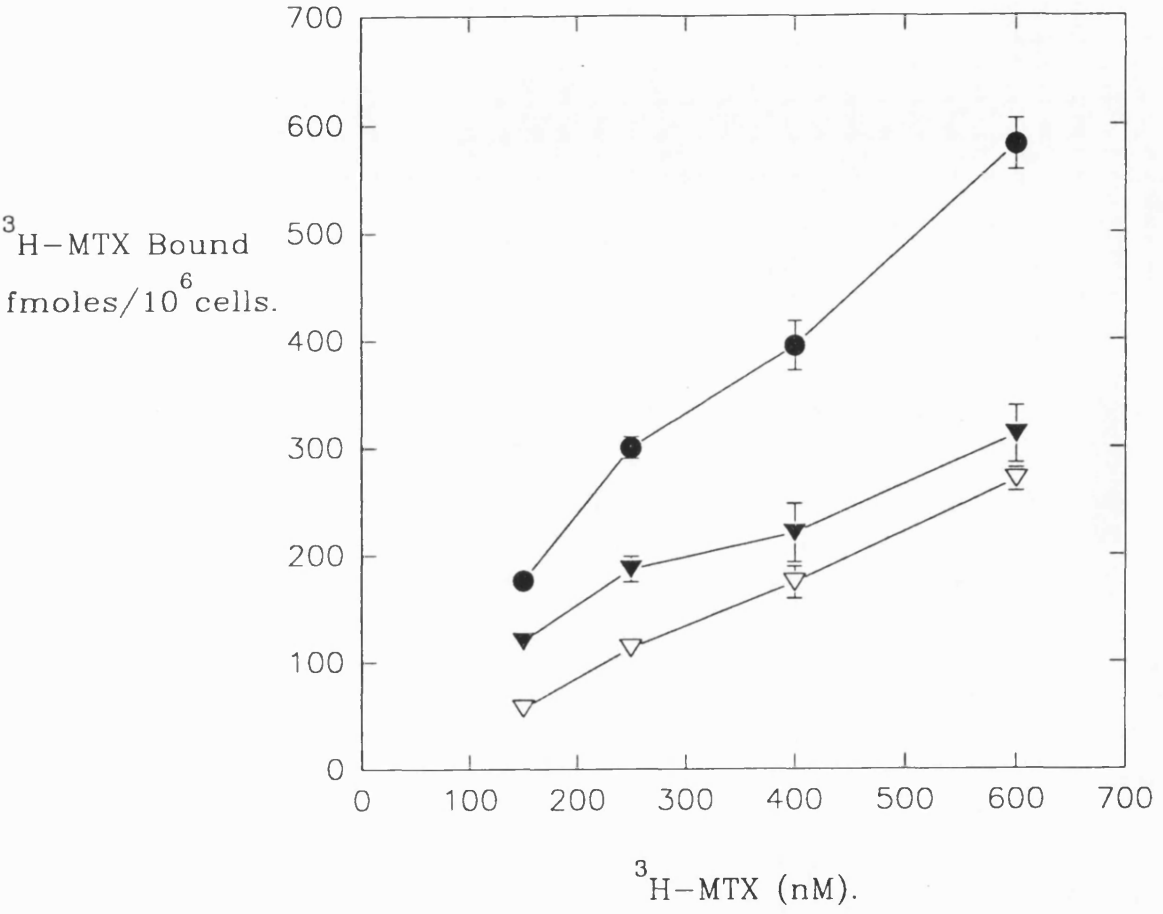

Figure 4.6: I. Adsorption isotherm of high concentrations of ^{3}H-MTX incubated with B16 cells at 4^0C for 30 minutes at pH 7.4. Each point represents the mean±sd for 6 wells. Total (●), specific (▼) and non-specific (▽) binding respectively.

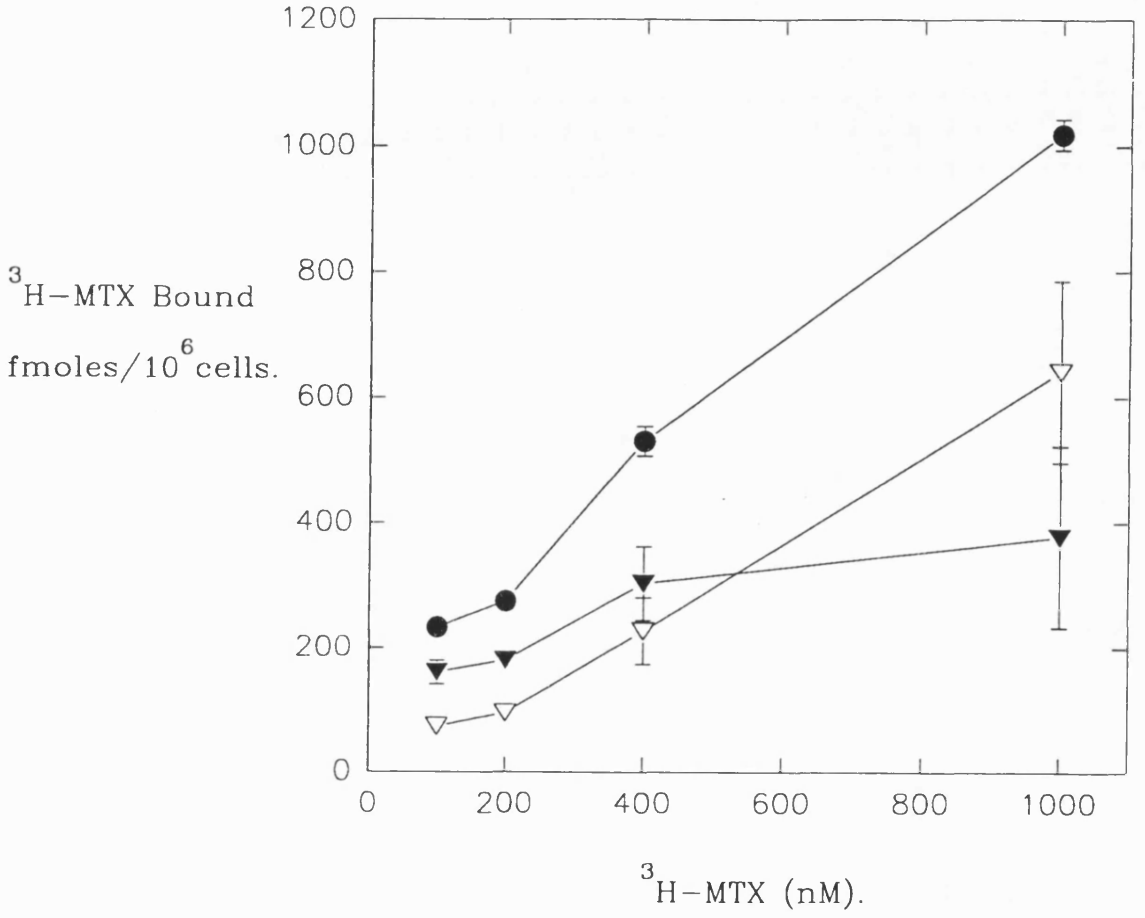

Figure 4.7: II. Adsorption isotherm of high concentrations of ^{3}H-MTX incubated with B16 cells at 4^{0}C for 30 minutes at pH 7.4. Each point represents the mean±sd for 6 wells. Total (●), specific (▼) and non-specific (▽) binding respectively.

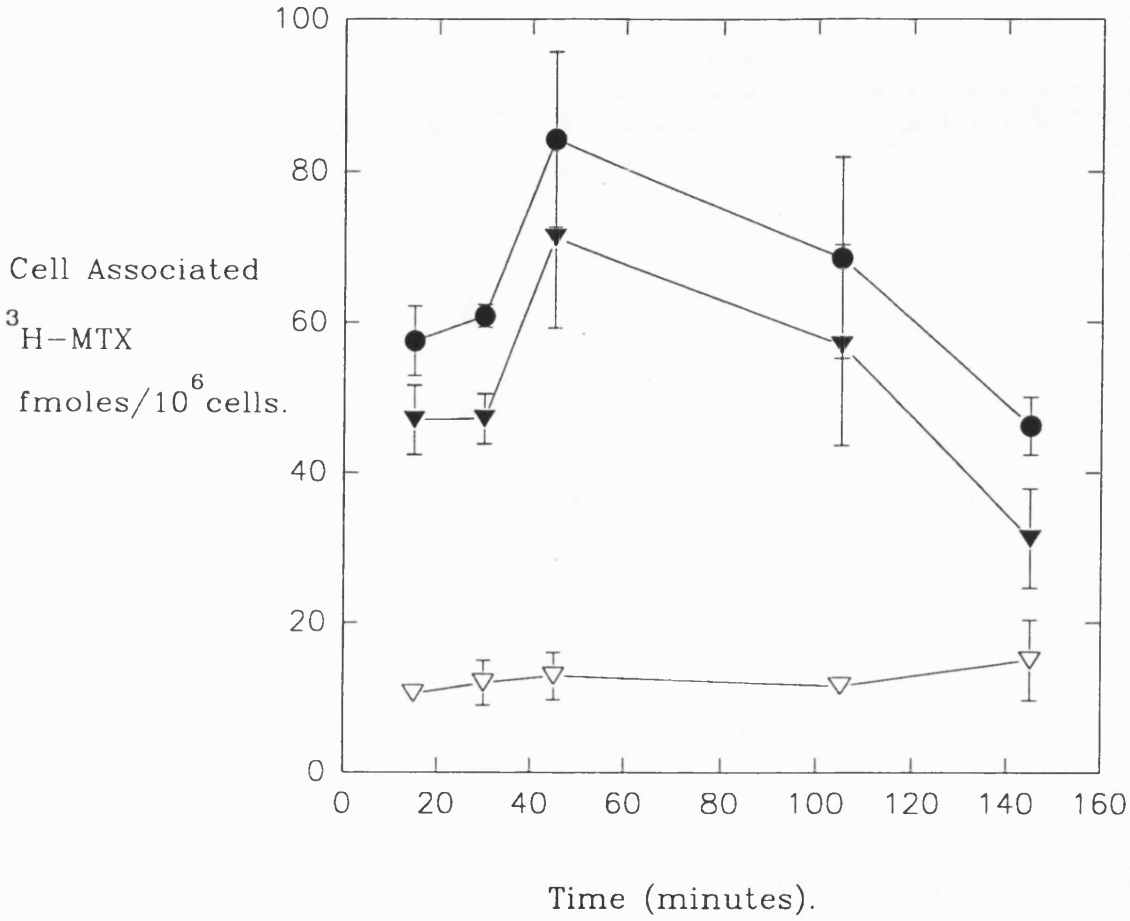

Figure 4.8: Incubation of 50nM ^{3}H-MTX with B16 cells at 37^{0}C with time. Each point represents the mean±sd for 6 wells. Total (●), specific (▼) and non-specific (▽) binding respectively.

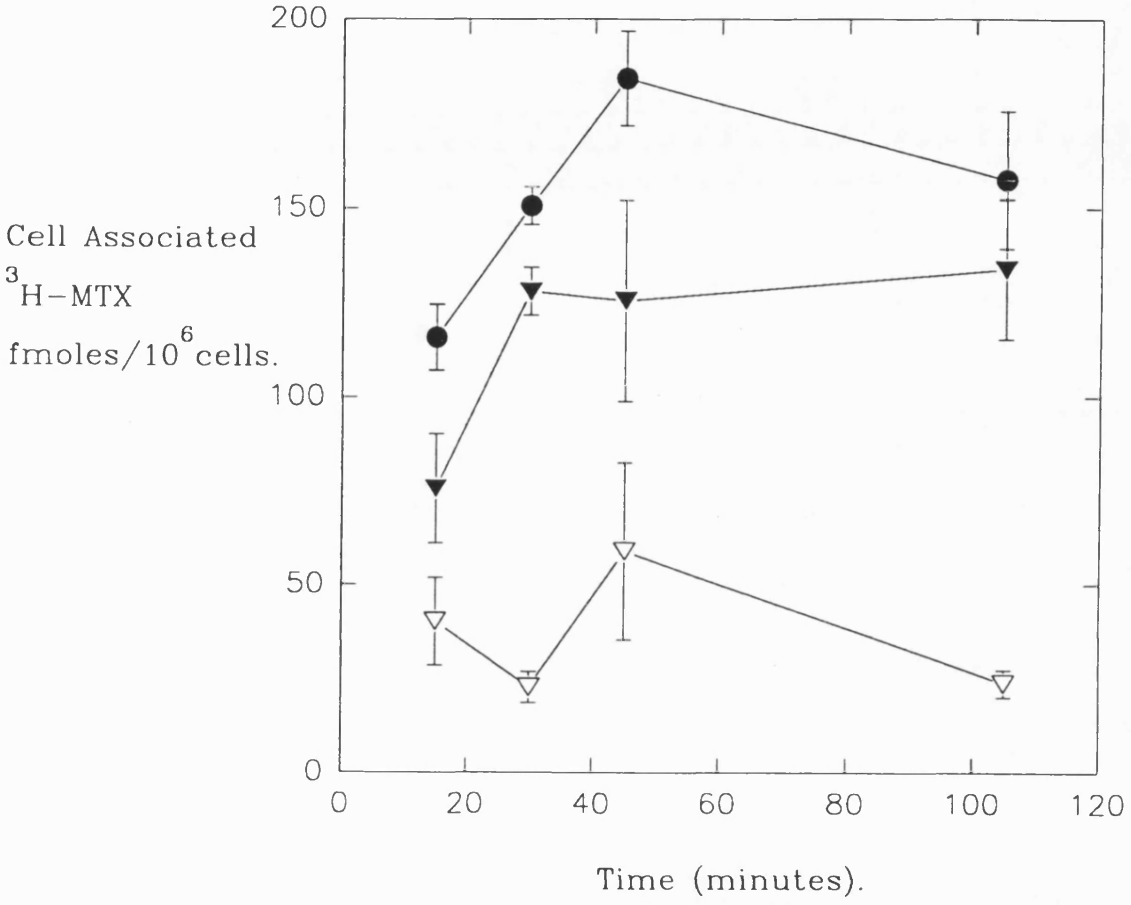

Figure 4.9: Incubation of 100nM ^{3}H-MTX with B16 cells at 37^{0}C with time. Each point represents the mean±sd for 6 wells. Total (●), specific (▼) and non-specific (▽) binding respectively.

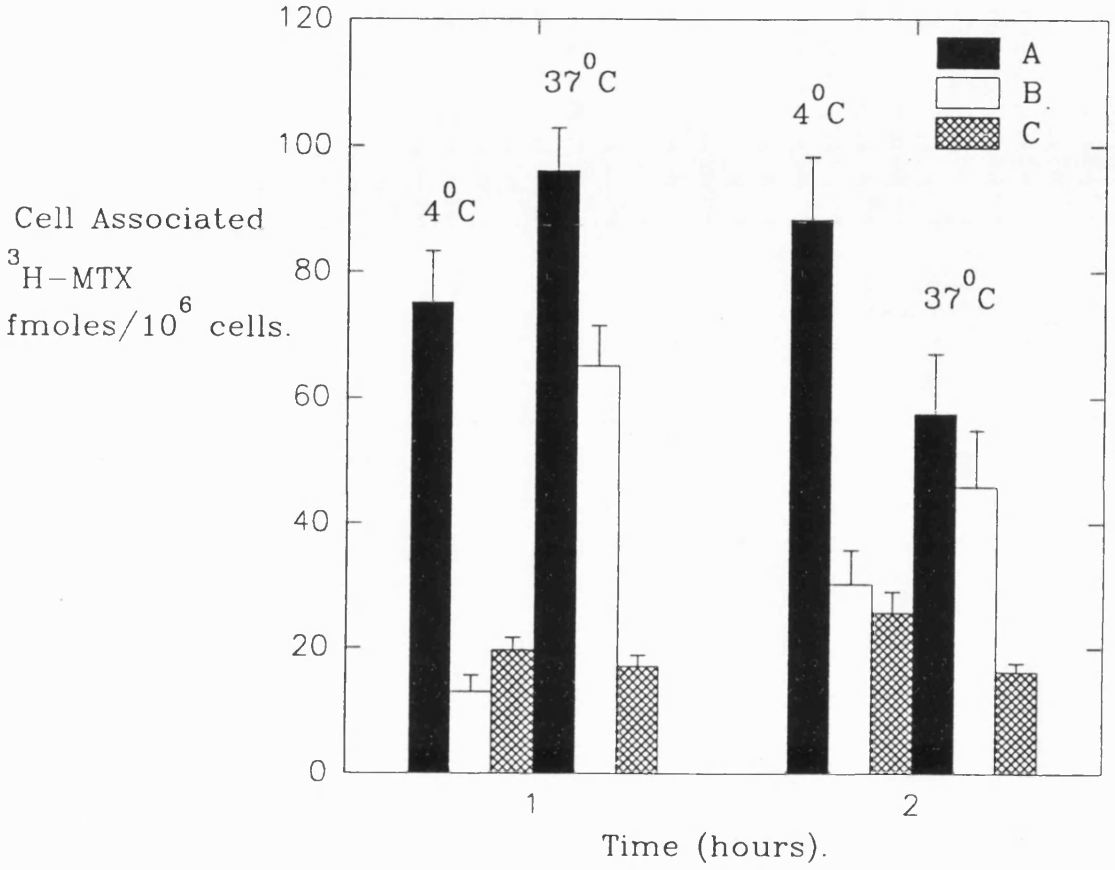

Figure 4.10: Incubation of 100nM ^{3}H-MTX with B16 cells at 4^{0}C and 37^{0}C respectively for 1 and 2 hours. Each incubation was terminated with ice-cold PBS after which a set of wells at each time point (exposed to labelled tracer only) received a 5 minute (4^{0}C) acid-wash. All wells were then treated in the usual manner. Each bar represents the mean±sd for six wells. Total binding (A), acid-washed cells (B) and non-specific binding (C).

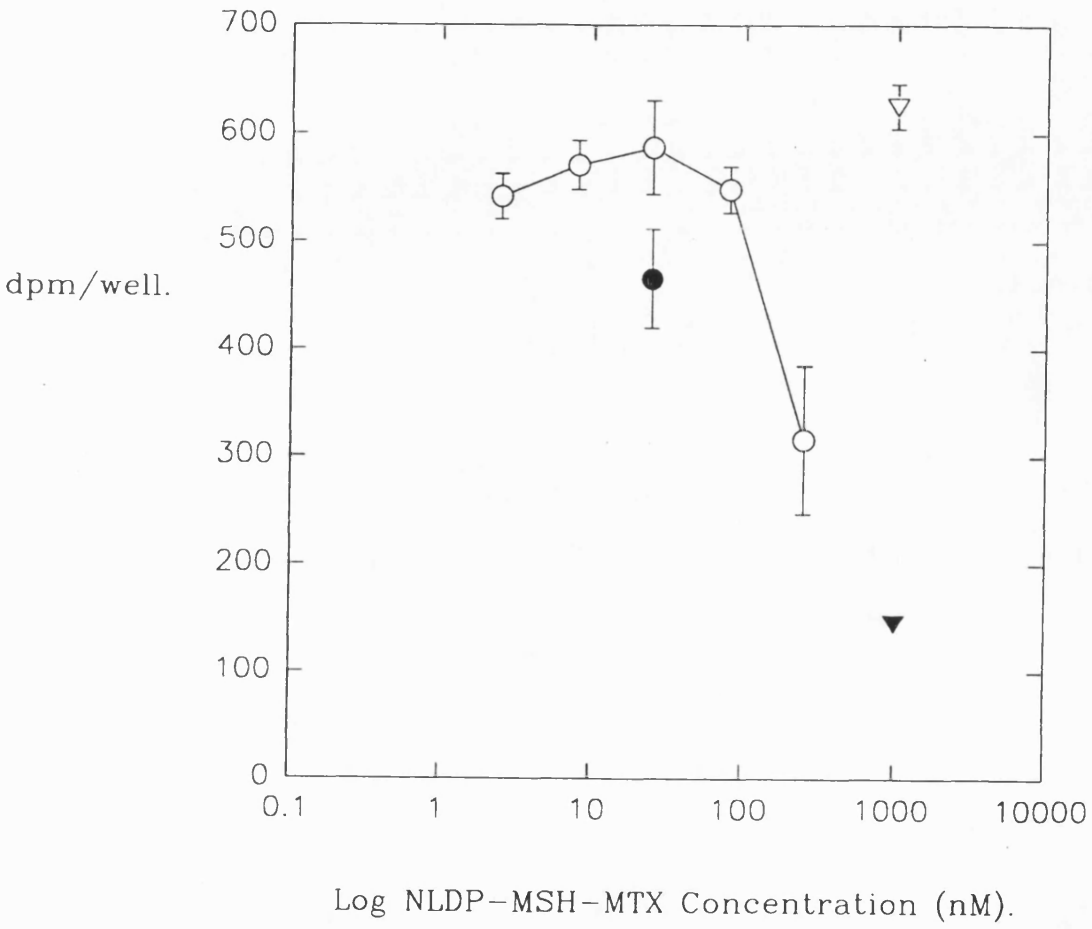

Figure 4.11: I. ^{3}H activity after incubation of 25nM ^{3}H-MTX with B16 cells at 4^{0}C for 30 minutes in the presence of increasing concentrations of the two conjugate forms of NLDP-MSH-MTX, G0133/1 (O) and G0133/3 (●). Each point represents the mean±sd for 6 wells, total (▽) and non-specific (▼) binding from 12 wells was measured in the absence of NLDP-MSH-MTX.

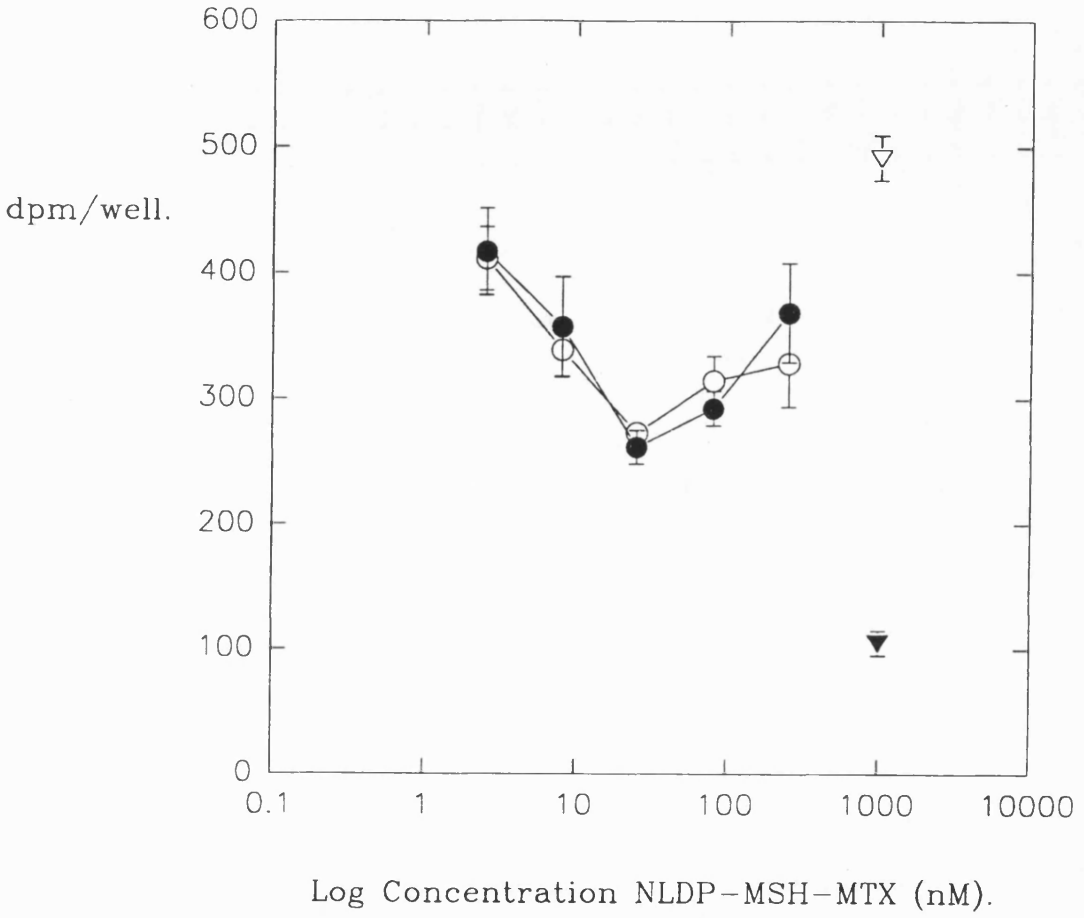

Figure 4.12: II. ^{3}H activity after incubation of 25nM ^{3}H-MTX with B16 cells at $4^{0}C$ for 30 minutes in the presence of increasing concentrations of the two conjugate forms of NLDP-MSH-MTX, G0133/1 (○) and G0133/3 (●). Each point represents the mean±sd for 6 wells, total (▽) and non-specific (▼) binding from 12 wells was measured in the absence of NLDP-MSH-MTX.

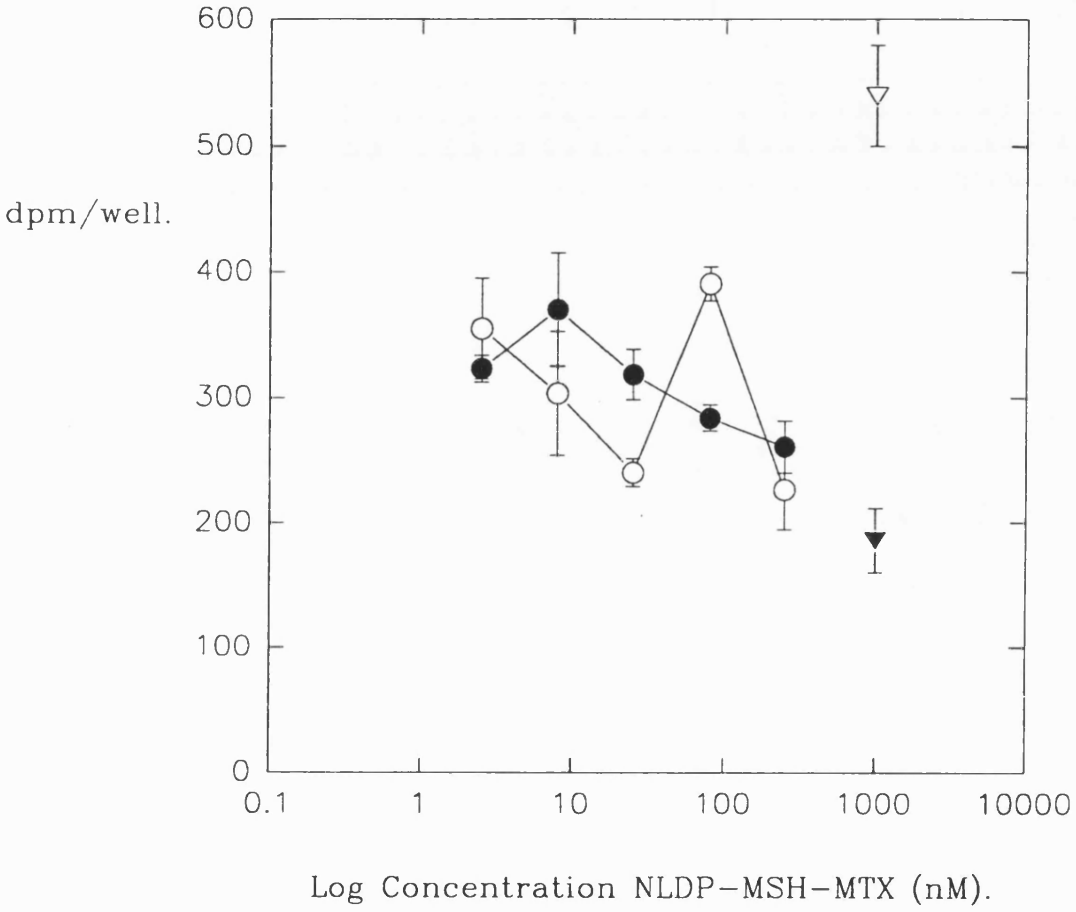

Figure 4.13: III. ^{3}H activity after incubation of 25nM ^{3}H-MTX with B16 cells at 4^{0}C for 30 minutes in the presence of increasing concentrations of the two conjugate forms of NLDP-MSH-MTX, G0133/1 (○) and G0133/3 (●). Each point represents the mean±sd for 6 wells, total (▽) and non-specific (▼) binding from 12 wells was measured in the absence of NLDP-MSH-MTX.

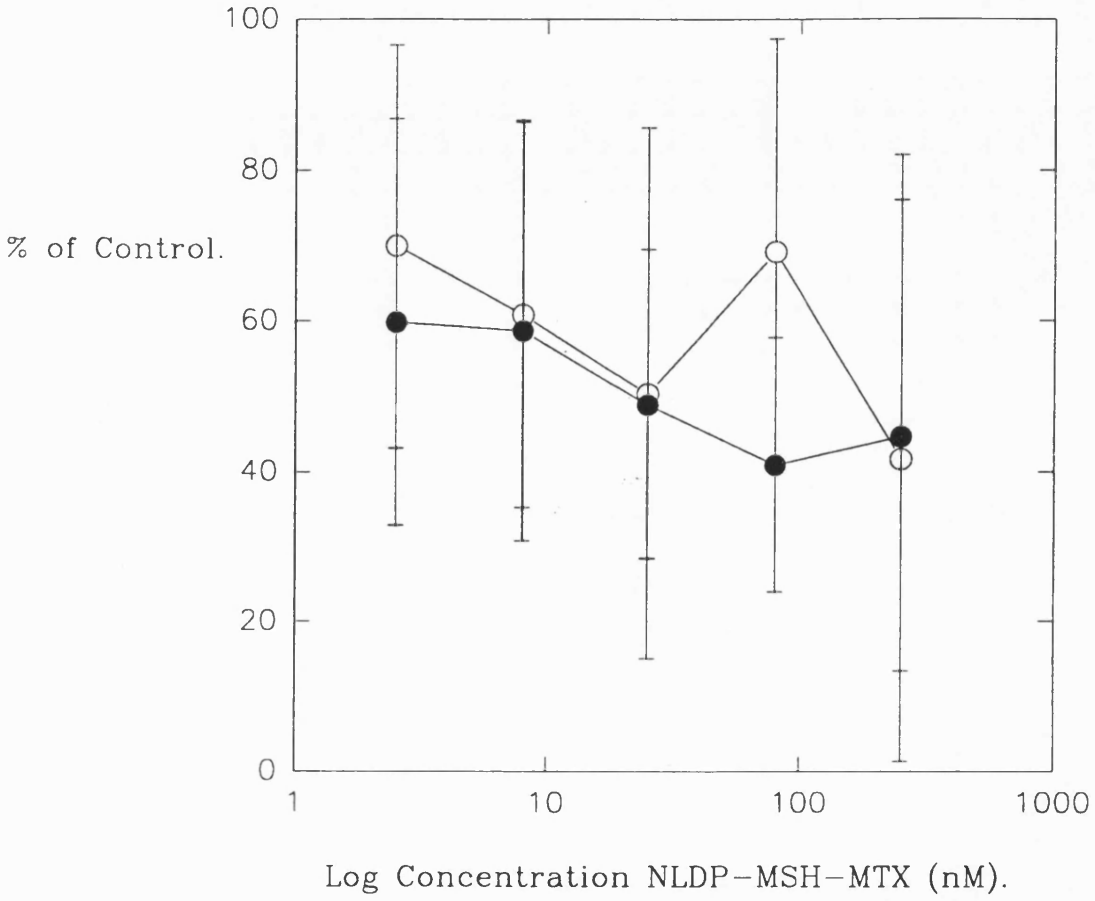

Figure 4.14: Inhibition of 25nM ^{3}H-MTX binding with B16 cells at 4^{0}C by two conjugates of NLDP-MSH-MTX for 30 minutes. Values are expressed as a % of the control binding (control equals specific binding of ^{3}H-MTX in the absence of conjugate) from single wells in individual experiments and represents the mean±sd from a minimum of 12 wells per point. G0133/1 (O) and G0133/3 (●).

4.4 Discussion

The cellular uptake of MTX briefly mentioned in the introduction to this thesis has been well reviewed by Sirotnak [120], when the difference in membrane transport of this folate analogue was compared between normal and tumour growing mammalian cells. Normal cells of varying types and sources display large variability in V_{max} and K_m at 37^0C, 0.003-220nmol/min/g dry weight and 0.6-2300μM respectively. Whereas tumour cells show greater similarity, 1.1-12.2nmol/min/g for V_{max} and 2.3-26.2μM for K_m. This has been described as the classical 'high affinity, low capacity' folate system in tumour cells which displays high saturability for reduced folates (5-methyltetrahydrofolate and 5-formyltetrahydrofolate) but very poor affinity for folic acid. Sirotnak suggested, in review of other work, that this effective transport of serum folates may be essential for tumour growth as these cells may rely more strongly on de novo synthesis of nucleic acid precursors, a process highly folate dependent.

Much work has focused on the presence of a second membrane folate binding protein which has been observed specifically in cell lines grown under physiological levels of folates [124, 125, 126, 127, 128, 190], or in the continued presence of MTX [188]. Normal tissue culture media contains folic acid in the order of 2μM, whereas serum concentration of folates (5-methyltetrahydrofolate being the predominant folate) are 5-50nM [189]. Jansen et al. [124] grew L1210 mouse leukemic cells in progressively decreasing concentrations of folate and discovered the cells expressed high levels of a membrane-associated folate binding protein in addition to the 'classical' high affinity/low capacity carrier as described by Sirotnak [120]. Similar findings were also found by Henderson et al. [128] with the same cell line. In support of this, multiple membrane associated folate binding proteins have been observed in human leukemic and epidermoid carcinoma cells [191, 192].

The significance of this second folate binding protein in MTX binding and uptake is unclear. Attempts to grow B16 cells in low folate medium proved unsuccessful

in the time scale tested. Cell growth became almost static presumably due to the lack of intracellular folate. Growth was slightly increased upon the addition of 5-methyltetrahydrofolate indicating some uptake had occurred and when the cells were re-incubated in standard media cell growth returned to normal (as compared to control cells) in only three passages. This demonstrated the cells retained the ability to transport folates into the cell.

Although growth became static at one point, binding experiments may have revealed the presence of a high affinity binding protein which has shown even greater affinity for folates upon cell incubation in completely folate free media [125].

The likelihood of this second binding protein being expressed in cells cultured in standard medium is unlikely, its presence/activity could have been measured in two ways. Firstly measuring the binding activity of ^{3}H-folic acid at low concentrations. The membrane binding protein has a far greater affinity for folic acid compared to the reduced folate carrier [126]. Secondly measuring the uptake of ^{3}H-MTX in the presence of thiamine pyrophosphate which inhibits transport via the reduced folate carrier but not by the membrane binding protein [66]. The binding data for ^{3}H-MTX at 4^0C was therefore treated with a least squares minimisation programme for one binding site (although a fit could be obtained for two sites the errors were much greater). The values obtained for the binding dissociation constant K_d, and the maximum amount bound were in the order of 0.21μM and 453fmoles/10^6cells respectively. Few values for the binding affinity for MTX at 4^0C are available in the literature for cells grown in normal tissue culture media. Henderson using mouse leukemic L1210 cells [187] obtained a K_d value of 0.35μM. Human epidermoid carcinoma cells grown in low folate media had a K_d for surface binding of MTX of c.0.2μM, other cell lines under similar conditions have displayed greater affinity than B16 cells, L1210 cells 30-35nM [126], and monkey kidney cells 20nM [193].

Uptake of ^{3}H-MTX by B16 cells was initially difficult to establish with only a

measure of cell-association being obtainable. Once a suitable acid-wash technique was available uptake was demonstrated after a 1 and 2 hour incubation with 100nM extracellular ^{3}H-MTX at 37^{0}C. An identical incubation at 4^{0}C using an acid-wash effectively removed all surface-bound ligand from the cells, showing no uptake had occurred. Although uptake has occurred at 37^{0}C, this does not confirm its occurrence directly via the binding site (at 4^{0}C), but transport was inhibited by PCMPS and thiamine pyrophosphate, both known inhibitors of the reduced folate carrier. One method to resolve this problem would be to allow binding at 4^{0}C, wash the cells and reincubate in ligand free medium at 37^{0}C for various time periods followed by an acid-wash treatment. There are many examples of MTX transport via the reduced folate carrier [187, 188, 194], in the review by Sirotnak [120] the V_{max} at 37^{0}C varies from 1-12nmol/min/g in various tumour cell types.

Uptake of MTX has also been demonstrated via the folate binding protein present in cells grown at physiological levels of folate [66, 124, 126, 195, 129, 196, 130, 131]. Westerhof et al. [132] even demonstrated the uptake of MTX in a previously MTX transport resistant human leukemic cell line, transferred to growth in low folate medium. The folate binding protein unlike the reduced folate carrier has high affinity for folic acid K_d 0.9nM [126], 0.07nM [66], 0.7nM [132], which is greater than for the reduced folates, whilst MTX has a low affinity. It appears that transport via this protein is regulated by the intracellular folate content of the cell [193, 130], whilst binding is relatively unaffected. The exact nature of influx is unclear however some authors have pointed towards receptor-mediated endocytosis and recycling of the protein [66, 126, 193, 130, 131, 132, 133], partly due to the relatively slow rate of uptake (2.1 molecules of ^{3}H-MTX/binding site/hour for L1210-JT3 human leukemic cells in low folate medium [132]).

The question arises as to what degree do either of these transport pathways play in the uptake of folates and in particular the antifolate MTX. This problem has recently been addressed by Westerhof et al. [126] using L1210 cells and a subline L1210-B73 grown in low folate media which expressed both the reduced folate

carrier and the folate membrane binding protein. Exploiting the difference in affinities for various compounds by the two binding/transport sites, they were able to evaluate uptake of folates and antifolates. They discovered the membrane folate binding protein mainly mediated the influx of folic acid (c.98%) and 5-formyltetrahydrofolate (c.81%), as opposed to MTX which was less than 30%. They concluded the membrane transport (and therefore the cytotoxicity) of MTX in the L1210-B73 cells was predominantly via the reduced folate carrier, this is not suprising since the folate binding protein has poor affinity for MTX. Similar findings were reported by Jansen and Schnoragel in a human leukemic cell line [195]. It must be noted at this point that these experiments have all occurred in tumour cell lines in culture, the role of these transport routes in vivo is not yet established.

From this brief overview of folate and MTX transport in tumour cell lines it is apparent that the influx of any NLDP-MSH-MTX conjugate in B16 melanoma cells due to the MTX moiety is likely to occur via the reduced folate carrier, the binding to which will give an indication to the amount of uptake expected. The maximum amount of binding of ^{3}H-MTX at 4^{0}C corresponded to c.270,000 binding sites/cell with a K_d value of 0.21μM. Uptake, under the culture conditions used, did not proceed continuously. The total cell-associated ^{3}H-MTX was similar at 37^{0}C and 4^{0}C, the only difference being that at 37^{0}C MTX had been internalised. The binding experiments with NLDP-MSH-MTX displayed no specific inhibition of 25nM ^{3}H-MTX by the conjugate up to a ten-fold greater concentration. It can only be concluded from this that the NLDP-MSH-MTX has at least ten-fold less affinity than MTX for the reduced folate carrier.

Chapter 5

Binding and Uptake of ^{125}I-Nle^4-D-Phe^7-αMSH

5.1 Introduction

In the design of a site-specific drug conjugate the targeting moiety is one of the most important factors. Without direction to the desired cell type the whole basis of drug targeting is undermined. The targeting component chosen in this study was alpha MSH (melanocyte stimulating hormone) or rather its analogue Nle^4-D-Phe^7-MSH (NLDP-MSH). This structure has been reported to have increased biological activity (measured by the activation of cell cAMP levels and tyrosinase activity) in mouse melanomas [197, 198, 199, 114, 200] and is less susceptible to enzymatic breakdown [114, 200, 201]. The binding of this analogue as with MSH, displays great specificity for sites on melanoma cells with a high binding affinity [198, 199, 114, 202, 203].

The radio-iodinated derivative of NLDP-MSH was used first for binding experiments as the procedure for its preparation has been well reported [113] and the high activity of the purified radio-isotope allows the detection of low receptor

populations. Cultures derived from the B16 mouse melanoma cell line have been used previously in binding and biological activity [197, 199, 114] studies of MSH.

The purpose of this study was to investigate the binding characteristics of ^{125}I-NLDP-MSH and its fate after interaction with B16 cells at 37^{0}C.

5.2 Methods

All methods are described in full in section 2.4. The use of 0.3mM 1,10-phenanthroline, an endopeptidase inhibitor [204], was based on its reported stabilising effect on MSH binding assays. The mechanism of stabilisation is thought to be prevention of degradation of the peptide [198, 199, 201, 203], which has been reported to occur in cell culture.

5.3 Results

5.3.1 Iodination of NLDP-MSH

The identity of the peptide was confirmed by FAB-MS, figure 5.1, (molecular weight 1647, calculated weight 1646). The protocol for the iodination procedure was based mainly on work by Eberle and colleagues [113] who used chloramine T as an oxidant. The purification of the reaction products was a two stage chromatographic procedure using a SepPak column and then HPLC. A typical trace from the latter (figure 5.2) displayed three peaks eluting at 30.5, 33.75 and 38 minutes respectively. Sixteen 1ml fractions were collected from 27 minutes onwards and their activity (figure 5.3) contained two main peaks which correspond well with the second two peaks on the trace. There was no significant activity associated with the first peak.

5.3.2 Washing Procedure

With the 12-well plates used in all the experiments, three washes of 3ml ice-cold PBS were sufficient to result in the removal of non-bound radio-ligand from the wells, as shown in table 5.1.

Wash Number	Experiment A	Experiment B
1	22,438.6	21,272.9
	21,445.7	21,534.4
	21,502.6	21,578.5
2	1,546.1	1,470.5
	1,153.1	1,871.0
	1,376.0	1,548.9
3	27.5	16.6
	15.0	10.6
	41.3	32.0

Table 5.1: The recorded washing activities (cpm) in 1ml taken from a total of 3ml PBS used per well. Each well was incubated with 1ml of 0.1nM ^{125}I-NLDP-MSH (c.300,000cpm). Incubation was for 8 hours at 4^0C in the absence (Experiment A) and presence (Experiment B) of excess unlabelled NLDP-MSH (1μM).

5.3.3 Binding of ^{125}I-NLDP-MSH at 4^0C

Incubation of B16 cells at 4^0C with 0.1 and 0.4nM ^{125}I-NLDP-MSH from 2-22 hours is displayed in figures 5.4 and 5.5. These concentrations were chosen to reflect the range used for binding isotherm experiments with the expectation that the low concentration would be more sensitive to the experimental conditions governing binding. Non-specific binding was recorded in the presence of 0.1μM unlabelled NLDP-MSH. The specific binding was obtained by subtracting the non-specific binding from the total binding.

At 0.4nM ^{125}I-NLDP-MSH binding effectively reached an equilibrium after 8 hours at 6fmoles/10^6cells, there being no significant increase over the next 14 hours. Non-specific binding represented approximately 40% of the total bound after 22 hours. At the lower concentration of 0.1nM almost identical binding kinetics were observed with out any discernable increase in binding after 8 hours. Non-specific binding again increased with time and represented about 40% of the total bound after 22 hours. All data points represent the mean and standard deviation from six wells and showed a small degree in variation. On the basis of this experiment an incubation period of 8 hours at 4^0C was chosen for the construction of a binding isotherm. Overnight incubation was avoided as prolonged time periods caused cells to be predominantly in a rounded state and liable to detachment.

The time taken to reach equilibrium at 4^0C appeared particulary long although it was in agreement with published work [199]. It was decided to investigate if the presence of the BSA (0.2%) in the binding medium delayed the time course of ^{125}I-NLDP-MSH binding to the cells. Albumin is well known to bind weakly with many compounds, indeed its presence in the medium is to 'coat' the plastic of the well and hence decrease the amount of non-specific binding. However it could also bind some of the tracer so prevent and/or delay the establishment of equilibrium binding to the cells. For this reason the bovine milk protein casein was chosen as a readily available substitute to examine any difference in binding kinetics.

An identical experiment to that represented in figure 5.4 was undertaken using an extracellular concentration of 0.1nM ^{125}I-NLDP-MSH (figure 5.6). The use of 0.2% casein resulted in a slow increase in binding over 22 hours with no sign of equilibrium occuring. Although the amount bound after 22 hours, 1.5fmoles/10^6cells, was identical to that determined with 0.2% BSA in the medium, binding in the presence of casein was still increasing after 22 hours. Initial values of specific binding were lower in the presence of casein and after 8 hours had not yet reached 1fmole/10^6cells. One advantage however was the apparent lower amount of non-specific binding which displayed only a small increase over the

time period, reaching c.0.3fmoles/10^6cells. BSA was chosen as the most suitable protein to use in the assay since binding equilibrium was attained after 8 hours.

Two separate binding isotherms are represented in figures 5.7 and 5.8 using extracellular concentrations of ^{125}I-NLDP-MSH ranging from 0.01 to 1.0nM. In the first experiment (figure 5.7) specific binding increased to reach 5fmoles/10^6cells at 0.8nM before decreasing to 3fmoles/10^6cells at 1.0nM. A similar degree of maximal binding was seen in figure 5.8 of 4fmoles/10^6cells at 1.0nM, whilst non-specific binding remained low reaching a maximum of 1fmole/10^6cells. However the second experiment displayed a greater increase in non-specific binding at 0.8 and 1.0nM to reach values of almost 3fmoles/10^6cells. This increase observed in the final two points could have been due to inadequate washing of the wells.

The mathematical procedure for determining binding parameters from the data was used, as described for ^{3}H-MTX (see chapter 4). Values for the association or affinity constant and the number of binding sites/cell are displayed in table 5.2. One class of binding site for MSH derivatives was assumed.

Experiment Number	K_a x$10^{-9}M^{-}1$	B_{max} fmoles/10^6cells	N sites/cell
1	1.15 ± 0.53	8.90 ± 2.69	5361 ± 1620
2	2.67 ± 1.13	5.62 ± 1.29	3384 ± 777

Table 5.2: The affinity constant (K_a), maximum bound (B_{max}) and the number of binding sites per cell (N) for the two binding isotherms, were obtained using a least squares minimisation fit to the data with the computer programme MINSQ.

The values for the affinity constant of 8.9 and 5.6 x $10^{-9}M^{-1}$ can be expressed as dissociation constants of 0.87 and 0.37nM respectively. The two experiments gave similar estimates of the number of binding sites/cell, considering binding was undertaken on cells of different passage number. A weighting value of one was used for the least squares fit as the majoritory of data points were located at the beginning of the isotherm, and also due to the relatively larger standard deviations at higher extracellular ^{125}I-NLDP-MSH concentrations.

5.3.4 Uptake of ^{125}I-NLDP-MSH by B16 cells at 37^{0}C

The cell association of the radio-ligand with B16 cells was measured at 37^{0}C (figure 5.9) using an extracellular concentration of 0.1nM. The cells were incubated for varying periods of time before being washed with ice-cold PBS, after which some wells received an acid-wash treatment identical to that used in chapter 4 with ^{3}H-MTX.

Specific binding of the tracer reached a maximum of 0.8fmoles/10^{6}cells after 30 minutes before steadily decreasing over the remainder of the experiment. It was discovered that with all 37^{0}C work a degree of cell detachment occurred after 120 minutes, therefore subsequent incubations at this temperature were limited to 80 minutes. Non-specific binding remained relatively low except for an apparent small increase at 30 and 40 minutes, the reason for which is unknown. The data from the acid-washed cells showed a gradual increase to reach c.3fmoles/10^{6}cells after 60 minutes. Some of the decrease in binding beyond 60 minutes may have been due to some cell detachment. Acid-washed treatment removed all extracellular bound ligand (as will be demonstrated subsequently) and thereby represented internalised ^{125}I-label. At 37^{0}C ^{125}I-NLDP-MSH was internalised (either complete or in a fragmented form) by B16 cells, the amount increasing with time. After 1 hour approximately 40% of the cell-associated radioactivity was within the cell.

Cell surface binding was more rapid at 37^{0}C, reaching a value of 0.8fmoles/10^{6}cells in 30 minutes, whereas at 4^{0}C it took 2 hours to reach 1fmole/10^{6}cells.

The internalisation observed at 37^{0}C could have been explained by mechanisms other than the MSH binding site. To investigate further, cells were first incubated at 4^{0}C for 1 hour with 0.5nM ^{125}I-NLDP-MSH to allow binding to occur. Cells were then washed (to remove unbound radioligand) and reincubated at 37^{0}C in the absence (figures 5.10 and 5.11) or presence (figures 5.12 and 5.13) of excess unlabelled NLDP-MSH.

Attempts were primarily made using a lower concentration of ligand for a longer time period at 4^0C but cells were observed to detach upon re-incubation at 37^0C. This problem was circumvented by using a shorter period at 4^0C which necessitated increasing the concentration of tracer to achieve a reasonable amount of binding.

Experiments in figures 5.10 and 5.11 show very similar trends, initial specific binding in the range of 4-6fmoles/10^6cells after the 4^0C incubation. Acid-washing in all these experiments after incubation at 4^0C displayed complete removal of ^{125}I-NLDP-MSH, i.e. all the ligand was surface bound at zero time, prior to re-incubation. For the experiment shown in figure 5.11 acid-wash treatment on cells incubated with excess unlabelled NLDP-MSH at 4^0C (non-specific binding), gave almost identical results to the same treatment in the absence of cold NLDP-MSH (0.86fmoles/10^6cells). However this value is a little lower than that for non-specific binding (1.41fmoles/10^6cells) indicating the possible removal of a small amount of non-specific bound radioligand.

On re-incubation at 37^0C the total specific binding decreased rapidly over the 80 minute period. Internalisation of the tracer in both figures 5.10 and 5.11 reached a maximum of c.1.75fmoles/10^6cells after 10-20 minutes before declining over the remaining 60 minutes. Non-specific binding decreased at 37^0C and (as in figure 5.10) there was little difference between it and the acid-wash values.

To investigate whether cooperativity could have occurred identical experiments were performed as described previously except the incubation buffer at 37^0C contained excess unlabelled NLDP-MSH (0.5μM). The results as shown in figures 5.12 and 5.13 show no discernable difference in the internalisation, decrease in specific binding or the degree of non-specific binding. Both experiments as in figures 5.10 and 5.11, exhibited similar values for specific binding (4-6fmoles/10^6 cells) after the 4^0C exposure, which then decreased with incubation at 37^0C. The profiles of the four graphs were very similar with the amount of surface-bound ^{125}I-NLDP-MSH decreasing rapidly at 37^0C with a corresponding small amount

of internalisation.

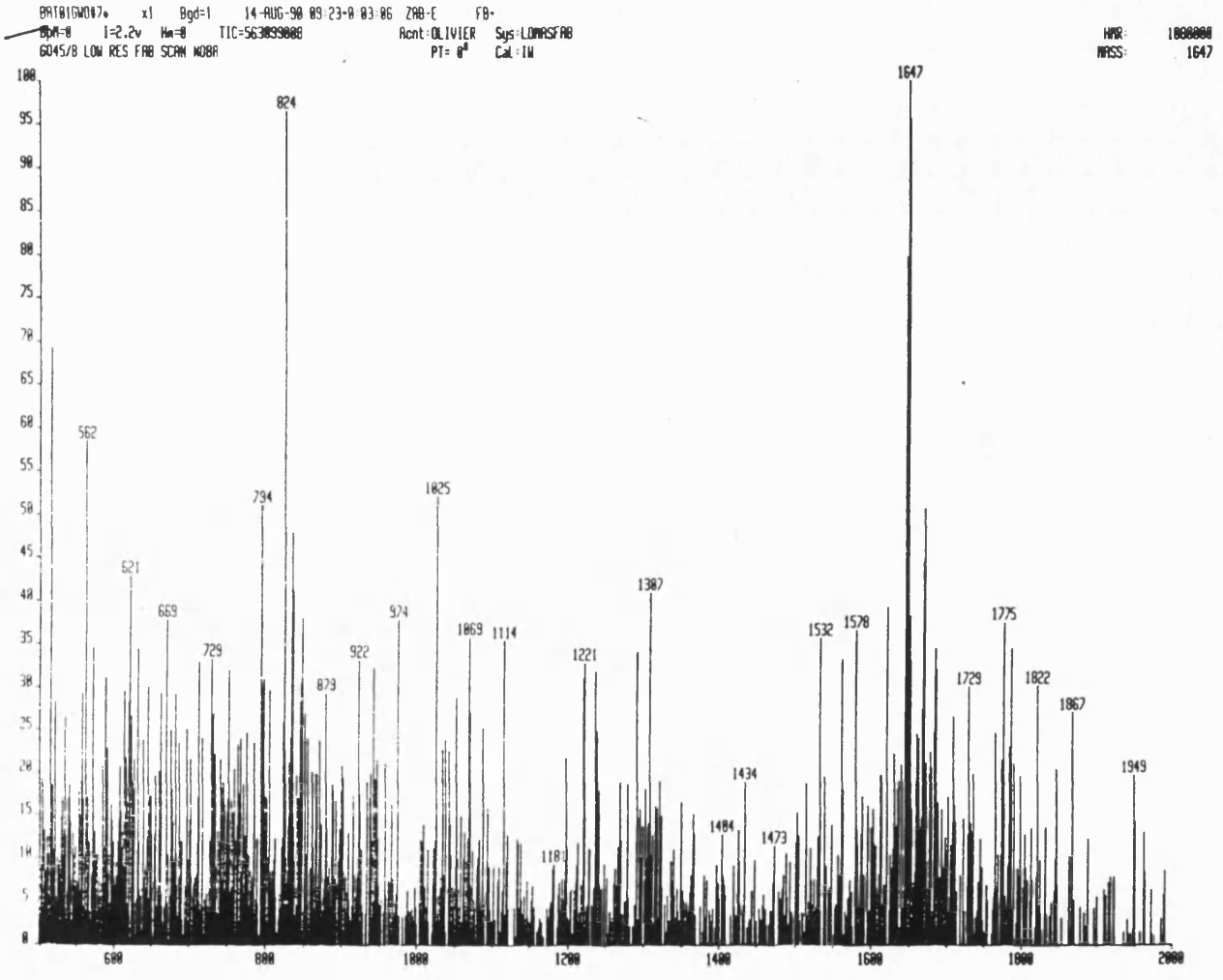

Figure 5.1: The FAB mass spectrometry of NLDP-MSH.

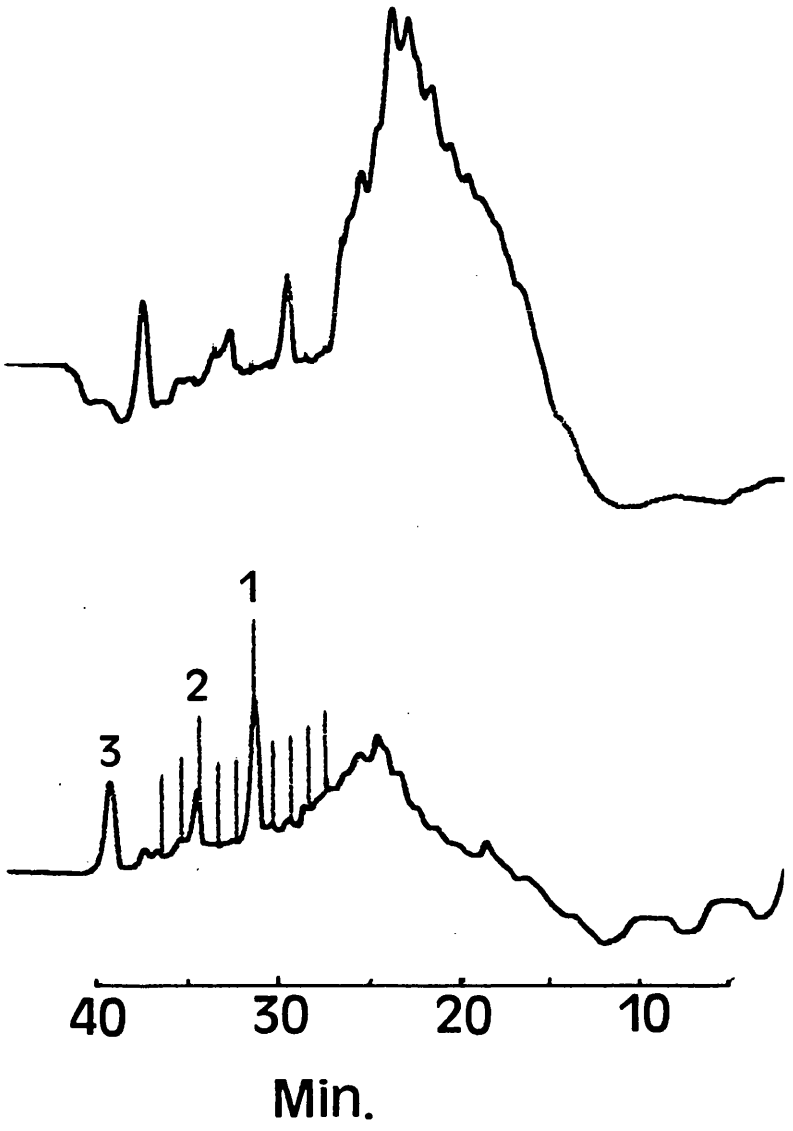

Figure 5.2: HPLC purification of the reaction products from the iodination of NLDP-MSH as measured by UV adsorption at 217nm. Peaks 1, 2 and 3 are thought to represent non-labelled, mono-iodinated and di-iodinated peptide respectively.

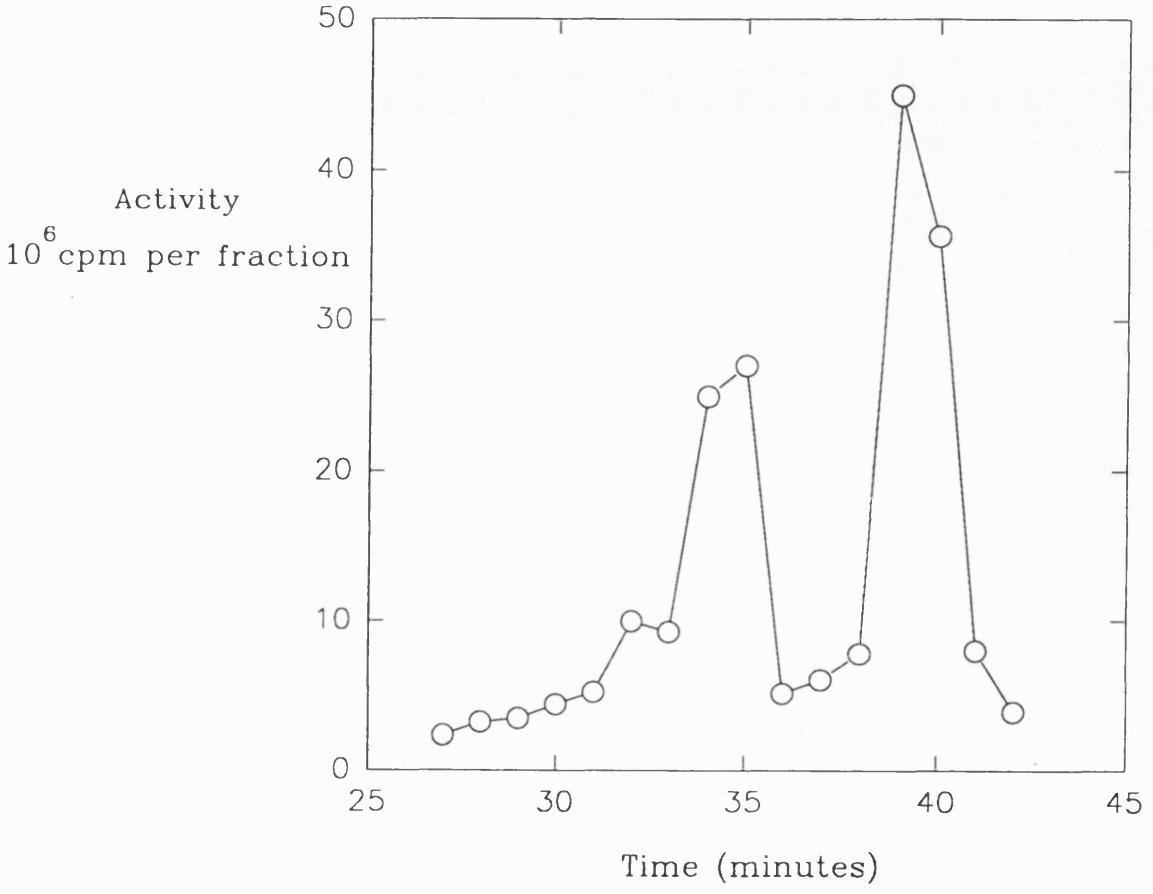

Figure 5.3: Activity per 1ml fraction from the HPLC purification of radio-iodinated NLDP-MSH from 27 minutes after the injection sample (flow rate 1ml/minute).

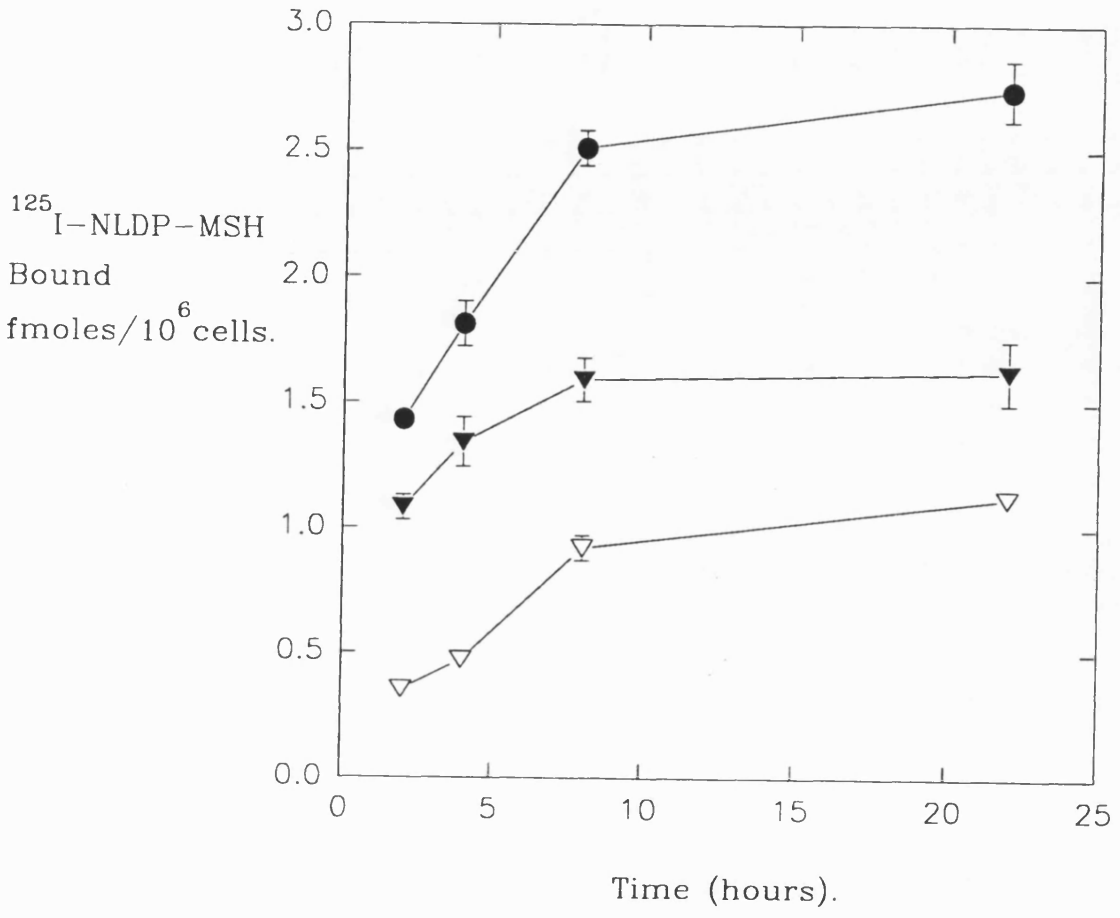

Figure 5.4: Binding of 0.1nM ^{125}I-NLDP-MSH with B16 cells at 4°C with time in a Hepes based buffer containing 0.2% BSA, pH 7.4. Each point represents the mean±sd from 6 wells. Total (●), specific (▼) and non-specific binding (▽) respectively.

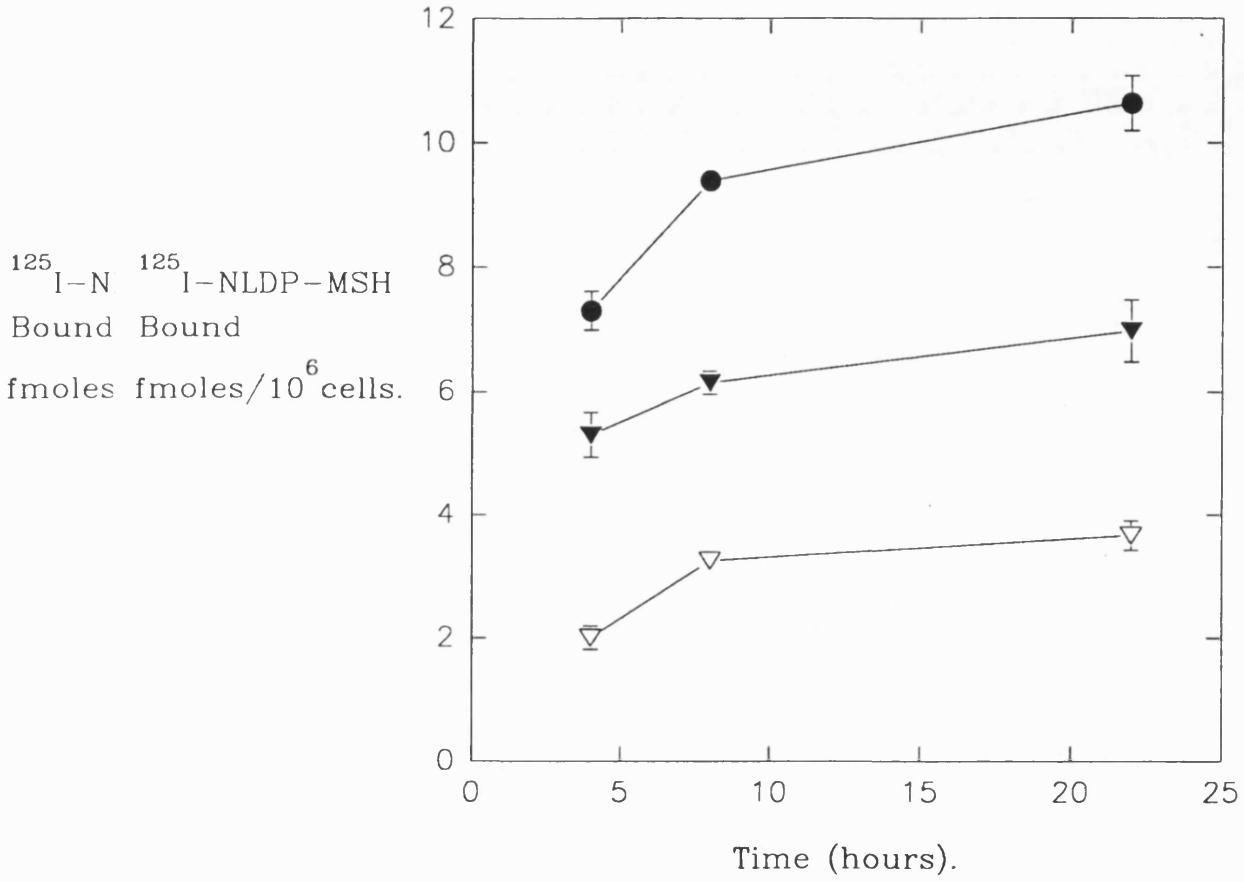

Figur
in a
the n
respe

Figure 5.5: Binding of 0.4nM ^{125}I-NLDP-MSH with B16 cells at 4^{0}C with time in a Hepes based buffer containing 0.2% BSA, pH 7.4. Each point represents the mean±sd from 6 wells. Total (●), specific (▼) and non-specific binding (▽) respectively.

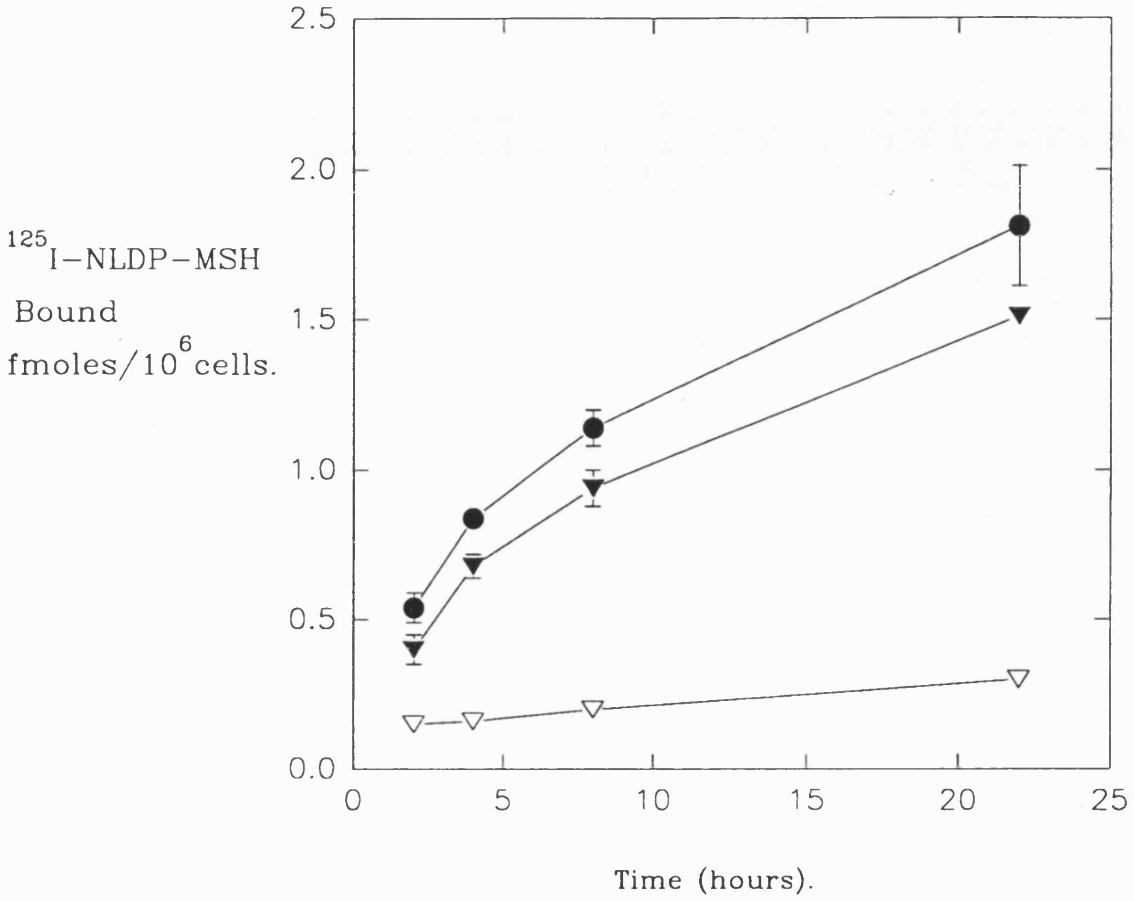

Figure 5.6: Binding of 0.1nM ^{125}I-NLDP-MSH with B16 cells at 4^{0}C with time in a Hepes based buffer containing 0.2% casein, pH 7.4. Each point represents the mean±sd from 6 wells. Total (●), specific (▼) and non-specific binding (▽) respectively.

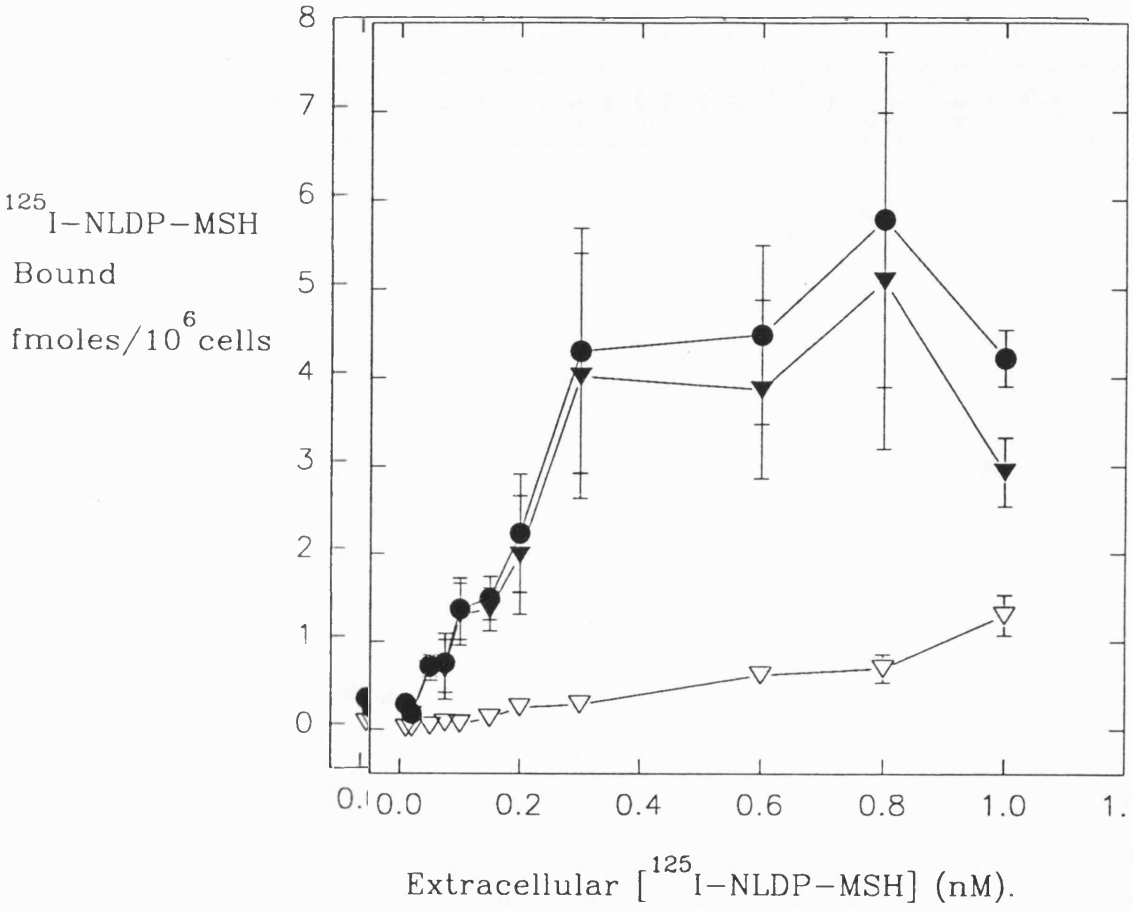

Figure 5.7: Adsorption isotherm of increasing concentrations of ^{125}I-NLDP-MSH incubated with B16 cells at 4^{0}C for 8 hours at pH 7.4. Each point represents the mean±sd from 6 wells. Total (●), specific (▼) and non-specific binding (▽) respectively.

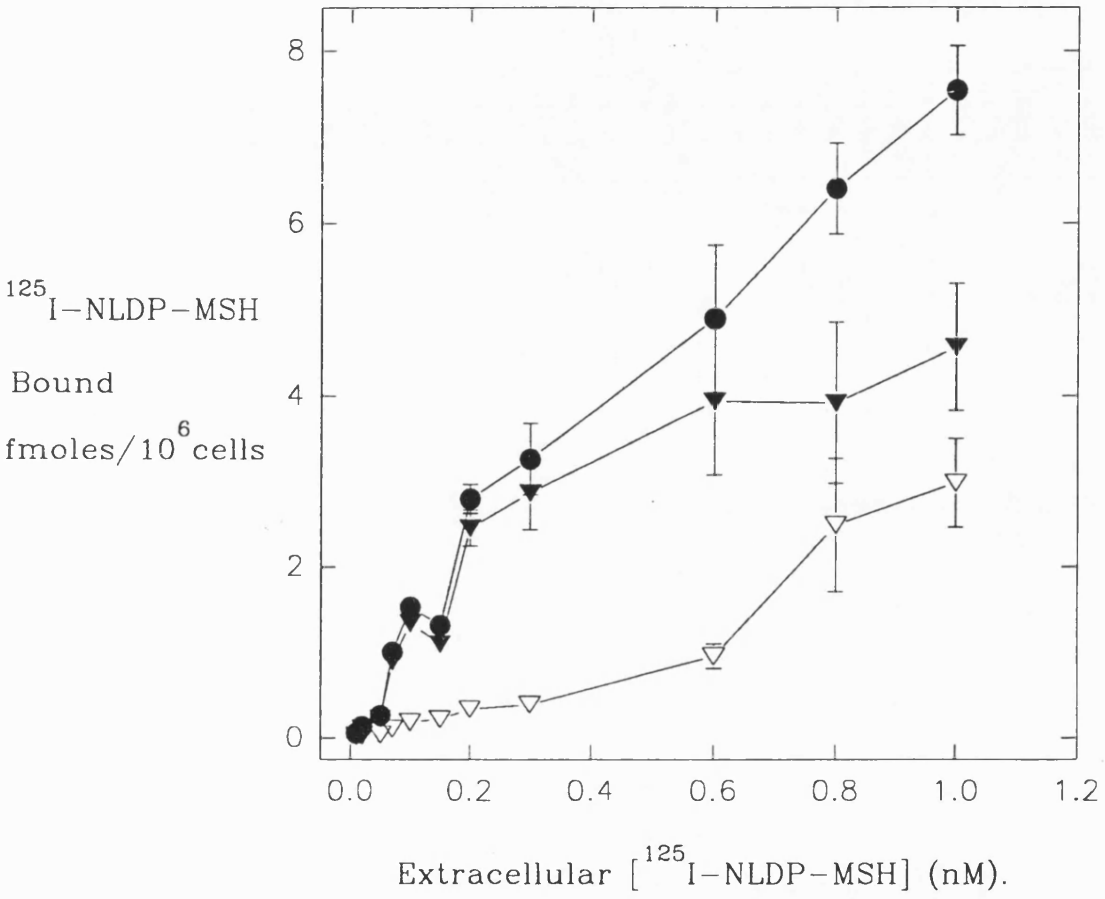

Figure 5.8: Second adsorption isotherm of increasing concentrations of ^{125}I-NLDP-MSH incubated with B16 cells at 4^{0}C for 8 hours at pH 7.4. Each point represents the mean±sd from 6 wells. Total (●), specific (▼) and non-specific binding (▽) respectively.

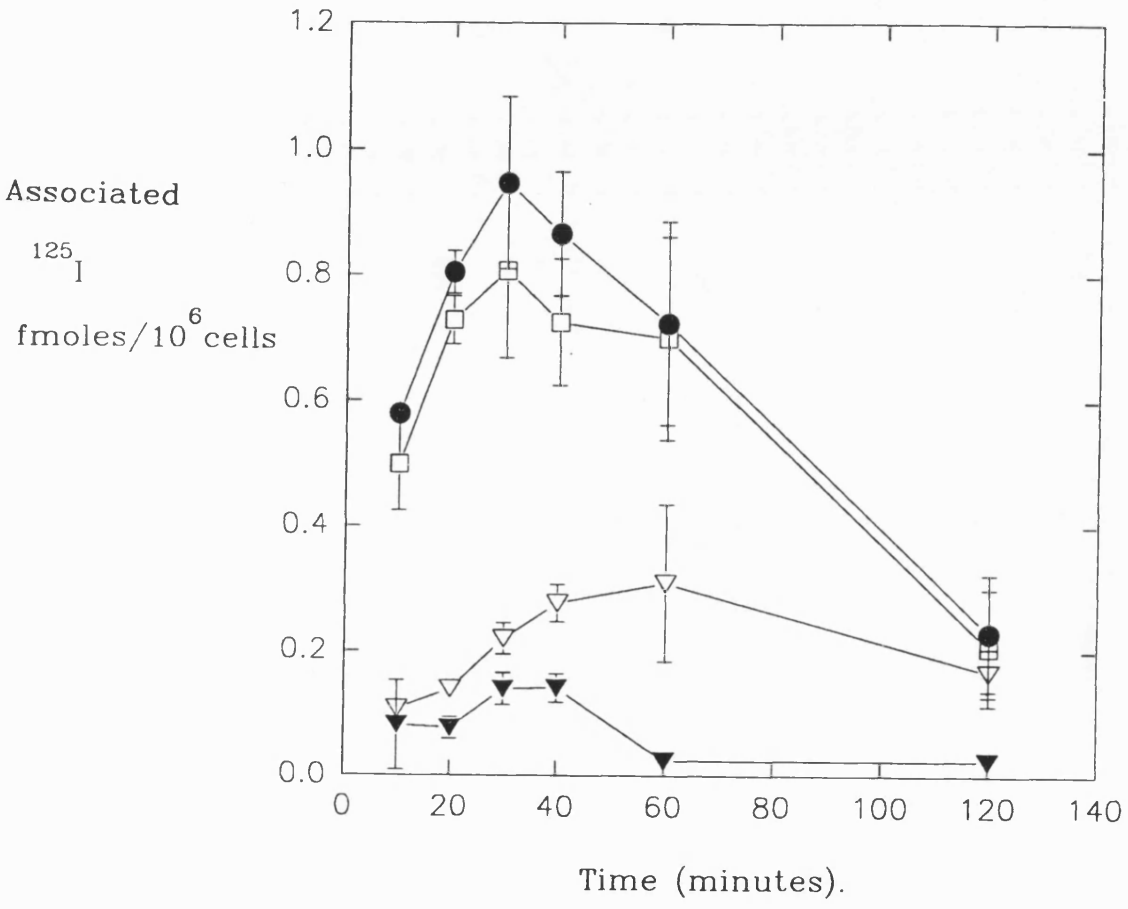

Figure 5.9: ^{125}I activity after incubation of 0.1nM ^{125}İ-NLDP-MSH with B16 cells at 37^{0}C with time. Each incubation was terminated with ice-cold PBS after which a set of wells at each time point (exposed to labelled tracer only) received a 5 minute 4^{0}C acid-wash. All wells were then treated in the usual manner. Each point represents the mean±sd from 4 wells. Total (●), specific (□) and non-specific binding (▼) respectively, and acid-washed cells (▽).

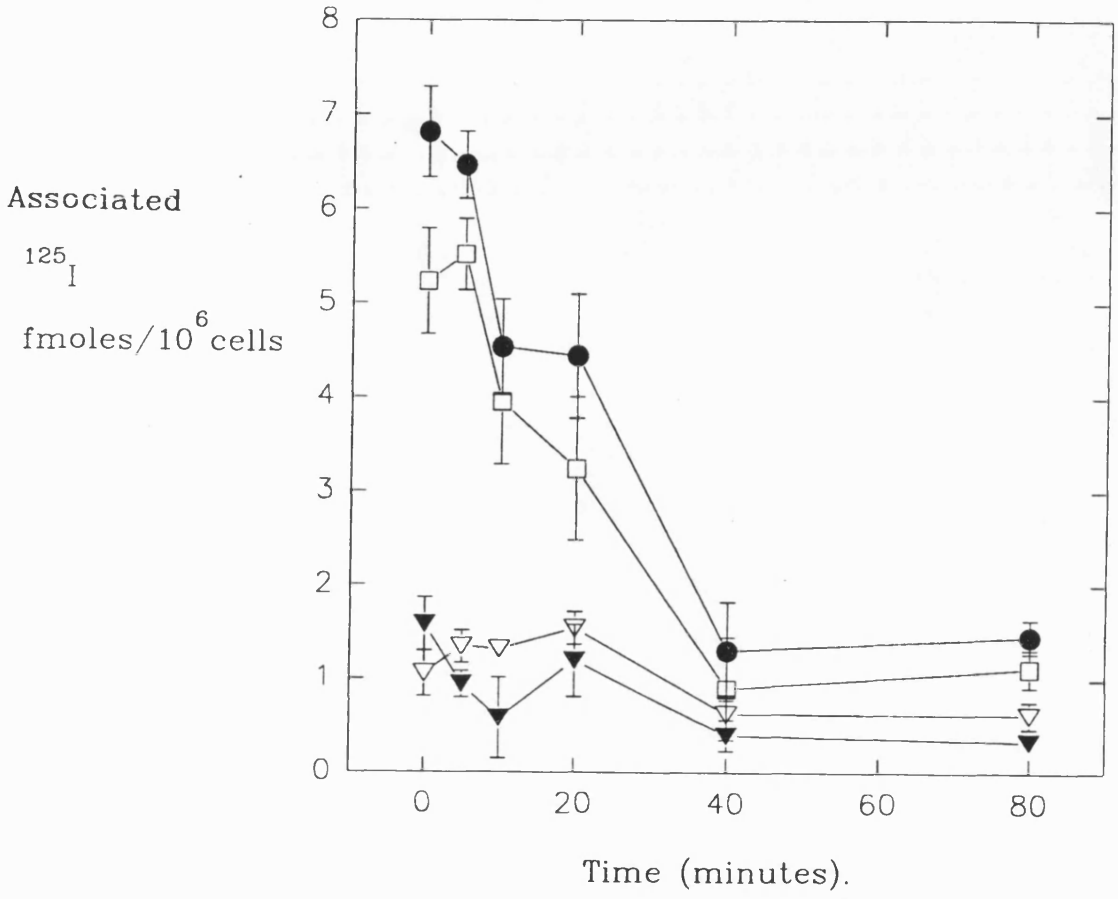

Figure 5.10: Incubation of B16 cells at 37^{0}C with time in normal Hepes binding buffer, pH 7.4. Cells were previously exposed to 0.5nM ^{125}I-NLDP-MSH for 1 hour at 4^{0}C before being washed with ice-cold PBS (time zero) and then reincubated at 37^{0}C. Each point represents the mean±sd from 4 wells. Total (●), specific (□) and non-specific binding (▼) respectively, and acid-washed cells (▽).

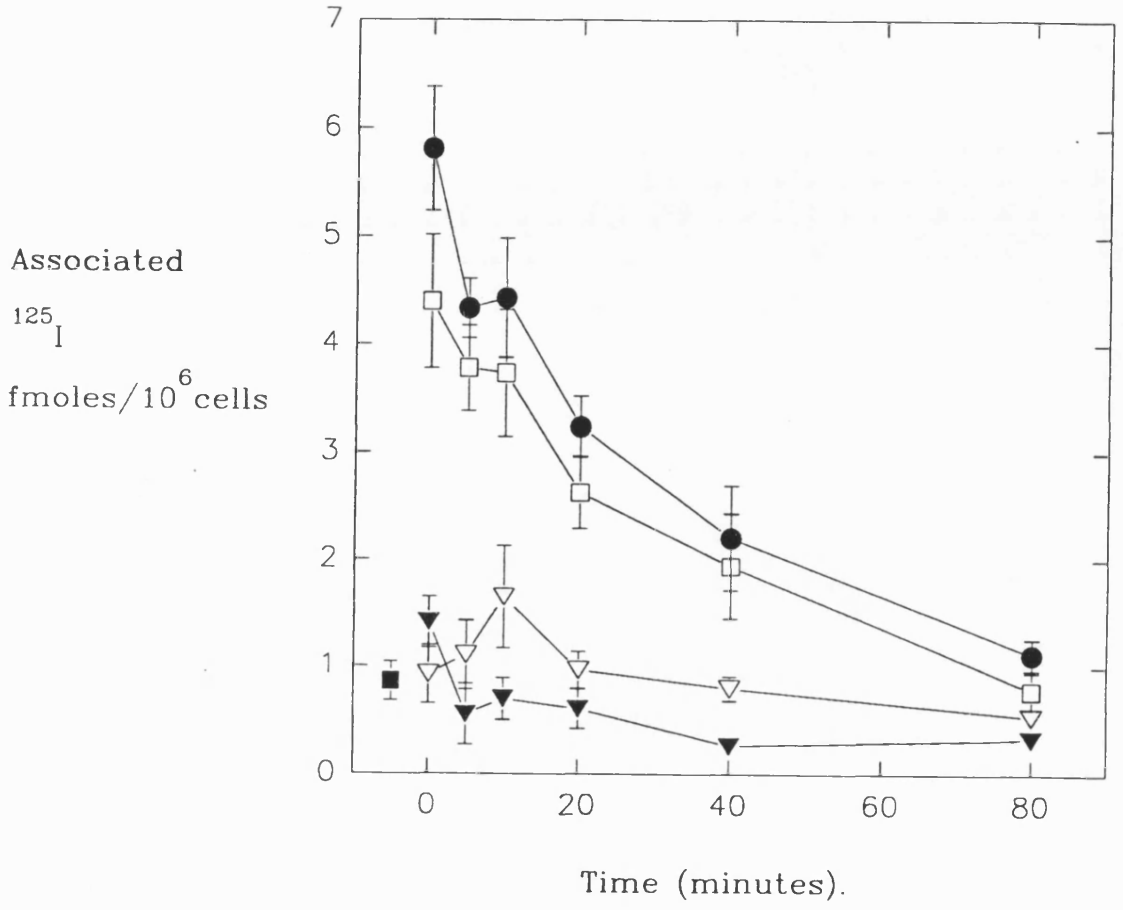

Figure 5.11: Second incubation of B16 cells at 37^{0}C with time in normal Hepes binding buffer, pH 7.4. Cells were previously exposed to 0.5nM ^{125}I-NLDP-MSH for 1 hour at 4^{0}C before being washed with ice-cold PBS (time zero) and then reincubated at 37^{0}C. Each point represents the mean±sd from 4 wells. Total (●), specific (□) and non-specific binding (▼) respectively, and acid-washed cells (▽). Also an acid-wash of cells exposed to the radio-ligand in the presence of an excess of unlabelled NLDP-MSH (■).

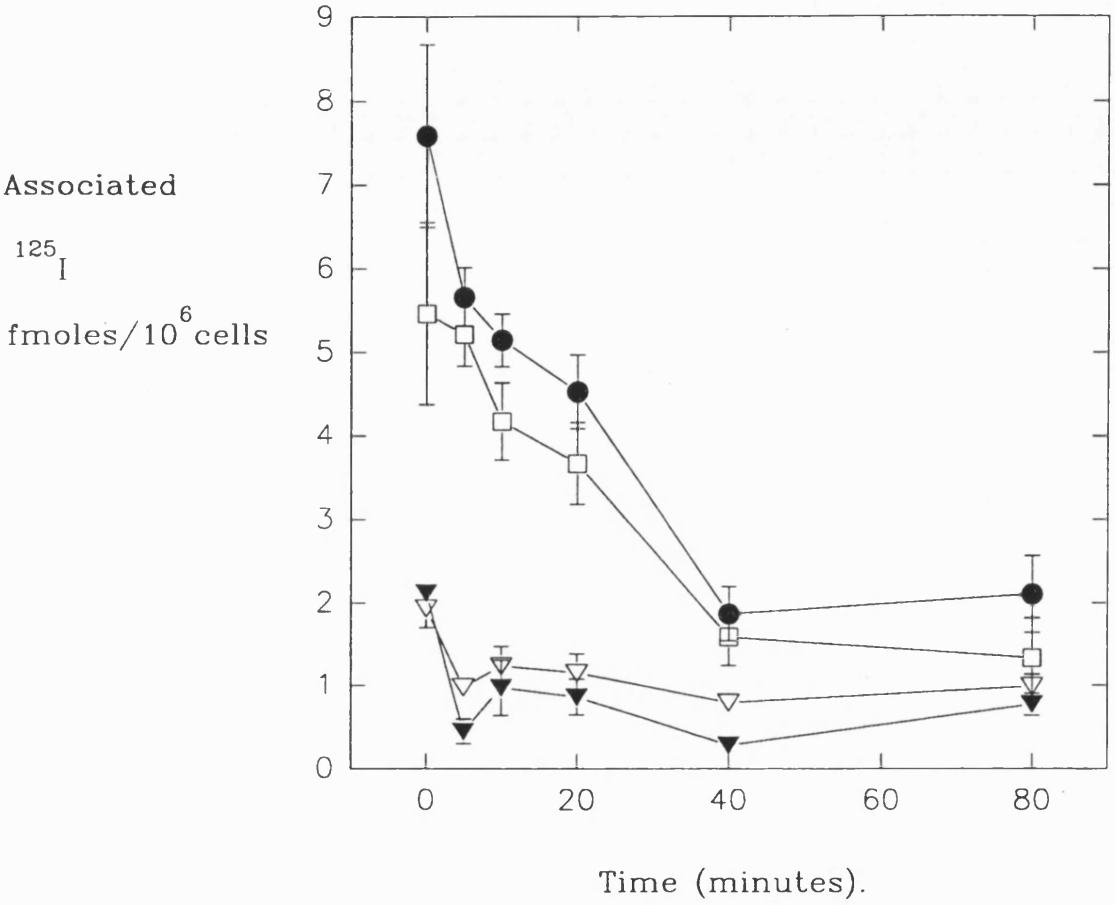

Figure 5.12: Incubation of B16 cells at 37^{0}C with time in normal Hepes binding buffer supplemented with 0.5μM NLDP-MSH, pH 7.4. Cells were previously exposed to 0.5nM ^{125}I-NLDP-MSH for 1 hour at 4^{0}C before being washed with ice-cold PBS (time zero) and then reincubated at 37^{0}C. Each point represents the mean±sd from 4 wells. Total (●), specific (□) and non-specific binding (▼) respectively, and acid-washed cells (▽).

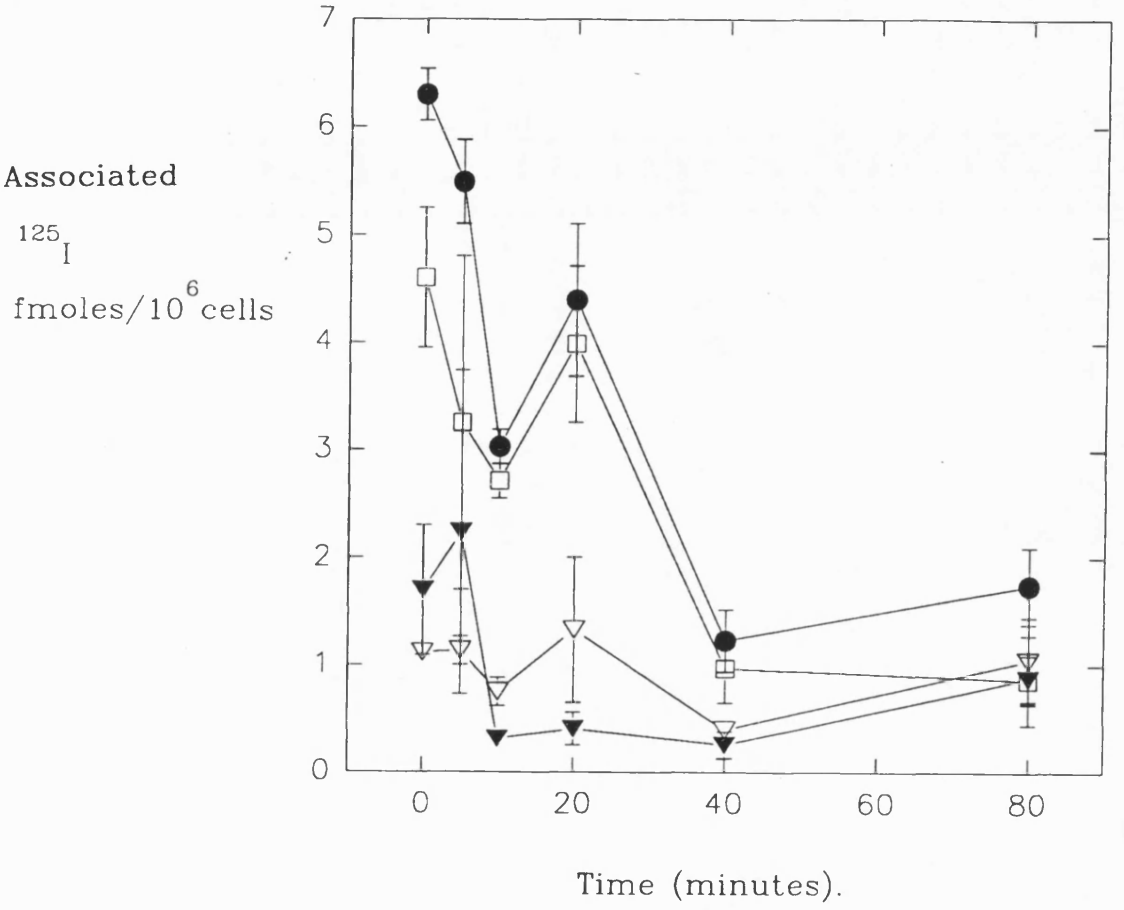

Figure 5.13: Second incubation of B16 cells at 37^{0}C with time in normal Hepes binding buffer supplemented with 0.5μM NLDP-MSH, pH 7.4. Cells were previously exposed to 0.5nM ^{125}I-NLDP-MSH for 1 hour at 4^{0}C before being washed with ice-cold PBS (time zero) and then reincubated at 37^{0}C. Each point represents the mean±sd from 4 wells. Total (●), specific (□) and non-specific binding (▼) respectively, and acid-washed cells (▽).

5.4 Discussion

The elution of the iodination products by HPLC revealed three peaks, two of which were associated with increased radioactivity. The first peak corresponded to non-labelled peptide (as no radioactivity above background was associated with it), the second and third corresponded to mono and di-iodinated NLDP-MSH respectively. These findings are almost identical to those of Eberle [113], elution times being slightly different. The iodination reactions proved very reproducible with a workable yield of mono-iodinated peptide being produced.

The binding of ^{125}I-NLDP-MSH at 4^{0}C reached equilibrium after 8 hours which was a relatively long time for a small peptide with a high binding affinity. Siegrist et al [199] observed similar kinetics with the analogue NLeu^4-αMSH. After 8 hours at 4^{0}C binding had still not yet reached a plateau. In contrast Panasci et al. [114] used NLDP-MSH but with a different radio-label (^{3}H-norleucine being incorporated into the peptide); they achieved constant binding between 30 minutes and 24 hours. Both authors used similar binding buffers and cells derived from the same line as in the present study. Panasci et al. used the F1 varient of B16 cells but did not state how the cells varied from those of the parent cell line. The presence of the ^{125}I atom may have altered the binding kinetics of the peptide as opposed to the use of a tritium label. Certainly Siegrist et al. [203] failed to find any significant difference in the binding affinity between iodinated and unlabelled peptide (similar results to the latter have been observed in our own laboratories).

The reason for this long equilibriation period is unclear, the fact that Siegrist et al. [199] obtained similar results with a related peptide on the same cell line indicates that it was not peculiar to the experimental protocol. They undertook binding studies in suspension, removing unbound tracer via centrifugation. The same group later failed to find any difference in binding of ^{125}I-αMSH to a human cell line in suspension or as a monolayer.

Specific binding of ^{125}I-NLDP-MSH at 4^{0}C increased up to c.1nM extracellular

concentration of the ligand, whilst it was felt the non-specific binding could have been limited for the same reasons in the use of ^{3}H-MTX, i.e. the use of a smaller size well. An isotherm fit was processed for one binding site as reports in the literature and in our own laboratories have reported the presence of only a single binding site [197, 198, 114, 203, 205]. This was further supported by the photoaffinity labelling of a single membrane protein in the order of 45kDa [206, 207] which has subsequently been found to be a glycoprotein. Gerst et al. [208] have reported two membrane proteins of 43 and 46kDa respectively but this may be an artifact of the cell system or methodology used.

The values of K_d obtained from the isotherm model fit, 0.87 and 0.37nM, compare favourably with other results from the same laboratory (with a slightly modified binding protocol) 0.395-0.588nM (unpublished data). However the apparent number of binding sites per cell is variable and has been estimated as 5900-35,700. The figures determined here 5361 and 3384 are representative under normal culture conditions. Both the values for K_d and the number of binding sites per cell are in the same range as reported in the literature for identical or closely related peptides with B16 cells. Siegrist et al. [198] 15^{0}C, 0.32$\pm$0.13nM (K_d) and 9570 $\pm$ 1750 sites/cell, Tatro et al. [205] 23^{0}C, 0.056 $\pm$ 0.019nM and 2805 $\pm$ 589 sites/cell, Panasci et al. [114] 4^{0}C, 0.059nM and 4570 sites/cell (all experiments used B16 cells, the temperature of the binding assay is indicated).

The binding and biological response of MSH has been demonstrated to be dependant on extracellular calcium ions [209, 210, 211], which were absent in the binding buffer used. This appears not to have affected the assay to a great extent as similar results were obtained in the same laboratory with a calcium replete buffer. The variation in the number of binding sites/cell could be due to phenotypic drift as the cells are being continuously passaged. Kameyama et al. [212] discovered that over six months cells retained the same affinity (22.0nM) for ^{125}I-αMSH but were less sensitive to the hormone with a decrease in the receptor density. Siegrist et al. [203] also found that progressive subculturing of one cell line lead to the loss of receptor expression. Conversely Ghanem et al. [213] found

binding characteristics for ^{125}I-αMSH with a human melanoma cell line to remain fairly constant over two months.

It appears from published work that the value for B_{max} is not a true reflection of receptor number of all cells within a population. Many authors have reported non-uniform binding/labelling of cell populations [214, 215, 216, 217] which may be due to their non-synchronised state. Varga et al. [217] and McLane and Pawelek [218] reported binding of the MSH hormone to occur predominantly in the G2 (and possibly late S) phase of the cell cycle and was associated with the Golgi complex [215], although Fuller and Brookes [219] dispute this point. However these authors failed to follow binding through more than one cell cycle as they reported loss in synchronisation. Shimizu et al. [220] have reported insulin receptor regulation through the cell cycle in mouse melanoma cells with the highest activity in the S-phase. Others have found some melanoma cell lines failing to express any MSH peptide binding [198, 213]. Both these instances have occurred with various human melanoma cell lines, others seem to express a greater affinity for MSH but tend to have a lower receptor density when compared to murine melanoma cell lines [203]. The advent of more potent analogues such as NLDP-MSH has in one case revealed the presence of previously undetected binding sites (Libert et al. [221]), of course good radiolabel purification is required to measure small receptor populations.

Although the results reported here demonstrate binding to B16 cell membranes, which can be displaced by excess unlabelled NLDP-MSH, it does not provide evidence for interaction with the αMSH receptor. Binding of a fixed amount of ^{125}I-NLDP-MSH in the presence of increasing concentrations of extracellular αMSH would confirm this specificity. This has been demonstrated for unlabelled NLDP-MSH in mouse and human melanomas by Siegrist et al. [199, 203] against ^{125}I-Nleu-αMSH and αMSH.

Apparent cellular binding of ^{125}I-NLDP-MSH was more rapid at 37^{0}C, reaching a maximum at 30 minutes before apparently declining. Of course at this tem-

perature metabolic processes are operative. The rate of association was similar to other reports [198, 199, 114]. The subsequent decrease in specific binding was paralled by an increase in the acid-resisitant cell associated radioactivity. Acid-wash treatment removed surface bound ligand which revealed all tracer to be on the cell surface at 4^0C. The remaining portion at 37^0C must therefore have been internalised whole or fragmented peptide within the cell.

The decrease in bound ligand at 37^0C has been observed by other workers using similar conditions. Siegrist et al. [199] used ^{125}I-Nleu-αMSH with B16 cells, where association of the ligand also reached a maximum value after 30 minutes. The rate of dissociation however was very rapid which they accounted for due to degradation by tissue proteases. Panasci et al. [114] used ^{3}H-NLDP-MSH with a B16 variant and also achieved maximum cell-association of ligand at 30 minutes with a decline thereafter at 37^0C. They demonstrated that the tracer was not degraded in the medium or within the cells for up to 2 hours which was not suprising as unlike the native peptide and some of its analogues, NLDP-MSH is more resisitant to enzymatic lysis [200, 201]. This is partly the reason for its greater biological activity compared to αMSH.

The measure of internalised (acid-resisitant) ^{125}I-NLDP-MSH was in good agreement with Panasci et al. [114] who also employed an acid-wash. A maximum amount was reached at 60 minutes with a following decline. The question that arises is can the internalisation of the ligand be related to the decrease of cell surface binding ? The latter is unlikely to be caused by NLDP-MSH degradation and although Siegrist et al. [199] demonstrated rapid dissociation of ligand at 37^0C, that was using ^{125}I-Nleu-αMSH, which they found to have far less affinity for the binding site than NLDP-MSH. Two further results by Panasci et al. [205] concerned the appearance of partial degradation products within the cell after 4 hours at 37^0C, and an increase in the amount of internalised ligand in the presence of ammonium chloride. This acidotrophic agent is known to increase the pH enviroment of endosomes and lysosomes, which restricts lysosomal enzyme degradation and prevents vesicle fusion events in the endocytic pathway [71, 72].

The increase in the amount of internalised tracer could be due to non-degradation and subsequent accumulation of ligand, or the non-dissociation from internalised receptors which are now trapped inside the cell.

A possible explanation for the decline of surface binding at 37^{0}C could be attributed to internalisation of ligand-receptor complex with a temporay loss of membrane binding sites. Covalent labelling of the receptor and monitoring its movement after binding would help resolve the reasoning behind this decrease observed.

Of course the internalisation observed at 37^{0}C of ^{125}I-NLDP-MSH need not have necessarily occurred via the binding previously observed at 4^{0}C (even though membrane binding was seen at the former temperature). For this reason in the last series of experiments the radio-tracer was allowed to bind at 4^{0}C, excess unbound ligand removed, and the incubation temperature increased to 37^{0}C. This resulted in a steady decline in membrane or surface bound ^{125}I-NLDP-MSH with a concomitant appearance of internalised tracer. The latter was very small and displayed a maximum at 10-20 minutes. It therefore seems ^{125}I-NLDP-MSH was internalised into B16 cells at 37^{0}C possibly associated with the receptor/binding site. The decrease in internalised ligand after one hour at 37^{0}C could either be due to recycling of receptor and ligand back to the cell surface with dissociation of the ligand (but an increase in membrane binding would occur unless the receptor was in an inactive form), or release of ligand either degraded or whole back into the medium. Receptor labelling and subcellular fractionation studies would give a greater insight into the internalisation process, of which there are very few examples in the literature. Siegrist et al. [198] observed the removal of 70-75% of surface bound ^{125}I-Nleu-αMSH from B16 cells at 37^{0}C compared to 90-95% of ^{125}I-αMSH in human melanoma cells. Other authors have also failed to observe internalisation [214, 216, 222] in human and mouse melanomas of MSH peptides in order to exert their biological action. It is interesting to note that Shimizu et al. [202] recorded the binding and subsequent uptake of iodinated insulin in Cloudman S-91 mouse melanoma cells which then underwent degradation.

It appeared that internalisation of ^{125}I-NLDP-MSH occurred via its binding site at 4^0C although this was not definitive evidence for such a process. Also the experiments failed to demonstrate if the ^{125}I-NLDP-MSH was internalised complete or in a fragmented form, whether the ^{125}I was still attached to its binding site or dissociated and entered via a different route. If internalisation did occur by a receptor-mediated process it may be influenced by the subsequent binding of more ligand, i.e. display cooperativity. McLane and Pawlek [218] proposed positive cooperativity to have occurred in synchronised cultures of Cloudman S91 mouse melanoma cells in response to β-MSH binding. However when excess NLDP-MSH was present in the medium no increase in the amount of internalisation was observed.

Chapter 6

NLDP-MSH-MTX Conjugate: Iodination and Cellular Interaction

6.1 Introduction

The targeting agent NLDP-MSH and the antimetabolite MTX can be combined to form a potentially site-specific drug conjugate. However the attachment must be performed to cause minimal loss of targeting or binding by the NLDP-MSH. Therefore the 'binding sequence' of this tridecapeptide must be established before conjugation can occur.

Eberle et al. [223] reported in 1977 that αMSH contained two message sequences capable of triggering melanophore receptors, a central portion and the C-terminal Try-Glys-Lys-Prol-Val.NH_2. The N-terminal sequence Ac-Ser-Tyr-Ser-Met- did not exhibit any biological activity alone but potentiated the activity of the C-terminal portion when combined. Further work [224] with the C-terminal structure demonstrated the importance of lysine and proline at positions 11 and 12

respectively, whilst valine was not essential at 13 but a residue must be present for no loss in activity. This pointed towards a central to C-terminal binding sequence in the peptide. When αMSH was coupled to human serum albumin, thyroglobulin or tobacco mosaic virus via the N-terminal the complexes still retained good activity. But when linked via lysine (position 11) the complexes were more than a 100-fold lower in activity than linked via the N-terminal.

From the quoted work a freely accessible C-terminus is essential for the biological (and therefore binding) activity of the native hormone. The shorter fragments (4-10 and 4-11) of NLDP-MSH have also demonstrated good biological potentcy [219]. For these reasons MTX was linked to NLDP-MSH via the N-terminal in the hope of retaining similar activity to the free analogue. The conjugate was iodinated and its interaction with B16 cells studied for a comparision of binding and most importantly uptake, to the free peptide.

6.2 Methods

All methods are described in detail in section 2.4.

6.3 Results

6.3.1 NLDP-MSH-MTX Synthesis

The conjugate was prepared by attachment through the glutamyl residue of MTX to the N-terminal of the peptide and purified by HPLC employing an identical procedure as for the free peptide, except UV detection was now at 300nm, utilising the chromophore of MTX. On analysis by HPLC four peaks were observed to elute very close together after 30 minutes (figure 6.1). The identity of this product was confirmed as the MTX conjugate by FAB-MS, figure 6.2 (molecular weight 2041,

calculated weight 2040). It appears that in the reaction the peptide couples through the α or γ carboxylic group of the glutamyl residue and forms a racemic mixture. Racemization is thought to occur at the α-carbon of the glutamine residue on MTX. Thus the four peaks observed are due to a di-isomeric racemic mixture.

6.3.2 Iodination of NLDP-MSH-MTX Conjugate

It was decided to use a similar iodination protocol as for the free peptide, however a difference in elution from the C18 SepPak was envisaged. Initially a preconditioned column was loaded with 5μl of stock conjugate (1mg/ml) in 0.5ml of PB buffer. A 2x1ml PB buffer wash of the column was first applied and discarded, followed by successive 2x1ml washes of 40, 50 and 60% methanol/1% TFA. Each 2ml fraction was collected and purified by HPLC using an identical procedure as for the free peptide.

Each methanolic wash revealed a peak at an identical elution time to an ordinary injection of the conjugate (i.e. c.29.5 minutes), figures 6.3, 6.4 and 6.5. The greatest yield and cleaner trace occurred with the 60% methanolic wash. It was decided to wash the SepPak column with 40 and 50% methanol and retain the 60% methanolic wash for further purification.

In all iodinations of the conjugate a stock volume of 5μl was used as opposed to 1μl of the free peptide as a poor yield would be expected due to the presence of the MTX. The first iodination used the standard 30 seconds reaction time with chloramine T. The resulting HPLC trace from the reaction (figure 6.6) displayed one large peak at the expected elution time for free or non-labelled conjugate. Fractions of 0.5ml were collected from 28-43 minutes at a flow rate of 1ml/minute, their activity was assayed by a gamma counter (figure 6.7). One main peak of radioactivity was observed reaching a maximum value at 35 minutes. When the profile of activity was superimposed on the HPLC trace with the correct time

scale (figure 6.8), the peak of ^{125}I activity did not coincide with the peak on the HPLC trace. With the knowledge of the order of iodination reaction products with the free peptide, it appeared that the peak observed on the trace was unlabelled conjugate. The mono-iodinated product, although displaying a peak via its activity was too small to measure by HPLC. Therefore using a 30 second iodination reaction gave a yield of mostly unlabelled conjugate. In theory if the reaction time is extended more mono-iodinated will be formed and a time will eventually be reached when di-iodinated conjugate would be predominant.

The reaction time was arbitarily extended to 5 minutes and again the products were purified with HPLC (figure 6.9) with 0.5ml fractions collected and the activity quantified (figure 6.10). Two peaks on the trace (labelled 1 and 2) had similar profiles to the pure conjugate, the first eluting at 31.5 minutes, the second at 34 minutes. The activity in the fractions displayed two distinct peaks, the first of which when superimposed on the trace (figure 6.11), coincided with peak 2. This was most probably the mono-iodinated, peak 1 the unlabelled and the second activity peak may represent the minor peak following number 2 on the trace (likely to be the di-iodinated). The yield of mono-iodinated product was greater using the extended reaction, as reflected by the level of activity recorded. A maximum of c.60 million cpm as opposed to just under 250,000. The mono-iodinated conjugate appeared in the four 0.5ml fractions from 34-35.5 minutes inclusive.

Figures 6.6 and 6.9 represent 0.5ml of a total of 2ml from the iodination. When the remaining 1.5ml were run through the HPLC very similar results occurred with the mono-iodinated peak of activity eluting in the same fractions.

From the above experiments an iodination reaction time of 5 minutes chloramine T exposure was chosen. However it was noted that complete separation between the various products had not occurred and fraction collection of mono-iodinated conjugate may involve the risk of contamination with non-labelled or di-iodinated, and/or the complete omission of one of the four conjugate isomers.

An experiment was performed to increase the chloramine T reaction time to 30 minutes to observe if mainly di-iodinated product was formed. This resulted in one large broad peak obviously composed of mono and di-iodinated products together, figure 6.12 (HPLC trace) and figure 6.13 (^{125}I activity). Although the activity associated with the fractions did display some resolution between the two labelled forms (figure 6.13).

6.3.3 Binding Competition with ^{125}I-NLDP-MSH

The binding affinity of the conjugate at 4^{0}C was assessed by a competition assay on B16 cells against a fixed concentration (0.25nM) of ^{125}I-NLDP-MSH for 8 hours. The conjugate concentration ranged from 0.05 to 0.5μM, the presence of the MTX being likely to decrease the binding affinity of the NLDP-MSH moiety compared to the free peptide.

The results of two experiments, figure 6.14, displayed good similarity. Values for total and non-specific binding of the free peptide showed little variation and were consistant with earlier findings. As the concentration of the conjugate increased there was a greater degree of binding inhibition. At 0.2-5.0μM binding of ^{125}I-NLDP-MSH reached non-specific values.

The experiments can be described by equation 6.1, assuming that both ligands bind to the same receptor, the level of non-specific binding is identical and there is no significant depletion of the ligand in the binding medium.

$$F = \frac{[RLF]}{([RLF] + K_{rl}.[CF]/K_c)} \tag{6.1}$$

where F is the relative fractional binding of the radioligand, [RLF] is its free molar concentration, [CF] is the free molar concentration of the competitor, K_{rl} and K_c are the dissociation constants for binding of radioligand and competi-

tor respectively. Estimates for K_c were obtained by fitting the data (cpm) to equation 6.2 using non-linear regression.

$$cpm_{test} = (cpm_{max} - cpm_{ns}).\frac{[RLF]}{([RLF] + K_{rl}.[CF]/K_c)} + cpm_{ns} \qquad (6.2)$$

The subscripts test, max and ns refer to the cpm obtained in the presence of a binding inhibitor, the absence of inhibitor and the non-specific binding. The dissociation constants of NLDP-MSH-MTX for the two experiments were 5.56 ± 1.82 and 7.49 ± 1.81nM respectively.

6.3.4 Incubation of ^{125}I-NLDP-MSH-MTX at 37^{0}C with B16 cells

The cell association of the iodinated conjugate at 37^{0}C was very similar to the free peptide, figure 6.15. Binding increased to reach a maximum at 30 minutes of c.9fmoles/10^{6}cells, followed by a fairly rapid decrease in the amount bound. Although similar to NLDP-MSH, the levels of internalisation throughout the experiment, as determined by acid-washing, were low. This was probably due to the degradation and subsequent exocytosis of internalised ligand and a corresponding loss of receptor expression on the cell surface.

Further experiments allowed the conjugate to first bind at 4^{0}C for 2 hours; excess tracer was then removed by washing, and the cells reincubated at 37^{0}C for varying time periods (figures 6.16, 6.17 and 6.18). After 2 hours at 4^{0}C the amount bound ranged from 3.5-10fmoles/10^{6}cells. This was all surface bound as determined by acid-washing which decreased all activity to around non-specific values except in figure 6.16. Here non-specific binding appeared relatively high at time zero, but fell to expected values at the next time point.

As incubation at 37^{0}C proceeded surface bound ^{125}I-NLDP-MSH-MTX decreased.

After 60 minutes in figure 6.17 no specific binding remained, whilst in the remaining two experiments there was a 50% reduction after 30 minutes. After 10 minutes an acid-wash resistant fraction began to appear, representing internalised radioligand. Its value, c.0.5-1fmoles/10^6cells remained almost constant throughout the experiment. Non-specific binding remained low for the three experiments all of which displayed similar profiles, i.e. a decrease in surface bound ligand with the appearance of internalised radiolabel (also similar to identical experiments with ^{125}I-NLDP-MSH).

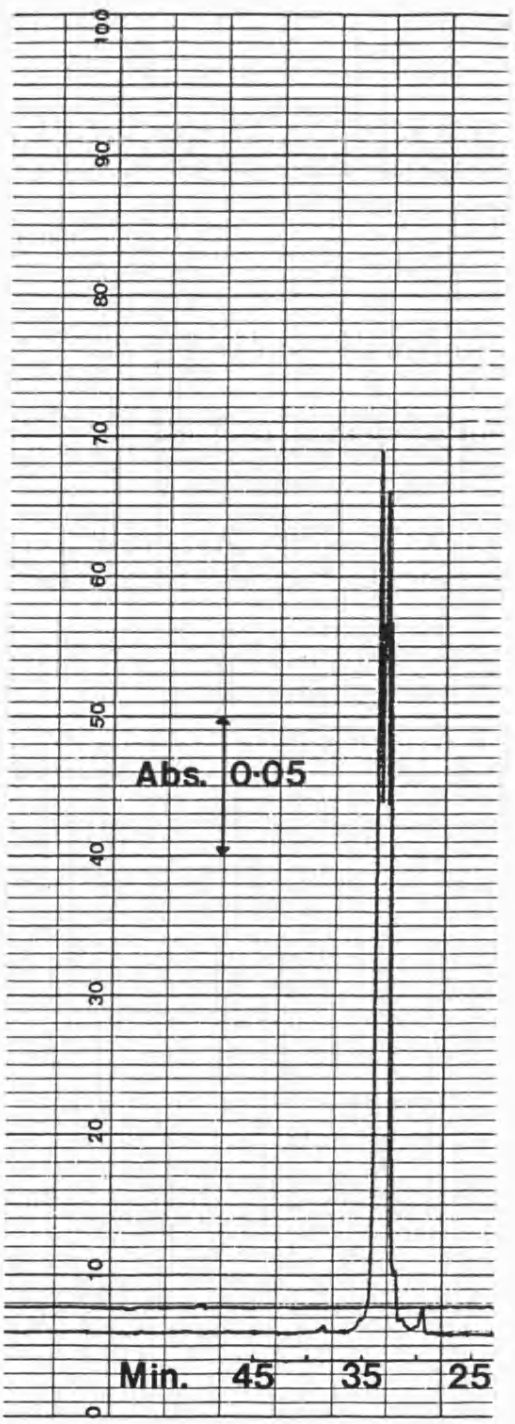

Figure 6.1: The HPLC purification of NLDP-MSH-MTX measured by UV absorbance at 300nm (vertical large squares represent $5x10^{-3}$ absorbance units).

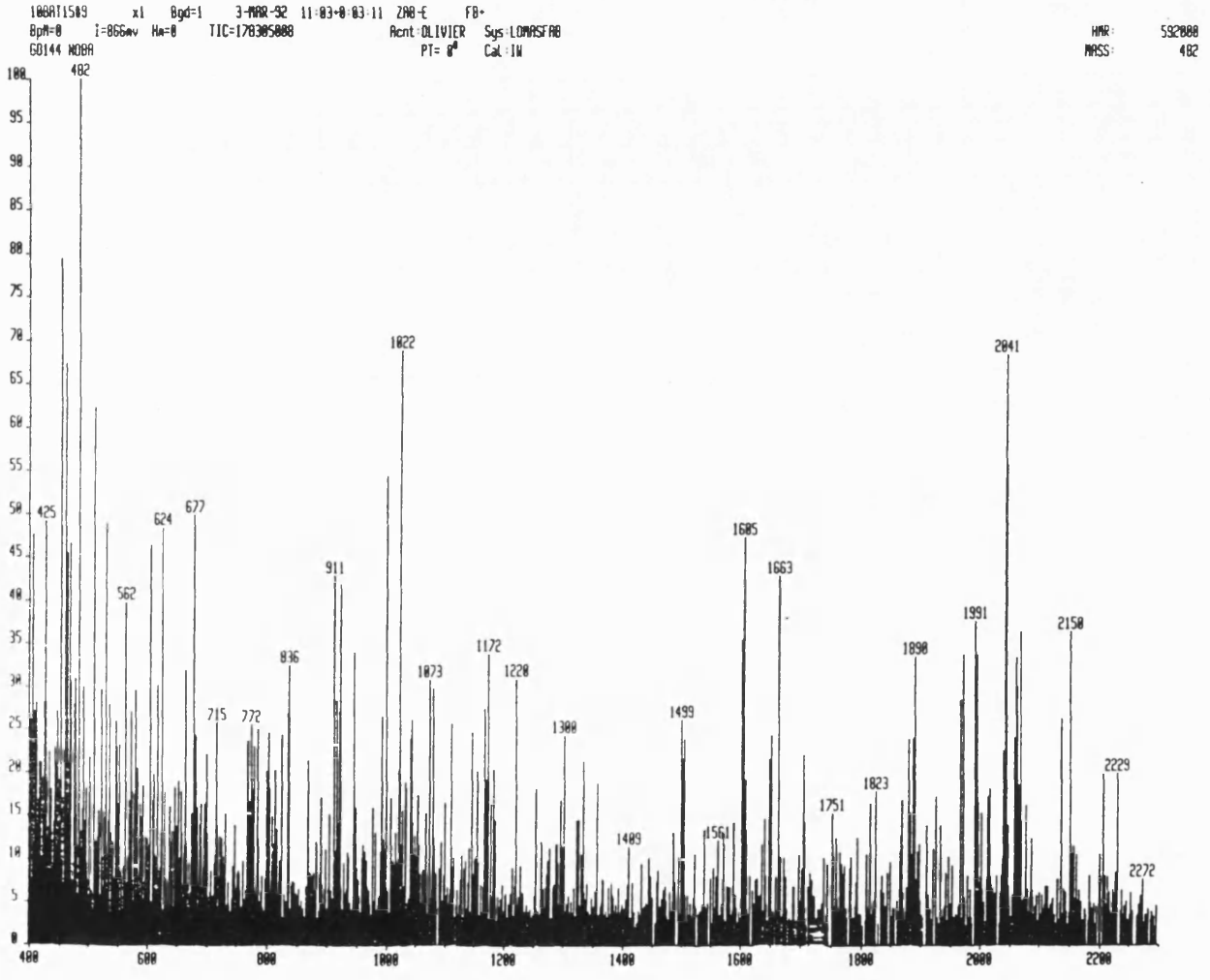

Figure 6.2: The FAB mass spectrometry of NLDP-MSH-MTX

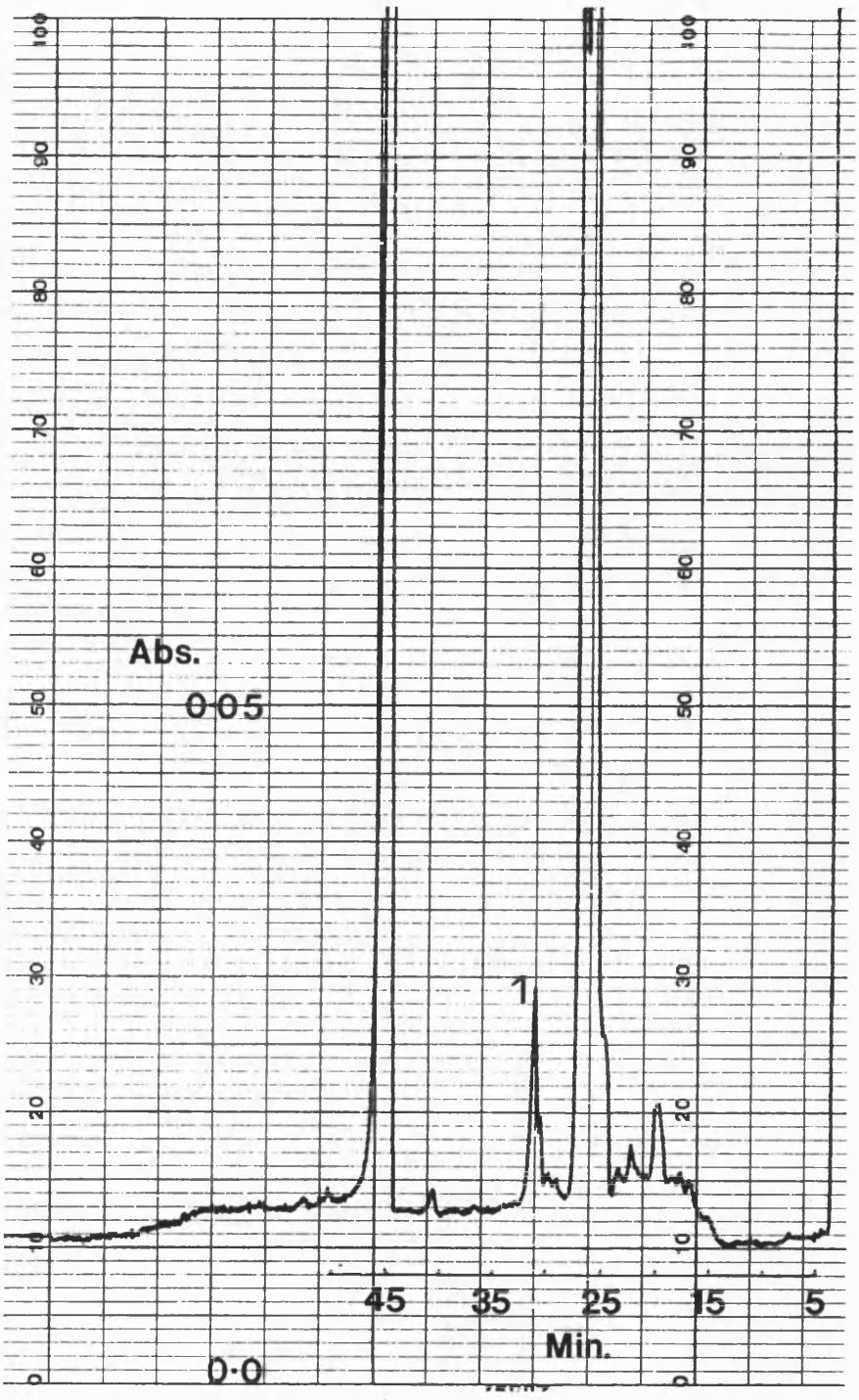

Figure 6.3: The HPLC trace of a 2x1ml 40% methanolic wash of a C18 SepPak column pre-loaded with 5μl of NLDP-MSH-MTX (1mg/ml stock). Peak 1 represents the conjugate (vertical large squares represent $1x10^{-3}$ absorbance units).

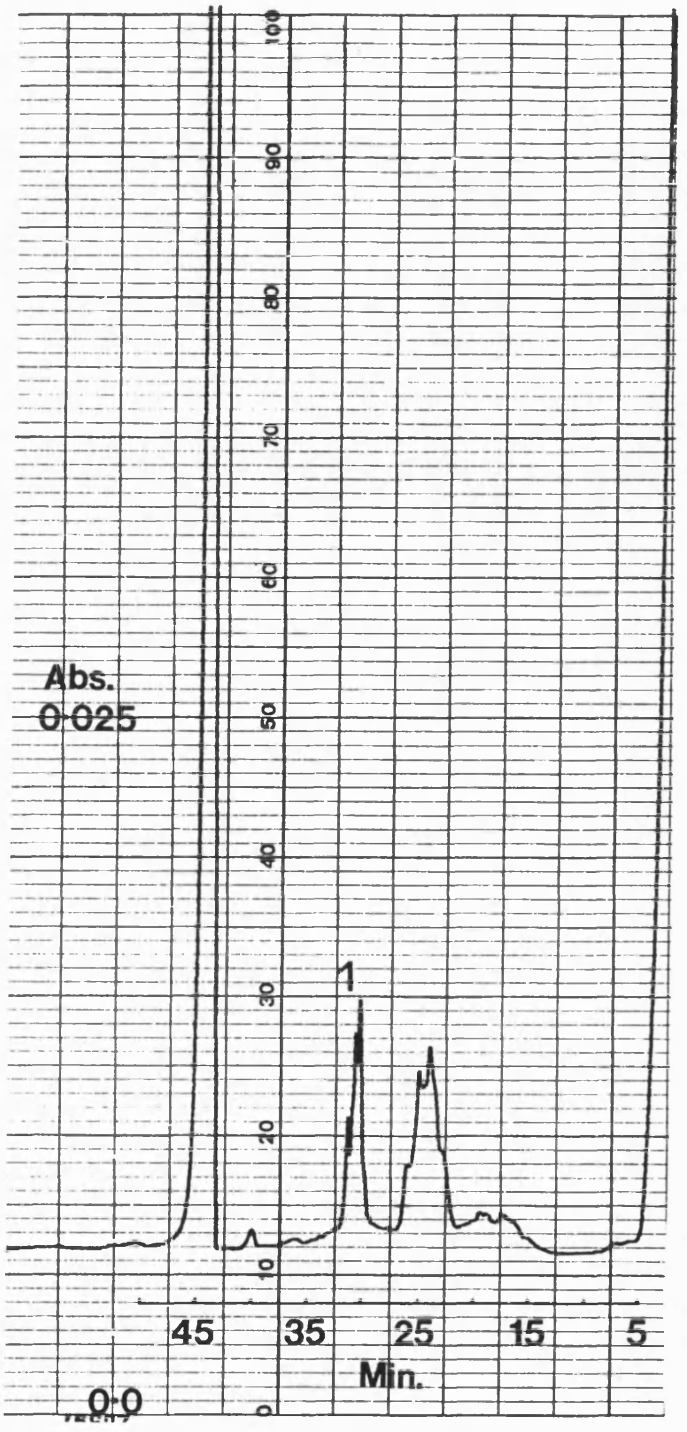

Figure 6.4: The HPLC trace of a 2x1ml 50% methanolic wash of a C18 SepPak column pre-loaded with 5μl of NLDP-MSH-MTX (1mg/ml stock). Peak 1 represents the conjugate (vertical large squares represent 5x10^{-3} absorbance units).

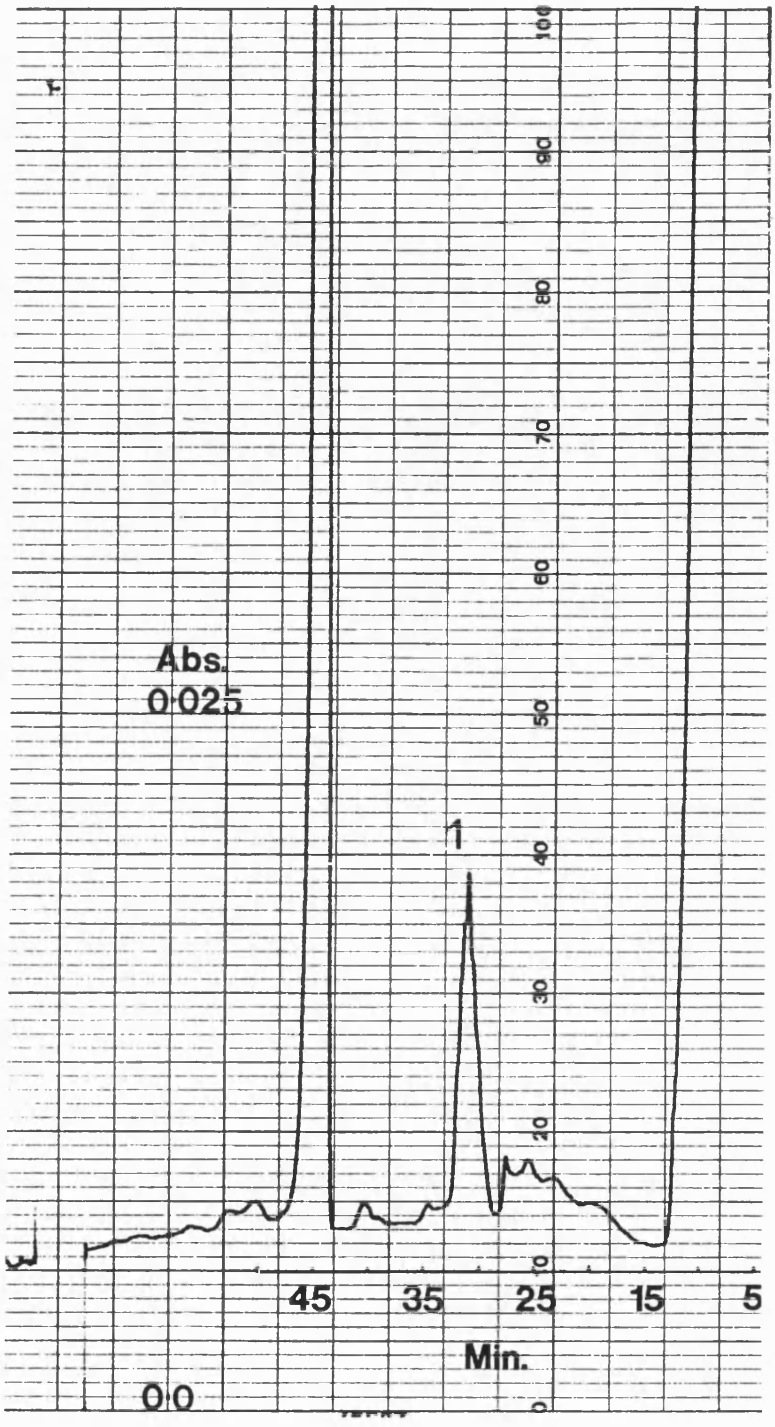

Figure 6.5: The HPLC trace of a 2x1ml 60% methanolic wash of a C18 SepPak column pre-loaded with 5μl of NLDP-MSH-MTX (1mg/ml stock). Peak 1 represents the conjugate (vertical large squares represent 5x10^{-3} absorbance units).

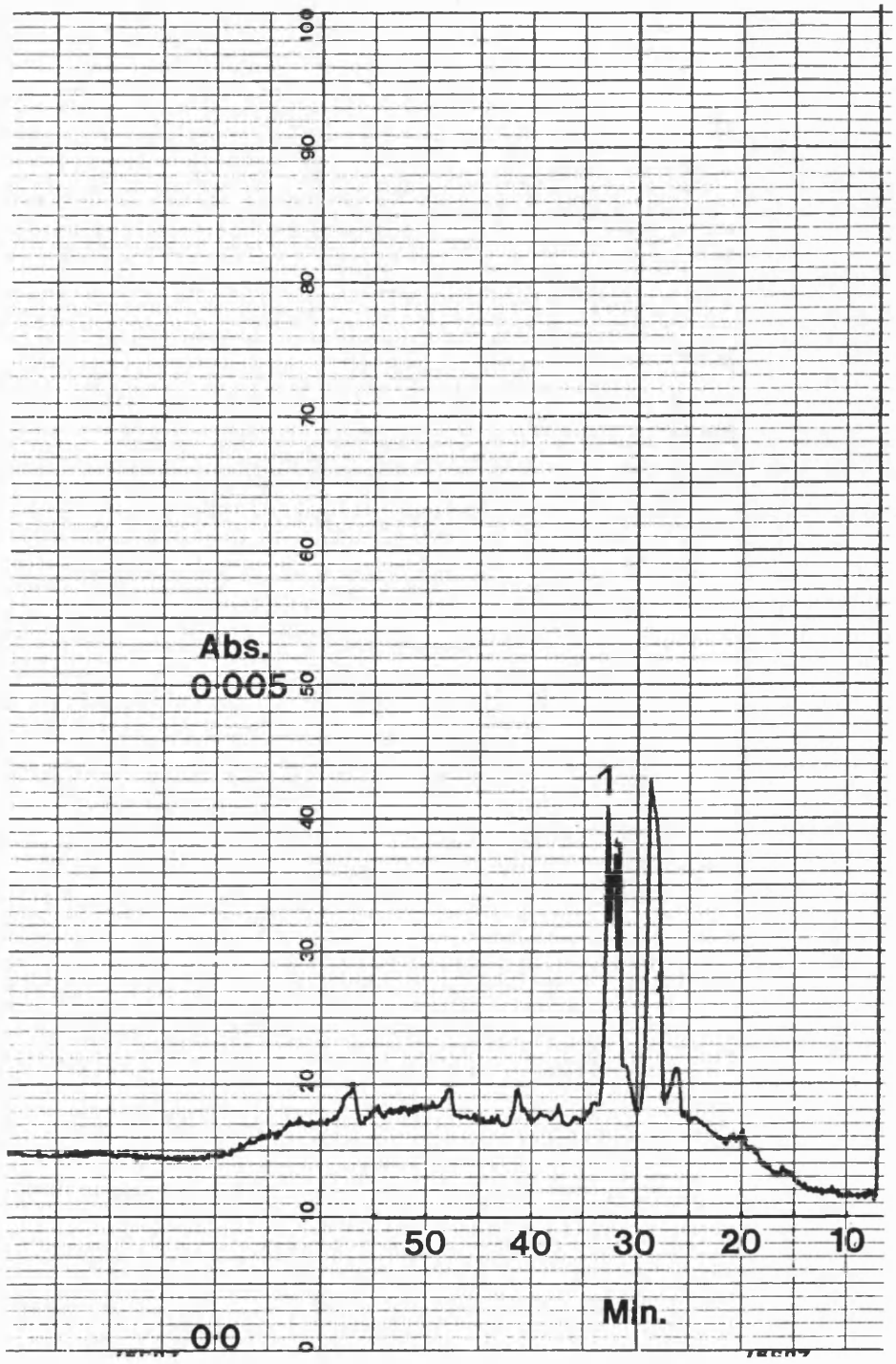

Figure 6.6: The HPLC trace of products from a 30 second chloramine T iodination reaction of NLDP-MSH-MTX. Peak 1 represents the conjugate (vertical large squares represent $1x10^{-3}$ absorbance units).

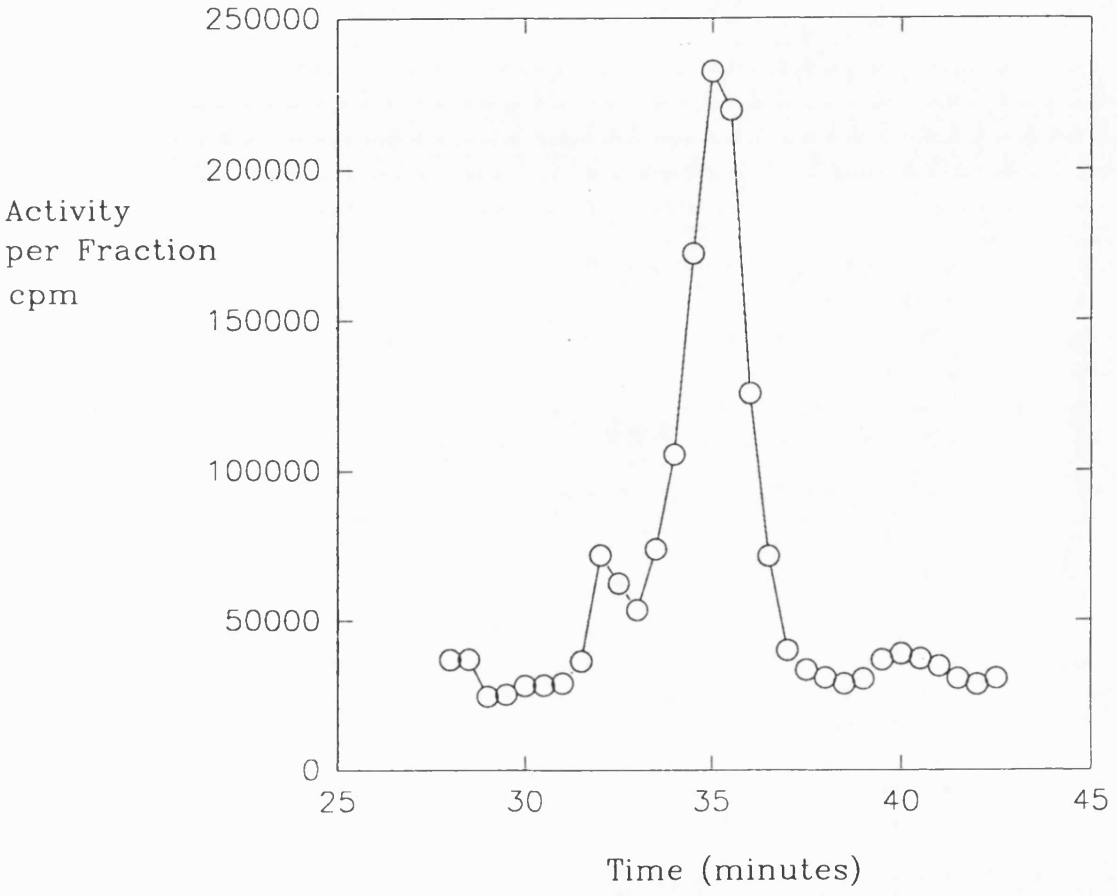

Figure 6.7: ^{125}I activity (cpm) per 0.5ml fraction of the HPLC purification (28-43 minutes after injection) of iodinated NLDP-MSH-MTX (after a 30 second chloramine T reaction). Flow rate was 1ml/minute.

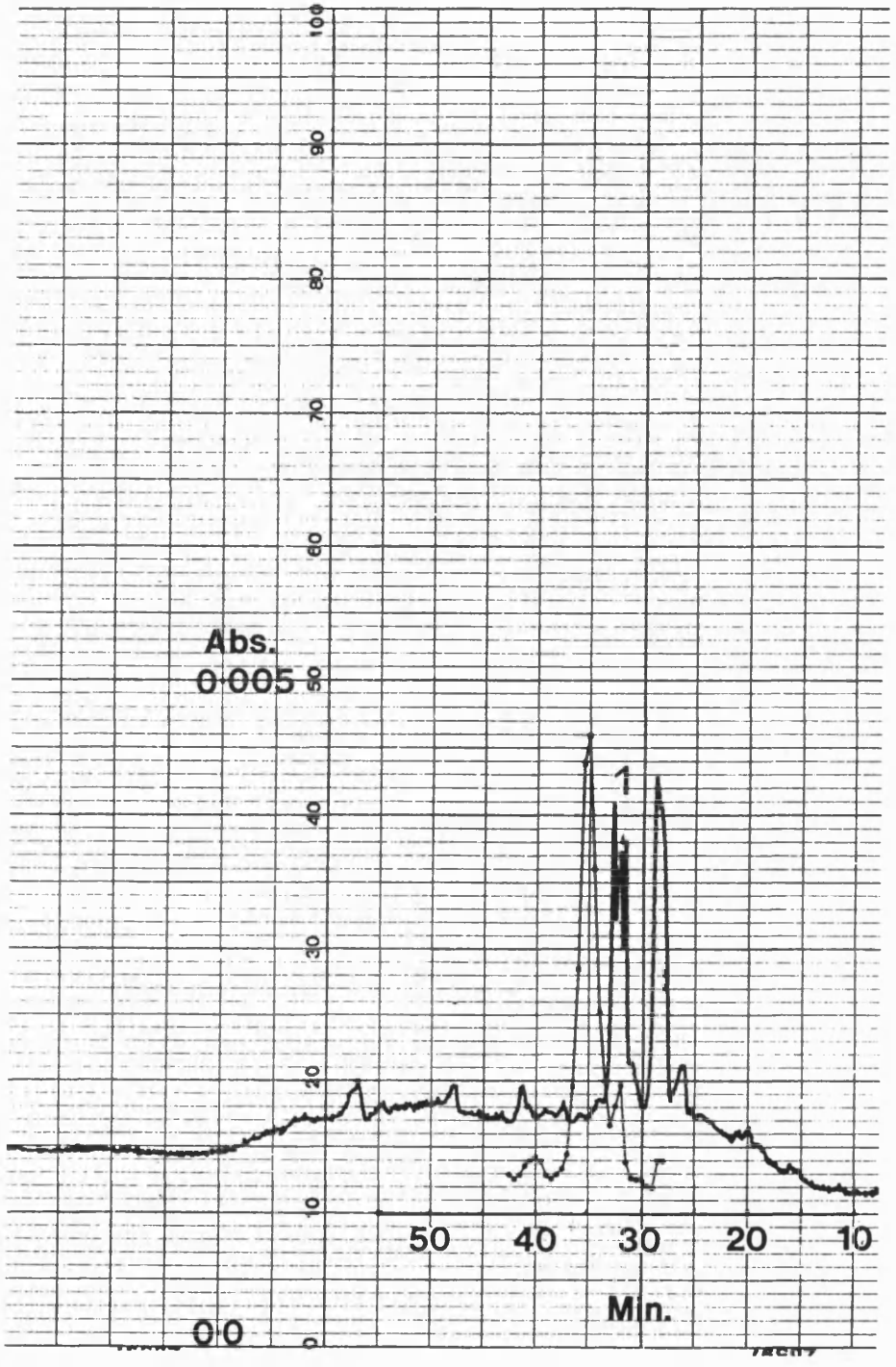

Figure 6.8: The HPLC trace of products from a 30 second chloramine T iodination reaction of NLDP-MSH-MTX, with the associated ^{125}I activity superimposed. Peak 1 represents the conjugate (vertical large squares represent $1x10^{-3}$ absorbance units).

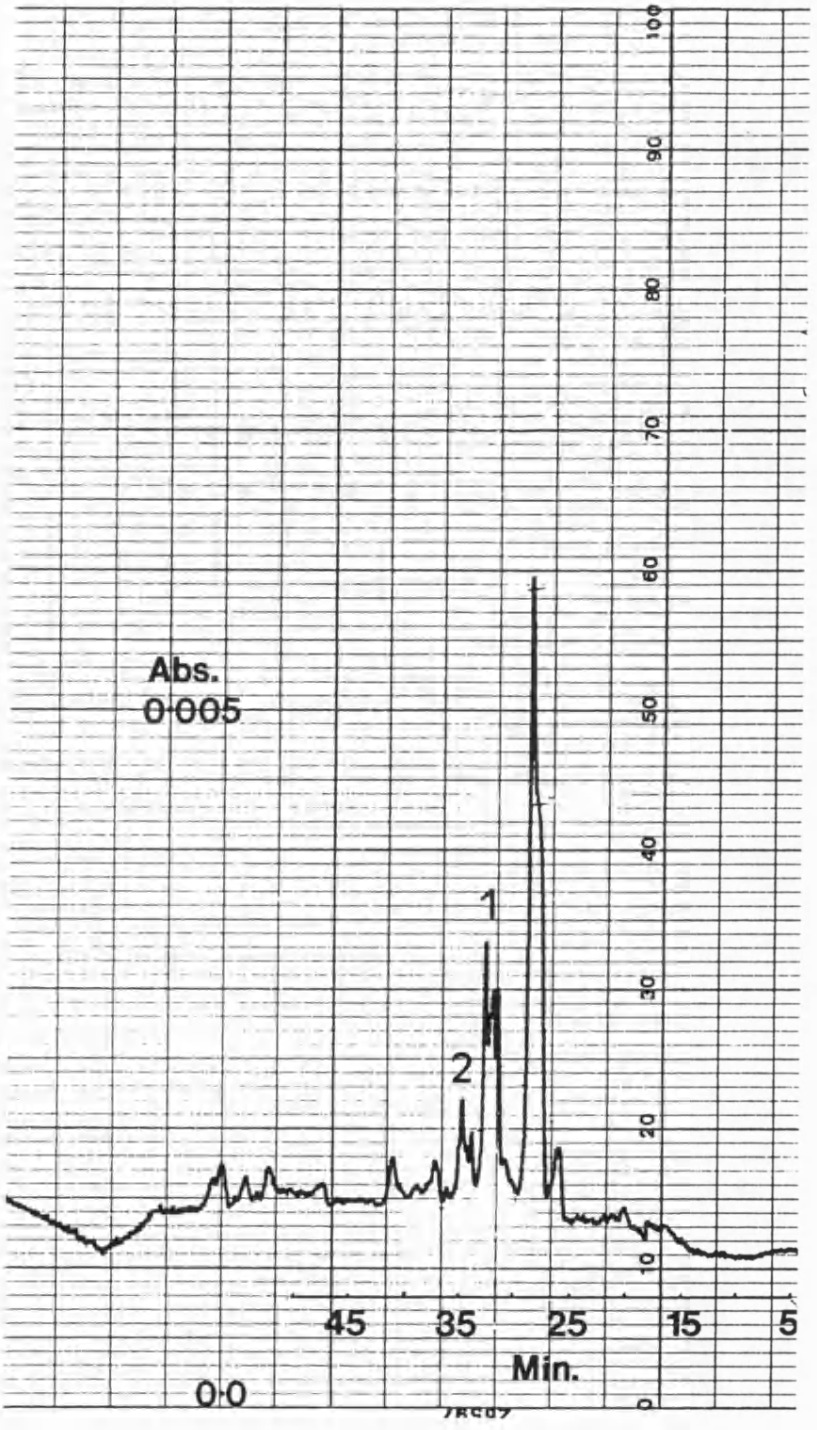

Figure 6.9: The HPLC trace of products from a 5 minute chloramine T iodination reaction of NLDP-MSH-MTX. Peak 1 and 2 are thought to represent the conjugate (vertical large squares represent $1x10^{-3}$ absorbance units).

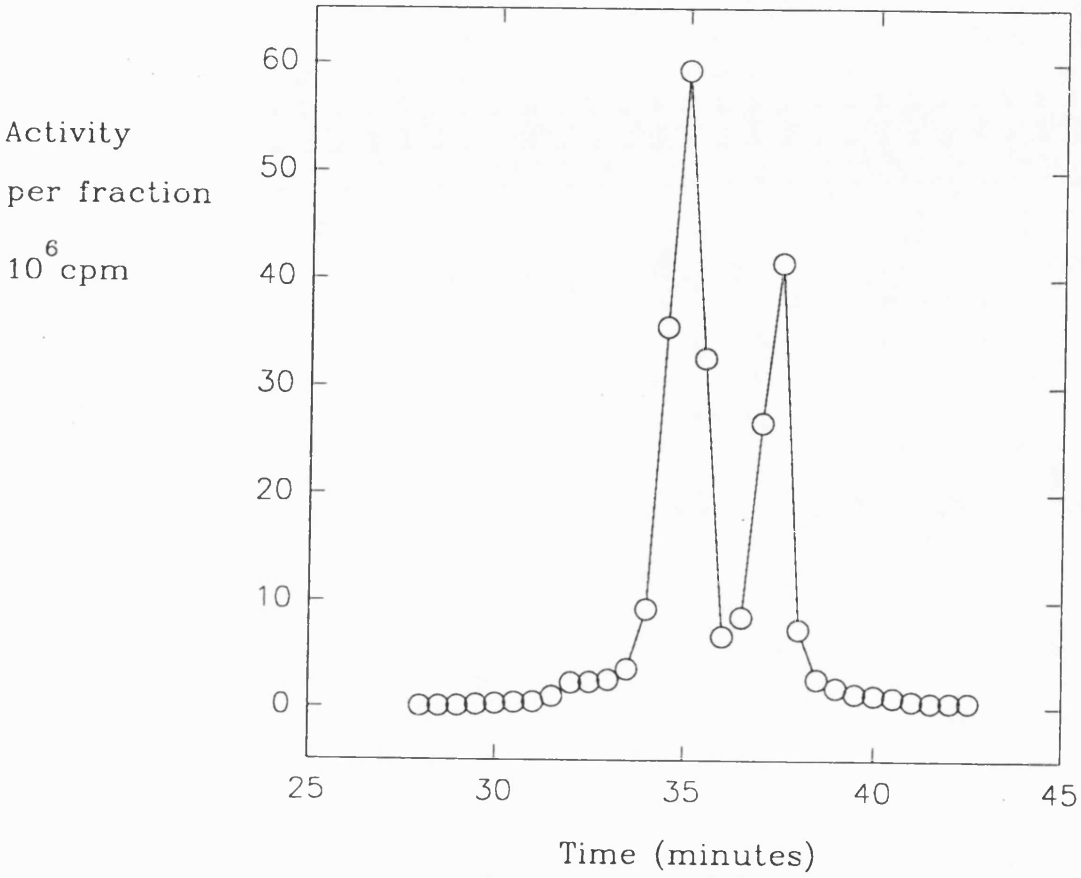

Figure 6.10: ^{125}I activity (cpm) per 0.5ml fraction of the HPLC purification (28-43 minutes after injection) of iodinated NLDP-MSH-MTX (after a 5 minute chloramine T reaction). Flow rate was 1ml/minute.

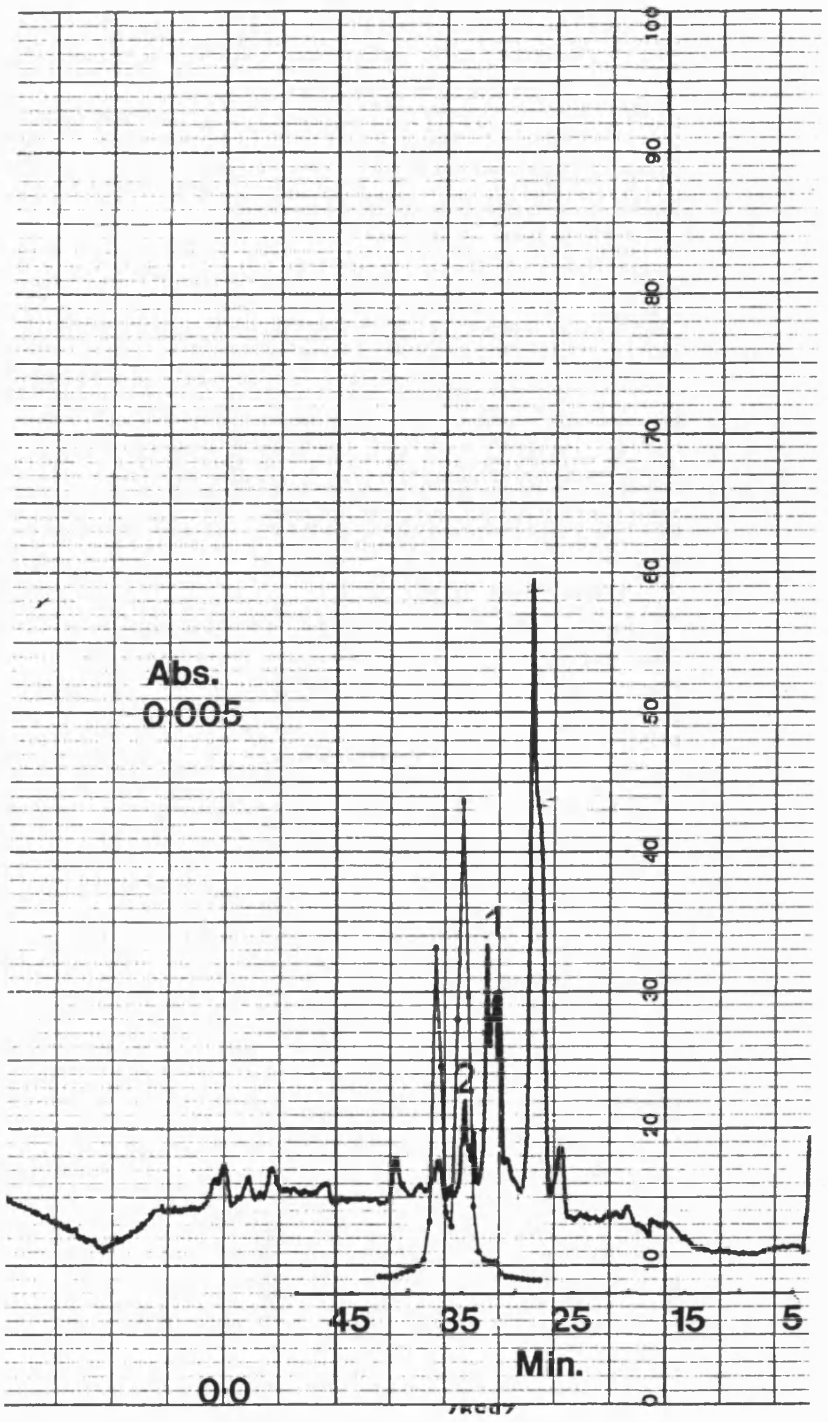

Figure 6.11: The HPLC trace of products from a 5 minute chloramine T iodination reaction of NLDP-MSH-MTX, with the associated ^{125}I activity superimposed. Peak 1 is thought to represent the unlabelled conjugate, and peak 2 the mono-iodinated (vertical large squares represent 1x10^{-3} absorbance units).

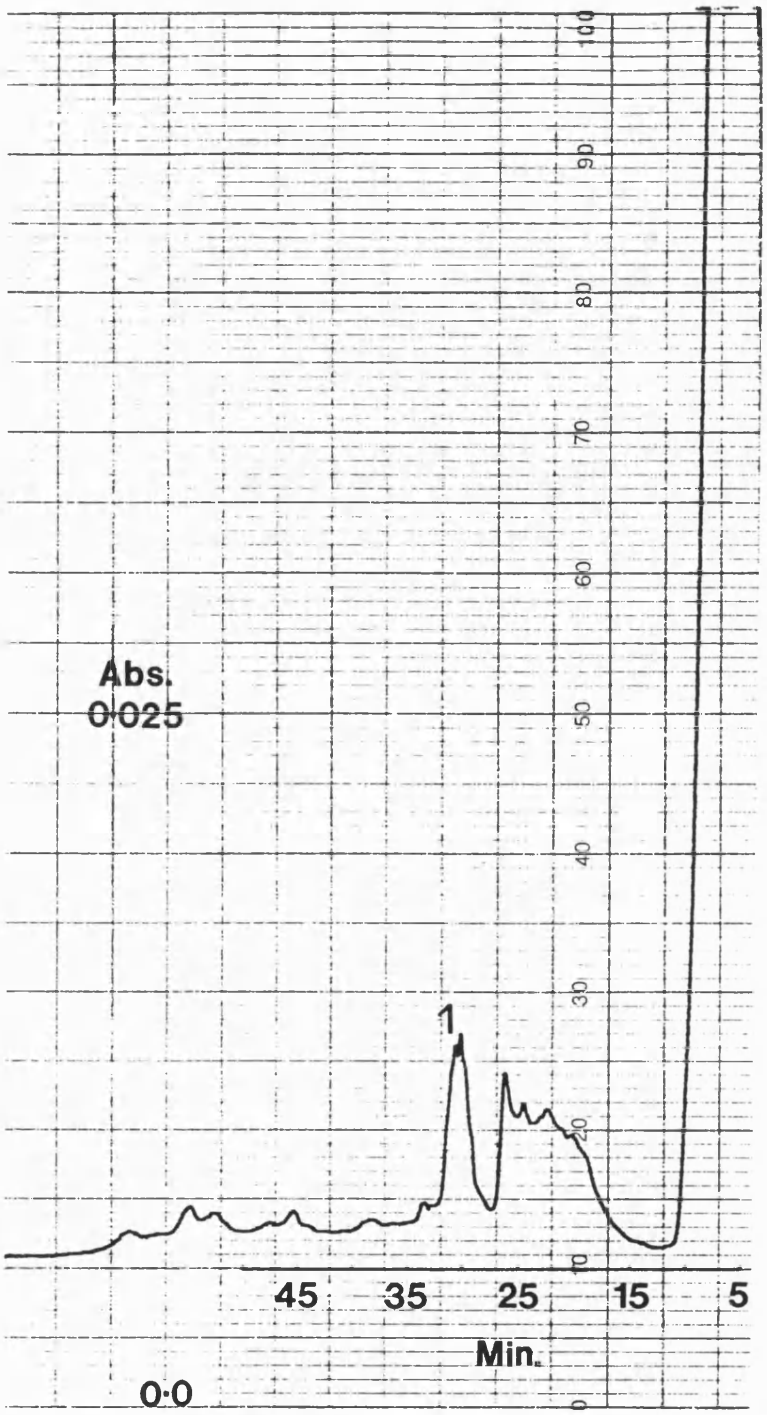

Figure 6.12: The HPLC trace of products from a 30 minute chloramine T iodination reaction of NLDP-MSH-MTX. Peak 1 is thought to represent the mono and di-iodinated conjugate (vertical large squares represent $5x10^{-3}$ absorbance units).

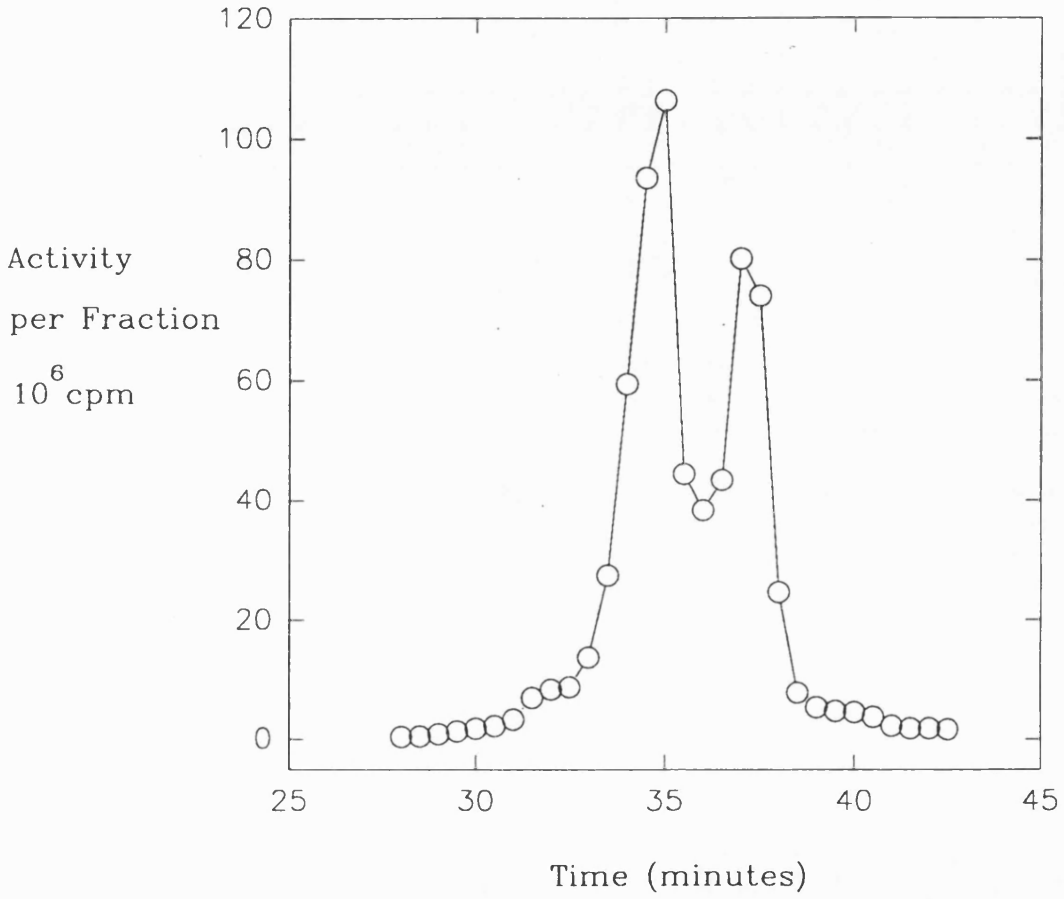

Figure 6.13: ^{125}I activity (cpm) per 0.5ml fraction of the HPLC purification (28-43 minutes after injection) of iodinated NLDP-MSH-MTX (after a 30 minute chloramine T reaction). Flow rate was 1ml/minute.

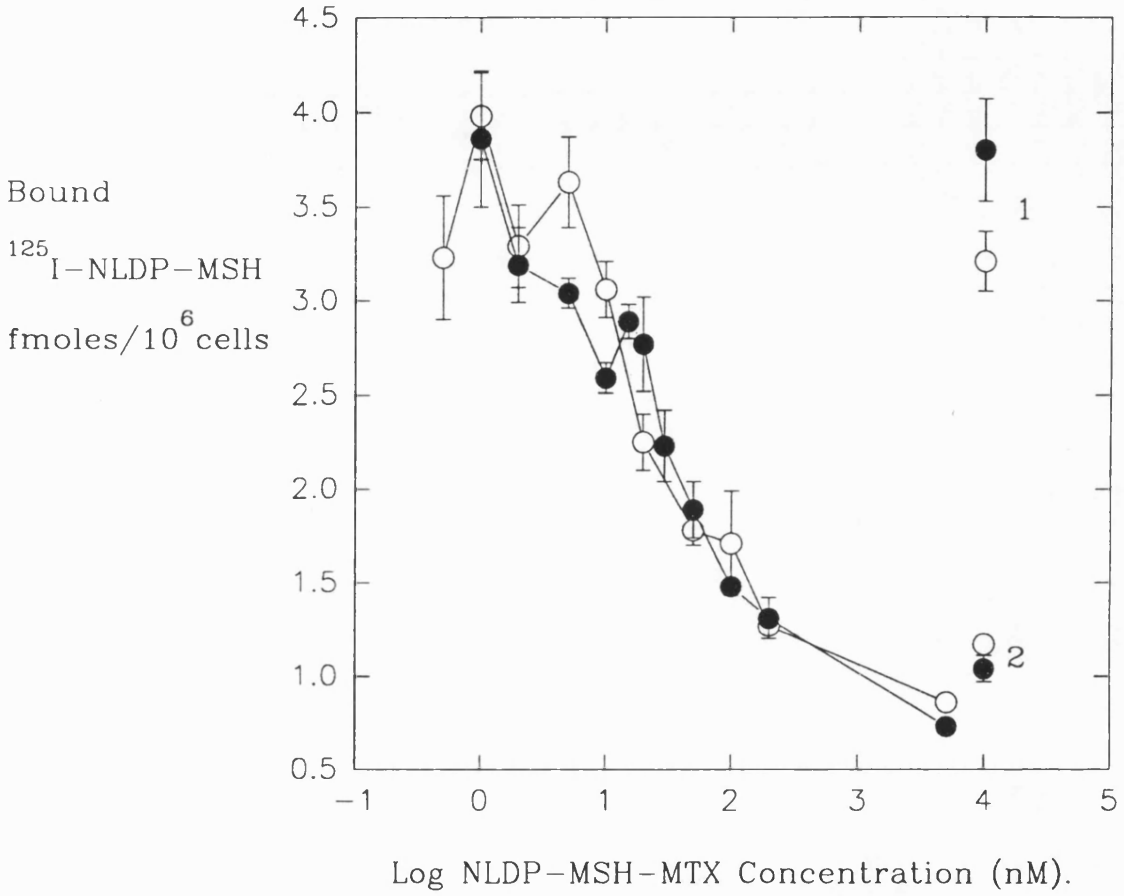

Figure 6.14: Binding competition assay (representing two individual experiments) of 0.25nM ^{125}I-NLDP-MSH incubated with increasing concentrations of NLDP-MSH-MTX at 4^{0}C for 8 hours. The total (1) and non-specific (2) binding are displayed for the two sets of data, each point represents the mean±sd from 6 wells.

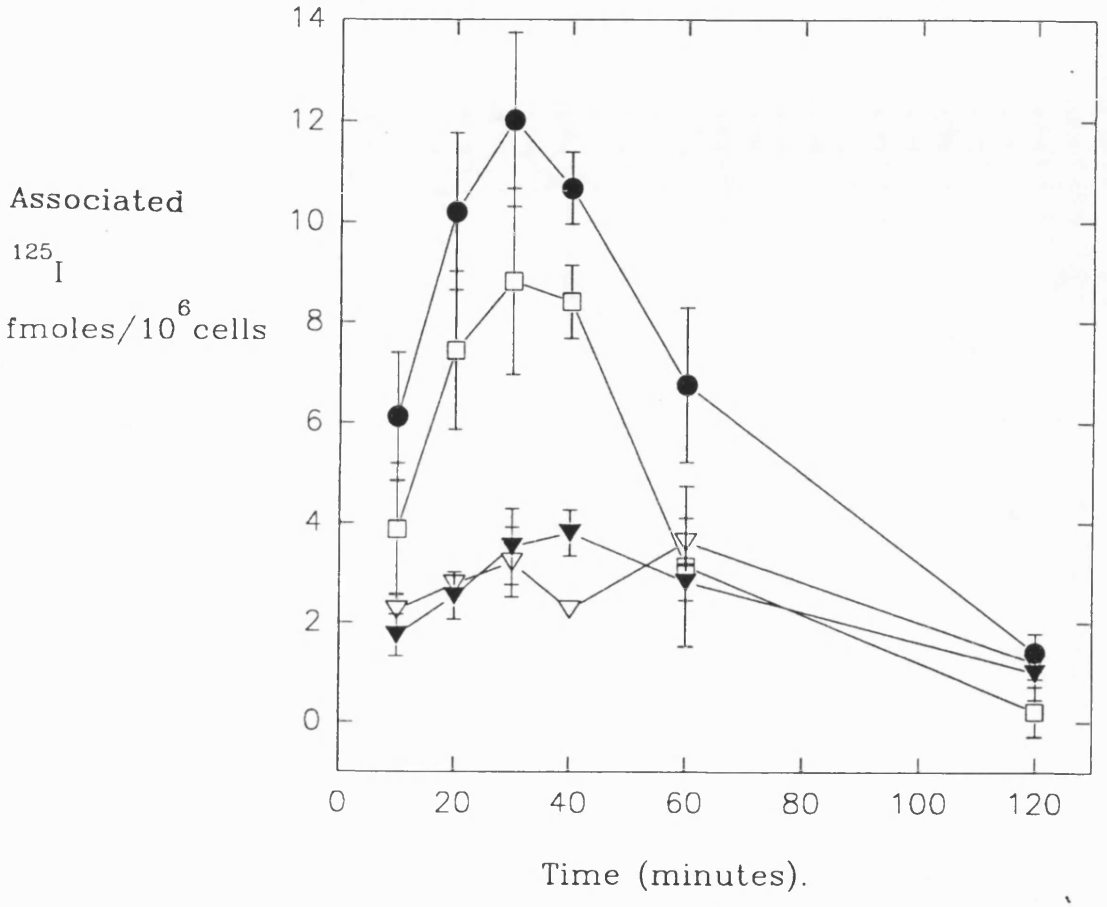

Figure 6.15: Cell associated ^{125}I activity after incubation of 1nM ^{125}I-NLDP-MSH-MTX with B16 cells at 37^{0}C with time. Each point represents the mean±sd from 4 wells. Total (●), specific (□) and non-specific (▼) binding respectively, and acid-washed cells (▽).

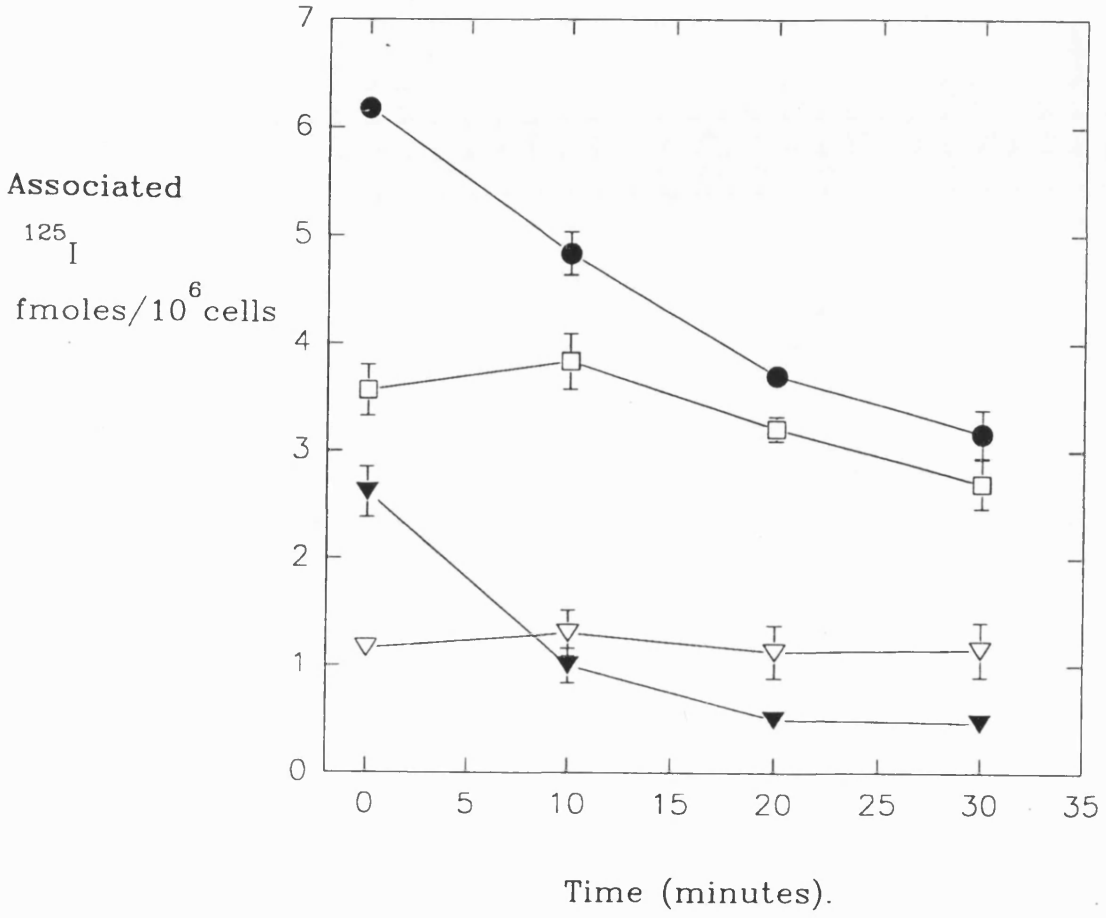

Figure 6.16: 1. Incubation of B16 cells at 37^{0}C with time in normal Hepes binding buffer, pH 7.4. Cells were previously exposed to 1nM ^{125}I-NLDP-MSH-MTX for 2 hour at 4^{0}C before being washed with ice-cold PBS (time zero) and then reincubated at 37^{0}C. Each point represents the mean±sd from 4 wells. Total (●), specific (□) and non-specific (▼) binding respectively, and acid-washed cells (▽).

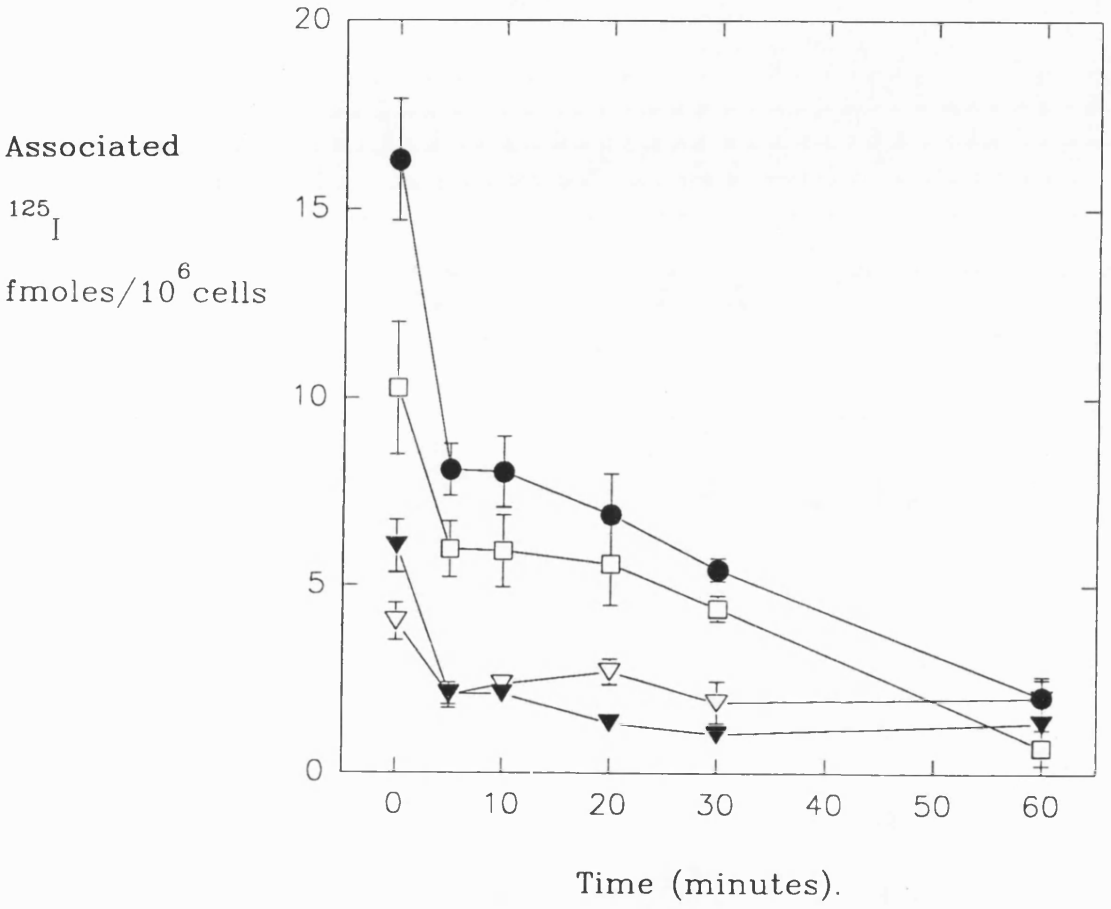

Figure 6.17: II. Incubation of B16 cells at 37^{0}C with time in normal Hepes binding buffer, pH 7.4. Cells were previously exposed to 1nM ^{125}I-NLDP-MSH-MTX for 2 hour at 4^{0}C before being washed with ice-cold PBS (time zero) and then reincubated at 37^{0}C. Each point represents the mean±sd from 4 wells. Total (●), specific (□) and non-specific (▼) binding respectively, and acid-washed cells (▽).

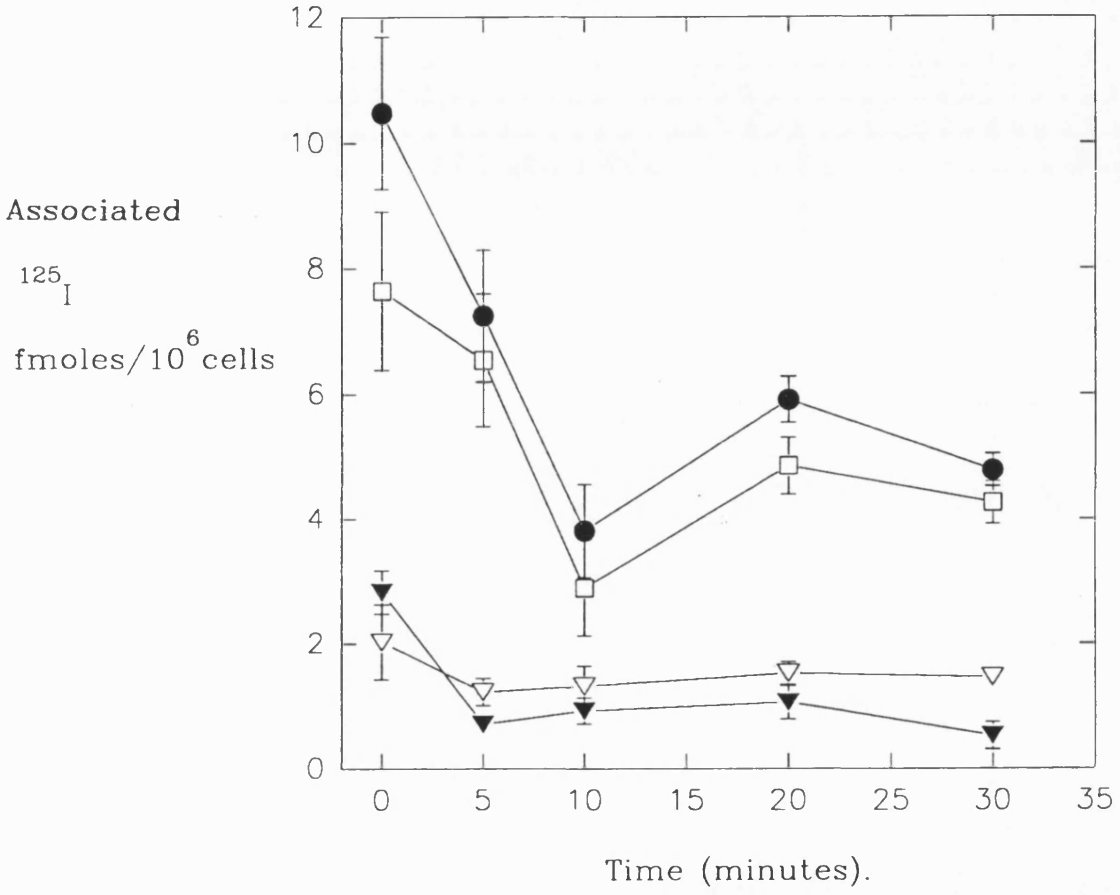

Figure 6.18: III. Incubation of B16 cells at 37^{0}C with time in normal Hepes binding buffer, pH 7.4. Cells were previously exposed to 1nM ^{125}I-NLDP-MSH-MTX for 2 hour at 4^{0}C before being washed with ice-cold PBS (time zero) and then reincubated at 37^{0}C. Each point represents the mean±sd from 4 wells. Total (●), specific (□) and non-specific (▼) binding respectively, and acid-washed cells (▽).

6.4 Discussion

The elution time of the unlabelled conjugate on the HPLC system was almost identical to that of the free peptide. Detection with UV was easier due to the MTX moiety, allowing the wavelength to be increased from 217 to 300nm. Upon iodination, products eluted in the same order as those for NLDP-MSH, i.e. non-labelled first, then mono and lastly di-iodinated peptides. However the reaction time was increased from 30 seconds to 5 minutes in order to improve the yield of mono-iodinated. Presumably the presence of MTX on the peptide decreased the efficiency of the reaction. It is also likely that 30 seconds is not the optimal reaction time for the iodination of NLDP-MSH. Resolution between the products was fairly good but by no means complete, as shown by both the HPLC trace and the activity of the fractions. Mono-iodinated conjugate was contained in fractions collected between 34-35.5 minutes inclusive, in two subsequent injections.

In retrospect the purity of the mono-iodinated conjugate could have been partially confirmed by re-injection of the chosen fractions. If totally mono-iodinated then one peak would have appeared, but it would be difficult to assess if all four forms of the conjugate were present.

The affinity of the unlabelled conjugate with B16 cells was assessed by a competition assay with ^{125}I-NLDP-MSH at 4^0C, the main assumption being that the two ligands were interacting with the same single class of receptors. The binding inhibition observed was sigmoidal in appearance, but a few more samples at lower concentrations would have been an improvement. The results from the two experiments were very close indicating a good consisitency in the assay. Values for the dissociation constant of 5.56$\pm$1.82 and 7.49$\pm$1.81nM were obtained. If the average of these two values are compared to those of ^{125}I-NLDP-MSH they are approximately ten-fold greater, thereby indicating the conjugate has a ten-fold lower affinity for the MSH receptor.

To achieve a similar level of receptor occupancy to ^{125}I-NLDP-MSH, 1nM of

labelled conjugate was incubated at 37^{0}C with B16 cells. The profile of specific binding for the conjugate was similar to the free peptide with maximal values at 30 minutes after which a decline was observed. However the maximal value attained by the conjugate was in the order of ten-fold greater (9fmoles/10^{6}cells compared to 0.8fmoles). This may reflect a significant change in binding affinity of the conjugate at 37^{0}C compared to 4^{0}C, which was not observed with NLDP-MSH; or a change in affinity due to the radiolabel (this did not occur with NLDP-MSH). Another possibility was greater receptor expression by the cells at that particular instance, but this was unlikely as similar passage numbers were used.

There was no clear evidence of internalisation during the 37^{0}C incubation, though the internalised ^{125}I may have been masked by a higher level of non-specific binding. It has been previously stated that a smaller size well may improve the assay by reducing non-specific binding, although levels were expected to increase as a greater amount of radioactivity was used (1nM ^{125}I-NLDP-MSH-MTX).

Uptake clearly occurred in experiments when the conjugate was allowed to bind to the cells at 4^{0}C, with excess ligand removed prior to reincubation at 37^{0}C in ligand free buffer. A lower level of non-specific binding in this technique may have been responsible for revealing the small amount of internalised label. These experiments displayed similar profiles to the free peptide with a decrease in specific binding with time at 37^{0}C. Both sets of experiments displayed an internalisation of ligand in the order of 0.5fmoles/10^{6}cells but this did not demonstrate if the ligands entered the cells complete or in a fragmented form.

Chapter 7

Enzyme Inhibition by NLDP-MSH-MTX and its Lysosomal Degradation products

7.1 Introduction

As mentioned previously (chapter 1), MTX exerts its cytotoxic action primarily through inhibition of dihydrofolate reductase (DHFR). MTX binding to DHFR is extremely tight and rapid [225] and inhibition is stoichiometric at pH 6.0 [226]. At physiological pH the binding affinity is lower and becomes similar to the substrate dihydrofolate (FH_2) [225]. The K_m for the natural substrate is generally in the micromolar range (pH 7.4) while the K_i for MTX is below 10^{-10}M [227].

In this part of the study it was decided to compare the inhibitory activities of MTX and the NLDP-MSH-MTX conjugate. The latter was expected to have lower activity because racemisation of the glutamate moiety was suspected. It was also of interest to determine how much activity was lost by conjugation of the peptide to MTX. However the cytotoxic action of the conjugate is not expected to

be due to the complete molecule. Targeting of this complex to cells is expected to result in receptor-mediated uptake and subsequent delivery of the complex to the lysosomes. Here degradation is likely to occur followed by the possible release of metabolites into the cell cytosol which may or may not lead to a cytotoxic effect. To study this hypothesis, NLDP-MSH-MTX was incubated with a lysosomal enzyme extract for various time periods and the degradation products assayed for DHFR inhibitory activity as a mixture. This hypothesis is comparable with reports of the in vivo effectiveness of a daunorubicin conjugate [228] which was found to be related to its susceptibility to lysosomal degradation (with release of free drug) and was more effective than daunorubicin alone. The latter study confirmed the cytotoxic action was due to endocytosis of the daunorubicin conjugate. In other studies the change in pH experienced by compounds entering lysosomes has been used as a means of drug release [229].

In the present study a spectrophotometric assay was employed using bovine liver DHFR, an easily obtainable and well documented enzyme. The human enzyme is not freely available due to difficulties in preparation as human tissue contains little DHFR [119]. Bovine DHFR was preferred to bacterial DHFR due to its closer homology with human DHFR. Although amino-acid sequence homology [230] is less than 30% between bacterial and vertebrate sources (75-90% homology in different vertebrates), X-ray crystallographic studies [231, 232, 233, 234] have shown that the overall tertiary structures are very similar. This is reflected in the very close binding requirements of DHFR from various sources for substrates and inhibitors alike. Differences are observed however in the varying affinities of inhibitors for the enzymes, e.g. trimethoprim is a potent inhibitor of bacterial DHFR but is several thousand fold less effective against mammalian DHFR [230]. Thus the bovine DHFR used in this study should be a good reflection of the results expected with the human enzyme.

7.2 Results

7.2.1 Assay Conditions

The enzyme assay was based on the method of Peterson et al. [166] who established a high yield purification of bovine liver DHFR. The reaction was measured by the rate of change in absorbance as dihydrofolate was converted to tetrahydrofolate in the presence of NADPH as a co-factor. FH_2 and FH_4 at identical concentrations display a variation in absorbance (figure 7.1), the reaction being performed at a wavelength that maximises this difference. A scan of absorbance against wavelength demonstrated this wavelength to be 343nm on the spectrophotometer used (table 7.1).

All experiments were performed with a saturating concentration of the substrate in order to ensure that the reaction proceeded at its maximum rate. This was established by increasing the FH_2 concentration in the cuvette until there was no further difference in the rate of absorbance change during the reaction (table 7.2). A value of 120μM FH_2 was found to saturate the enzyme and was employed throughout the study.

The assay was quantified by the rate of change in absorbance which proceeded with a close to linear relationship until the FH_2 became depleted. The absorbance was recorded every 30 seconds for 10 minutes during which a linear rate of absorbance change was recorded (figure 7.2). The use of rate of change in absorbance ensured that any differences in absorbance due to 'unmatched' quartz cuvettes would be nullified in quantification of the experiment.

Wavelength	FH_2	FH_4	Difference
330	0.631	0.442	0.189
331	0.619	0.418	0.201
332	0.602	0.385	0.217
333	0.587	0.356	0.231
334	0.572	0.330	0.242
335	0.560	0.311	0.249
336	0.552	0.295	0.257
337	0.540	0.276	0.264
338	0.529	0.261	0.268
339	0.520	0.248	0.272
340	0.510	0.236	0.274
341	0.505	0.231	0.274
342	0.497	0.222	0.275
343	0.491	0.216	0.275
344	0.484	0.210	0.274
345	0.480	0.207	0.273
346	0.475	0.202	0.273
347	0.470	0.199	0.271

Table 7.1: Absorbance values and difference between equimolar (0.1mM) concentrations of dihydrofolate (FH_2) and tetrahydrofolate (FH_4) at different wavelengths.

FH_2 Concentration (μM)	Gradient of ΔA
60	0.0155
70	0.0161
80	0.0184
100	0.0211
120	0.0217

Table 7.2: The gradients of the rate of absorbance change with increasing concentrations of the enzyme substrate FH_2.

7.2.2 Inhibition by MTX and NLDP-MSH-MTX

The rate of absorbance change for each experiment was calculated by performing linear regression on the data obtained. The control gradient, essentially absorbance change due to NADPH oxidation alone, was subtracted from all other gradients which were then expressed as a percentage of the maximum (120μM FH_2 with no inhibitor present).

Increasing concentrations of free MTX were added and a decline in the reaction rate was observed. An example of a typical experiment, figure 7.3, shows the test and control reactions plus three different concentrations of MTX. As the amount of MTX increased there was a corresponding decrease in the reaction rate. Complete inhibition occurred when the reaction had an identical rate to that of the control. The linear regression of the data also demonstrated the close linear relationship of the reaction and the validity of using linear regression.

Dose-inhibition curves for MTX and NLDP-MSH-MTX exhibited similar profiles as would be expected for genuine competitive inhibition (figure 7.4). The inhibition from 100% approximately to 20% of the test activity occurring over 2 to 3 log cycles for both compounds. Inhibition was thought to take place through the same mechanism, both being competitive with FH_2 for the enzyme. The data was fitted to equation 7.1, where A represents the % of DHFR activity, C the concentration of inhibitor, and B the IC_{50} for the respective inhibitor. A value of 0.7 was assigned to m, using a parameter estimate from an initial fit of the data for MTX.

$$A = 100 \times \frac{1 - C^m}{C^m + B^m} \tag{7.1}$$

The IC_{50} values for MTX and NLDP-MSH-MTX were 8.98 ± 1.32 and $364.25 \pm$ 121.15nM respectively.

7.2.3 Inhibition by the lysosomal degradation products of NLDP-MSH-MTX

A concentration of the conjugate was chosen which exhibited an inhibitory effect whilst overlying part of the free MTX inhibition curve in order to compare the inhibitory effects of degradation products with both conjugate and free drug. A concentration of 20nM NLDP-MSH-MTX was chosen which allowed the reaction to proceed at 85% of the maximum rate of the test reaction. The corresponding reaction in the presence of 20nM MTX proceeded at 30% of the maximum rate. The concentration of conjugate exposed to the lysosomal enzymes was 0.25mM. The lysosomal reaction mixture was then serially diluted in the sodium acetate and KCl buffer (pH 6.0), in order to minimise effects of the low pH buffer and the proteins themselves.

Two degradation reactions were performed at 37^0C (reactions A and B) on different days with samples removed at 0, 2, 4 and 16 hours. The inhibitory activity was then assessed in the DHFR enzyme assay (table 7.3). Generally products of the lysosomal reaction mixtures displayed an increase in inhibitory activity as the length of lysosome degradation increased. Control samples at 0 hours retained almost identical activity to the undegraded conjugate thus demonstrating no effect on the assay by buffer or lysosomal enzymes being carried over to the DHFR assay. No explanation is available why the 2 hour sample from reaction B exhibited a greater inhibitory action than at 4 hours. In reaction A the 16 hour sample was more inhibitory than the corresponding concentration of free MTX (18.65±2.54% activity compared to 30.25±2.94%)whilst the same time sample from reaction B was similar to MTX (28.15±0.58%).

Incubation Time (hours)	Percentage of DHFR Activity	
	Reaction A	Reaction B
0	84.63 ± 6.38	88.77 ± 34.04
2	68.53 ± 12.29	26.15 ± 4.02
4	34.66 ± 1.07	41.20 ± 8.01
16	18.65 ± 2.54	28.15 ± 0.58

Table 7.3: The percentage of DHFR activity (mean±sd) in the presence of the degradation products of NLDP-MSH-MTX after various lengths tritosomal incubation (from two different reaction mixtures, A and B).

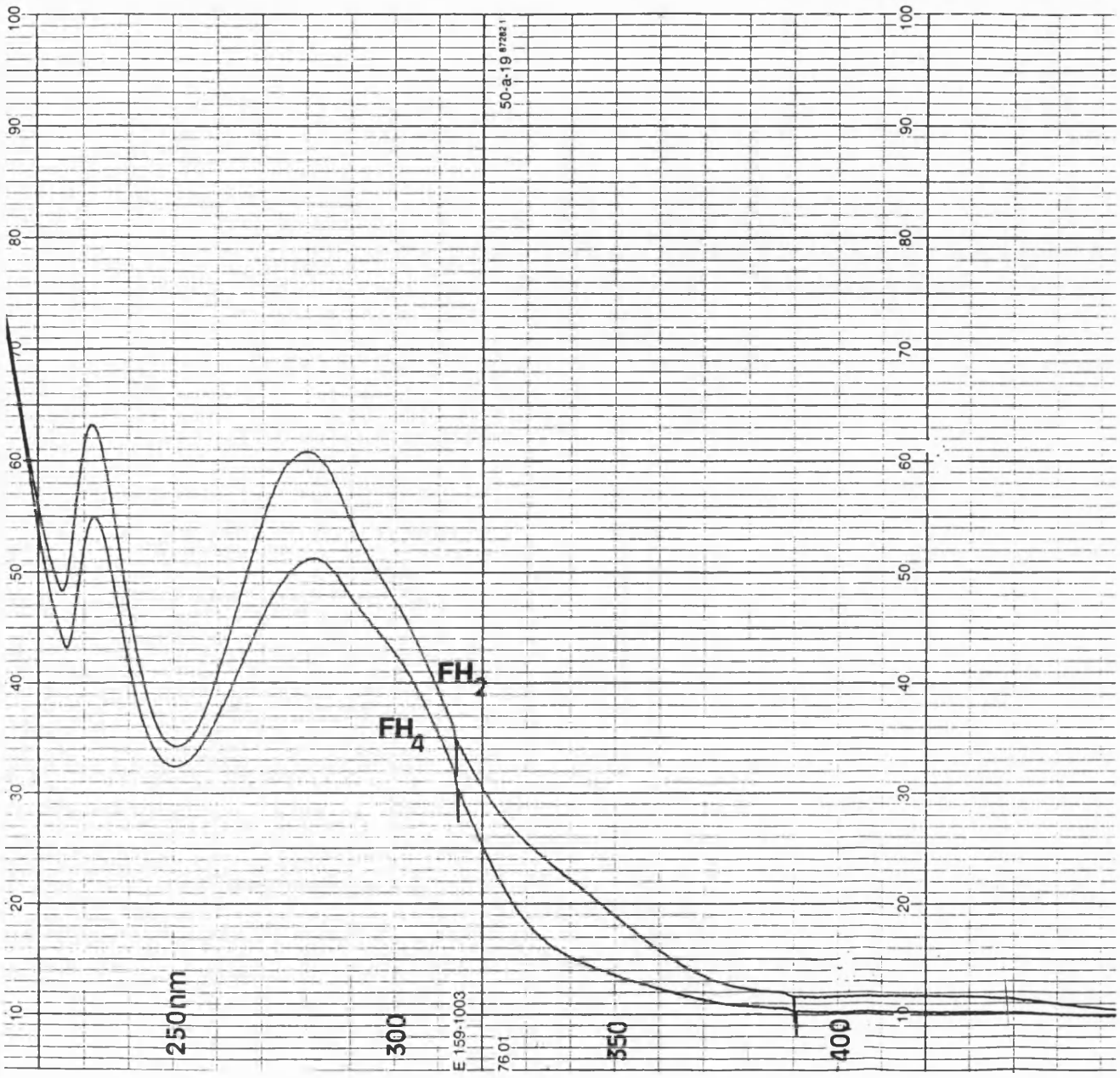

Figure 7.1: Absorbance scan against wavelength of 1μM FH_2 and FH_4 at room temperature.

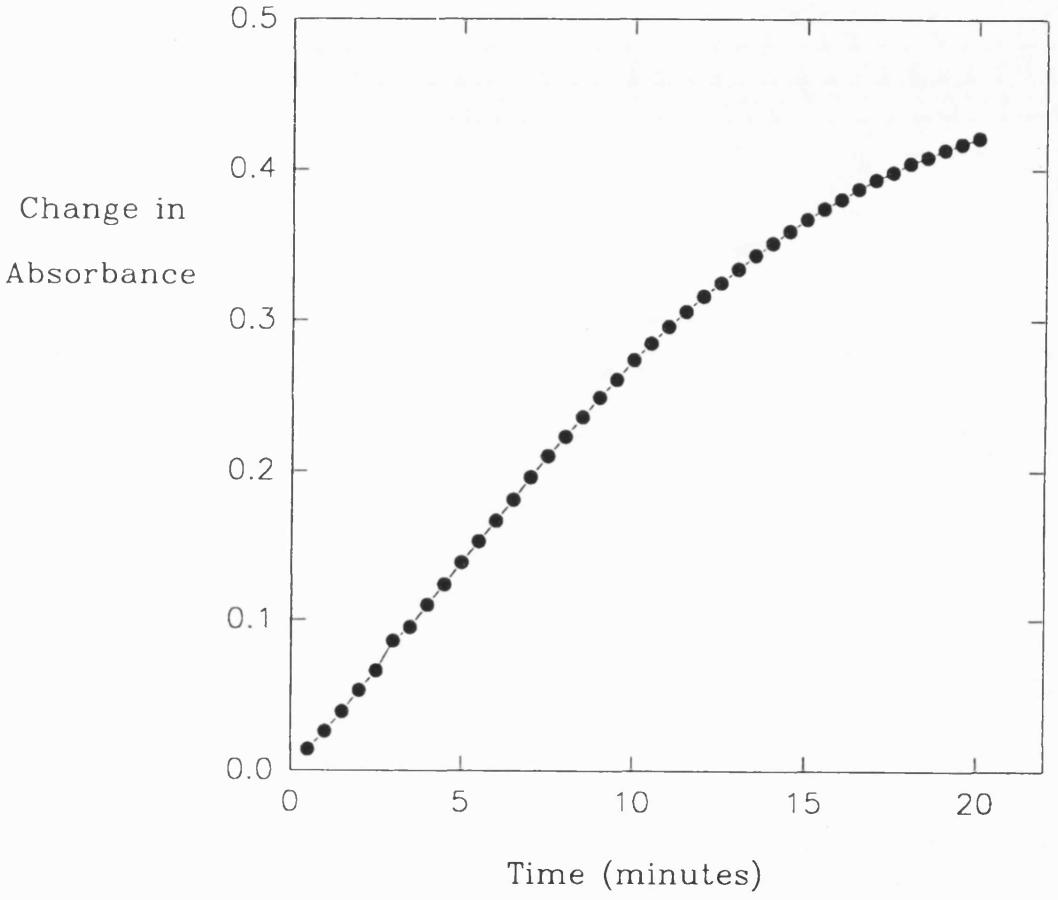

Figure 7.2: The rate of change of absorbance at 343 nm of 120μM FH_2 incubated with DHFR at 37^{0}C in the presence of 50μM NADPH

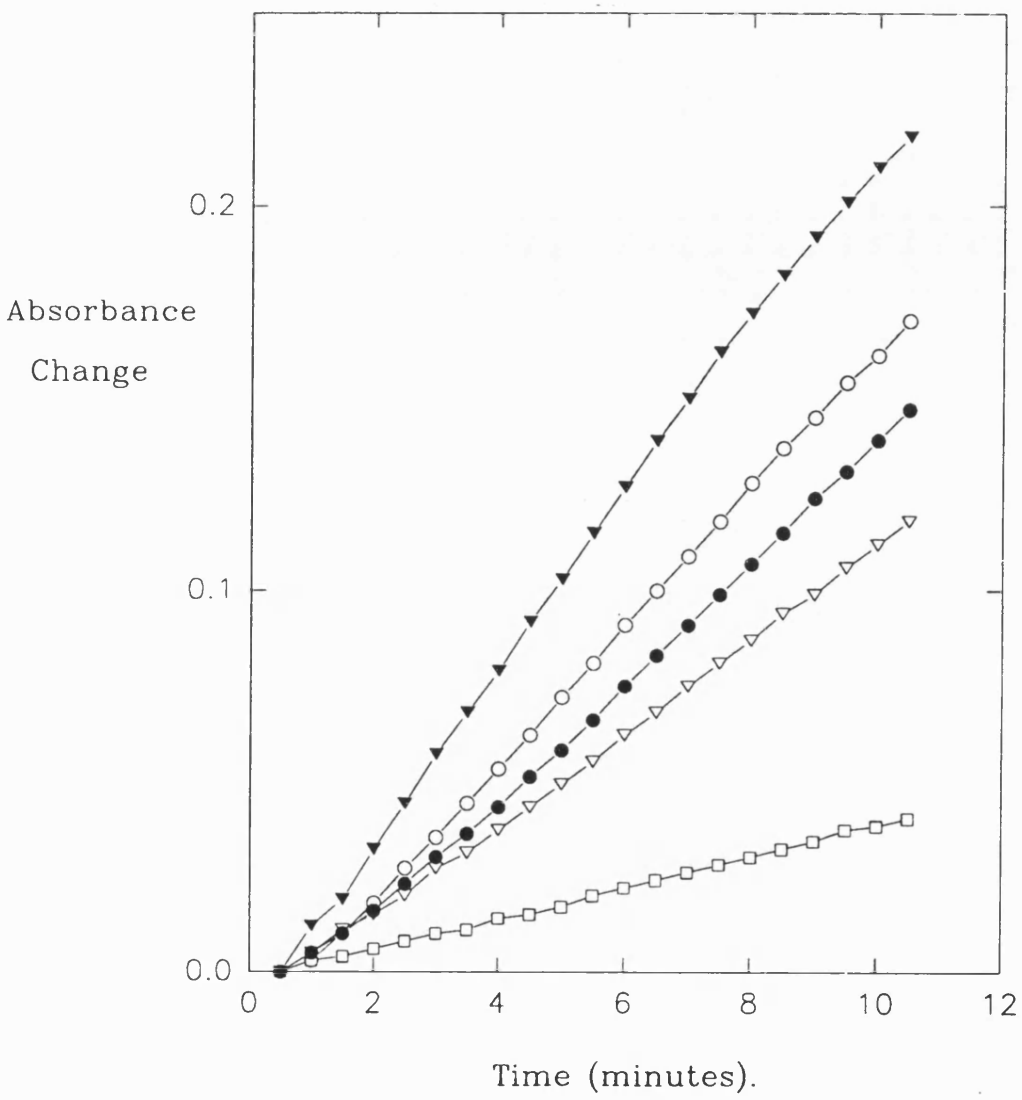

Figure 7.3: Rate of change of absorbance at 37^{0}C, 343 nm, of 120μM FH_2 with DHFR, 50μM NADPH in the absence and presence of varying MTX concentrations. The control represents DHFR and NADPH alone. 120μM FH_2 (▼), 1 nM (○), 2 nM (●) and 10 nM MTX (▽), and the control (□).

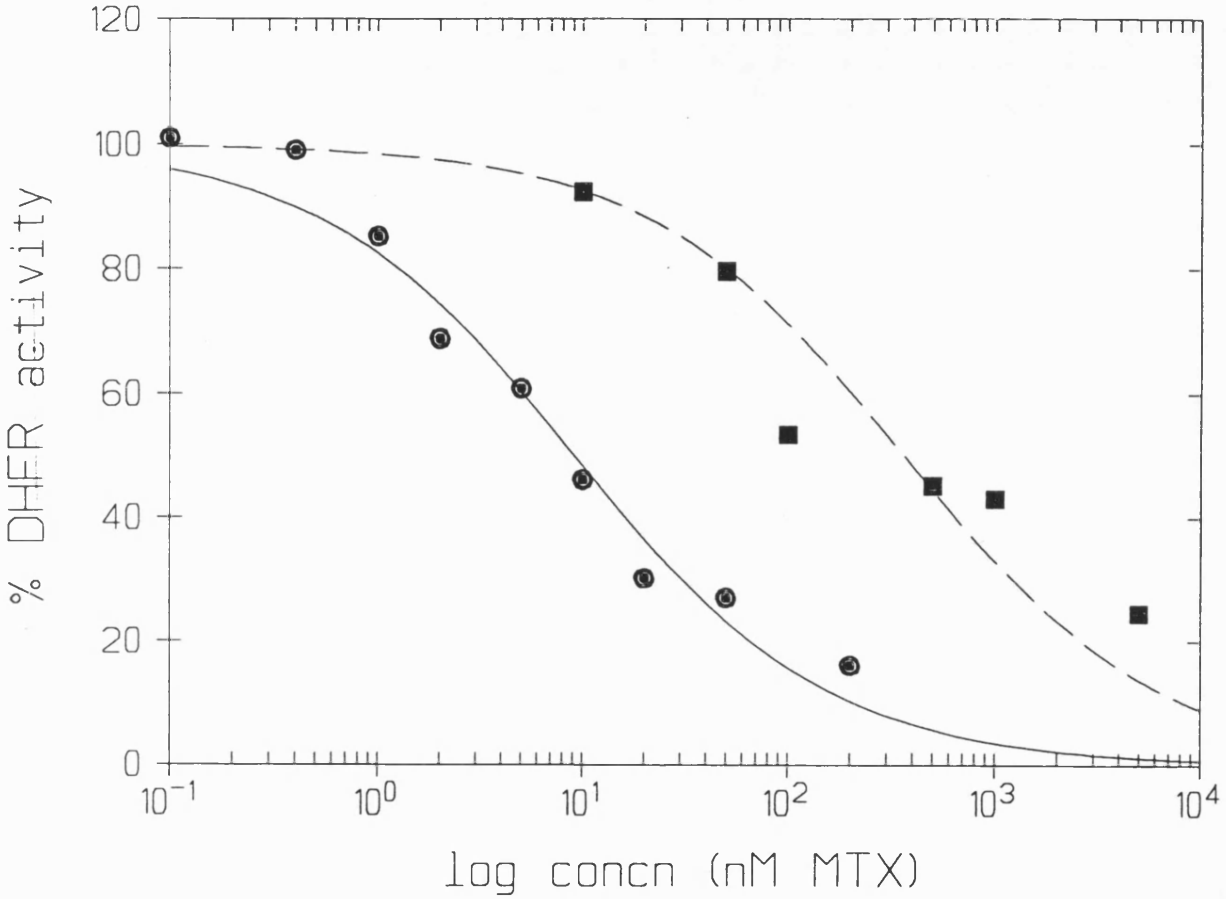

Figure 7.4: Inhibition of DHFR at 37°C by MTX (●) and NLDP-MTX (■) expressed as a percentage of maximum activity (120μM FH_2 represents 100%).

7.3 Discussion

The spectrophotometric assay employed enabled the measurement of initial rate of reduction of FH_2 by the DHFR system. This permitted the comparision between three different MTX derivatives, namely free MTX, the conjugate form NLDP-MSH-MTX and the degradation products of the latter after lysosomal attack. The validity of using the first ten minutes of the reaction to calculate reaction rate was established as the rate of absorbance change was very close to linear.

Inhibition of DHFR by free MTX occurred in a dose related manner with up to about 80% inhibition being achieved at 0.2μM. This degree of inhibition was gradual taking place over 2 to 3 log cycles which proved too shallow to model by the standard procedures for a sigmoidal dose/response relationship. Similar profiles were obtained by Peterson et al. [166] using bovine DHFR at pH 8 and Thillet and Picket with the mouse enzyme [235]. The response could infer negative cooperativity however this has not been suggested to occur with this well documented enzyme.

When the conjugate NLDP-MSH-MTX was used a similar dose/inhibition response was observed, however this was shifted to the right corresponding to increased inhibitor concentrations. The IC_{50} values corresponded to 8.98 ± 1.32 and 364.25 ± 121.15nM for MTX and NLDP-MSH-MTX respectively. The conjugate thus had a 41 fold lower affinity for the enzyme than the free drug. The parallel profiles of the two inhibitors indicated that they both acted as competitive inhibitors with FH_2 for the same site on the enzyme.

The decrease in affinity by the conjugate can easily be explained when the stereochemistry of MTX inhibition of DHFR is examined. Early x-ray studies of the bacterial DHFR/MTX complex pointed towards two important features of inhibitor binding [236]. Firstly the possible inversion of the MTX pteridine ring relative to that of FH_2 in the binding site of DHFR, and secondly the hydrogen

bonding via the α-carboxyl group of the glutamate moiety of MTX. The proposal of the former by Matthews et al. [236] was later confirmed by Charlton et al. [237] using DHFR from Lactobacillus casei and Bolin et al. [231] with an identical enzyme source plus Escherichia coli. Similar findings were later observed with human DHFR and MTX in a crystalline structure [233, 234] and in solution [232].

During the aforementioned studies the importance of hydrogen-bonding via the α-carboxyl group was also noted in all DHFR sources whereas interaction through the γ-carboxylate appeared weak and non-specific. This was supported with the study of DHFR inhibition by various analogues and conjugates of MTX involving its terminal glutamate residue. When Rosowsky et al. [238] prepared amide derivatives of MTX via the α and γ carboxyl groups together there was a dramatic increase in the IC_{50} values for DHFR inhibition compared to free MTX. However a γ-monohydroxamine acid analogue which had a free α-carboxylate retained similar activity to MTX. Other findings reported by Piper et al. [239] who used α and γ substituted amides, peptides and esters of MTX led to similar conclusions. Inhibition of DHFR showed little variation when the α carboxyl group remained intact, but when substituted with Gly, Asp or Glu there resulted in a 100,000 fold incease in the values of K_i for DHFR inhibition in mouse L1210 cells.

When Fan et al. [240] synthesised a fluorescein-MTX conjugate they obtained similar reaction products as those obtained here with NLDP-MSH-MTX, i.e. α and γ isomers, which on further investigation were found to have undergone racemization of the l-glutamate moiety in MTX. When the isomers were resolved the α conjugate was found to be almost 60 times less effective in DHFR inhibition than the γ isomer, which in turn was 5.5 times less effective than free MTX. This would imply that the NLDP-MSH-MTX conjugate, which is also thought to comprise of the α and γ isomers, would be expected to demonstrate weaker DHFR inhibition than MTX, in particular the α form. If the two isomers were to be separated a difference in the IC_{50} values would almost undoubtably be observed, with the γ form perhaps displaying a lower value than the one recorded with the

mixed isomer conjugate.

Other conjugates of MTX have been reported with varying degrees of DHFR inhibition, they all observed a similar inhibitory profile for the free drug i.e. inhibition over approximately 2 to 3 log cycles. Antibody conjugates of MTX synthesised by different methods (ECDI reaction or the active ester method) displayed similar activities compared to MTX [241]. Conjugates prepared by either method were about 2.5 and 3.8 fold weaker inhibitors of DHFR activity (at 40% inhibition) with incorporation levels of 5 and 12 moles of MTX per mole of antibody respectively. Kulkarni et al. [80] prepared a MTX conjugate with an antibody and its $F(ab)_2$ fragment. Both had identical inhibitory action against DHFR and had an IC_{50} value two fold greater than free MTX.

Various polymer-linked MTX derivatives displayed more diversity in DHFR inhibition [242] when bound to poly-l-lysine or carboxycellulose, IC_{50} values were 1 and 2 log cycles greater than free MTX respectively. A co-polymer of divinylether-maleic anhydride had very similar activity to MTX. This latter observation was unexpected as the polymer was bound to the pteridine ring of MTX which is essential for binding. In this case hydrolysis of the conjugate and the release of MTX was suggested. Although not tested in the enzyme assay, stability of the NLDP-MSH-MTX was thought to be high.

Although inhibitory activity of the complete conjugate is almost desirable in some respects, certain non-specific uptake processes e.g. via the MTX membrane transport protein, will allow entry to non-targeted cells avoiding the lysosomal pathway hence the conjugate remains intact inside the cell cytoplasm. In this case a low inhibitory action would be advantageous with the cytotoxic ability only being released upon lysosomal contact. It is envisaged that the majority of the cellular uptake of NLDP-MSH-MTX will occur via receptor-mediated endocytosis terminating in exposure to the lysosomes (although a portion may be recycled to the cell exterior if still attached to the MSH receptor which may undergo this process). In this situation DHFR inhibition is expected to be the result of the

lysosomal degradation products of the conjugate, which have been emulated in this present study with the use of rat liver lysosomes.

The results of two separate lysosomal incubations of the conjugate revealed similar results with greatest inhibitory activity after 16 hours incubation. This may indicate the reaction has not yet reached optimal conditions and further periods of incubation are worth investigating. The inhibition by the 2 hour incubation in reaction B appeared rather strong and is possibly explained by inadequate mixing before sample removal or variability in the reaction, which at that stage was probably in its initial phase.

All time points displayed increased inhibitory action than the undegraded conjugate implying the formation or release of more toxic component(s). The activity of the mixtures after the longest incubation periods, 18.65±2.54% and 28.15±0.58% were similar, and in the former case greater, than the activity of the free drug at the equivalent concentration. This would suggest the possible release of free MTX from the conjugate or alternatively MTX derivatives with an increased affinity for the enzyme. Separation and individual testing of the degradation products would give a clearer indication of the mechanisms of the inhibitory action observed.

A similar investigation was performed with trypsin by Shen and Ryser [74] using a poly-l-lysine conjugate which had an IC_{50} value 400 fold greater than free MTX. After the conjugate was incubated with trypsin the IC_{50} value decreased to 20 fold greater. Cell lysates incubated with the conjugate revealed a peak of low molecular weight material which eluted just before MTX after HPLC separation. This was believed to be a digestive product of the conjugate, presumably MTX-lysine or MTX-oligolysine. A corresponding experiment with NLDP-MSH-MTX may reveal similar findings.

The release of cytotoxic agents from macromolecules has been investigated over the last fifteen years, with various reports of efforts to increase the efficiency of drug release. Early studies discovered the necessity of employing spacer linkages

between the carrier and the drug in question, in order to allow access to the lysosomal enzymes. Trouet et al. [228] conjugated daunorubicin to succinylated serum albumin directly or with up to four amino acid residues as spacer linkages. The direct linkage proved resistant to lysosomal attack whilst a single amino acid spacer resulted in very slow release. A slight improvement was attained with a di-peptide spacer when 8% of the daunorubicin was released. However when the tri- and tetra-peptide spacers were used, 60 and 75% of the drug was cleaved respectively. Duncan et al. [243] investigated the degradation of peptide side chains of poly-N-(2-hydroxypropyl)-methacrylamide derivatives to release a terminal 4-nitroaniline residue. Spacers varied from 2-4 amino acids in length but out of 22 tested only 4 were digestable. This demonstrated that release was not purely based on physical distance from the linear backbone of the macromolecule but was also dependent on the structure of the linkage. This was later confirmed with further studies with the same polymer backbone [244, 104].

In order to rationalise this approach for linkage design the basis behind the degradation had to be elucidated. Studies of the proteases involved [245, 246] revealed that the enzymes posessed a large active site performing two main functions; binding of the substrate, and catalysis of the reaction. The active site has been conveniently divided into subsites which interact with one amino acid residue of the substrate. Each site is aligned such that the -CO-NH- group to be hydrolysed always occupies the same position. Therefore the efficiency of cleavage will be dependent on the amino acids that occupy each enzyme subsite. This explains why 3/4 residues are required for spacer linkage but also why their identity is very important.

The precise requirements of all the lysosomal enzymes have yet to be elucidated, however, an example of conjugate design using the existing knowledge has been demonstrated [247]. It was discovered that the cleavage of the peptide spacers employed in the system was due to proteases, mainly cathepsins B, L and H. Cathepsin L was known to be a thiol dependent enzyme requiring hydrophobic residues in two of its subsites [248]. When phenylalanine or valine were introduced

at certain positions in the spacer linkage, an increase in the amount of cleavage occurred.

Although the NLDP-MSH-MTX conjugate would be unlikely to require a spacer linkage as such (due to the relatively small size of the peptide and the linkage of MTX to the N-terminus), rearrangement of the last 3-4 terminal amino acid residues before the MTX component, or even the addition of further residues, may yield a conjugate with an increased efficiency of lysosomal MTX release. However this may alter the binding properties of the peptide to the MSH receptor even though the residues thought to be involved are at the C-terminus (see chapter 6). It should also be noted that as well as the structure of the amino acids being important for interaction with the subsites on the enzymes, the terminal moiety will also determine the rate of release [249].

Chapter 8

Discussion

Site-specific drug delivery requires the direction of the therapeutic agent in question, to a specified site of action. An immense task when the physiological barriers involved are considered, but through the use of macromolecular carriers and/or targeting groups, success has been achieved to a limited extent. These targeting moieties or homing devices are generally employed to maximise the interaction of the drug-conjugate with the target cells and through this, minimise non-specific binding to other cells. However this would imply the sole expression of the targeted binding site on the selected cells which is rarely the case. In cancer chemotherapy the increased expression of the receptor/antigen site in tumour cells over the healthy cell population, is usually encountered. Therefore the plasma membrane interaction of a conjugate must be carefully assessed in vitro in order to partially predict its chances of successful site-specific delivery in vivo.

The conjugate employed in this study, although not available until the later stages of the work, consisted of two components, both capable of binding to cell membranes. The antifolate MTX enters cells through the reduced folate carrier, present on almost all human cells due to the dependence on extracellular reduced folate sources. The drug not suprisingly exhibits a very low specificty

against tumor cells due to an increased folate requirement. However the peptide analogue of MSH, NLDP-MSH, interacts with high affinity to specific membrane receptors and will thus have a more defined mode of cellular binding.

Before studying the fate of NLDP-MSH-MTX with the selected B16 murine melanoma cell line, the individual components of the conjugate were examined with respect to membrane binding and subsequent fate. Particulary in view of the proposed mode of cellular uptake for MTX in the conjugate form, which was expected to be different to the uptake of free drug. Would this new route of drug delivery be as efficient as the former, and if not would therapeutic intracellular levels be achieved ?

MTX binding and subsequent uptake in tumour cells is predominantly through the reduced-folate carrier, often described as a 'high affinity, low capacity' system, with respect to MTX and reduced folates [120]. However this nomenclature is misleading as the affinities usually encountered for MTX and reduced folates are in the micro-Molar range. Indeed when ^{3}H-MTX binding at 4^{0}C with B16 cells was assayed, a value for K_d in the order of 0.21μM was recorded, which in fact is a relatively low affinity for a ligand/receptor complex. Although the presence of a second membrane folate binding protein has been reported [124], which does display an affinity for folic acid in the nM range, it has a low affinity for MTX which appears to undergo intracellular uptake predominantly through the reduced-folate carrier [126].

Uptake of MTX initially proved difficult to measure until a reliable acid-wash buffer was established. Although the amount of cell associated ^{3}H- activity was essentially identical after 24 hours at 4^{0}C and 37^{0}C, the majority of the latter was acid-resistant or internalised within the cells (presumably retained associated with MTX). The validity of in vitro cell culture models in comparision to the in vivo state has to be questioned since the cells are grown in an abundance of extracellular folate far above serum levels in the body; thereby perpetually possessing high intracellular levels of folate. The inability of B16 cells to grow in

low folate media without the use of a gradual decline in the extracellular folate concentration, did not permit binding or uptake experiments upon cells under these conditions.

Although the MTX moiety of the conjugate may have the potential for a wide degree of specific binding via the reduced-folate carrier (c.270,000 binding sites per B16 cell as an estimate), it has a low binding affinity. Indeed it was this low affinity that was responsible for the problems encountered in the work involving the radio-labelled ligand. Notably the danger of a degree of dissociation during the washing procedure, and the relatively high levels of non-specific binding encountered. Binding of the NLDP-MSH-MTX conjugate to the MTX transport proteins was weak and would be minimal in comparision to its binding to the MSH receptor.

Although ^{125}I-NLDP-MSH did display specific binding of a higher affinity, K_d 0.37-0.87nM, there was a much lower number of binding sites (4000-5000 per B16 cell). Since uptake of the conjugate is unlikely via the reduced-folate carrier, internalisation after NLDP-MSH binding would be essential for action. Although MSH elicits its biological action through binding to the MSH membrane receptor, it is unresolved whether or not this process also involves internalisation of the ligand/receptor complex. Experiments at 37^{0}C revealed the appearance of acid-resistant ^{125}I activity with B16 cells, but it was impossible to ascertain if this was still associated with the peptide, without analysis of the cell contents via chromatographic techniques. Further experiments revealed the likelihood of this internalisation process occurring after binding to the receptor. When permitted to bind at 4^{0}C, the amount of the surface-bound tracer decreased upon transfer to a 37^{0}C enviroment, with about 40% appearing internalised. However these experiments were not performed at a saturating concentration of the ligand. This resulted in difficulties in the detection of acid-resistant ^{125}I activity above non-specific levels. Further experiments should be carried out at higher receptor occupancy with a larger population of cells, to reduce non-specific effects.

Of course at 37^{0}C many cellular processes are occurring, including pinocytosis. The question arises as to whether the appearance of acid-resistant activity can be attributed to the constitutive process of membrane internalisation reflected by pinocytosis ? The rate of fluid-phase endocytosis, or more strictly the lysosomal accumulation of extracellular fluid, for B16 cells at 37^{0}C was established as 0.038μl/hr/10^6cells. If one makes the assumption that endocytic vesicles are 0.2μm in diameter, and the average diameter of a B16 cell is 15μm (considering the cell for theoretical purposes as a smooth spherical body), then 150 vesicles are formed per minute per cell. This represents a cell-surface membrane internalisation rate of 2.7% per minute, i.e. the entire cell membrane will be internalised after 37 minutes. So can the appearance of 40% of the original bound ^{125}I-NLDP-MSH activity within the cells after 10 minutes be attributed to constitutive membrane turnover ? From these predictions, and assuming an even receptor distribution on the cell surface, 27% of the surface-bound peptide will be internalised after 10 minutes. This theoretical value is not too disimilar to that recorded experimentally.

A similar calculation can be considered when examining the data from the continual exposure of B16 cells at 37^{0}C in the presence of 0.1nM ^{125}I-NLDP-MSH. After 60 minutes the acid-resistant fraction had increased to 0.3fmoles/10^6 cells which is equivalent to 180 molecules per cell. The determined amount delivered by pinocytosis to the lysosomes after 1 hour would be 2.28 molecules per cell. This does not include molecules present in the endosomal compartment, which was estimated to have a volume of approximately 109nl/cell. This translates to 6.6 molecules per cell. Therefore fluid-phase uptake could account for about 9 molecules of ^{125}I-NLDP-MSH per cell in 1 hour at 37^{0}C. This is obviously exceeded by the value of 180 molecules/cell as expected due to the membrane interaction of the peptide. However can constitutive membrane internalisation account for the observed amount of internalisation ? An extracellular concentration of 0.1nM ^{125}I-NLDP-MSH was approximately one tenth of the receptor saturating concetration, the latter determined as c.4500 sites/cell, i.e. approx-

imately 450 binding sites would be occuppied by the tracer. It was calculated earlier that the entire cell surface area of the cell membrane would be internalised after 37 minutes, however a value of only 180 molecules per cell was attained, less than half the expected amount. There are a number of possible reasons for this observation:

1. Binding to 450 sites was not achieved, or a lower amount of receptor expression than previously recorded.
2. Cells exhibited a decreased rate of membrane internalisation.
3. The assumption of the cell as a spherical body has resulted in an unacceptably low value for the cell surface area.
4. After 60 minutes some radio-label has been internalised and subsequently exited the cell.

It should also be noted that the surface-bound activity achieved a maximum at 30 minutes before declining, i.e. there was a decrease in the number of membrane binding sites. A plausible hypothesis to these observations and theoretical calculations would be a constant recycling of the receptor due to membrane internalisation and subsequent reappearance at the cell surface (e.g. as is the case for LDL and transferrin receptors [250]). After the binding of ^{125}I-NLDP-MSH, the fate of the receptor could be a return to the cell surface in a state unable to bind further ligand, or the receptor could be processed intracellulary. Either fate will result in a decrease in the number of available binding sites on the cell surface, which would account for the decrease in bound labelled peptide. Cycling from plasma membrane to early endosome and back is likely to be rapid with some delivery to the lysosome which accounts for the observed intracellular ^{125}I activity.

The fate of the ligand is very difficult to predict from the current data as we only have a measure of the ^{125}I activity. Once internalised the ligand may dissociate

from the receptor in the endosomes and be transferred further along the vesicular pathway to the lysosomes. Alternatively it may return to the cell exterior either in solution or bound to the receptor with subsequent dissociation. If the ligand/receptor complex was recycled intact back to the cell surface, dissociation would be expected to occur slowly due to the high affinity of the peptide. Dissociation would be too slow to explain the decrease in specifically bound ligand observed.

The low activity inside the cell (180 molecules/cell) could be an underestimate as ligand may have been returned to the extracellular medium, or the iodine label may also be returned either passively or actively after separation from the peptide (possibly after exposure to lysosomal enzymes). The latter is certainly possible, fluid-phase markers appear in the lysosomal compartment from 10 minutes after exposure to a cellular enviroment [179].

To summarise; the measure of acid-resistant activity at 37^0C was probably an underestimate of total internalised peptide due to the subsequent loss of iodine-label back to the extracellular medium, either as ^{125}I-NLDP-MSH or a derivative of the peptide. It can be postulated that the internalisation of the ligand/receptor complex is unecessary for the biological action of NLDP-MSH, and is only a mode of desensitisation or termination of the stimulus. Thus the receptor is constantly being recycled until ligand is bound which then alters the fate of the receptor, probably being processed further along the vesicular endocytic pathway.

Some membrane receptors are known to recycle, e.g. LDL and transferrin are thought to be internalised 4 and 10 times an hour respectively, whilst others, e.g. EGF, remain for longer periods at the cell membrane surface [250]. Saturating levels of ligand binding result in the majority of EGF receptors being internalised with a half-time of 2.5 minutes [251]. The existence of relatively long term membrane proteins suggests that not all the regions of the cell membrane are recycled. Thus the MSH receptor may also escape recycling. The presence of the receptor at the cell surface could be further investigated by two methods.

The first would involve initial exposure of B16 cells to a saturating concentration of unlabelled peptide at 4^0C. Unbound ligand would be subsequently removed, the cells re-incubated at 37^0C, and challenged after various time periods to assay the number of membrane binding sites. Due to the high binding affinity of the peptide, ligand dissociation would be minimal, thus the radio-ligand will bind only to new or unoccupied receptors arriving at the cell surface.

Secondly, exposing the cell to a salt of a weak base, such as ammonium chloride, and then challenging the cells with radio-ligand after various time periods, will indicate if the receptors are involved with membrane turnover. Weak bases can alter vesicle pH and fusion events leading to the entrappment within the cell of surface receptors, e.g. the presence of monensin prevented the recycling of LDL receptors [252]. A loss of membrane binding sites in the absence of ligand indicated the internalisation of empty receptors can occur.

The receptor recycling proposed for the NLDP-MSH binding site presents many questions with respect to site-specific drug delivery:

1. Are there sufficient cell surface binding sites to account for an increased accumualtion of a conjugate within tumour cells ?
2. Once internalised is the peptide recycled to the cell exterior or processed within the cell ?
3. What is the time period before full receptor expression is reinstated at the cell surface after exposure to the ligand ?
4. Will NLDP-MSH-MTX follow an identical pathway to the parent peptide, and if so will sufficient drug levels be attained within the cell for a therapeutic effect ?

It is important to assess the subsequent fate of the ligand/receptor complex after internalisation. This is probably optimally achieved with covalent labelling of

the receptor in conjunction with subcellular fractionation and electronmicroscope studies. Also the use of ionophores (e.g. monensin) or weak bases which are able to increase the intraluminal pH of endosomes and lysosomes, have profound effects on the fate of ligand/receptor complexes.

From the results presented here it can be predicted that interaction between the NLDP-MSH-MTX conjugate and the B16 cell plasma membrane was predominantly via binding to the high affinity MSH receptor. The MTX moiety was expected to display little specific binding which was duly demonstrated. The conjugate, with at least a ten-fold lower binding affinity than free MTX, displayed no specific displacement of the latter at 4^0C. However in a similar binding inhibition experiment with ^{125}I-NLDP-MSH the conjugate exhibited only a ten-fold lower affinity for the MSH receptor. This confirmed the conjugate was binding predominantly via the NLDP-MSH component, but would it be internalised ?

When 1nM of the successfully iodinated conjugate was incubated at 37^0C with B16 cells, a similar profile of surface binding was demonstrated, although internalised ^{125}I activity was masked by non-specific binding. This indicated the conjugate may be following the same route as the labelled peptide. When the conjugate was initially permitted to bind at 4^0C before further incubation at 37^0C (after washing), similar results to ^{125}I-NLDP-MSH were again obtained. The degree of internalisation was difficult to assess with certainty due to the levels of non-specific binding. Subsequent assay experiments must employ an increased cell number to well size ratio, or a similar cell suspension technique to that used for the measurement of fluid-associated ^{125}I-PVP uptake.

As the conjugate retained a relatively high affinity for the binding sites on B16 cells, uptake was assummed to occur by an identical mechanism to the parent peptide. However would adsorptive endocytosis with maximum receptor occupation be sufficient to achieve therapeutic levels of drug within the cell ? This is very much dependant on the toxicity of the drug in question, MTX, which is estimated to require c.1 million molecules to cause cell death, is unlikely to attain

such levels in this system. Conversely, toxins such as ricin A-chain, which require only one or two molecules to be internalised, will achieve sufficient amounts. Toxins are likely though to prove too potent for clinical use, with only small levels required for non-specific cell death, whereas MTX is at the opposite end of the scale. The clinical situation requires increased drug levels in tumour cells over the normal healthy cells in the body. For malignant melanoma, which is the focus of this study, this necessitates a sufficient level of receptor expression on the tumour cells with low levels of uptake by non-specific processess in other cell types. Non-malignant melanocytes which will also express MSH receptors are likely to accumulate some of the conjugate, however this will probably result in non-fatal de-pigmentation.

From binding studies on human melanoma cell lines, the number of binding sites is generally lower than murine melanomas, e.g. from undetectable to c.2000 sites/cell [113]. If the rate of internalisation is slow (albeit by receptor-mediated or adsorptive endocytosis) then improvements to the drug conjugate have to be made, e.g. a more potent cytotoxic component and/or analogue, or an increased drug incorporation ratio (although this is likely to decrease the binding affinity of the peptide). The rate of receptor recycling and subsequent re-expression at the cell surface also need to be assessed.

The amount of non-specific cellular uptake by non-melanotic cells must be established. The assay system in this study, although not employed with a non-target cell line, would prove unsuitable to measure the predicted uptake, due to relative high background levels of ^{125}I activity. A similar experimental system to the assay of fluid-phase uptake would be required. The likely route for this non-specific internalisation would be either pinocytosis or adsorptive endocytosis, the latter due to any membrane binding of the conjugate, e.g. through the MTX moiety or the hydrophobic nature of the peptide.

As the work in chapter 3 demonstrated, the rate and profile of fluid-phase uptake is very dependent on the tissue type and origin. Human SVK-14 keratinocytes

appeared to accumulate little or no extracellular fluid in the lysosomes and would therefore be expected to display minimal toxicity due to the conjugate. Even the pinocytic rate of B16 cells would account for little toxicity, if 10^6 cells were incubated at 37^0C in 1ml of a 1nM solution of a non-polar compound, only 23 molecules would be internalised per cell per hour. Although this is a poor reflection of an in vivo enviroment, the number of molecules internalised per cell is very low. Thus fluid-phase endocytosis would account for a very small amount of the toxic effects of a macromolecular-drug conjugate. However the rate of adsorptive endocytosis can be a hundred to a thousand fold greater [44], again depending on the degree of membrane binding and the rate of cell membrane turnover.

It should be noted that due to the structural similarity between MSH and related peptides, e.g. ACTH, a drug conjugate may cross react with other membrane binding sites of these peptides, leading to a degree of non-selectivity. Conversely these other peptides, in addition to the natural MSH produced by the host, may block some of the available binding sites on the tumour cells. This is one of the disadvantages of hormone-targeted conjugates, although circulating hormone levels are generally of a very low concentration e.g. 10^{-12}-10^{-10}M, and their plasma levels are not usually sustained for long periods.

The internalisation of a drug-conjugate does not necessarily result in toxic effects on the cell. Generally the drug(s) must first be released from the macromolecular carrier in an active form. The cellular uptake of most conjugates will occur through endocytosis [253], resulting in a disposition towards the lysosomal compartment of the cell. The degradative processes then experienced being responsible for some release of active drug. Therefore once inside the lysosomes there are two factors determining the appearance of active drug in the cell cytosol, the efficiency of lysosomal degradation, and the diffusion of these products across the lysosomal membrane. The former of these was investigated in this present study, the activity of the active drug and drug-derivatives assayed for their inhibitory action on DHFR.

The intact conjugate displayed a forty fold lower affinity for DHFR compared to the free drug. The levels of intact conjugate expected in the cell cytosol are minimal, and in conjunction with a lower affinity, little DHFR inhibition would be envisaged. However when the conjugate was incubated with a rat lysosomal extract, an increase in DHFR inhibition was demonstrated (which increased with the length of incubation in the presence of the extract). Optimal reaction conditions had not yet been achieved by 16 hours when the inhibitory action of the degradation products was equivalent to that of free MTX at an identical concentration. This suggested the release of free MTX, or MTX derivatives with a similar affinity for DHFR. Further work would involve the identification of these degradation products, and the lysosomal incubation of non-conjugated NLDP-MSH and MTX.

Although the formation of active degradation products was demonstrated, their ability or efficiency to cross the lysosomal membrane remains unknown. The time period of lysosomal incubation was a good representation of the in vivo situation where lysosomes are generally regarded as the terminal vesicular department. Most molecules are resident indefinitely or enzymatically degraded and lost to the cell cytosol.

It must be remembered that the NLDP-MSH-MTX consisted of four compounds of equal concentrations, as yet unseperated. Of course a homogenous yield is essential for further work, particulary in the assessment of lysosomal degradation and cytotoxic studies. One of the four compounds may display more efficient MTX release or active MTX-derivatives. An identical situation applies to other cellular processes, e.g. membrane binding.

To briefly summarise, some of the properties established in this work, for the interaction of the NLDP-MSH-MTX conjugate and NLDP-MSH with B16 cells; are listed below.

1. The MSH analogue NLDP-MSH has a high affinity (<1.0nM) for specific

membrane sites on the cell surface of B16 cells.

2. There are c.4500 binding sites/cell.

3. The peptide was internalised at 37^0C through the binding site.

4. From the measurement of fluid-associated ^{125}I-PVP uptake, theoretical calculations predicted the internalisation of ^{125}I-NLDP-MSH could conceivably occur through adsorptive endocytosis.

5. NLDP-MSH-MTX was successfully iodinated for experimental use.

6. NLDP-MSH-MTX was internalised via an identical route to the free peptide.

7. NLDP-MSH-MTX demonstrated little or no specific membrane binding through the MTX moiety.

8. NLDP-MSH-MTX had a forty fold lower affinity for DHFR than MTX, and inhibited the enzyme through an identical mechanism to the free drug.

9. The lysosomal degradation products of NLDP-MSH-MTX had an equivalent inhibitory activity on DHFR as free MTX.

In addition to providing information for macromolecular-drug targeting via the MSH receptor, this study has proposed a pathway for the natural interaction and fate of the native hormone and receptor membrane stability. Further work in this direction would necessitate the employment of more suitable probes and an improved definition of the intracellular location of the ligand and receptor. The process of ligand/receptor uncoupling remains a relatively unknown function with only a change in the pH enviroment as a plausible mechanism. It would be interesting to study in detail the stability of bound NLDP-MSH at about pH 6.0, a value experienced in the endosomes where uncoupling is thought to occur. However from the present work the complex would be expected to be quite stable, as an acid-wash of pH 2.5 was required to remove all extracellular

bound peptide. Therefore it is likely that uncoupling of receptors and ligand is quite slow.

NLDP-MSH-MTX certainly has potential as an experimental model system, it is internalised within the cell and active products are formed from lysosomal enzyme degradation. In practice MTX should presumably be replaced by a more potent toxic agent, but the MTX conjugate would prove a useful tool for in vivo studies. Even if a conjugate was successful in vitro, it may still prove ineffective due to the one characteristic fundamental to site-specific cancer chemotherapy;- an identical biodistribution to the metastases of the tumour which must involve extravasation from the vasculature. The fatality of this disease is primarily due to the widespread growth of secondary tumours which makes malignant melanoma a very siutable in vivo model system, with its high metatastatic potential.

Hormones may prove useful tools for drug targeting, due to their high affinity for specific membrane receptors. There are few reports of drug conjugates utilising the MSH system. A daunomycin-β-MSH conjuagte has been synthesised and demonstrated to posess a more toxic effect than free drug in melanoma cells [13, 254]. However in vivo it displayed a distinct lack of success, possibly due to a rapid clearance, or endogenous ligands competing for a finite number of cell surface receptors.

Undoubtedly the study of drug-targeting via MSH (or other hormones) involves many different aspects with apparently insurmountable problems, e.g. the establishment of a suitable model for the study of transcytosis in the endothelial vasculature, or a successful biodistribution of the conjugate in vivo. However I hope this study has formed part of the platform for the advancement of further work.

References

[1] H. Sezaki and M. Hashida. Macromolecule-drug conjugates in targeted cancer chemotherapy. *CRC Critical Reviews in Therapeutic Drug Carrier Systems*, 1:1–38, 1984.

[2] D. R. Friend and S. Pangburn. Site-specific drug delivery. *Med. Res. Rev.*, 7:53–106, 1987.

[3] G. Gregoriadis, editor. *Drug Carriers in Biology and Medicine.* Academic Press, London, 1979.

[4] G. Gregoriadis. Targeting of drugs with molecules, cells and liposomes. *Trends in Pharmacol. Sci.*, 4:304–307, 1983.

[5] E. Tomlinson and J. J. Burger. *Polymers in Controlled Drug Delivery*, pages 27–48. Wright, Bristol, 1987.

[6] U. Zimmerman. *Targeted Drugs*, pages 153–200. Wiley, New York, 1983.

[7] M. V. Pimm. Drug-monoclonal antibody conjugates for cancer therapy: potentials and limitations. *CRC Critical Reviews in Therapeutic Drug Carrier Systems*, 5:189–227, 1988.

[8] G. J. O'Neill. *Drug Carriers in Biology and Medicine*, pages 23–41. Academic Press, London, 1979.

[9] A. Trouet, R. Baurain, D. D. Campeneere, M. Masquelier, and P. Pirson. pages 19–30.

[10] E. Schacht. *Ploymers in Controlled Drug Delivery*, pages 131–151. 1987.

[11] R. E. Counsell and R. C. Pohland. Lipoproteins as potential site-specific delivery systems for diagnostic and therapeutic agents. *J. Med. Chem.*, 25:1115–1120, 1982.

[12] W. T. Shier. *Drug Carriers in Biology and Medicine*, pages 43–70. Academic Press, London, 1979.

[13] J. M. Varga and N. Asato. *Targeted Drugs*, pages 73–88. John Wiley and Sons Inc., New York, 1983.

[14] L. Moleteni. *Drug Carriers in Biology and Medicine*, pages 107–128. Academic Press, London, 1979.

[15] A. Trouet. *Polymeric Delivery Systems*, pages 157–173. Gordon and Breach, New York, 1978.

[16] J. Kopecek and R. Duncan. *Polymers in Controlled Drug Delivery*, pages 152–187. Wright, Bristol, 1987.

[17] E. Tomlinson. Theory and practice of site-specific drug delivery. *Adv. Drug Del. Rev.*, 1:87–198, 1987.

[18] F. K. Jansen, H. E. Blythman, D. Carriere, P. Casellas, O. Gros, J. C. Laurent, F. Paolucci, B. Pau, P. Poucelet, G. Richer, H. Vidal, and G. A. Voisin. Immunotoxins: Hybrid molecules combining high specificity and cytotoxicity. *Immunol. Rev.*, 62:185–216, 1982.

[19] N. R. Worrell, A. J. Cumber, G. D. Parnell, A. Mirza, J. A. Forrester, and W. C. J. Ross. Effect of linkage variation on pharmacokinetics of ricin A chain-antibody conjugates in normal rats. *Anticancer Drug Des.*, 1:179–188, 1986.

[20] M. Hashida, A. Kato, Y. Takakura, and H. Sezaki. Disposition and pharmacokinetics of a polymeric prodrug of mitomycin C, mitomycin C-dextran conjugate, in the rat. *Drug Metab. Disposition*, 12, 1984.

[21] W. C. Shen, J. Wan, and H. Ekrami. (C) Means to enhance penetration. (3) Enhancement of polypeptide and protein absorption by macromolecular carriers via endocytosis and transcytosis. *Adv. Drug Del. Rev.*, 8:93–113, 1992.

[22] J. M. Besterman and R. B. Low. Endocytosis: A review of mechanisms and plasma membrane dynamics. *Biochem. J.*, 210:1–13, 1983.

[23] J. S. Rodman, R. W. Mercer, and P. D. Stahl. Endocytosis and transcytosis. *Curr. Op. Cell Biol.*, 2:664–672, 1990.

[24] A. L. Hubbard. Endocytosis. *Current Op. Cell Biol.*, 1:675–683, 1989.

[25] B. Van Deurs, O. W. Peterson, S. Olsnes, and K. Sandvig. The ways of endocytosis. *Int. Rev. Cytol.*, 117:131–177, 1989.

[26] C. Watts. Rapid endocytosis of the transferrin receptor in the absence of bound transferrin. *J. Cell Biol.*, 100:633–637, 1985.

[27] R. B. Dickson, J. A. Hanover, M. C. Willingham, and I. Pastan. Prelysosomal divergence of transferrin and epidermal growth factor during receptor-mediated endocytosis. *Biochem.*, 22:5667–5674, 1983.

[28] J. R. Glenney, W. S. Chen, C. S. Lazar, G. M. Walton, L. M. Zokas, M. G. Rosenfeld, and G. N. Gill. Ligand-induced endocytosis of the EGF receptor is blocked by mutational inactivation and by microinjections of anti-phosphotyrosine antibodies. *Cell*, 52:675–684, 1988.

[29] A. Dautry-Varsat. Receptor-mediated endocytosis: the intracellular journey of transferrin and its receptor. *Biochimie*, 68:375–381, 1986.

[30] W. J. Schneider. The low density lipoprotein receptor. *Biochim. Biophys. Acta*, 988:303–317, 1989.

[31] N. Ghinea and N. Simionescu. Anionized and cationized hemeundecapeptides as probes for cell surface charge and permeability studies: differenti-

ated labeling of endothelial plasmalemmal vesicles. *J. Cell Biol.*, 100:606–612, 1985.

[32] C. G. Davis, M. A. Lehrnum, D. W. Russell, R. G. W. Anderson, M. S. Brown, and J. L. Goldstein. The J. D. Mutation in Familial Hypercholesterolemia: Amino acid substitution in cytoplasmic domain impedes internalization of LDL receptors. *Cell*, 45:15–24, 1986.

[33] S. Schmid, R. Fuchs, M. Kielian, A. Helenius, and I. Mellman. Acidification of endosome subpopulations in wild-type Chinese hamster ovary cells and temperature-sensitive acidification-defective mutants. *J. Cell Biol.*, 108:1291–1300, 1989.

[34] H. J. Geuze, J. W. Slot, G. J. A. M. Strous, H. F. Lodish, and A. L. Schwartz. Intracellular site of Asialglycoprotein receptor-ligand uncoupling: Double-label immunoelectron microscopy during receptor-mediated endocytosis. *Cell*, 32:277–287, 1983.

[35] D. Yamashiro and F. R. Maxfield. Regulation of endocytic processes by pH. *Trends Pharmacol. Sci.*, 9:190–193, 1988.

[36] A. L. Schwartz, S. E. Fridovich, and H. F. Lodish. Kinetics of internalisation and recycling of the asialglycoprotein receptor in a Hepatoma cell line. *J. Biol. Chem.*, 257:4230–4237, 1982.

[37] R. D. Klausner, J. V. Renswoude, G. Ashwell, C. Kemph, A. M. Schechter, A. Dean, and K. R. Bridges. Receptor-mediated endocytosis of transferrin in K562 cells. *J. Biol. Chem.*, 258:4715–4724, 1983.

[38] I. Mellman and H. Plunter. Internalisation and degradation of macrophages Fc receptors bound to ploy valent immune complexes. *J. Cell Biol.*, 98:1170–1177, 1984.

[39] D. McVey Ward, R. Ajioka, and J. Kaplan. Cohort movement of different ligands and receptors in the intracellular endocytic pathway of alveolar macrophages. *J. Biol. Chem.*, 264:8164–8170, 1989.

[40] A. Helenius, I. Mellman, D. Wall, and A. Hubbard. Endosomes. *Trends Biochem.*, 8:245–250, 1983.

[41] B. Mullock, W. J. Branch, M. Van Schaik, K. L. Gilbert, and J. P. Luzio. Reconstitution of an endosome-lysosome interaction in a cell-free system. *J. Cell Biol.*, 108:2093–2099, 1989.

[42] J. Lippincott-Schwarz and D. M. Fambrough. Cycling of the membrane glycoprotein, LEP100, between plasma membrane and lysosomes: Kinetic and morphological analysis. *Cell*, 49:669–677, 1987.

[43] S. Diment and P. Stahl. Macrophage endosomes contain proteases which degrade endocytosed protein ligands. *J. Biol. Chem.*, 260:15311–15317, 1985.

[44] W. C. Shen and H. J. P. Ryser. Conjugation of poly-L-lysine to albumin and horseradish peroxidase: A novel method of enhancing the cellular uptake of proteins. *Proc. Natl. Acad. Sci. U.S.A.*, 75:1872–1876, 1978.

[45] W. M. Pardridge, A. K. Kumagai, and J. B. Eisenberg. Chimeric peptides as a vehicle for peptide pharmaceutical delivery through the blood-brain barrier. *Biochem. Biophys. Res. Commun.*, 146:307–313, 1987.

[46] N. K. Gonatas and S. Avrameas. Detection of plasma membrane carbohydrates with lectin peroxidase conjugates. *J. Cell Biol.*, 59:536–543, 1989.

[47] R. D. Broadwell, B. J. Balin, and M. Sakman. Transcytotic pathway for blood-borne protein through the blood-brain barrier. *Proc. Natl. Acad. Sci. U.S.A.*, 85:632–646, 1988.

[48] E. Galis, L. Ghitescu, and M. Simionescu. Fatty acids binding to albumin increases its uptake and transcytosis by the lung capillary endothelium. *Eur. J. Cell Biol.*, 47:358–365, 1988.

[49] D. B. Cawley, H. R. Herschman D. G. Gilliland, and R. J. Collier. Epidermal growth factor-toxin A chain conjugates: EGF-ricin A is a potent toxin while EGF-diptheria fragment A is non-toxic. *Cell*, 22:563–570, 1980.

[50] G. Bergamaschi, M. Cazzola, L. Dezza, E. Savino, L. Consonni, and D. Lappi. Killing of K562 cells with conjugates between human transferrin and a ribosome-inactivating protein (SO-6). *Br. J. Hematol.*, 68:379–384, 1988.

[51] J. Kralovec, M. Singh, M. Mammen, A. H. Blair, and T. Ghose. Synthesis of site-specific methotrexate-IgG conjugates: Comparision of stability and antitumor activity with active-ester-based conjugates. *Can. Immunol. Immunother.*, 29:293–302, 1989.

[52] Y. Tsukada, K. Ohkawa, and N. Hibi. Therapeutic effect of treatment with polyclonal or monoclonal antibodies to alpha-fetoprotein-producing rat hepatoma tumor model. *Can. Res.*, 47:4293–4295, 1987.

[53] C. De Duve, T. De Barsy, B. Poole, A. Trouet, P. Tulkens, and F. Van Hoof. Lysosomotropic Agents. *Biochem. Pharmacol.*, 23:2495–2531, 1974.

[54] W. C. Shen and H. J. P. Ryser. Cis-Aconityl spacer between daunomycin and macromolecular carrier: a model of pH-sensitive linkage releasing drug from a lysosomtropic conjugate. *Biochem. Biophys. Res. Commun.*, 102:1048–1054, 1981.

[55] R. L. Pisoni, T. L. Acker, K. M. Lisowski, R. M. Lemons, and J. G. Theone. A cysteine-specific lysosomal transport system provides a major route for the delivery of thiol to human fibroblast lysosomes: Possible role in supporting lysosomal hydrolysis. *J. Cell Biol.*, 110:327–335, 1990.

[56] S. Olsnes and K. Sandvig. *Receptor-Mediated Endocytosis*, pages 187–236. Chapman and Hall, New York, 1983.

[57] E. S. Vietta. Immunotoxins: New therapeutic reagents for autoimmunity, cancer and AIDS. *J. Clin. Immunol.*, 10:15S–18S, 1990.

[58] P. N. Kulkarni, A. Huntley Blair, and T. I. Ghose. Covalent binding of methotrexate to immunoglobulins and the effect of antibody-linked drug on tumor growth in vivo. *Can. Res.*, 41:2700–2706, 1981.

[59] G. F. Rowland, R. G. Simmonds, J. R. F. Corvalan, R. W. Baldwin, J. P. Brown, M. J. Embleton, C. H. J. Ford, K. E. Hellstrom, I. Hellstrom, J. T. Kemshead, C. E. Newman, and C. S. Woodhouse. Monoclonal antibodies for targeted therapy with vindesine. *Protides Biol. Fluids Proc. Colloq.*, 30:375–379, 1983.

[60] M. C. Garnett, M. J. Embleton, E. Jacobs, and R. W. Baldwin. Preparation and properties of a drug-carrier-antibody conjugate showing selective antibody-directed cytotoxicity in vitro. *Int. J. Cancer*, 31:661–670, 1983.

[61] R. W. Baldwin, M. J. Embleton, M. C. Garnett, and M. V. Pimm. Conjugates of monoclonal antibody 791T/36 with methotrexate in cancer therapy. *NCI Monogr.*, 3:95–99, 1987.

[62] L. B. Shih, R. M. Sharkey, F. J. Primus, and D. M. Goldenberg. Site-specific linkage of methotrexate to monoclonal antibodies using an intermediate carrier. *Int. J. Cancer*, 41:832–839, 1988.

[63] J. W. Paxton. Protein binding of methotrexate in sera from normal human beings: Effect of drug concentration, pH, temperature and storage. *J. Pharm. Met.*, 5:203–213, 1981.

[64] G. W. Halbert, A. T. Florence, and J. F. B. Stuart. Characterization of in-vitro drug release and biological activity of methotrexate-bovine serum albumin conjugates. *J. Pharm. Pharmacol.*, 39:871–876, 1987.

[65] N. Endo, Y. Takeda, N. Umemoto, K. Kishida, K. Watanabe, M. Saito, Y. Kato, and T. Hara. Nature of linkage and mode of action of methotrexate conjugated with antitumor antibodies: implications for future preparation of conjugates. *Can. Res.*, 48:3330–3335, 1988.

[66] G. B. Henderson and B. P. Strauss. Methotrexate transport via the high-affinity folate binding protein of L1210 cells. *Chemistry and Biology of Pteridines*, pages 1227–1237, 1990.

[67] M. Singh, J. Kralovec, M. Mezei, and T. Ghose. Inhibition of human renal cancer by methotrexate linked to a monoclonal antibody. *J. Urology*, 141:428–431, 1989.

[68] A. J. Rowland, M. E. Harper, D. W. Wilson, and K. Griffiths. The effect of an anti-membrane antibody-methotrexate conjugate on the human prostatic tumour line PC3. *Br. J. Can.*, 61:702–708, 1990.

[69] N. Umemoto, Y. Kato, N. Endo, Y. Takeda, and T. Hara. Preparation and in vitro cytotoxicity of a methotrexate-anti-MM46 monoclonal antibody conjugate via an oligopeptide spacer. *Int. J. Cancer*, 43:677–684, 1989.

[70] M. C. Garnett, E. Jacobs, M. J. Embleton, and R. W. Baldwin. Studies on the mechanism of action of a drug-carrier-antibody conjugate. *Biochem. Soc. Trans.*, 12:1035–1036, 1984.

[71] P. O. Seglen, B. Grindle, and A. E. Solhein. Inhibition of the lysosomal pathway of protein degradation in isolated rat hepatocytes by ammonia, methylamine, chloroquine and leupeptin. *Eur. J. Biochem.*, 95:215–225, 1979.

[72] S. Okhuma and B. Poole. Fluoresence probe measurement of the intralysosomal pH in living cells and the perturbation of pH by various agents. *Proc. Natl. Acad. U.S.A*, 75:3327–3331, 1978.

[73] W. C. Shen, B. Ballou, H. J. P. Ryser, and T. R. Hakala. Targeting, internalization, and cytotoxicity of methotrexate-monoclonal anti-stage-specific embryonic antigen-1 antibody conjugates in cultured F-9 teratocarcinoma cells. *Can. Res.*, 46:3912–3916, 1986.

[74] W. C. Shen and H. J. P. Ryser. Poly (L-lysine) and poly (D-lysine) conjugates of methotrexate: Different inhibitory effect on drug resistant cells. *Mol. Pharmacol.*, 16:614–622, 1979.

[75] T. Ghose, A. Guclu, R. R. Raman, and A. Huntley Blair. Inhibition of a mouse hepatoma by the alkylating agent trenimon linked to immunoglobulins. *Can. Immunol. Immunother.*, 13:185, 1982.

[76] M. V. Pimm, J. A. Clegg, M. C. Garnett, and R. W. Baldwin. Biodistribution and tumour localisation of a methotrexate-monoclonal antibody 791T/36 conjugate in nude mice with human tumour xenografts. *Int. J. Can.*, 41:886–891, 1988.

[77] D. C. Blakey, G. J. Watson, P. P. Knowles, and P. E. Thorpe. Effect of chemical deglycosylation of ricin A chain on the in vivo fate and cytotoxic activity of an immunotoxin composed of ricin A chain and anti-Thy 1.1 antibody. *Can. Res.*, 47:947–952, 1987.

[78] M. V. Pimm, R. A. Robins, M. J. Embleton, E. Jacobs, A. J. Markham, A. Charleston, and R. W. Baldwin. A bispecific monoclonal antibody against methotrexate and a human tumour associated antigen augments cytotoxicity of methotrexate-carrier conjugate. *Br. J. Can.*, 61:508–513, 1990.

[79] S. Persiani, B. Ballou, W. C. Shen, H. J. P. Ryser, J. M. Reiland, and T. R. Hakala. In vivo antitumor effect of methotrexate conjugated to a monoclonal IgM antibody specific for stage-specific embryonic antigen-1, on MH-15 mouse teratocarcinoma. *Can. Immunol. Immunother.*, 29:167–170, 1989.

[80] P. N. Kulkarni, A. Huntley Blair, T. I. Ghose, and M. Mammen. Conjugation of methotrexate to IgG antibodies and their $F(ab)_2$ fragments and the effect of conjugated methotrexate on tumor growth in vivo. *Can. Immunol. Immunother.*, 19:211–214, 1985.

[81] A. Jarlozinska, R. Richter, Z. Albert, and H. Zawadzka. Antigan heterogeneity of human lung cancers. *J. Natl. Can. Inst.*, 70:427–433, 1983.

[82] P. H. Hand, M. Nuti, D. Colcher, and J. Schlom. Definition of antigenic heterogeneity and modulation among human mammary carcinoma cell populations using monoclonal antibodies to tumor-associated antigens. *Can. Res.*, 43:728–735, 1983.

[83] M. V. Pimm, A. C. Perkins, N. C. Armitage, and R. W. Baldwin. The characteristics of blood-borne radiolabels and the effect of anti-mouse IgG antibodies on localization of radiolabeled monoclonal antibody in cancer patients. *J. Nucl. Med.*, 26:1011–1023, 1985.

[84] P. G. Balboni, A. Minia, M. P. Grossi, G. Barbanti-Brodano, A. Mattioli, and L. Fiume. Activity of albumin conjugates of 5-fluorodeoxyuridine and cytosine arabinoside on poxviruses as a lysosomotropic approach to antiviral chemotherapy. *Nature*, 264:181–183, 1976.

[85] B. C. F. Chu and J. M. Whiteley. Control of solid tumor metastases with a high molecular-weight derivative of methotrexate. *J. Natl. Cancer Inst.*, 62:79–82, 1979.

[86] J. M. Whiteley, Z. Nimec, and J. Galivan. Treatment of Reuber H35 Hepatoma cells with carrier-bound methotrexate. *Mol. Pharm.*, 19:505–508, 1981.

[87] R. T. Dean. *Drug Carriers in Biology and Medicine*, pages 71–86. Academic Press, London, 1979.

[88] G. Ashwell and A. G. Morrell. The role of surface carbohydrates in the hepatic recognition and transport of circulating glycoproteins. *Adv. Enzymology*, 41:99–128, 1974.

[89] L. Fiume, C. Busi, A. Mattioli, P. G. Balboni, G. Balboni-Brodano, and T. Wieland. *Targeting of Drugs*, pages 1–17. Plenum, New York, 1982.

[90] M. Szekerke, R. Wade, and M. E. Whisson. The use of macromolecules as carriers of cytotoxic groups. I. conjugates of nitrogen mustards with

proteins, polypeptidyl proteins and polypeptides. *Neoplasia*, 19:211–215, 1972.

[91] A. Kato, Y. Takakura, M. Hashida, T. Kimura, and H. Sezaki. Physicochemical and antitumor characteristics of high molecular weight prodrugs of mitomycin C. *Chem. Pharm. Bull.*, 30:2951–2957, 1982.

[92] M. Hashida, A. Kato, T. Kohima, S. Muranishi, H. Sezaki, N. Tanigawa, K. Satomura, and Y. Hikasa. Antitumor activity of mitomycin C-dextran conjugate against various murine tumors. *Gann.*, 72:226–234, 1981.

[93] R. Arnon and E. Hurwitz. *Targeted Drugs*, pages 23–55. John Wiley and Sons Inc., New York, 1983.

[94] H. J. P. Ryser. *Rehovot Symposium on Peptides.* John Wiley and Sons Inc., New York, 1974.

[95] J. Hugues, P. Ryser, and W. C. Shen. Conjugation of methotrexate to poly (L-lysine) increases drug transport and overcomes drug resistance in cultured cells. *Proc. Natl. Acad. Sci. U.S.A.*, 75:3867–3870, 1978.

[96] B. C. Chu and S. B. Howell. Differential toxicity of carrier-bound methotrexate toward human lymphocytes, marrow and tumor cells. *Biochem. Pharmacol.*, 30:2545–2552, 1981.

[97] B. C. Chu and S. B. Howell. Differential toxicity of carrier-bound methotrexate against tumor/bone marrow cells in vivo. *Biochem. Pharmacol.*, 31:3513–3517, 1982.

[98] Z. A. Cohn and E. Parks. The regulation of pinocytosis in mouse macrophages: II. Factors including vesicle formation. *J. Exp. Med.*, 125:213–232, 1967.

[99] G. Atassi, M. Duarte-Karim, and H. J. Targon. Comparision of adriamycin with DNA-adriamycin complex in chemotherapy of experimental tumors and metastases. *Eur. J. Cancer*, 11:309–316, 1975.

[100] A. Bosly, J. Prignot, C. Ledent, G. Sokal, and A. Trouet. Adriamycin and adriamycin-DNA in inoperable bronchogenic carcinoma. A randomised study with cyclophosamide vinblastine. *Eur. J. Cancer*, 14:639–644, 1978.

[101] G. Ashwell and J. Harford. Carbohydrate-specific receptors of the liver. *Ann. Rev. Biochem.*, 51:531–554, 1982.

[102] E. F. Neufield and G. Ashwell. *The Biochemistry of Glycoproteins and Proteoglycans*, pages 241–256. New York: Plenum, 1980.

[103] R. Duncan and J. Kopecek. *Advances in Polymer Science*, pages 51–101. Springer-Verlag, 1983.

[104] J. Kopecek. Controlled biodegradability of polymers- a key to drug delivery systems. *Biomaterials*, 5:19–25, 1984.

[105] B. Rihova, J. Kopecek, K. Ulbrich, J. Pospisil, and P. Mancal. Effect of the chemical structure of N-(2-hydroxypropyl)-methacrylamide copolymers on their ability to induce antibody formation in inbred strains of mice. *Biomaterials*, 5:143–148, 1984.

[106] T. Kitao and K. Hattori. Concanavalin A as a carrier of daunomycin. *Nature*, 265:81–82, 1977.

[107] J. Y. Lin, J. S. Li, and T. C. Tung. Lectin derivatives of methotrexate and chlorambucil as chemotherapeutic agents. *J. Natl. Cancer Inst.*, 66:523–528, 1981.

[108] D. G. Gilliland, R. J. Collier, J. N. Moehring, and T. J. Moehring. Chimeric toxins: toxic, disulfide-linked conjugate of concanavalin A with fragment A from diptheria toxin. *Proc. Natl. Acad. Sci. U.S.A.*, 75:5319–5323, 1978.

[109] E. P. Goldberg, H. Iwata, R. N. Terry, W. E. Longo, M. Levy, T. A. Lindheimer, and J. L. Cantrell. *Affinity Chromatography and Related Techniques*, page 375. Elsevier, 1982.

[110] T. M. Chang, A. Dazord, and D. M. Neville. Artificial hybrid protein containing a toxic protein fragment and a cell membrane receptor-binding moiety in a disulfide conjugate. *J. Biol. Chem.*, 252:1515–1522, 1977.

[111] T. N. Oeltmann and E. C. Heath. A hybrid protein containing the toxic subunit of ricin and the cell-specific subunit of Human Chorionic Gonadotropin. *J. Biol. Chem.*, 254:1028–1032, 1979.

[112] D. B. Cowley, H. R. Herschmann, D. G. Gillilard, and R. J. Collier. Epidermal Growth Factor-toxin A chain conjugates: EGF-Ricin A is a potent toxin while EGF-Diptheria Fragment A is nontoxic. *Cell*, 22:563–570, 1980.

[113] A. N. Eberle. *The Melanotropins: Chemistry, Physiology and Mechanism of Action.* Karger, Switzerland, 1988.

[114] L. C. Panasci, A. McQuillan, and M. Kaufman. Biological activity, binding, and metabolic fate of Ac-[Nle^4,D-Phe^7]α-$MSH_{4-11}NH_2$ with the F_1 variant of B16 melanoma cells. *J. Cell. Physiol.*, 132:97–103, 1987.

[115] D. R. Seeger, D. B. Cosulich, J. M. Smith, and M. E. Hultquist. Analogs of Pteroylglutamic acid. III. 4-Amino derivatives. *J. Am. Chem. Soc.*, 71:1753–1758, 1949.

[116] L. K. A. Rahman and S. R. Chhabra. The chemistry of methotrexate and its analogues. *Med. Res. Rev.*, 8:95–156, 1988.

[117] J. Jolivet, K. H. Cowan, G. A. Curt, N. J. Clendeninn, and B. A Chabner. The pharmacology and clinical use of methotrexate. *New Eng. J. Med.*, Nov. 3:1094–1102, 1983.

[118] J. D. Borsi and P. J. Moe. New aspects of clinical and cellular pharmacodynamics of methotrexate. *Acta Paediatrica Scandinavica*, Suppl. 34:1–31, 1987.

[119] B. A. Kamen, P. A. Nylen, V. M. Whitehead, H. T. Abelson, B. J. Dolnick, and D. W. Peterson. Lack of dihydrofolate reductase in human tumor and leukemia cells in vivo. *Cancer Drug Delivery*, 2:133–138, 1985.

[120] F. M. Sirotnak. Obligate genetic expression in tumor cells of a fetal membrane property mediating 'folate' transport: Biological significance and implications for improved therapy of human cancer. *Can. Res.*, 45:3992–4000, 1985.

[121] I. D. Goldman. The characteristics of membrane transport of amethopterin and the naturally occurring folates. *Ann. N. Y. Acad. Sci.*, 186:400–422, 1971.

[122] M. Dembo, F. M. Sirotnak, and D. M. Moccio. Effects of metabolic deprivation on methotrexate transport in L1210 leukemia cells: further evidence for seperate influx and efflux systems with different energetic requirements. *J. Membrane Biol.*, 78:9–17, 1984.

[123] D. W. Fry, J. C. White, and I. D. Goldman. Effects of 2,4-dinitrophenol and other metabolic inhibitors on the bidirectional fluxes, net transport and intracellular binding of methotrexate in Ehrlich ascites tumor cells. *Can. Res.*, 40:3669–3673, 1980.

[124] G. Jansen, I. Kathmann, B. C. Rademaker, B. J. M. Braakhuis, G. R. Westerhof, G. Rijksen, and J. H. Schornagel. Expression of a folate binding protein in L1210 cells grown in low folate medium. *Can. Res.*, 49:1959–1963, 1989.

[125] G. Jansen, G. R. Westerhof, I. Kathmann, B. C. Rademaker, G. Rijksen, and J. H. Schornagel. Identification of a membrane-associated folate-binding protein in human leukemic CCRF-CEM with transport-related methotrexate resistance. *Can. Res.*, 49:2455–2459, 1989.

[126] G. R. Westerhof, G. Jansen, N. van Emmerik, I. Kathmann, G. Rijksen, A. L. Jackman, and J. H. Schornagel. Membrane transport of natural folates and antifolate compounds in murine L1210 leukemia cells: Role of carrier- and receptor-mediated transport systems. *Can. Res.*, 51:5507–5513, 1991.

[127] M. A. Kane, R. M. Portillo, P. C. Elwood, A. C. Antony, and J. F. Kolhouse. The influence of extracellular folate concentration on methotrexate uptake by human KB cells. *J. Biol. Chem.*, 261:44–49, 1986.

[128] G. B. Henderson, J. M. Tsuji, and H. P. Kumar. Mediated uptake of folate by a high-affinity binding protein in sublines of L1210 cells adapted to nanomolar concentrations of folate. *J. Membrane Biol.*, 101:247–258, 1988.

[129] G. Jansen, G. R. Westerhof, M. J. A. Jarmuszewski, G. Rijksen, and J. H. Schornagel. Methotrexate transport in variant human CCRF-CEM leukemia cells with elevated levels of the reduced folate carrier. *J. Biol. Chem.*, 265:18272–18277, 1990.

[130] B. A. Kamen, M. T. Wang, A. J. Streckfuss, X. Peryea, and R. G. W. Anderson. Delivery of folates to the cytoplasm of MA104 cells is mediated by a surface membrane receptor that recycles. *J. Biol. Chem.*, 263:13602–13609, 1988.

[131] J. C. Deutsch, P. C. Elwood, R. M. Portillo, M. G. Macey, and J. F. Kolhouse. Role of the membrane-associated folate binding protein (folate receptor) in methotrexate transport by human KB cells. *Archiv. Biochem. Biophys.*, 274:327–337, 1989.

[132] G. R. Westerhof, G. Jansen, G. A. M. Kathmann, J. H. Schornagel, and G. Rijksen. Characterization of receptor-mediated (anti)folate uptake in human CCRF-CEM cells. *Chemistry and Biology of Pteridines*, pages 1286–1287, 1990.

[133] C. P. Leamon and P. S. Low. Delivery of macromolecules into living cells: A method that exploits folate receptor endocytosis. *Proc. Natl. Acad. Sci. U.S.A.*, 88:5572–5576, 1991.

[134] W. C. Werkheiser. The Biochemical, Cellular, and Pharmacological Action and Effects of the Folic Acid Antagonists. *Can. Res.*, 23:1277–1285, 1963.

[135] J. E. Gready. Dihydrofolate reductase: Binding of substrates and inhibitors and catalytic mechanism. *Adv. Pharmacol. Chemo.*, 17:37–102, 1980.

[136] M. Cohen, R. A. Bender, R. Donehower, C. E. Myers, and B. A. Chabner. Reversibility of high affinity binding of methotrexate in L1210 leukemia cells. *Can. Res.*, 38:2866–2870, 1978.

[137] J. C. White. Reversal of methotrexate binding to dihydrofolate reductase by dihydrofolate. *J. Biol. Chem.*, 254:10889–10895, 1979.

[138] J. C. White, S. Lotfield, and I. D. Goldman. Mechanism of action of methotrexate. part III. *Mol. Pharmacol.*, 11:287–297, 1975.

[139] A. V. Hofflerend and E. Tripp. Unbalanced deoxyribonucleotide synthesis caused by methotrexate. *Br. Med. J.*, 2:140–142, 1972.

[140] J. M. Covey. Polyglutamate derivatives of folic acid coenzymes and methotrexate. *Life Sci.*, 26:665–678, 1980.

[141] R. G. Mathews and C. M. Baugh. Interactions of pig liver methylenetetrahydrofolate reductase with methylenetetrahydropteroylpolyglutamate substrates and with dihydropteroylpolyglutamate inhibitors. *Biochem.*, 19:2040–2045, 1980.

[142] S. A. Jacobs, C. J. Derr, and D. G. Johns. Accumulation of methotrexate diglutamate in human liver during methotrexate therapy. *Biochem. Pharmacol.*, 26:2310–2313, 1977.

[143] C. M. Baugh, C. L. Krumdieck, and M. G. Nair. Polygammaglutamyl metabolites of methotrexate. *Biochem. Biophys. Res. Commun.*, 52:27–34, 1973.

[144] V. M. Whitehead. Synthesis of methotrexate polyglutamates in L1210 murine leukemia cells. *Can. Res.*, 37:408–412, 1977.

[145] S. A. Jacobs, R. H. Adamson, B. A. Chabner, C. J. Derr, and D. G Johns.

[146] J. Jolivet and B. A. Chabner. Intracellular pharmacokinetics of methotrexate polyglutamates in human breast cancer cells. *J. Clin. Invest.*, 72:773–778, 1983.

[147] J. E. Baggott. Inhibition of purified avian liver amidoimidazole-carboxamide ribotide transformylase by polyglutamates of methotrexate and oxidised folates. *Fed. Proc.*, 42:667, 1983.

[148] D. W. Fry, J. C. Yalowich, and I. D. Goldman. Rapid formation of polygammaglutamyl derivatives of methotrexate and their association with dihydrofolate reductase as assessed by high pressure liquid chromatography in the Ehrlich ascites tumor cells in vitro. *J. Biol. Chem.*, 257:1890–1896, 1982.

[149] J. Galivan and Z. Nimec. Effects of folinic acid on hepatoma cells containing methotrexate polyglutamates. *Can. Res.*, 43:551–555, 1983.

[150] D. Neithammer and R. C. Jackson. Changes of molecular properties associated with the development of resistance against methotrexate in human lymphoblastoid cells. *Eur. J. Can.*, 11:846–854, 1975.

[151] R. C. Jackson, D. Neithammer, and F. M. Huennenkens. Enzymatic and transport mechanisms of amethopterine resistance in L1210 mouse leukemia cells. *Can. Biochem. Biophys.*, 1:151–155, 1975.

[152] F. M. Sirotnak, D. M. Moccio, L. E. Kelleher, and L. J. Goutas. Relative frequency and kinetic properties of transport-defective phenotypes among methotrexate resistant L1210 clonal cells derived in vivo. *Can. Res.*, 41:4447–4452, 1981.

[153] J. R. Bertino, E. Mini, A. Sobrero, B. A. Moroson, T. Love, M. Jastreboff, M. Carmen, S. Srimatkandada, and S. Dube. Methotrexate resistant cells as targets for selective chemotherapy. *Adv. Enz. Reg.*, 24:3–11, 1986.

[154] W. F. Flintoff and K. Essani. Methotrexate resistant Chinese hamster ovary cells contain a dihydrofolate reductase with an altered affinity for methotrexate. *Biochem.*, 19:4321–4327, 1980.

[155] D. A. Haber, S. M. Berverly, M. L. Kiely, and R. T. Schimke. Properties of an altered dihydrofolate reductase in cultured mouse fibroblasts. *J. Biol. Chem.*, 256:9501–9510, 1981.

[156] J. H. Goldie, G. Krystal, D. Hartley, G. Gudauskas, and S. Dedhar. A methotrexate insensitive variant of folate reductase present in two lines of methotrexate resistant L5178Y cells. *Eur. J. Can.*, 16:1539–1546, 1980.

[157] U. J. Hanggi and J. W. Littlefield. Isolation and characterization of the multiple forms of dihydrofolate reductase from methotrexate resistant hamster cells. *J. Biol. Chem.*, 249:1390–1397, 1974.

[158] J. R. Bertino, S. Srimatkandada, M. D. Carman, M. Jastreboff, M. Mehlmann, W. D. Medina, E. Mini, B. A. Moroson, A. R. Cashmore, and S. K. Dube. *New Experimental Modalities in the Control of Neoplasia*, pages 183–193. Plenum Press, New York, 1986.

[159] C. J. Bostock, E. M. Clark, N. G. L. Harding, P. M. Mounts, C. Tyler-Smith, V. van Heyningen, and P. M. Walker. The development of resistance to methotrexate in a mouse melanoma cell line. *Chromosoma*, 74:153–177, 1979.

[160] K. H. Cowan and J. Jolivet. A novel mechanism of resistance to methotrexate in human breast cancer cells: Lack of methotrexate polyglutamate formation. *Clin. Res.*, 31:508a, 1983.

[161] D. McCloskey, B. G. Rowan, and J. J. McGuire. Defective polyglutamation caused by an altered folypolyglutamate synthetase as a mechanism of resistance in human leukemia. *Proc. Amm. Assoc. Can. Res.*, 1989.

[162] R. G. Moran, M. Mulkins, and C. Heidlelberger. Role of thymidylate synthetase activity in development of methotrexate cytotoxicity. *Proc. Natl. Acad. Sci. U.S.A.*, 76:5924–5928, 1979.

[163] B. I. Schweitzer, A. P. Dicker, and J. R. Bertino. Dihydrofolate reductase as a therapeutic target. *FASEB J.*, 4:2441–2452, 1990.

[164] I. G. England, L. Naess, R. Blomhoff, and T. Berg. Uptake, intracellular transport and release of ^{125}I-poly(vinylpyrrolidone) and [^{14}C]-sucrose-asialofetuin in rat liver parenchymal cells. *Biochem. Pharmacol.*, 35:201–208, 1986.

[165] E. Atherton and R. C. Sheppard. *Solid Phase Peptide Synthesis. A Practical Approach.* IRL Press, Oxford.

[166] D. L. Peterson, J. M. Gleinser, and R. L. Blakley. Bovine liver dihydrofolate reductase: Purification and properties of the enzyme. *Biochem.*, 14:5261–5267, 1975.

[167] A. Trouet. *Methods in Enzymology*, pages 323–329. Academic Press, New York, 1974.

[168] R. J. Marriott. *Synthesis and Characterisation of Macromolecular Carriers of Methotrexate.* PhD thesis, Department of Pharmacy and Pharmacology, University of Bath, 1990.

[169] J. Munniksma, M. Noteborn, T. Kooistra, S. Steinstra, J. M. W. Bouma, M. Gruber, A. Brouwer, D. Praaning-Van Dalen, and D. L. Knook. Fluid endocytosis by rat liver and spleen. *Biochem. J.*, 192:613–621, 1980.

[170] L. Ose, T. Ose, R. Reinertsen, and T. Berg. Fluid endocytosis in isolated rat parenchymal and non-parenchymal liver cells. *Exp. Cell Res.*, 126:109–119, 1980.

[171] C. A. Price. *Centrifugation in Density Gradients.* Academic Press, New York, 1982.

[172] M. K. Pratten, K. E. Williams, and J. B. Lloyd. A quantitative study of pinocytosis and intracellular proteolysis in rat peritoneal macrophages. *Biochem. J.*, 168:365–372, 1977.

[173] K. E. Williams, E. H. Kidston, F. Beck, and J. B. Lloyd. Quantitative studies of pinocytosis. I. Kinetics of uptake of [^{125}I]-polyvinylpyrrolidone by rat yolk sac cultured in vitro. *J. Cell Biol.*, 64:113–122, 1975.

[174] A. V. S. Roberts, K. E. Williams, and J. B. Lloyd. The pinocytosis of ^{125}I-labelled poly(vinylpyrrolidone), [^{14}C]-sucrose and colloidal [^{198}Au]-gold by rat yolk sac cultured in vitro. *Biochem. J.*, 168:239–244, 1977.

[175] A. V. S. Roberts, S. E. Nicholls, P. A. Griffiths, K. E. Williams, and J. B. Lloyd. A quantitative study of pinocytosis and lysosome function in experimentally induced lysosomal storage. *Biochem. J.*, 160:621–629, 1976.

[176] D. N. McKinley and H. S. Wiley. Reassessment of fluid-phase endocytosis and diacytosis in monolayer cultures of human fibroblasts. *J. Cell. Physiol.*, 136:389–397, 1988.

[177] F. L. Guillot, K. L. Audis, and T. L. Raub. Fluid-phase endocytosis by primary cultures of bovine brain microvessel endothelial cell monolayers. *Microvas. Res.*, 39:1–14, 1990.

[178] C. J. Adams, K. M. Maurey, and B. Storrie. Exocytosis of pinocytic contents by Chinese hamster ovary cells. *J. Cell Biol.*, 93:632–637, 1982.

[179] R. M. Steinman, S. E. Brodie, and Z. A. Cohn. Membrane flow during pinocytosis. *J. Cell Biol.*, 68:665–687, 1976.

[180] J. M. Besterman, J. A. Airhart, R. C. Woodworth, and R. B. Low. Exocytosis of pinocytosed fluid in cultured cells: Kinetic evidence for rapid turnover and compartmentation. *J. Cell Biol.*, 91:716–727, 1981.

[181] B. Goud, C. Jouanne, and J. C. Antoine. Reversible pinocytosis of horseradish peroxidase in lymphoid cells. *Exp. Cell Res.*, 153:218–235, 1984.

[182] R. M. Steinman, J. M. Silver, and Z. A. Cohn. Pinocytosis in fibroblasts. *J. Cell Biol.*, 63:949–969, 1974.

[183] V. S. Goldmacher, N. L. Tinnel, and B. C. Nelson. Evidence that pinocytosis in lymphoid cells has a low capacity. *J. Cell Biol.*, 102:1312–1319, 1986.

[184] A. W. Sasaki, S. K. Williams, M. Jain, and R. C. Wagner. Mechanism of sucrose uptake by isolated rat hepatocytes. *J. Cell Physiol.*, 133:175–180, 1987.

[185] R. M. Steinman, I. S. Mellman, W. A. Muller, and Z. A. Cohn. Endocytosis and the recycling of plasma membrane. *J. Cell Biol.*, 96:1–27, 1983.

[186] K. A. Casey, K. M. Maurey, and B. Storrie. Characterization of early compartments in fluid phase pinocytosis: A cell fractionation study. *J. Cell Sci.*, 83:119–133, 1986.

[187] G. B. Henderson, B. Grzelakowska-Sztabert, E. M. Zeverly, and F. M. Huennekens. Binding properties of the 5-Methyltetrahydrofolate/Methotrexate transport system in L1210. *Archiv. Biochem. Biophys.*, 202:144–149, 1980.

[188] B. T. Hill, B. D. Bailey, J. C. White, and I. D. Goldman. Characteristics of transport of 4-amino antifolates and folate compounds by two lines of L5178Y lymphoblasts, one with impaired transport of methotrexate. *Can. Res.*, 39:2440–2446, 1979.

[189] W. S. Beck. *Hematology*, pages 334–350. Cambridge, Press, 1977.

[190] M. McHugh and Y. C. Cheng. Demonstration of a high affinity folate binder in human cell membranes and its characterization in cultured human KB cells. *J. Biol. Chem.*, 254:11312–11318, 1979.

[191] A. C. Antony, M. A. Kane, R. M. Portillo, P. C. Elwood, and J. F. Kolhouse. Studies of the role of a particulate folate-binding protein in the uptake of

5-Methyltetrahydrofolate by cultured human KB cells. *J. Biol. Chem.*, 260:14911–14917, 1985.

[192] P. C. Elwood, M. A. Kane, R. M. Portillo, and J. F. Kolhouse. The isolation, characterization, and comparision of the membrane-associated and soluble folate-binding proteins from human KB cells. *J. Biol. Chem.*, 261:15416–15423, 1986.

[193] B. A. Kamen and A. Capdevila. Receptor-mediated folate accumulation is regulated by the cellular folate content. *Proc. Natl. Acad. Sci. U.S.A.*, 83:5983–5987, 1986.

[194] G. B. Henderson, M. R. Suresh, K. S. Vitols, and F. M. Huennekens. Transport of folate compounds in L1210 cells: Kinetic evidence that folate influx proceeds via the high-affinity transport system for 5-Methyltetrahydrofolate and methotrexate. *Can. Res.*, 46:1639–1643, 1986.

[195] G. Jansen and J. H. Schornagel. Tumor cell sensitivity and resistance to folate analogues: The role of carrier- and receptor-mediated transport systems. *Chemistry and Biology of Pteridines*, pages 1247–1252, 1990.

[196] L. H. Matherly, C. A. Czajkowski, and S. M. Angeles. Identification of a highly glycosylated methotrexate membrane carrier in K562 human erythroleukemia cells up-regulated for tetrahydrofolate cofactor and methotrexate transport. *Can. Res.*, 51:3420–3426, 1991.

[197] F. F. A. Solca, Y. Salomon, and A. N. Eberle. Heterogeneity of the MSH receptor among B16 murine melanoma subclones. *J. Rec. Res.*, 11:379–390, 1991.

[198] W. Siegrist, F. Solca, S. Stutz, L. Giuffre, S. Carrel, J. Girard, and A. N. Eberle. Characterization of receptors for α-Melanocyte-Stimulating Hormone on human melanoma cells. *Can. Res.*, 49:6352–6358, 1989.

[199] W. Siegrist, M. Oestreicher, S. Stutz, J. Girard, and A. N. Eberle. Radioreceptor assay for α-MSH using mouse B16 melanoma cells. *J. Rec. Res.*, 8:323–343, 1988.

[200] T. K. Sawyer, P. J. Sanfilippo, V. J. Hruby, M. H. Engel, C. B. Heward, J. B. Burnett, and M. E. Hadley. 4-Norleucine, 7-phenylalanine-α-Melanocyte-Stimulating Hormone: A highly potent α-melanotropin with ultralong biological acivity. *Proc. Nat. Acad. Sci. U.S.A.*, 77:5754–5758, 1980.

[201] M. Deschodt-Lanckman, Y. Vanneste, B. Loir, A. Michel, A. Libert, G. Ghanem, and F. Lejeune. Degradation of alpha-Melanocyte Stimulating Hormone (alpha-MSH) by CALLA/endopeptidase 24.11 expressed by human melanoma cells in culture. *Int. J. Can.*, 46:1124–1130, 1990.

[202] A. N. Eberle, V. J. Verin, F. Solca, W. Siegrist, C. Kuenlin, C. Bagutti, S. Stutz, and J. Girard. Biologically active monoiodinated α-MSH derivatives for receptor binding studies using human melanoma cells. *J. Rec. Res.*, 11:311–322, 1991.

[203] W. Siegrist, S. Stutz, J. Girard, and A. N. Eberle. Binding assay for the study of melanoma cell MSH receptors. *Progress in Can. Res. Ther.*, 35:314–317, 1988.

[204] C. M. Lee, E. B. Sandberg, M. R. Hanley, and L. L. Iversen. Purification and characterisation of a membrane-bound substance-P-degrading enzyme from human brain. *Eur. J. Biochem.*, 114:315–327, 1981.

[205] J. B. Tatro, M. L. Entwistle, B. R. Lester, and S. Reichlin. Melanotropin receptors in murine melanoma characterized in cultured cells and demonstrated in experimental tumors in situ. *Can. Res.*, 50:1237–1242, 1990.

[206] F. Solca, W. Siegrist, R. Drozdz, J. Girard, and A. N. Eberle. The receptor for α-melanotropin of mouse and human melanoma cells. *J. Biol. Chem.*, 264:14277–14281, 1989.

[207] T. Scimonelli and A. N. Eberle. Photoaffinity labelling of melanoma cell MSH receptors. *FEBS*, 226:134–138, 1987.

[208] J. E. Gerst, J. Sole, E. Hazum, and Y. Salomon. Identification and characterization of melanotropin binding proteins from M2R melanoma cells by covalent photoaffinity labeling. *Endocrinology*, 123:1792–1797, 1988.

[209] A. M. Lucas, A. J. Thody, and S. Shuster. The role of calcium in MSH stimulated melanosome dispersion. *Peptides*, 8:955–960, 1987.

[210] Y. Salomon. Melanocortin receptors: Targets for control by extracellular calcium. *Mol. Cell. Endo.*, 70:139–145, 1990.

[211] J. E. Gerst, J. Sole, and Y. Salomon. Dual regulation of β-Melanotropin receptor function and adenylate cyclase by calcium and guanosine nucleotides in the M2R melanoma cell line. *Mol. Pharmacol.*, 31:81–88, 1986.

[212] K. Kameyama, P. M. Montague, and V. J. Hearing. Expression of Melanocyte Stimulating Hormone receptors correlates with mammalian pigmentation, and can be modulated by interferons. *J. Cell. Physiol.*, 137:35–44, 1988.

[213] G. E. Ghanem, G. Comunale, A. Libert, A. Vercammen-Grandjean, and F. J. Lejeune. Evidence for alpha-Melanocyte-Stimulating Hormone (α-MSH) receptors on human malignant melanoma cell lines. *Int. J. Can.*, 41:248–255, 1988.

[214] F. Legros, J. Coel, A. Doyen, P. Hanson, N. Van Tieghem, A. Vercammen-Grandjean, J. Fruhling, and F. J. Lejeune. α-Melanocyte-Stimulating Hormone binding and biological activity in a human melanoma cell line. *Can. Res.*, 41:1539–1544, 1981.

[215] J. M. Varga, G. Moellmann, P. Fritsch, E. Godawska, and A. B. Lerner. Association of cell surface receptors for melanotropin with the Golgi region in mouse melanoma cells. *Proc. Nat. Acad. Sci. U.S.A.*, 73:559–562, 1976.

[216] A. DiPasquale, J. M. Varga, G. Moellmann, and J. McGuire. Synthesis of a hormonally active conjugate of α-MSH, ferritin, and fluorescein. *Anal. Biochem.*, 84:37–48, 1978.

[217] J. M. Varga, A. DiPasquale, J. Pawelek, J. S. McGuire, and A. B. Lerner. Regulation of Melanocyte Stimulating Hormone action at the receptor level: Discontinuous binding of hormone to synchronised mouse melanoma cells during the cell cycle. *Proc. Nat. Acad. Sci. U.S.A*, 71:1590–1593, 1974.

[218] J. A. McLane and J. M. Pawelek. Receptors for β-Melanocyte-Stimulating Hormone exhibit positive cooperativity in synchronised melanoma cells. *Biochem.*, 27:3743–3747, 1988.

[219] Z. A. Abdel Malek, K. L. Kreutzfeld, M. M. Marwan, M. E. Hadley, V. J. Hruby, and B. C. Wilkes. Prolonged stimulation of S91 melanoma tyrosinase by [Nle^4, D-Phe^7]-substitued α-Melanotropins. *Can. Res.*, 45:4735–4740, 1985.

[220] N. Shimizu, Y. Shimizu, and B. B. Fuller. Cell-cycle analysis of insulin binding and internalisation on mouse melanoma cells. *J. Cell Biol.*, 88:241–244, 1981.

[221] A. Libert, G. Ghanem, R. Arnould, and F. J. Lejeune. Use of an alpha-Melanocyte-Stimulating Hormone analog to improve alpha-Melanocyte-Stimulating Hormone receptor-binding assay in human melanoma. *Pig. Cell Res.*, 2:510–518, 1989.

[222] A. DiPasquale and J. McGuire. MSH stimualtes adenylate cyclase and tyrosinase in cultivated melanoma cells in the presence of cytochalasin B. *Exp. Cell Res.*, 102:264–268, 1976.

[223] A. N. Eberle, V. M. Kriwaczek, and R. Schwyzer. Hormone-receptor interactions: Melanotropic activities of covalent serum albumin complexes with α-melanotropin, α-melanotropin fragments, and enkephalin. *FEBS Letters*, 80:246–250, 1977.

[224] A. N. Eberle. Studies on melanotropin (MSH) receptors of melanphores and melanoma cells. *Biochem. Soc. Trans.*, 9:37–39, 1981.

[225] J. R. Bertino. *Antineoplastic and Immunosuppressive Agents II*, pages 468–483. Springer, New York, 1975.

[226] W. C. Werkheiser. Specific binding of 4-aminofolic acid analogues by folic acid reductase. *J. Biol. Chem.*, 236:888–893, 1961.

[227] B. A. Kamen. *Metabolism and Action of Anti-cancer Drugs*, pages 141–161. Taylor and Francis, London, 1987.

[228] A. Trouet, M. Masquelier, R. Baurain, and D. Deprez de Campeneere. A covalent linkage between daunorubicin and proteins that is stable in serum and reversible by lysosomal hydrolases, as required for a lysosomotropic drug-carrier conjugate: In vitro and in vivo studies. *Proc. Natl. Acad. Sci. USA*, 79:626–629, 1982.

[229] W. C. Shen and H. J. P. Ryser. Cis-aconityl spacer between daunomycin and macromolecular carriers: A model of pH-sensitive linkage releasing drug from a lysosomotropic conjugate. *Biochem. Biophys. Res. Comm.*, 102:1048–1054, 1981.

[230] J. N. Champness, L. F. Kuyper, and C. R. Beddell. Interaction between dihydrofolate reductase and certain inhibitors. *Trends in Mol. Pharmcol.*, 3:335–362, 1989.

[231] J. T. Bolin, D. J. Filman, D. A. Matthews, R. C. Hamlin, and J. Kraut. Crystal structures of Escherichia coli and Lactobacillus casei dihydrofolate reductase refined at 1.7Å resolution. *J. Biol. Chem.*, 257:13650–13662, 1982.

[232] B. J. Stockman, N. R. Nirmala, G. Wagner, T. J. Declamp, M. T. De-Yarman, and J. H. Freisheim. Methotrexate binds in a non-productive orientation to human dihydrofolate reductase in solution, based on NMR spectrscopy. *FEBS*, 283:267–269, 1991.

[233] C. Oefner, A. D'Arcy, and F. K. Winkler. Crystal structure of human dihydrofolate reductase complexed with folate. *Eur. J. Biochem.*, 174:377–385, 1988.

[234] J. F. Davies, T. J. Declamp, N. J. Prendergast, V. A. Ashford, J. H. Freisheim, and J. Kraut. Crystal structures of human dihydrofolate reductase complexed with folate and 5-deazafolate. *Biochem.*, 29:9467–9479, 1990.

[235] J. Thillet and R. Pictet. Transfection of $DHFR^-$ and $DHFR^+$ mammalian cells using methotrexate-resistant mutants of mouse dihydrofolate reductase. *FEBS*, 269:450–453, 1990.

[236] D. A. Matthews, R. A. Alden, J. T. Bolin, D. J. Filman, S. T. Freer, R. Hamlin, W. G. L. Hol, R. L. Kisliuk, E. J. Pastore, L. T. Plante, N. H. Xuong, and J. Kraut. Dihydrofolate reductase from Lactobacillus casei. *J. Biol. Chem.*, 253:6946–6954, 1978.

[237] P. A. Charlton and D. W. Young. Stereochemistry of reduction of folic acid using dihydrofolate reductase. *J.C.S. Chem. Comm.*, pages 922–924, 1979.

[238] A. Rosowsky, C. S. Yu, J. Uren, H. Lazarus, and M. Wick. Methotrexate analogues. 13. Chemical and pharmacological studies on amide, hydrazide, and hydroxamic acid derivatives of the glutamate side chain. *J. Med. Chem.*, 24:559–567, 1981.

[239] J. R. Piper, J. A. Montgomery, F. M. Sirotnak, and P. L. Chello. Syntheses of α- and γ-substituted amides, peptides, and esters of methotrexate and their evaluation as inhibitors of folate metabolism. *J. Med. Chem.*, 25:182–187, 1982.

[240] J. Fan, L. E. Pope, K. S. Vitols, and F. M. Huennekens. Covalent labelling of dihydrofolate reductase and folate transport proteins by fluorescein methotrexate. *Chemistry and Biology of Pteridines*, pages 1162–1165, 1989.

[241] P. N. Kularni, A. Huntley Blair, and T. I. Ghose. Covalent binding of methotrexate to immunoglobulins and the effect of antibody-linked drug on tumor growth in vivo. *Can. Res.*, 41:2700–2706, 1981.

[242] W. P. Fung, M. Przbylski, H. Ringsdorf, and D. Szaharko. In vitro inhibitory effects of polymer-linked methotrexate derivatives on tetrahydrofolate dehydrogenase and murine L5178Y cells. *J. Natl. Can. Inst.*, 62:1261–1264, 1979.

[243] R. Duncan, J. B. Lloyd, and J. Kopecek. Degradation of side chains of N-(2-hydroxypropyl) methacrylamide copolymers by lysosomal enzymes. *Biochem. Biophys. Res. Comm.*, 94:284–290, 1980.

[244] V. Subr, J. Kopecek, and R. Duncan. Degradation of oligopeptide sequences connecting poly[N-(2-hydroxypropyl)-methacrylamide] chains by lysosomal cysteine proteinases. *Makromol. Chem.*, 186:133–146, 1985.

[245] I. Schechter and A. Berger. On the size and active site in proteinases. I. Papain. *Biochem. Biophys. Res. Comm.*, 27:157–162, 1967.

[246] K. Kurachi, J. C. Powers, and P. E. Wilcox. Kinetics of the Reaction of Chymotrypsin A_α with Peptide Chloromethyl Ketones in Relation to its Subsite Specificity. *Biochem.*, 12:771–777, 1973.

[247] J. Kopecek. *IUPAC Macromolecules*, pages 305–320. Pergamon Press, Oxford, 1982.

[248] R. Duncan, H. C. Cable, J. B. Lloyd, P. Rejmanova, and J. Kopecek. Degradation of side-chains of N-(2-hydroxypropyl)-methacrylamide copolymers by lysosomal thiol proteinases. *Biosci. Reports*, 2:1041–1046, 1982.

[249] R. Duncan, P. Kopeckova-Rejmanova, J. Strohalm, I. Hume, H. C. Cable, J. Pohl, J. B. Lloyd, and J. Kopecek. Anticancer agents coupled to N-(2-hydroxypropyl)-methacrylamide copolymers. I. Evaluation of daunomycin and puromycin conjugates in vitro. *Br. J. Can.*, 55:165–174, 1987.

[250] E. Tomlinson and S. S. Davies, editors. *Site-Specific Drug Delivery.* J. Wiley and Sons Ltd, 1986.

[251] G. Carpenter and S. Cohen. Epidermal Growth Factor. *Ann. Rev. Biochem.*, 48:193–216, 1979.

[252] M. S. Brown, R. G. W. Anderson, and J. L. Goldstein. Recycling receptors: The round-trip itinerary of migrant membrane proteins. *Cell*, 32:663–667, 1983.

[253] S. K. Basu. Receptor-mediated endocytosis of macromolecular conjuagtes in selective drug delivery. *Biochem. Pharmacol.*, 40:1941–1946, 1990.

[254] J. M. Varga, N. Asato, S. Lande, and A. B. Lerner. Melanotropin-daunomycin conjugate shows receptor-mediated cytotoxicity in cultured murine melanoma cells. *Nature*, 267:56–58, 1977.

Appendix A

Experimental Data for Chapter 3

TIME	Fluid Uptake (μl/10^6cells)			
(minutes)	A	B	C	D
10	0.102	0.132	0.069	0.151
15	0.108	0.135	0.073	0.150
30	0.123	0.154	0.078	0.167
45	0.130	0.163	0.099	0.165
60	0.141	0.183	0.103	0.179
75	0.148	0.180	0.112	0.184
90	0.154	0.197	0.125	0.180
105	0.188	0.201	0.128	0.170

Table A.1: Fluid-associated uptake of ^{125}I-PVP by B16 cells in suspension at 37^{0}C for four individual experiments (A-D).

TIME (minutes)	Fluid Uptake (μl/10^6cells)		
	A	B	C
10	0.055	0.124	0.103
15	0.061	0.136	0.108
30	0.073	0.099	0.128
45	0.077	0.107	0.143
60	0.082	0.112	0.142
75	0.079	0.127	0.148
90	0.092	0.128	0.151
105	0.093	0.160	0.153
150	0.086	0.138	0.155

Table A.2: Fluid-associated uptake of ^{125}I-PVP by HMB-2 cells in suspension at 37^{0}C for three individual experiments (A-C).

TIME (minutes)	Fluid Uptake (μl/10^6cells)	
	A	B
10	0.186	0.117
15	0.184	0.113
30	0.162	0.105
45	0.167	0.106
60	0.154	0.104
75	0.159	0.120
90	0.165	0.114
105	0.159	0.115
150	0.196	0.164

Table A.3: Fluid-associated uptake of ^{125}I-PVP by SVK-14 cells in suspension at 37^{0}C for two individual experiments (A and B).

Appendix B

Experimental Data for Chapter 4

TIME (hours)	^{3}H-MTX Bound (fmoles/10^6cells).		
	Total Binding	Non-Specific Binding	Specific Binding
0.25	50.41 ± 3.46	9.18 ± 1.02	41.23 ± 3.61
0.50	68.55 ± 4.82	15.50 ± 2.01	53.05 ± 5.22
1.00	87.69 ± 5.03	27.41 ± 2.54	60.28 ± 5.64
2.00	81.75 ± 6.88	24.53 ± 1.89	57.22 ± 7.14
4.00	58.26 ± 4.97	20.21 ± 1.98	38.05 ± 5.35

Table B.1: Binding of 25nM ^{3}H-MTX with B16 cells at 4^0C with time in a Hepes based buffer, pH 7.4 (n=6).

^{3}H-MTX (nM)	^{3}H-MTX Bound (fmoles/10^6cells).		
	Total Binding	Non-Specific Binding	Specific Binding
1.0	3.59 ± 0.32	2.03 ± 0.16	1.56 ± 0.36
2.0	5.41 ± 0.32	2.69 ± 0.14	2.72 ± 0.35
4.0	16.20 ± 0.74	3.35 ± 0.21	12.85 ± 0.77
8.0	20.48 ± 0.72	5.91 ± 0.33	14.57 ± 0.79
12.0	24.48 ± 0.99	7.05 ± 0.42	21.43 ± 1.08
15.0	37.78 ± 1.49	8.78 ± 1.17	29.00 ± 1.90
20.0	54.69 ± 2.86	11.52 ± 0.52	43.17 ± 2.91
25.0	59.86 ± 2.79	12.14 ± 0.27	47.72 ± 2.80
30.0	71.42 ± 1.21	16.84 ± 0.45	54.58 ± 1.29
50.0	124.25 ± 5.35	32.09 ± 2.00	92.16 ± 5.71
60.0	157.19 ± 5.59	46.63 ± 10.13	110.56 ± 11.57
70.0	177.95 ± 5.45	66.45 ± 10.34	111.50 ± 11.69
150.0	295.23 ± 9.30	91.94 ± 4.07	203.29 ± 10.15

Table B.2: I. Adsorption isotherm of increasing concentrations of ^{3}H-MTX incubated with B16 cells at 4^0C for 30 minutes (pH 7.4), n=6.

^{3}H-MTX (nM)	^{3}H-MTX Bound (fmoles/10^6cells).		
	Total Binding	Non-Specific Binding	Specific Binding
1.0	6.15 ± 0.26	3.02 ± 0.18	3.13 ± 0.32
2.0	10.56 ± 0.57	4.22 ± 0.35	6.34 ± 0.67
4.0	16.07 ± 1.17	5.55 ± 0.46	10.52 ± 1.26
8.0	26.17 ± 1.31	6.58 ± 0.27	19.59 ± 1.36
12.0	42.35 ± 1.34	9.20 ± 0.47	33.15 ± 1.42
15.0	58.73 ± 3.40	11.86 ± 0.43	46.87 ± 3.43
20.0	62.73 ± 1.19	18.01 ± 1.44	44.72 ± 1.87
25.0	70.08 ± 1.69	19.20 ± 1.29	50.88 ± 2.13
30.0	75.11 ± 1.97	20.17 ± 2.25	54.94 ± 2.99
50.0	129.33 ± 3.87	45.17 ± 3.28	84.16 ± 5.07
60.0	117.19 ± 3.37	45.19 ± 2.33	72.00 ± 4.10
70.0	197.97 ± 8.81	52.32 ± 2.59	145.65 ± 9.18

Table B.3: II. Adsorption isotherm of increasing concentrations of ^{3}H-MTX incubated with B16 cells at 4^0C for 30 minutes (pH 7.4), n=6.

^{3}H-MTX (nM)	^{3}H-MTX Bound (fmoles/10^6cells).		
	Total Binding	Non-Specific Binding	Specific Binding
1.0	5.59 ± 0.66	3.31 ± 0.34	2.28 ± 0.74
2.0	13.93 ± 1.44	5.95 ± 1.00	7.98 ± 1.75
4.0	14.60 ± 0.44	5.17 ± 0.19	9.43 ± 0.48
8.0	29.60 ± 1.61	8.62 ± 0.84	20.98 ± 1.82
12.0	34.79 ± 1.31	11.04 ± 1.04	23.75 ± 1.67
15.0	37.10 ± 0.92	9.29 ± 0.49	27.81 ± 1.04
20.0	44.78 ± 1.99	9.95 ± 0.22	34.83 ± 2.00
25.0	48.64 ± 1.45	12.5 ± 1.15	36.14 ± 1.85
30.0	55.53 ± 2.00	10.76 ± 0.94	42.77 ± 2.21
50.0	113.48 ± 3.76	34.66 ± 8.10	78.82 ± 8.93
60.0	143.18 ± 14.50	14.50 ± 1.85	118.32 ± 14.62
70.0	158.44 ± 9.73	27.71 ± 3.79	130.73 ± 10.44

Table B.4: III. Adsorption isotherm of increasing concentrations of ^{3}H-MTX incubated with B16 cells at 4^0C for 30 minutes (pH 7.4), n=6.

^{3}H-MTX (nM)	^{3}H-MTX Bound (fmoles/10^6cells).		
	Total Binding	Non-Specific Binding	Specific Binding
150	176.30 ± 9.36	56.83 ± 3.00	119.47 ± 9.83
250	299.99 ± 10.19	113.02 ± 6.05	186.97 ± 11.85
400	394.34 ± 22.80	174.06 ± 14.94	220.28 ± 27.26
600	581.27 ± 23.95	269.77 ± 10.95	311.50 ± 26.33

Table B.5: I. Adsorption isotherm of high concentrations of ^{3}H-MTX incubated with B16 cells at 4^0C for 30 minutes (pH 7.4), n=6.

^{3}H-MTX (nM)	^{3}H-MTX Bound (fmoles/10^6cells).		
	Total Binding	Non-Specific Binding	Specific Binding
100	233.25 ± 14.21	72.74 ± 12.79	160.51 ± 19.12
200	275.36 ± 10.41	94.82 ± 7.38	180.54 ± 12.76
400	530.12 ± 23.88	226.95 ± 53.44	303.17 ± 58.53
1000	1018.04 ± 24.05	640.59 ± 144.62	377.45 ± 144.61

Table B.6: II. Adsorption isotherm of high concentrations of ^{3}H-MTX incubated with B16 cells at 4^0C for 30 minutes (pH 7.4), n=6.

TIME (minutes)	Cell-Associated ^{3}H-MTX fmoles/10^6cells		
	Total Binding	Non-Specific Binding	Specific Binding
15	57.56 ± 4.62	10.56 ± 0.59	47.00 ± 4.66
30	60.87 ± 1.53	12.00 ± 3.00	47.13 ± 3.37
45	84.18 ± 11.53	12.92 ± 3.16	71.26 ± 11.96
105	68.53 ± 13.30	11.58 ± 1.39	56.95 ± 13.37
145	46.19 ± 3.87	15.01 ± 5.34	31.18 ± 6.60

Table B.7: Incubation of 50nM ^{3}H-MTX with B16 cells at 37^0C with time, n=6.

TIME (minutes)	Cell-Associated ^{3}H-MTX fmoles/10^6cells		
	Total Binding	Non-Specific Binding	Specific Binding
15	115.72 ± 8.71	40.18 ± 11.72	75.54 ± 14.60
30	150.63 ± 5.01	22.71 ± 4.01	127.92 ± 6.42
45	184.38 ± 12.49	58.90 ± 23.60	125.48 ± 26.70
105	157.54 ± 18.21	23.72 ± 3.55	133.82 ± 18.55

Table B.8: Incubation of 100nM ^{3}H-MTX with B16 cells at 37^{0}C with time, n=6.

TIME (hours)	Cell-Associated ^{3}H-MTX fmoles/10^6cells		
	Total Binding	Non-Specific Binding	Acid-Washed Cells
4^0C			
1	75.13 ± 8.16	13.03 ± 2.61	19.67 ± 1.98
2	88.28 ± 9.92	30.19 ± 5.50	25.63 ± 3.41
37^0C			
1	96.11 ± 6.74	65.04 ± 6.41	17.07 ± 1.78
2	57.50 ± 9.42	45.81 ± 8.96	16.28 ± 1.40

Table B.9: Incubation of 100nM ^{3}H-MTX with B16 cells at 4^0C and 37^0C for 1 and 2 hours, n=6.

NLDP-MSH-MTX	^{3}H Activity (dpm/well)	
Conc. (nM)	G0133/1	G0133/3
2.5	541.4 ± 21.0	
8.0	570.8 ± 22.8	
25.0	587.5 ± 43.4	465.5 ± 45.9
80.0	548.2 ± 21.4	
250.0	315.5 ± 68.9	

Table B.10: I. ^{3}H activity after incubation of 25nM ^{3}H-MTX with B16 cells at 4^0C for 30 minutes in the presence of increasing concentrations of the two conjugate forms of NLDP-MSH-MTX, G0133/1 and G0133/3 (n=6). The total and non-specific binding (n=12) in the absence of the conjugate were 625.1 ± 20.8 and 145.6 ± 8.0 respectively.

NLDP-MSH-MTX	^{3}H Activity (dpm/well)	
Conc. (nM)	G0133/1	G0133/3
2.5	411.3 ± 25.2	416.9 ± 34.6
8.0	338.4 ± 20.6	356.9 ± 40.0
25.0	272.6 ± 8.4	261.4 ± 13.3
80.0	313.9 ± 19.8	292.0 ± 13.8
250.0	327.7 ± 34.4	367.9 ± 39.4

Table B.11: II. ^{3}H activity after incubation of 25nM ^{3}H-MTX with B16 cells at 4^0C for 30 minutes in the presence of increasing concentrations of the two conjugate forms of NLDP-MSH-MTX, G0133/1 and G0133/3 (n=6). The total and non-specific binding (n=12) in the absence of the conjugate were 491.1 ± 17.9 and 104.9 ± 9.9 respectively.

NLDP-MSH-MTX	^{3}H Activity (dpm/well)	
Conc. (nM)	G0133/1	G0133/3
2.5	354.9 ± 40.0	323.1 ± 10.7
8.0	303.2 ± 49.4	370.0 ± 45.1
25.0	240.1 ± 11.3	318.4 ± 20.1
80.0	390.5 ± 13.3	283.7 ± 10.5
250.0	226.3 ± 31.8	260.8 ± 20.7

Table B.12: III. ^{3}H activity after incubation of 25nM ^{3}H-MTX with B16 cells at 4^{0}C for 30 minutes in the presence of increasing concentrations of the two conjugate forms of NLDP-MSH-MTX, (n=6). The total and non-specific binding (n=12) in the absence of the conjugate were 539.6 ± 40.0 and 185.7 ± 25.6 respectively.

NLDP-MSH-MTX	% of Control	
Conc. (nM)	G0133/1	G0133/3
2.5	69.89 ± 26.70	59.82 ± 26.95
8.0	60.78 ± 25.55	58.68 ± 27.94
25.0	50.33 ± 35.26	48.88 ± 20.50
80.0	69.08 ± 28.35	40.88 ± 16.93
250.0	41.66 ± 40.31	44.65 ± 31.29

Table B.13: Inhibition of 25nM ^{3}H-MTX binding with B16 cells at 4^{0}C for 30 minutes in the presence of increasing concentrations of the two conjugate forms of NLDP-MSH-MTX, G0133/1 and G0133/3 (n>12). Values are expressed as a % of the control binding (specific binding of ^{3}H-MTX in the absence of conjugate) from single wells in individual experiments.

Appendix C

Experimental Data for Chapter 5

TIME (hours)	^{125}I-NLDP-MSH Bound (fmoles/10^6cells).		
	Total Binding	Non-Specific Binding	Specific Binding
2	1.43 ± 0.03	0.35 ± 0.04	1.08 ± 0.05
4	1.81 ± 0.09	0.47 ± 0.04	1.34 ± 0.10
8	2.51 ± 0.07	0.92 ± 0.05	1.59 ± 0.09
22	2.74 ± 0.12	1.12 ± 0.04	1.62 ± 0.13

Table C.1: Binding of 0.1 nM ^{125}I-NLDP-MSH with B16 cells at 4^0C with time in a Hepes based buffer containing 0.2% BSA, pH 7.4, n=6

TIME (hours)	^{125}I-NLDP-MSH Bound (fmoles/10^6cells).		
	Total Binding	Non-Specific Binding	Specific Binding
4	7.30 ± 0.31	2.00 ± 0.19	5.30 ± 0.36
8	9.39 ± 0.11	3.25 ± 0.15	6.14 ± 0.19
22	10.63 ± 0.44	3.66 ± 0.24	6.97 ± 0.50

Table C.2: Binding of 0.4nM ^{125}I-NLDP-MSH with B16 cells at 4^0C with time in a Hepes based buffer containing 0.2% BSA, pH 7.4, n=6

TIME (hours)	^{125}I-NLDP-MSH Bound (fmoles/10^6cells).		
	Total Binding	Non-Specific Binding	Specific Binding
2	0.54 ± 0.05	0.15 ± 0.01	0.40 ± 0.05
4	0.84 ± 0.03	0.16 ± 0.02	0.68 ± 0.04
8	1.14 ± 0.06	0.20 ± 0.01	0.94 ± 0.06
22	1.81 ± 0.20	0.30 ± 0.01	1.51 ± 0.02

Table C.3: Binding of 0.1nM ^{125}I-NLDP-MSH with B16 cells at 4^0C with time in a Hepes based buffer containing 0.2% casein, pH 7.4, n=6

^{125}I-NLDP-MSH (nM)	^{125}I-NLDP-MSH Bound (fmoles/10^6cells).		
	Total Binding	Non-Specific Binding	Specific Binding
0.010	0.291 ± 0.042	0.014 ± 0.003	0.195 ± 0.042
0.020	0.182 ± 0.096	0.015 ± 0.003	0.167 ± 0.096
0.050	0.720 ± 0.127	0.039 ± 0.004	0.682 ± 0.127
0.075	0.755 ± 0.337	0.076 ± 0.018	0.680 ± 0.338
0.100	1.369 ± 0.353	0.063 ± 0.010	1.306 ± 0.353
0.150	1.491 ± 0.247	0.127 ± 0.002	1.364 ± 0.248
0.200	2.232 ± 0.673	0.249 ± 0.035	1.983 ± 0.674
0.300	4.300 ± 1.382	0.284 ± 0.104	4.016 ± 1.386
0.600	4.486 ± 1.008	0.618 ± 0.071	3.868 ± 1.010
0.800	5.781 ± 1.887	0.693 ± 0.162	5.089 ± 1.894
1.000	4.222 ± 0.319	1.299 ± 0.231	2.933 ± 0.394

Table C.4: I. Adsorption binding isotherm of increasing concentrations of ^{125}I-NLDP-MSH incubated with B16 cells at 4^0C for 8 hours at pH 7.4, n=6.

^{125}I-NLDP-MSH (nM)	^{125}I-NLDP-MSH Bound (fmoles/10^6cells).		
	Total Binding	Non-Specific Binding	Specific Binding
0.01	0.056 ± 0.009	0.019 ± 0.005	0.037 ± 0.010
0.02	0.136 ± 0.017	0.023 ± 0.004	0.113 ± 0.018
0.05	0.270 ± 0.044	0.040 ± 0.014	0.229 ± 0.046
0.07	1.005 ± 0.053	0.110 ± 0.036	0.896 ± 0.064
0.10	1.528 ± 0.102	0.186 ± 0.026	1.342 ± 0.105
0.15	1.316 ± 0.109	0.220 ± 0.025	1.097 ± 0.111
0.20	2.795 ± 0.168	0.340 ± 0.123	2.455 ± 0.208
0.30	3.259 ± 0.418	0.395 ± 0.094	2.864 ± 0.429
0.60	4.893 ± 0.850	0.958 ± 0.143	3.936 ± 0.862
0.80	6.400 ± 0.526	2.486 ± 0.779	3.910 ± 0.939
1.00	7.535 ± 0.517	2.977 ± 0.518	4.559 ± 0.732

Table C.5: II. Adsorption binding isotherm of increasing concentrations of ^{125}I-NLDP-MSH incubated with B16 cells at 4^0C for 8 hours at pH 7.4, n=6.

Time (minutes)	Cell Associated ^{125}I-NLDP-MSH (fmoles/10^6cells).			
	Total Binding	Acid-Washed Cells	Non-Specific Binding	Specific Binding
10	0.579 ± 0.016	0.107 ± 0.013	0.081 ± 0.072	0.498 ± 0.074
20	0.805 ± 0.034	0.139 ± 0.006	0.076 ± 0.018	0.729 ± 0.038
30	0.947 ± 0.137	0.220 ± 0.025	0.139 ± 0.026	0.807 ± 0.139
40	0.866 ± 0.098	0.277 ± 0.030	0.141 ± 0.023	0.725 ± 0.101
60	0.724 ± 0.162	0.310 ± 0.126	0.024 ± 0.003	0.700 ± 0.162
120	0.230 ± 0.093	0.166 ± 0.039	0.024 ± 0.006	0.206 ± 0.094

Table C.6: ^{125}I activity after incubation of 0.1nM ^{125}I-NLDP-MSH with B16 cells at 37^0C with time, n=4.

Time (minutes)	Cell Associated ^{125}I-NLDP-MSH (fmoles/10^6cells).			
	Total Binding	Acid-Washed Cells	Non-Specific Binding	Specific Binding
0	6.812 ± 0.484	1.059 ± 0.243	1.582 ± 0.285	5.230 ± 0.562
5	6.461 ± 0.353	1.345 ± 0.173	0.945 ± 0.138	5.516 ± 0.379
10	4.534 ± 0.507	1.317 ± 0.108	0.583 ± 0.432	3.952 ± 0.667
20	4.440 ± 0.658	1.545 ± 0.174	1.200 ± 0.384	3.240 ± 0.762
40	1.303 ± 0.523	0.632 ± 0.203	0.402 ± 0.166	0.901 ± 0.548
80	1.456 ± 0.181	0.622 ± 0.146	0.338 ± 0.089	1.118 ± 0.202

Table C.7: I. Incubation of B16 cells at 37^0C with time in normal Hepes binding buffer, pH 7.4 (n=4). Cells were previously exposed to 0.5nM ^{125}I-NLDP-MSH for 1 hour at 4^0C before being washed and re-incubated at 37^0C.

Time (minutes)	Cell Associated ^{125}I-NLDP-MSH (fmoles/10^6cells).			
	Total Binding	Acid-Washed Cells	Non-Specific Binding	Specific Binding
0	5.811 ± 0.572	0.927 ± 0.268	1.413 ± 0.241	4.398 ± 0.620
5	4.333 ± 0.278	1.105 ± 0.323	0.556 ± 0.281	3.778 ± 0.395
10	4.427 ± 0.555	1.648 ± 0.480	0.696 ± 0.193	3.730 ± 0.587
20	3.327 ± 0.281	0.966 ± 0.176	0.609 ± 0.185	2.628 ± 0.336
40	2.206 ± 0.490	0.796 ± 0.111	0.265 ± 0.060	1.941 ± 0.494
80	1.114 ± 0.145	0.539 ± 0.047	0.333 ± 0.083	0.781 ± 0.168

Table C.8: II. Incubation of B16 cells at 37^0C with time in normal Hepes binding buffer, pH 7.4 (n=4). Cells were previously exposed to 0.5nM ^{125}I-NLDP-MSH for 1 hour at 4^0C before being washed and re-incubated at 37^0C. Also an acid-wash of cells exposed to the radio-ligand in the presence of excess unlabelled NLDP-MSH, 0.861 ± 0.179.

Time (minutes)	Cell Associated ^{125}I-NLDP-MSH (fmoles/10^6cells).			
	Total Binding	Acid-Washed Cells	Non-Specific Binding	Specific Binding
0	7.584 ± 1.087	1.935 ± 0.234	2.122 ± 0.066	5.462 ± 1.089
5	5.661 ± 0.350	0.979 ± 0.117	0.446 ± 0.148	5.215 ± 0.380
10	5.145 ± 0.319	1.237 ± 0.237	0.973 ± 0.336	4.172 ± 0.463
20	4.528 ± 0.441	1.155 ± 0.232	0.860 ± 0.214	3.668 ± 0.490
40	1.864 ± 0.324	0.790 ± 0.071	0.279 ± 0.111	1.585 ± 0.343
80	2.101 ± 0.462	0.989 ± 0.143	0.768 ± 0.133	1.333 ± 0.480

Table C.9: III. Incubation of B16 cells at 37^{0}C with time in normal Hepes binding buffer supplemented with 0.5nM NLDP-MSH, pH 7.4 (n=4). Cells were previously exposed to 0.5nM ^{125}I-NLDP-MSH for 1 hour at 4^{0}C before being washed and re-incubated at 37^{0}C.

Time (minutes)	Cell Associated ^{125}I-NLDP-MSH (fmoles/10^6cells).			
	Total Binding	Acid-Washed Cells	Non-Specific Binding	Specific Binding
0	6.300 ± 0.242	1.118 ± 0.091	1.698 ± 0.603	4.602 ± 0.650
5	5.493 ± 0.387	1.138 ± 0.132	2.238 ± 1.504	3.255 ± 1.553
10	3.031 ± 0.158	0.754 ± 0.130	0.316 ± 0.025	2.714 ± 0.160
20	4.398 ± 0.711	1.332 ± 0.677	0.410 ± 0.153	3.988 ± 0.728
40	1.230 ± 0.291	0.401 ± 0.072	0.258 ± 0.126	0.970 ± 0.318
80	1.743 ± 0.358	1.046 ± 0.402	0.880 ± 0.213	0.864 ± 0.417

Table C.10: IV. Incubation of B16 cells at 37^{0}C with time in normal Hepes binding buffer supplemented with 0.5nM NLDP-MSH, pH 7.4 (n=4). Cells were previously exposed to 0.5nM ^{125}I-NLDP-MSH for 1 hour at 4^{0}C before being washed and re-incubated at 37^{0}C.

Appendix D

Experimental Data for Chapter 6

NLDP-MSH-MTX Conc. (nM)	Bound ^{125}I-NLDP-MSH (fmoles/10^6cells)	
	Experiment A	Experiment B
0.50	3.23 ± 0.33	
1.00	3.98 ± 0.23	3.86 ± 0.36
2.00	3.29 ± 0.22	3.19 ± 0.20
5.00	3.63 ± 0.24	3.04 ± 0.08
10.0	3.06 ± 0.15	2.59 ± 0.08
15.0		2.89 ± 0.09
20.0	2.25 ± 0.15	2.77 ± 0.25
30.0		2.23 ± 0.19
50.0	1.78 ± 0.08	1.89 ± 0.15
100.0	1.71 ± 0.28	1.48 ± 0.05
200.0	1.27 ± 0.04	1.31 ± 0.11
5000	0.86 ± 0.01	0.73 ± 0.05

Table D.1: Binding competition assay (representing two individual experiments, A and B) of 0.25nM ^{125}I-NLDP-MSH incubated with increasing concentrations of NLDP-MSH-MTX at 4^0C for 8 hours, n=6. Experiment A total (3.21 ± 0.16) and non-specific (1.17 ± 0.04) binding. Experimnt B (3.80 ± 0.27) and non-specific (1.04 ± 0.07) binding.

Time (minutes)	Cell Associated ^{125}I-NLDP-MSH (fmoles/10^6cells).			
	Total Binding	Acid-Washed Cells	Non-Specific Binding	Specific Binding
10	6.119 ± 1.276	2.249 ± 0.328	1.742 ± 0.422	3.870 ± 1.317
20	10.205 ± 1.563	2.773 ± 0.198	2.538 ± 0.473	7.432 ± 1.575
30	12.027 ± 1.719	3.213 ± 0.700	3.523 ± 0.762	8.814 ± 1.856
40	10.677 ± 0.719	2.267 ± 0.140	3.799 ± 0.462	8.411 ± 0.732
60	6.754 ± 1.538	3.621 ± 0.475	2.820 ± 0.371	3.133 ± 1.610
120	1.410 ± 0.384	1.194 ± 0.321	0.992 ± 0.536	0.215 ± 0.500

Table D.2: Cell associated ^{125}I activity after incubation of 1.0nM ^{125}I-NLDP-MSH-MTX with B16 cells at 37^0C with time, n=4.

Time (minutes)	Cell Associated ^{125}I-NLDP-MSH (fmoles/10^6cells).			
	Total Binding	Acid-Washed Cells	Non-Specific Binding	Specific Binding
0	6.181 ± 0.053	1.162 ± 0.030	2.618 ± 0.232	3.563 ± 0.238
10	4.834 ± 0.199	1.304 ± 0.212	1.002 ± 0.163	3.833 ± 0.258
20	3.697 ± 0.063	1.125 ± 0.248	0.493 ± 0.093	3.205 ± 0.113
30	3.161 ± 0.220	1.147 ± 0.256	0.464 ± 0.071	2.697 ± 0.232

Table D.3: I. Incubation of B16 cells at 37^{0}C with time in normal Hepes binding buffer, pH 7.4 (n=4). Cells were previously exposed to 1.0nM ^{125}I-NLDP-MSH-MTX for 2 hour at 4^{0}C before being washed and re-incubated at 37^{0}C.

Time (minutes)	Cell Associated ^{125}I-NLDP-MSH (fmoles/10^6cells).			
	Total Binding	Acid-Washed Cells	Non-Specific Binding	Specific Binding
0	16.308 ± 1.615	4.035 ± 0.501	6.047 ± 0.703	10.260 ± 1.761
5	8.089 ± 0.689	2.075 ± 0.339	2.120 ± 0.293	5.969 ± 0.749
10	8.030 ± 0.944	2.359 ± 0.117	2.110 ± 0.213	5.920 ± 0.968
20	6.894 ± 1.088	2.696 ± 0.344	1.324 ± 0.164	5.569 ± 1.100
30	5.424 ± 0.309	1.881 ± 0.559	1.032 ± 0.143	4.393 ± 0.340
60	2.048 ± 0.465	2.017 ± 0.573	1.343 ± 0.058	0.705 ± 0.468

Table D.4: II. Incubation of B16 cells at 37^{0}C with time in normal Hepes binding buffer, pH 7.4 (n=4). Cells were previously exposed to 1.0nM ^{125}I-NLDP-MSH-MTX for 2 hour at 4^{0}C before being washed and re-incubated at 37^{0}C.

Time (minutes)	Cell Associated ^{125}I-NLDP-MSH (fmoles/10^6cells).			
	Total Binding	Acid-Washed Cells	Non-Specific Binding	Specific Binding
0	10.479 ± 1.210	2.029 ± 0.607	2.835 ± 0.349	7.644 ± 1.259
5	7.251 ± 1.051	1.228 ± 0.220	0.707 ± 0.141	6.543 ± 1.060
10	3.811 ± 0.746	1.317 ± %%[ΔPrinterError:ΔoutΔofΔpaperΔ]%%ΔΔ%%[		
20	5.913 ± 0.368	1.526 ± 0.182	1.059 ± 0.269	4.854 ± 0.456
30	4.784 ± 0.261	1.458 ± 0.116	0.521 ± 0.217	4.263 ± 0.339

Table D.5: III. Incubation of B16 cells at 37^{0}C with time in normal Hepes binding buffer, pH 7.4 (n=4). Cells were previously exposed to 1.0nM ^{125}I-NLDP-MSH-MTX for 2 hour at 4^{0}C before being washed and re-incubated at 37^{0}C.

Appendix E

Experimental Data for Chapter 7

Inhibitor Conc. (nM)	% of Maximum Activity	
	MTX	NLDP-MSH-MTX
0.1	101.00 ± 14.15	
0.4	99.05 ± 9.38	
1.0	85.17 ± 6.94	
2.0	68.86 ± 3.57	
5.0	60.91 ± 16.98	
10.0	46.15 ± 11.61	92.29 ± 21.32
20.0	30.25 ± 2.94	
50.0	27.07 ± 0.91	79.63 ± 1.84
100		53.54 ± 7.81
200	16.10 ± 5.36	
500		45.24 ± 3.60
1000		43.11 ± 4.07
5000		24.62 ± 4.49

Table E.1: Inhibition of DHFR at 37°C by MTX and NLDP-MSH-MTX, expressed as a percentage of maximum activity (120μM FH_2 represents 100% in the absence of inhibitor)